DEVELOPMENT OF EMPIRICAL MODELS FOR ESTIMATING TBM PENETRATION RATE IN ROCK MASS

Aitolkyn Yazitova

Lead Supervisor: Prof. Saffet Yagiz

Internal Co-supervisor: Prof. Amoussou C. Adoko

External Co-supervisor: Prof. Jafar Hassanpour

A thesis submitted in fulfillment of the requirements for the degree of

Doctor of Philosophy in Mining Engineering

Department of Mining Engineering

School of Mining and Geosciences

May 2025

Originality statement

“With this statement I hereby confirm that the submitted research proposal is my own work. To the best of my knowledge, it contains no sources or resources previously published or written by another person. Any contribution has been made to the research by others, with whom I am working at Nazarbayev University, explicitly will be acknowledged in the thesis. I have indicated all quotes, citations and references that were literally taken from publications, such as, academic articles, whether published or unpublished, as well as web sources, reports, papers, etc.”

Date: 03.05.2025

Signature:

Dedication

I would like to express my deepest and most heartfelt gratitude to my friends who have stood by me and shared in every step of this journey. Your encouragement, companionship, and unwavering belief in me have been a source of strength and inspiration throughout this project.

Above all, my most profound thanks to my beloved parents, Maxat Kuspanov and Aliya Kuspanova. Your constant love, sacrifices, and steadfast moral support have shaped the person I am today. You have been my guiding light in every challenge and triumph, and this accomplishment would not have been possible without you.

With all my love, respect, and devotion,

Aitolkyn Yazitova

Acknowledgments

I would like to begin by extending my heartfelt gratitude to my supervisor, Prof. Saffet Yagiz, whose unwavering support, insightful feedback, and expert guidance have been instrumental throughout my PhD journey. His encouragement and mentorship have been a cornerstone in the successful completion of this thesis. I am equally grateful to my co-supervisor, Prof. Amoussou C. Adoko, for his dedication, patience, and invaluable insights. His willingness to devote countless hours to consultations and guidance has greatly enriched my work and contributed significantly to this achievement. I also thank to Prof. Jafar Hassanpour who was my external Co-Supervisor and also provided raw data from Iranian TBM tunnel projects for this study. Also, I would like to extend my sincere thanks to reviewers, Prof. Nasser Madani, Prof. Sergei Sabanov and also Prof. Murat Karakus who was kindly accept our invitation for the committee. Further, I would like to extend my gratitude the Nazarbayev University who provided fund via Faculty Competitive Grant Project (Grant No: 021220FD5151) for this research.

Abstract

Estimating the Rate of Penetration (ROP) of Tunnel Boring Machines (TBMs) is crucial in rock excavation and boreability, as it serves as a key input for scheduling and executing tunneling projects. Despite advancements in tunneling technologies, achieving a reliable ROP estimate remains challenging. In present one of the difficult tasks is to quantifying the properties of rock discontinuities to be use as input for the TBM performance models. Another issue is that utilizing the combination of intact rock, rock mass properties and TBM specification into the TBM performance prediction models.

This thesis aims to develop several empirical models using intact rock, rock mass, disc cutter and TBM specifications for predicting TBM penetration rates in hard rock conditions. In order to achieve this goal, extensive field and laboratory tests were conducted across six TBM projects, including the Queens Water Tunnel (USA), Manapouri hydropower tunnel (New Zealand), Miryang dam tunnel (South Korea), and three Iranian water tunnels (Karaj, Zagros and Ghomrood), resulting in a database of more than 550 cases. Each case consists of the intact rock, rock mass properties and TBM field parameters. The collected data underwent preprocessing and analysis. The raw data were thoroughly examined with the literature to ensure the research output was valuable and acceptable. Common TBM performance models used by researchers and industry were critically reviewed.

In order to develop the models, first of all, a rock mass fracture index (FI) was introduced using a weighting method. Then, numerous linear and nonlinear multivariable regression models were developed using the SPSS program. At least a hundred models were generated for the aim; then the best twenty of them were chosen for each case by means of the linear multiple regression (LMR) and Non-linear multiple regression (NLMR) to be evaluated and introduced. After examination of LMR and NLMR models, with the

top five models evaluated using performance indices and a total ranking approach introduced in the thesis, the rest of them are provided in the appendices. Six statistical measures—coefficient of determination, root mean square error, mean absolute deviation, mean absolute percentage error, relative root mean square error, and variance accounted for—were used to rank the models. The study confirmed that estimating TBM penetration rate is a complex, non-linear issue due to the heterogeneous nature of rock masses. The most accurate model was a NLMR with fewer input variables, achieving the highest-ranking score of 42 (Eq.5.17; Model 1-NLMR). This model, incorporating intact rock strength, a weighted fracture index, and operational machine parameters, was ultimately identified as a reliable tool for TBM tunneling. Finally, it is concluded that the introduced rock fracture index (FI) together with weighted fracture index (WFI) could be used for quantifying the discontinues of rock mass into the TBM performance prediction model to represent the rock mass parameters. Further, it is found that the developed model could be used for similar rock type and geological formation in practice; More, it is suggested that the alpha angle, that is the angle between plane of weakness including joint, faults and shear zone and TBM driving direction, could be added as an input into the model to obtain the more accurate result for project scheduling in practice.

Contents

List of Figures

List of Tables

CHAPTER 1：INTRODUCTION

1.1. Background

Mechanized excavation refers to the method of rock breakage where the rock is entirely removed from the excavation face by mechanized excavators. The characteristic advantages of mechanical excavation over a traditional drilling and blasting are increased safety, higher production rate, reduce labor-intensive operation, higher degree of automation, minimum damage to the walls, better control over the process, uniformity of product size, elimination of blast vibrations, and better ventilation in underground openings with a length of over 1.5 km in almost all ground conditions from weak through the hard rocks. The most common types of mechanized excavators are tunnel boring machines (TBMs), roadheader (RH), raise boring machine (RBM), continuous miner (CM), and longwall drum shear (LDS) to be used for either civil or mining construction. Depending on the ground condition, one of those excavators could be chosen to excavate rocks for variety of purposes such as drift development, ventilation shaft, highway, dam, or ground water transportation tunnels. Even though numerous models have been proposed for prediction of rate of penetration (ROP), the accuracy of the developed models for the aim depends on the original database from which they were driven, range of dataset used for the model as well as ground condition, type and specifications of excavator utilized in project.

For construction planning and for the selection of the most suitable excavation technology, the estimation of the TBM performance, in terms of rate of penetration (ROP), utilization factor (U), daily advancement (AR) has become significant parameters that should be measured or estimated for project scheduling related to time and cost implication. TBM performance assessment is a complex and non-linear problem to be

solved as real-world project scheduling due to that it is not simply can be estimated as a function of simple one parameter. Developed function for the aim should be non-linear with multiple input variables to obtain the most accurate output such as ROP, U and AR.

During the last decades a number of models have been developed for the prior-to-construction prediction of the TBM performance based on input parameters including intact rock, rock mass parameters and also TBM specifications (Table 1.1). In present, several models including Colorado School of Mines, CSM (Rostami, 1997; Cheema 1999; Yagiz, 2002), Norwegian University of Sciences and Technology, NTNU (Bruland, 1998; Macias et al. 2014; Macias, 2016), field penetration index (FPI) (Nelson et al. 1983; Hassanpour, et al. 2011), Q_{tbm} Model (Barton, 1999), Alpin Model (Gehring, 1995; Wilfing, 2016) can be mentioned herein. In fact, TBM performance prediction models can be divided into three main approaches, namely, theoretical and empirical models as well as artificial intelligence (AI).

Table 1.1. Common parameters influencing TBM penetration in the literature

Intact rock parameters	Rock mass parameters	Machine parameters
Uniaxial compressive strength	Rock mass fabric	Total thrust (F_t)
Point load Index	Rock texture	Normal force (F_n)
Brazilian tensile strength	Orientation of discontinuities	Cutter diameter
Rock brittleness, Toughness	Spacing between the fractures	Cutter tip width, RPM
Hardness	Rock Quality Designation	Spacing between the cutters
Drilling rate index (DRI)	Fissures	Number of Cutters
Thin section analysis	Grain size and minerals	Cutterhead Power

1.2. Problem Statement

TBM performance estimation prognosis be divided in two main categories: the empirical models, which represent the largest group with field and laboratory studies,

and the theoretical or semi-theoretical models refers to a basic understanding of rock fragmentation and explanations into the force versus penetration behavior of rocks. Due to the complexity of TBM performance prediction, artificial intelligence (AI) methods particularly machine learning algorithms also conducted in the literature (Grima, et al. 2000; Benardos and Kaliampakos, 2004). Even though numerous empirical, mathematical, Artificial Intelligence (AI) models were introduced in the literature, most of them are based on the rough dataset of one or two projects, simple correlations between two variables (such as ROP vs UCS) or without proper rock mass discontinuity properties that directly influence the ROP.

In order to address significance of input parameters (intact rock strength and TBM specification) and use them together with quantified rock fracture properties, this research is conducted based on six long mechanized tunnel projects where the database is developed. With this research, input variables are chosen, rock fracture index were developed and all together used for estimating the TBM performance in empirical approaches using statistical program.

1.3. Research Objectives

The main aim of this research is to develop several new empirical models which is powerful and useful in practice for predicting the ROP of TBM based on uniaxial compressive strength (UCS) of intact rock and rock fracture index (FI) measured in the field and TBM specification and cutter disc properties. To obtain the aims, the following are accomplished:

- Raw UCS data, rock mass data and TBM field data were obtained from six TBM tunnel projects including Queens fresh water (USA), Manapouri Hydropower (New Zeland), Miryang dam (S. Korea) and Iranian fresh water transfer tunnels (Iran).

- Obtained raw data is examined and then the database established base on available parameters including UCS, spacing between the discontinuities in rock mass, RPM, cutterhead diameter, power, torque and thrust of TBM as well as disc diameter, and individual cutter load.
- Introducing the rock fracture index (FI), weighted fracture index (WFI) and then examine the impact of each individual variable in the database on the estimation of the ROP
- Apply SPSS Statistics program to develop possible multiple variables linear and non-linear models for estimating the ROP.
- Check the validity of developed models and compare them to suggest the best one to be used for real world mechanized excavation project.

1.4. Thesis Organization

This is composed of several chapters that is related to from aim of it through the conclusions as follow:

Chapter 1: ***Introduction*** section of this research, in which the background of the research, problem statement, research objectives and thesis organization is presented.

Chapter 2: ***Comprehensive Literature Review*** related to general through the detail aim of the research which is about data analysis and TBM performance estimation. The chapter provides information related to current main input parameters and their influence on the estimated ROP as well as current models for estimating the ROP in the literature.

Chapter 3: ***Case Studies*** including geological and rock mass properties of the project. Laboratory and field observation of rock features and TBM specification and performance. General project overview of six TBM tunnel projects studied and investigated for the aim.

Chapter 4: ***Development of Rock Fracture Index*** and weighted fracture index as an input parameter related to discontinuities of rock mass for the estimation of TBM performance from weak through the hard rock mass conditions.

Chapter 5: Development of Empirical Linear and Non-linear Multivariable Models for estimating the TBM penetration rate. This section includes linear and non-linear multivariable regression models for the aim which is estimating the ROP. Then, comparing the obtained alternative models to suggest the best one among them.

Chapter 6: Application and Limitations that focus on application of developed models and their limitations that is related to rock and TBM specification as well as rock conditions.

Chapter 7: Conclusions and Recommendations. This section refers to conclude the output of this thesis, suggested model among the ones for the aims and also recommendations for future studies.

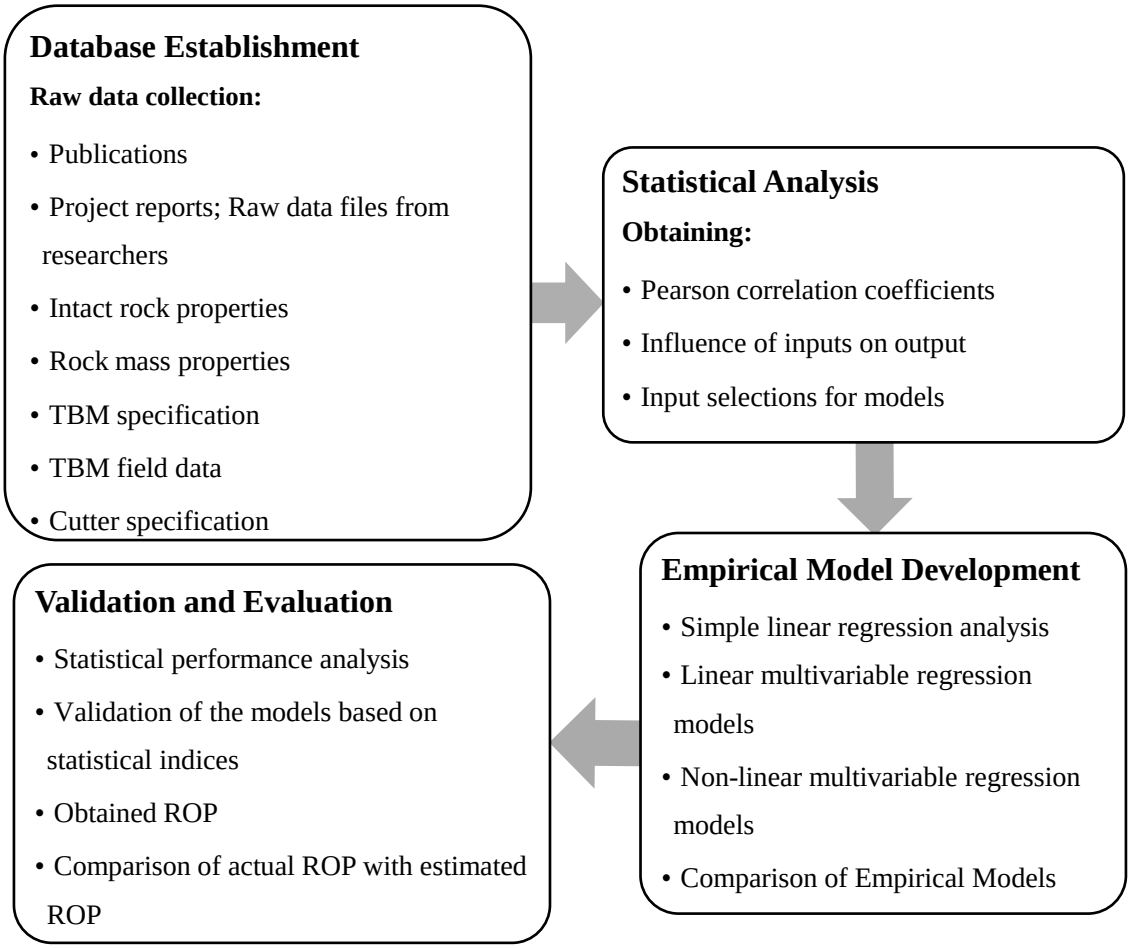

Figure 1.1. Diagram illustrated to research design

CHAPTER 2 : LITERATURE REVIEW

Since 1950's, many improvements have been carried out on the design of TBM and to improve the machine advancement (Figure 2.1). These changes have led to more powerful and efficient TBMs in a variety of ground conditions, from very hard to soft rocks having UCS of 80MPa to more than 300MPa respectively. For any tunneling project, one of the challenging issues is predicting the performance of TBM in difficult ground conditions (Nelson, 1993; Sapigni et al. 2002). Geological record and mapping provide valuable quantified and unquantified information about the geological conditions ahead of the tunnel face and the response of the rock mass to excavation progress. Rock mass weathering, intact rock strength (both UCS and BTS), geological structures and other conditions influence TBM performance in tunnelling project (Sapigni et al. 2002; Benardos and Kaliampakos, 2004). Therefore, prediction of TBM penetration is very crucial in planning the tunnel projects and selecting the suitable methods of construction, and it can decrease the risks related to high capital costs, which are very common for the mechanized excavation operations (Yagiz, 2002; Yagiz et al. 2009). A key component in the successful planning of TBM tunnelling is the accurate prediction of TBM performance parameters, the penetration rate (PR) and the advance rate (AR). Over the past few decades, there have been numerous research studies conducted, most of them in the developed countries such as USA, Germany and Norway, to estimate TBM performance in rock mass. At present, estimation of TBM performance may be made by means of penetration rate (ROP), the ratio of excavated distance to the operating time during continuous excavation phase, and advance rate (AR), the ratio of both mined and supported actual distance to the total time or field penetration index (FPI), that is the ratio of individual cutter load to RoP (Rostami, 1997; Yagiz, 2002; Hassanpour, et al. 2009, 2011; Adoko, et al. 2017; Yazitova, et al. 2025). Rostami (2016) stated that predicting

the performance of Tunnel Boring Machines (TBMs) is crucial for effective project scheduling and cost estimation. This process requires a deep understanding of the geological complexities of the site, the specifications of the machine, and site management practices. Over the years, various methods have been employed to estimate TBM performance in specific ground conditions. While many of these methods have proven to be accurate within acceptable limits, some have significantly deviated from the actual performance. Experience indicates that the most reliable approach to predicting TBM performance is to use multiple models to assess a range of estimated penetration and advance rates, and then select the rate that best aligns with the actual working conditions and the parameters of the model used. This strategy helps engineers avoid unexpected issues and identify the key factors influencing machine performance in each situation. The chapter reviews type of TBMs, intact rock, rock mass properties, disc and TBM operational parameters, and also the existing models for TBM performance prediction and discusses ongoing research aimed at developing more accurate models to enhance TBM performance.

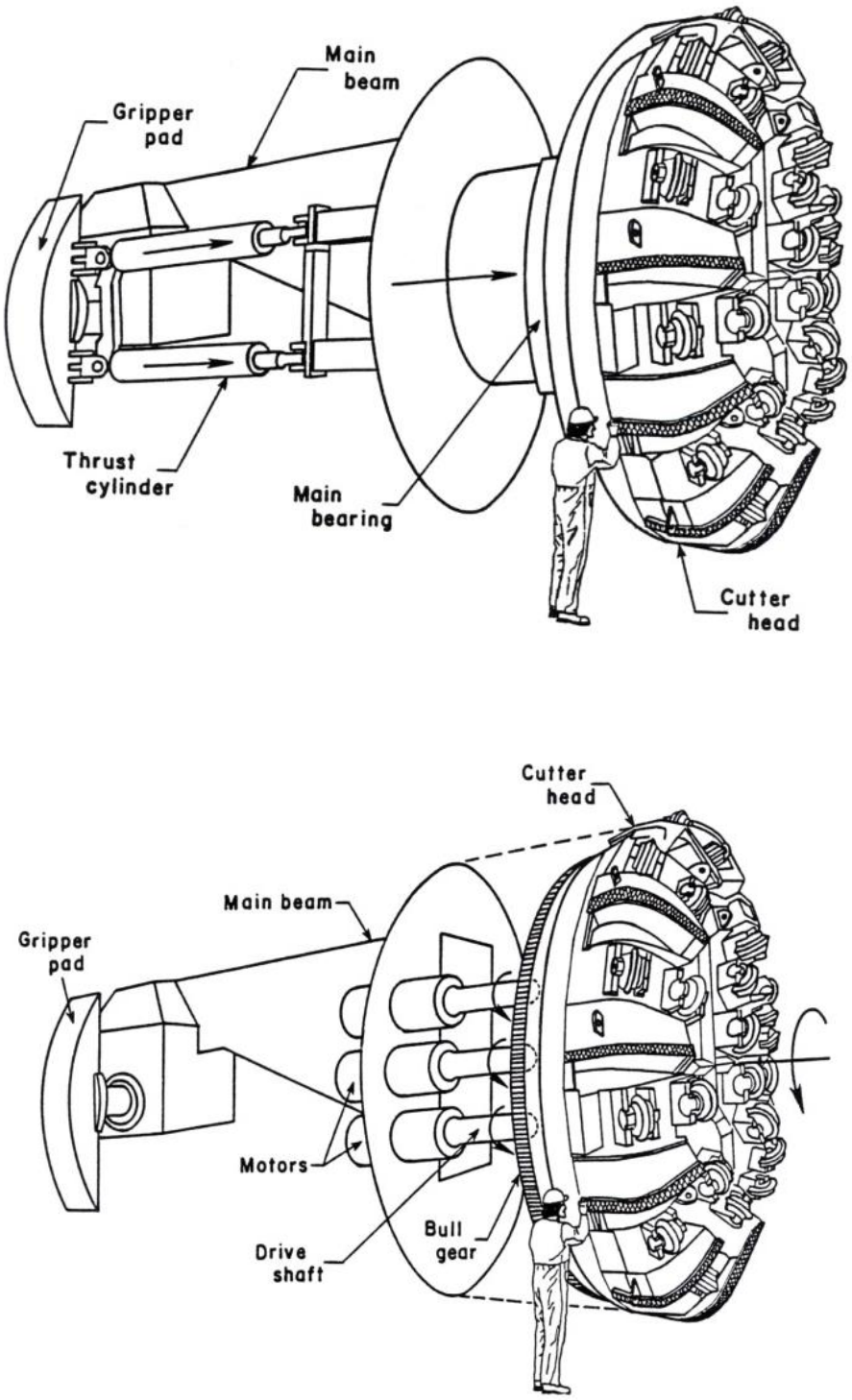

Figure 2.1. TBM thrust and torque system respectively (Nelson, 1993)

2.1. Type of Tunnel Boring Machine (TBM)

Various types of TBMs are in use today for the full-face excavation in rock condition from weak, medium to hard rocks. Since the research is related to TBMs,

general specification of the different type of TBMs are herein together with ground condition where selected type of TBM could be productive and applicable. Different TBMs may be selected on the ground condition from hard rock through the fractured rock with groundwater inflows (Figure 2.2).

Figure 2.2.Geological condition of ground condition and suggested TBM (Robbins Company)

Further, one of the most important distinctions in hard rock TBM classification is between the open (gripper) and the shield TBM as follow.

2.1.1. Open TBMs

The open type TBM, also called gripper TBM, is widely used for tunnel excavation where rock masses are characterized by good quality, rock strength can be characterized by medium to high strength, and stand-up time long enough to put in work the required supports in safety conditions. During the boring operation, two laterally mounted gripper plates anchor the rear part of the machine to the tunnel side walls, while the rotating cutterhead having disc cutters is pressed against the tunnel face. Due to the rolling movement of the cutters, single pieces (chips) of rock are cut out from the face and removed. The demonstration of Open TBMs is presented in Figure 2.3 where TBM has different type of component and each of them illustrated herein.

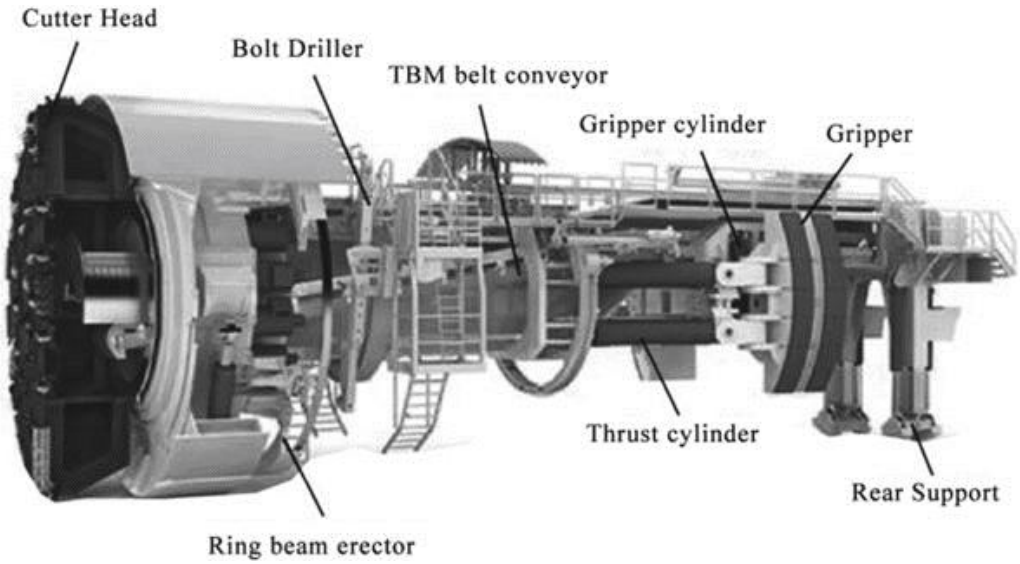

Figure 2.3. Principal components of Open TBMs (Chen et al. 2023)

2.1.2. Shielded TBMs

This group of TBMs is usually used to excavate jointed rock masses with low stand-up time; in these contexts, single shield TBMs can guarantee high tunnelling performances.

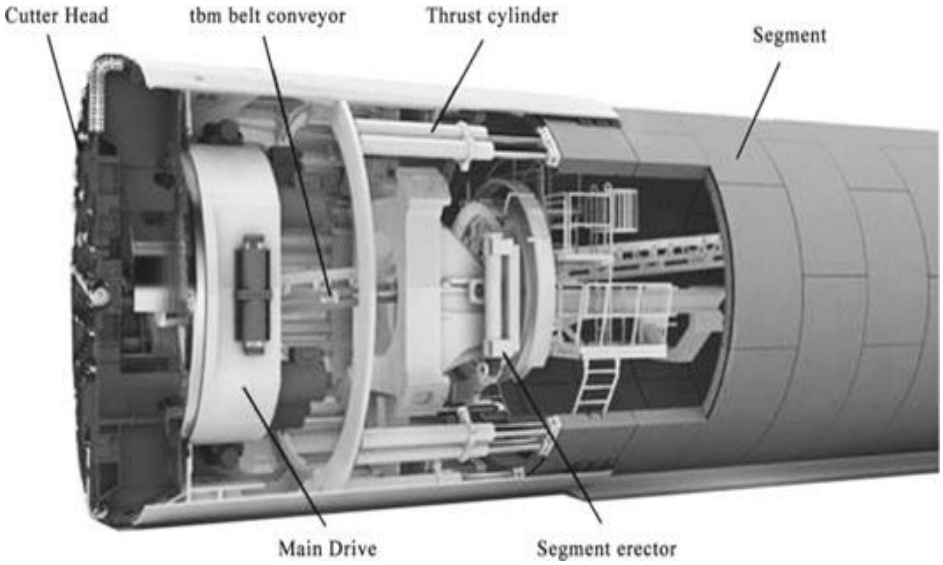

Figure 2.4. Principal components of a shield TBM (Chen et al. 2023)

The substantial difference between open and shield TBM is that in the first group the contrast required by thrust cylinders to transfer the thrust to the cutterhead is provided by rock tunnel walls, whereas in the second group the contrast is provided by lining, given that rock mass strength in which single shield TBMs are used generally lower that the one characterizing the rock mass in which open TBM are adopted (Paltrinieri, 2015). This TBM is applicable for rock characterized by low to high strengths. The demonstration of Shield TBMs is presented in Figure 2.4 where TBM has different type of component and each of them illustrated herein.

2.1.3. Double shielded TBMs

Double shield TBMs, also called telescopic shields, are frequently used in long tunnel excavation in hard rocks with high fractured or shear zones and/or fault zones in rock mass. The double shield TBMs are considered the most sophisticated ones because they are a combination of gripper and single shield machines. They guarantee very high tunnelling performances by working in continuous tunnelling method. They consist of two principal elements: a front shield with cutterhead, drive and main bearing; and a gripper shield with gripping units, auxiliary thrust cylinders, tail skin (Maidl et al. 2008) as shown in Figure 2.5. The two parts of the shield are connected by the main thrust cylinders and a telescopic shield protects them. The segments are installed in the tail skin section while the machine is tunnelling. When a bore stroke is completed the gripper, shoes are loosened and the auxiliary thrust cylinders make the gripper shield push behind the front shield.

The TBM simultaneously excavates and erects the tunnel lining (continuous cycle of excavation). The machine unifies the functional principles of gripper and single shield TBMs being equipped by two possible “thrust systems” which is adopted on the basis of the ground conditions: the jacks that push against the segment ring to create the thrust

for the TBM as well as the grippers (located on the second shield) that push against the excavated tunnel. In this sense the double shield machine can be considered as one of the most flexible types of machine. The demonstration of double shield TBMs is presented in Figure 2.5 where TBM has different type of component and each of them illustrated herein.

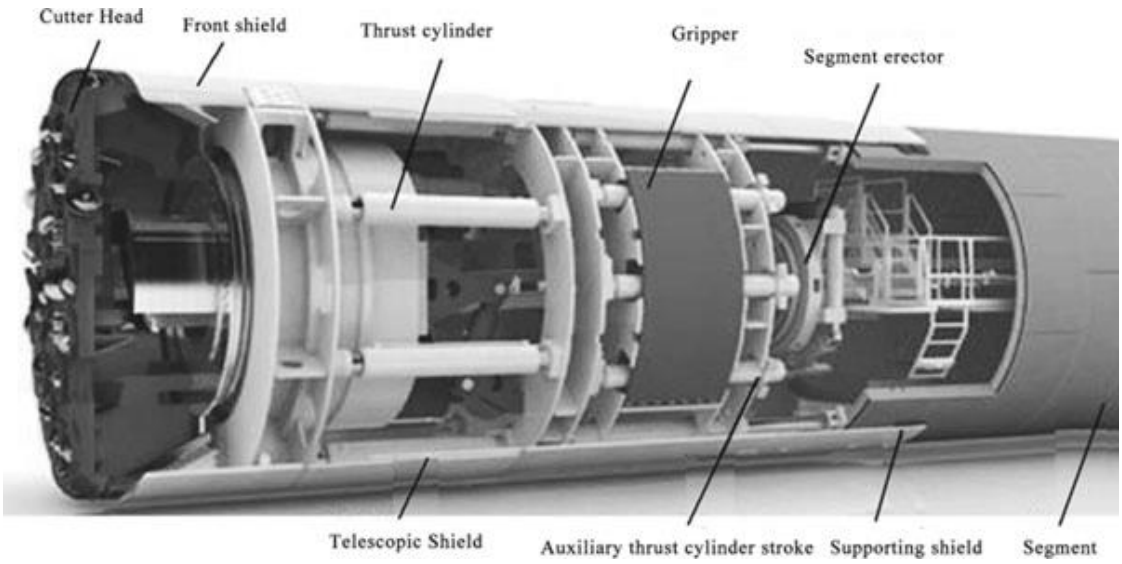

Figure 2.5. Principal components of a double shield TBM (Chen et al. 2023)

Table 2.1. Comparison between open TBM and shield TBM (Chen et al. 2023)

Comparison items	Open TBM	Double-shield TBM	Single-shield TBM
Geological adaptability	It is generally used in good geological conditions, featuring good adaptability to hard rock tunneling. In soft rock, stratum shall be reinforced in advance. It is suitable for tunnels dominated by Class II and III rocks	Its adaptability to hard rock tunneling is the same as that of open type. In soft rock tunneling, single shield is better than open type. It is suitable for tunnels dominated by Class III rocks	It is used under relatively poor geological conditions (but the excavation face can be self-stabilized). It is suitable for tunnels dominated by Class III and IV rocks
Tunneling performance	On the premise of giving full play to the advance speed, it is mainly suitable for hard rock stratum (50–150 MPa) with relatively complete to complete rock mass and good self-stability. When effective support measures are adopted, it can also be applied to soft rock tunnels, but the advance speed is limited	On the premise of giving full play to the advance speed, it is mainly suitable for soft rock to medium hard rock stratum (30–90 MPa) with relatively complete rock mass and certain self-stability	It is suitable for soft rock (5–60 MPa) with certain self-stability in medium-length
Construction speed	Only bolting and shotcreting is needed if the geological conditions are good. In this case, the supporting workload is small and the speed is fast. However, it needs to be reinforced in advance if the geological conditions	When the geological conditions are good, the tunnel wall is supported by grippers to provide the reverse thrust, and the tunneling and installation of the segment are carried out at the same time to speed up the progress. In soft ground, single	Tunneling and segment installation cannot be carried out at the same time, so the construction speed is limited

	are poor. In this case, the supporting workload is large and the speed is slow	shield tunneling is adopted, and tunneling and segment installation cannot be carried out at the same time, so the construction speed is limited	
Safety	Equipment and personnel are exposed to rocks, so protection should be strengthened	Personnel safety can be secured under the protection by shield. There is a danger of being stuck when the ground stress is high and the stratum is broken	Personnel safety can be secured under the protection by shield. There is a danger of being stuck when the ground stress is high and the stratum is broken
Advance speed	It is affected by geological conditions, but	Less affected than the open type	It is less affected by geological conditions than the open TBM
Lining mode	Secondary concrete lining can be carried out depending on specific situation	Segment lining is adopted	Segment lining is adopted
Geological conditions for construction	The lithological change of the tunnel wall can be directly observed during the tunneling process. It is convenient for geological map description. When the geological survey data is not detailed, it is less risky to choose open TBM for construction	It is difficult to systematically describe the construction geological conditions and measure the convergence deformity. The construction risk will be high if the geological survey data is not detailed	It is difficult to systematically describe the construction geological conditions and measure the convergence deformity. The construction risk will be high if the geological survey data is not detailed

2.2. Rock Breakage Process

There have been numerous studies conducted to explain the interaction between rock and mechanical cutting tools as well as the rock fragmentation process during the TBM operation. Rock fragmentation under disc cutter includes different procedures crushing, chipping and fracturing respectively (Rostami and Ozdemir, 1993). Each of these phenomena is representing one of the physical properties of rock and in combination with each other. The linear cutting machine (LCM) test on a rock block and theoretical results confirmed that beneath the CCS disc, three different zones can be observed, namely the crushed zone, the fracture zone, and the elastic zone; however, the most significant zones are crushed and fractured zone in terms of rock fragmentation and breakage. All authors agree that the fragmentation is divided into two parts (Figure 2.6): a zone of crushed material beneath the cutter (crushed zone) and the formation of rock chips (Sanio, 1985; Sato et al. 1991; Rostami and Ozdemir 1993; Yagiz, 2002; Bruland, 1998; Wilfing, 2016; Rostami, 2016; Hassanpour, 2018). Most of the researchers have confirmed and stated that, as the disc cutter penetrates the rock, it creates a crushed zone under a disc cutter; then this zone transfers of stresses applied by disc into the rock medium to initiate the crack. The spacing between joints occurring in a rock mass has a great influence on the chip forming process. The role of joint spacing on rock fragmentation under cutter action has been studied by many researchers (Sanio, 1985; Sato et al. 1991; Yagiz, 2002; Gong and Zhao, 2009; Thuro and Plinninger, 2006) by means of field tests, laboratory tests (e.g. indentation test) and numerical simulation methods.

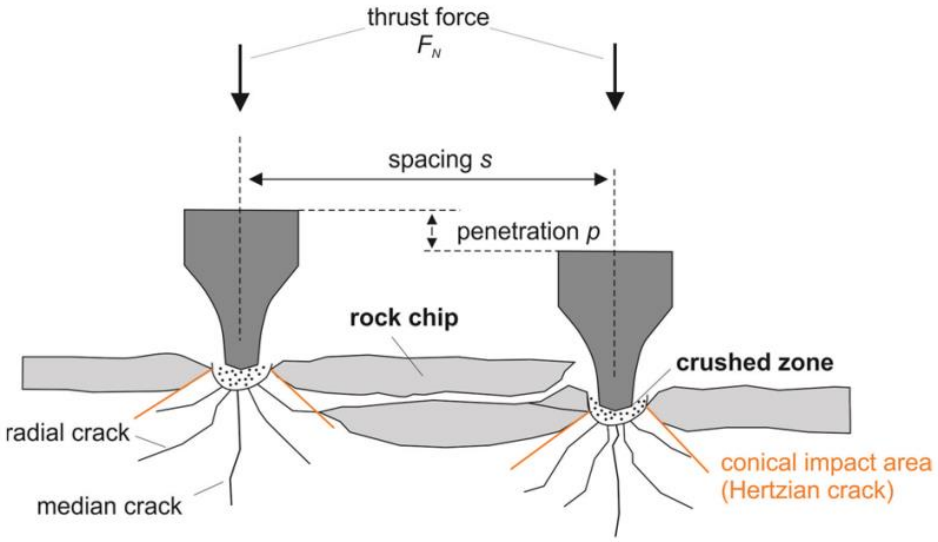

Figure 2.6. Schematic figure of the fragmentation process during rock excavation with disc cutters (Rostami, 1997; Wilfing 2016)

2.3. TBM Performance Parameters

In common, the penetration rate, advance rate, utilization and cutter wear are used to evaluate the TBM performance; however, field penetration rate is also another parameter that can be used for the aim. Main TBM performance parameters utilized to estimate the machine performance in the literature as follow:

The rate of penetration (ROP) or penetration rate (PR) is defined as the excavated length in a continuous phase during the effective boring time; it represents net penetration. This time does not consider TBM maintenance, excavation stop for reinforcement or support element.

$$\mathrm{ROP} = \frac{L_e}{T_e} \tag{2.1}$$

Where L_e is the excavated length and T_e is the effective boring time. ROP is usually expressed as meter/ hour.

In addition, ROP can be computed based on the distance bored per cutter head revolution; it is defined as an instantaneous penetration or the basic penetration rate (Bruland, 1998). Penetration per cutter head revolution, P_{rev}, can be used to investigate the mechanics of rock cutting as:

$$P_{rev} = \frac{1000 \cdot ROP}{60 \cdot RPM} \tag{2.2}$$

Where P_{rev} is penetration per revolution of cutterhead in mm/rev, and RPM is the rate of cutterhead revolutions per minute.

The advance rate (AR), is the ratio between excavated length and total time, which includes the time necessary to bore, to install supports and lining, the time needed for the TBM ordinary and extraordinary maintenance.

$$AR = \frac{L_e}{T_t} \tag{2.3}$$

Where L_e is the excavated length and T_t is the total time essential to do all the required operation. AR is usually expressed as meter/ hour.

Utilization (U), which is the ratio between AR and ROP and expressed as percentage (%). In stable rock mass condition, the AR is considerably lower than the ROP and U ranges from 30-50% due to machine daily maintenance.

$$U = \frac{AR}{ROP} \tag{2.4}$$

The field penetration index, FPI, (Nelson, et al. 1983; Tarkoy and Marconi, 1991; Klein, et al. 1995; Hassanpour, et al. 2011) is the ratio between the total force acting on each cutter and the penetration rate per revolution. It represents the force necessary to obtain a determinate penetration during a single individual disc revolution.

$$FPI = \frac{F_n}{ROP_{rev}} \quad (2.5)$$

Where, F_n is the force acting on each cutter. It can be expressed as kN/cutter/mm/rev

Specific penetration (SP) also represents the performance parameters and it is the inverse of FPI. It can be calculated as:

$$SP = \frac{ROP_{rev}}{F_n} \quad (2.6)$$

Where, SP is measured in mm/rev/kN/cutter acting on each cutter. It is introduced by Alber (2000) with the aim of combining the cutter force and cutter head revaluation.

The specific excavation rate (SER), was developed by Stevenson (1999) to combine the specific penetration and the tunnel cross area, in fact it can be calculated as the ratio between the excavated volume per each cutterhead revolution and the force per cutter.

$$SER = A \cdot SP \quad (2.7)$$

Where, A is the cross-section area of the tunnel. SER is measured in $(m^3/rev)/(kN/cutter)$.

2.4. Factors Influencing the TBM performance

During the rock excavation process, many factors affect TBM performance Table 2.2 where listed the important factors. Some factors directly and some of them indirectly influence the rate of penetration.

Table 2.2. Factors influencing TBM performance (Modified from Blindheim, 1979; Salimi, 2021)

Geological/Geotechnical	Machine and Operation	Organization
Rock material properties	TBM specifications	Work arrangements
• Strength: compressive, tensile, shear • Crushing strength • Rock toughness • Elasticity, rebound, hardness • Anisotropy • Porosity • Abrasivity •	• Thrust, net and total including friction • RPM, rolling speed • Torque capacity, installed and usable power • Number diameter, edge width, material • Cutterhead diameter, shape, and stiffness • Cutter change mode: front or back-loaded • Re-gripping principle: thrust on walls/roof or on segmented lining	• Available hours, work regulations • Shift schedule, buffer time • Crew organization authority of shift bosses, autonomous groups • Crew training and experience • Crew remuneration, bonus system
Rock Mass Features	Operation	Services
• Type of weakness planes; joints, fissures, partings, bedding planes • Spacing orientation and persistence	• Thrust and Torque • Utilization • Steering friction • Cutter change sequence	• Electricity, water etc. • Ventilation, cooling
Ground Conditions & Controls	Backup System	Safety
• Mixed face condition • Rock stresses • Fault zones • Groundwater • Gas • Water control measurement • Rock support measurement • Lining	• Transportation system for mucking and supplies	• Dust Control • Fire control • Light, vibrations, noise

Net penetration is influenced mainly by rock material and rock mass properties and machine parameters such as thrust and cutter spacing. The most important parameters with major impact on TBM penetration ca be classified as; Intact rock properties, rock mass properties, ground condition along the tunnel alignment and machine characteristics (power, thrust, torque, shape and disc of disc cutters). Further, Site management and logistics mainly influences utilization of TBM.

2.4.1. Intact Rock Properties

One of the most influencing parameters is the rock strength; generally, when it increases the penetration decreases and the thrust required to guarantee a penetration is high (Yagiz, 2008; Gong and Zhao, 2009; Hamidi, et al. 2010; Fatemi, 2018; Armetti, et al. 2018). Rock material strength is used as an important parameter in many rock classification systems as well as predicting boreability and drillability of rock (Yagiz, 2002; Salimi, 2021). Hence, the Uniaxial Compressive Strength of rock (UCS) is one of the most important engineering properties of rocks. It should be noted that, prediction models relying only on the UCS of intact rock may provide inaccurate results, since TBM performance is a non-linear function of multiple variables including rock material and rock mass properties and TBM specifications (Yazitova et al. 2025). Tensile strength is another common rock strength property used in making boreability predictions. Brazilian Tensile Strength (BTS) is generally intended to provide an indication of rock brittleness from a viewpoint of crack propagation between adjacent cutter paths (Yagiz, 2008).

As result, the UCS of rock was used to describe the rock crushing beneath the cutter tip while the tensile strength accounted for the chip formation between adjacent cuts (Rostami, 2016). It is remarkable that, great attention should be paid how to the sample failed during UCS or BTS testing whether structural or non-structural failure. Those samples, which were observed to fail along with existing rock defects, such as

joints, fractures, bedding, or foliation, must be classified as a structural failure otherwise should be noted as non-structural failure.

Another rock property, which affects rock boreability is the brittleness that is a highly desirable feature of the rock. In general, the rock cutting efficiency of any mechanical tool improves with increasing brittleness exhibited by the rock formation. Even though brittleness is one of the necessary properties of rock, there is no agreement in the engineering rock mechanics community to describe or measure it. There are several different methods used for the determination of rock brittleness; however, two common methods include the Punch penetration test (Gertsch, 2000; Yagiz, 2009; Yagiz, et al. 2020) and Brittleness value, S_{20} (Bruland, 1998) were found to influence the boreability of rock when assessing TBM performance (Gong and Zhao 2007; Yagiz, 2002, 2009; Altindag, 2010). Also, using difference alternatives of the ratio of UCS to BTS, the brittleness of rock has been estimated (Hucka and Das, 1984; Altindag, 2010). Among these rock brittleness approaches, Yagiz (2009) and Altindag (2010) were classified in the literature and useful for examining the rock boreability. Further, couple index properties of rock including density and porosity are also important parameters to defined the failure behavior of rock under the compression. More it is known that both these indices are related to brittleness of rock (Yagiz, et al. 2020).

2.4.2. Rock Mass Properties

The characteristic of the rock mass features and conditions is of major influence for examining the penetration rate of TBM. Rock mass properties are heavily influenced by the rock fabric which is described by discontinuity or cleavage characteristics in the field. Joints, faults, folding, bedding, foliation and any other weakness zone of the rock mass should be considered to examine the TBM performance by quantified features of discontinuities. Main aspect is the orientation of joints, fissures and faults relative to the

direction of tunnel advance herein. The parameter includes the strike direction and the dipping angle of discontinuities and also the distance between these planes of weakness must be considered. Besides rock mass characteristics, also the primary state of stress and the water inflow within the rock mass influence the performance of tunnel boring machines. However, these parameters have not yet been investigated adequately and are until now not implemented into prediction models (Wilfing, 2016). The main characteristics of rock mass that have a significant influence on TBM performance include:

• ***Discontinuity spacing*** that is the most significant rock mass property which has a undoubtfully great role to play on TBM performance. It is easy to realize that discontinuity and its feature can facilitate rock breakage because cracks induced by disc cutters easily develop along the existing discontinuities as compared to extending across the grains (Salimi, 2021). Rock quality designation-RQD (Deer, et al. 1969), Volumetric joints (Palmstrom, 1995), Joint spacing (Js) are three frequently used parameters to describe the discontinuity spacing (Khosravi et al. 2021). Yagiz (2002) also utilized orientation and spacing of fracture to adjust the CSM model basic penetration. The past investigations by the Norwegian University of Science and Technology (NTNU), decreasing joint spacing means the fracture factor (K_s) increases which has a direct impact and leads to an increased penetration rate of TBM (Bruland, 1998) as shown at Table 2.3. Barton (2000) in the Q_{TBM} model, used modified RQD, namely RQD_o (it must be oriented in the tunneling direction) for predicting TBM penetration. The RQD_o has a direct relationship with Q_{TBM} and an inverse relationship with the ROP. Recently, Yagiz, et al. (2024a, b) and Yazitova, et al. (2925) introduced rock fracture index and weighted fracture index to quantify the frequency of fractures in unit length of the excavated tunnel. Yazitova, et al. (2025) stated that rock fractures including faults, joint, foliation, crack

can be quantified as inverse of spacing between the discontinuities in rock mass as number of joints per meter along the tunnel alignment. They named as rock fracture index (FI) and then multiplying the FI with excavated length of the rock is named as weighed fracture index (WFI) as will be discussed further in this thesis.

Table 2.3. Fractures classes with distance between planes of weakness (Bruland, 1998)

Fracture Class (joints, fissures)	Distance between Plane of Weakness (mm)
0	-
0-I	1600
I-	800
I	400
II	200
III	100
IV	50

• ***Joint orientation relative to tunnel axis***: In foliated, jointed rock, foliation or any other discontinuities can play an important role in rock fracture propagation between cuts, depending on the orientation of discontinuities with respect to the direction of machine advance. The influence of the joint orientation on TBM penetration rate is widely observed in tunneling projects. Wanner (1975) and Aeberli & Wanner (1978) observed that, the advance rate of TBM increases with the increase of the angle between the TBM axis and the planes of schistosity in a homogeneous zone of schistose phyllite. Yagiz (2002, 2008) observed that the angle between plane of weakness and the TBM driven direction (so called alpha angle) influence the TBM performance. As the angle (α) increases the penetration rate increases until reaches to 55-60°, then the ROP decreases with the increase of α till 90 degrees (Figure 2.7).

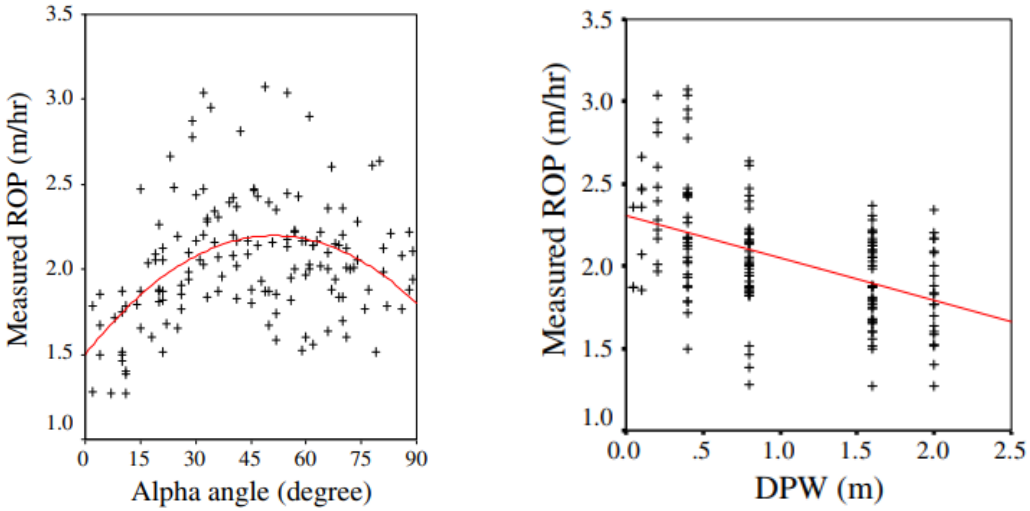

a) Relations between Alpha and ROP b) Relations between the DPW and ROP

Figure 2.7. Effect of joint orientation and distance between the pane of weakness (DPW) on TBM penetration rate (Yagiz, 2008)

Gong et al. (2005) simulated effects of joint orientation on rock fragmentation by TBM cutters with series of two-dimension numerical modelling using the discrete element method (DEM-UDEC). They also stated the maximum TBM penetration is obtained when the alpha reaches at 60 degrees.

2.4.3. TBM Parameters and Specifications

The TBM specifications, such as thrust and power are the key to provide a sufficient amount of forces and torque to support the excavation operation. TBM thrust provides enough force to efficiently penetrate the rock mass. Also, the cutterhead torque and power enable the head to rotate at a designated penetration rate to overcome the rolling resistance. Generally, tougher rocks with less fractures and joints require more thrust and relatively low torque/power (due to low penetration), compared to soft/jointed rock where low thrust and high torque are expected (as a result of high penetration) (Salami, 2021). Cutter parameters (type, profile, material, tip width, and diameter) have a great influence on TBM performance. In particular, Roxborough and Phillips (1975)

and Bilgin et al. (2013) declared that larger cutters require higher thrust to obtain the same ROP for a rock mass, being disc-rock contact area larger. The thrust capacity increases when cutter diameter increases and, as a consequence, the ROP.

2.5. Existing TBM Performance Prediction Models

Accurate estimation of both TBM penetration is of crucial significance for the successful completion of the mechanized excavation projects. It mainly includes the determination of the rock cutting force and efficiency under different cutter penetration depth and the determination of the optimum rock boring/cutting condition as well as tool consumption; however, this thesis focusses on the aspect of penetration prediction for hard rock tunnel boring machines. From past to present, many TBM performance estimation models are introduced (Graham 1976; Ozdemir 1977; Farmer and Glossop, 1980; Snowdon et al. 1982; Gehring, 1995; Rostami, 1997; Bruland, 2000; Barton, 2000; Yagiz 2002; Hassanpour, 2011; Wilfing 2014; Macias 2016; Yagiz 2008; Farrokh, et al. 2012; She et al. 2024) as summarized in Table 2.4.

Among those models, some are only based on simple one laboratory test and some based on practical tunnel construction data. Generally speaking, laboratory rock cutting tests on rock block are necessary, but they neither give a full picture of rock mass nor represent the full-scale operation of the TBM. A realistic prediction model should combine the laboratory tests data and site geological and rock mass conditions in the construction area. During the early period of TBM tunnelling and mechanized excavation, some simple empirical equations were developed from data on rock strength tests and force acting on a disc (Graham, 1976; Farmer and Glossop, 1980; Nelson, 1983; Huges, 1986).

Table 2.4. Summary of empirical equations developed for estimating the TBM penetration rate in the literature (Yazitova et al. 2025)

References	Equations	Inputs	Outputs
Grahan (1976)	$P_{rev} = 3940 \cdot F_n/\sigma_c$	F_n, σ_c	P_{rev}
Farmer and Glossop (1980)	$P_{rev} = 624 \cdot F_n/\sigma_c$	F_n, σ_c	P_{rev}
Cassinelli et al. (1982)	$ROP = -0.0059RSR + 1.59$	RSR	PR
Hughes (1986)	$ROP = 1.667 \cdot (F_n/\sigma_c)^{1.2} \cdot (2/d)^{0.6}$	F_n, σ_c, d	PR
Innaurato et al. (1991)	$ROP = {\sigma_c}^{-0.437} - 0.047 \cdot RSR + 3.15$	σ_c, RSR	PR
Rostami and Ozdemir (1993)	$ROP = (F_n, \sigma_c, \sigma_t, rpm, s, T, R, \emptyset)$	$F_n, \sigma_c, \sigma_t, rpm, s, T, R, \emptyset$	PR
Gehring (1995)	$ROP = 4 \cdot \frac{F_n}{\sigma_c}$	F_n, σ_c	P_{rev}
NTNU (Bruland, 1998)	$ROP = (f_n, \sigma_c, J_c, RPM, S, d, q, \alpha)$	f_n, σ_c, J_c, RPM, S, d, q, α	PR
Q_{TBM}(Barton, 1999)	$ROP = 5 \cdot {Q_{TBM}}^{-0.2}$; $Q_{TBM} = 5Q \cdot \gamma \cdot \sqrt[3]{Q \cdot \sigma_c/100/F_n}$	Q_{TBM}, Q, γ, σ_c, F_n	PR
Bieniawski et al. (2007)	$ARA_T = 0.324 \cdot RME - 6.8$ If UCS $\leq$ 45 MPa $ARA_T = 0.839 \cdot RME - 40.8$ If UCS $>$ 45 MPa	RME, UCS range	AR
Yagiz (2008)	$ROP = 1.039 + 0.028 \cdot BI - 0.003 \cdot \sigma_c + 0.437 \cdot \log(a) - 0.219 \cdot DPW$	Bi, σ_c, α, DPW	PR
Yagiz et al. (2009)	$ROP = -0.139UCS + 0.594BI - 0.234DPW + 0.634\alpha^{0.205} + 0.076$	UCS, BI, DPW, α	PR

Hassanpour et al. (2011)	$\mathrm{FPI} = \mathrm{Exp}(0.008 \cdot \mathrm{UCS} + 0.015 \cdot \mathrm{RQD} + 1.384)$	UCS, RQD	FPI
Farrokh et al. (2012)	$\mathrm{P_{rev}} = \exp(0.41 + 0.404\mathrm{D} - 0.027\mathrm{D}^2 + 0.0691\mathrm{RT_c} - 0.00431\sigma_c + 0.09\mathrm{RQD} + 0.0893\mathrm{F_n})$	$\mathrm{D}, \mathrm{RT_c}, \sigma_c,$ $\mathrm{RQD}, \mathrm{F_n}$	$\mathrm{P_{rev}}$
Oraee et.al. (2012)	$\mathrm{ROP} = 2.581 - 0.033 \cdot \mathrm{UCS} + 0.069 \cdot \mathrm{RQD} - 0.176 \cdot \mathrm{DPW} + 0.001\mathrm{UCS}^2 - 0.008\mathrm{RQD}^2$	UCS, RQD, DPW	PR
Rayatdust et.al. (2012)	$\mathrm{ROP} = -0.012 \cdot \mathrm{UCS} + 0.042\mathrm{J_v} + 0.01\alpha + 2.39$	$\mathrm{UCS}, \mathrm{J_v}, \alpha$	PR
Salimi and Esmaeili (2013)	$\mathrm{ROP} = -4.316 + 0.05\sigma_c + 0.05\sigma_t + 0.183\mathrm{PSI} - 0.005\alpha - 0.79\mathrm{DPW}$	$\sigma_c, \sigma_t, \mathrm{PSI},$ α, DPW	PR
Torabi et al. (2013)	$\mathrm{ROP} = 21.659 - 0.042\mathrm{UCS} - 0.545\mathrm{c} - 0.166\varphi - 31.261\nu$	$\mathrm{UCS}, \mathrm{C},$ φ, ν	PR
Benato and Oreste (2015)	$\mathrm{P_{rev}} = 5/8 \cdot [(\mathrm{F_n} - 14) \cdot (0.0132 - 0.00009\sigma_c) \cdot (100 - \mathrm{GSI})^2]$	$(\mathrm{F_n}, \sigma_c, \mathrm{GSI}$	$\mathrm{P_{rev}}$
Goodarzi et.al. (2021)	$\mathrm{ROP} = \exp(0.006\mathrm{F_n} - 0.016\sigma_c + 1.833)$	$\mathrm{F_n}, \sigma_c$	PR
Pourhashemi et al. (2021)	$\mathrm{P_{rev}} = 1.98 + 0.035\mathrm{F_n} - 0.03\sigma_c - 0.011\mathrm{GSI}$	$\mathrm{F_n}, \sigma_c, \mathrm{GSI}$	$\mathrm{P_{rev}}$
Xu et al. (2021)	$\mathrm{P_{rev}} = 16.888 - 0.025\sigma_c - 108243\mathrm{K_v}$	$\sigma_c, \mathrm{K_v}$	$\mathrm{P_{rev}}$

Note: ROP, penetration rate (m/h); P_{rev}, penetration per revolution (mm/rev); RPM, cutterhead rotation speed (rev/min); F_n, cutter normal force (kN/cutter); σ_c, uniaxial compressive strength of intact rock (MPa); σ_t, tensile strength of intact rock (MPa); BI, brittleness index; D, tunnel diameter (m); d, cutter diameter (m); RQD, rock quality designation; RMR, rock mass rating; RSR, rock structure rating; Q, rock mass quality rating; Q_{TBM}, rock mass quality rating for TBM driven tunnels; GSI, geological strength index; α, the angle between the tunnel axis and the joint plane; J_s, joint spacing; J_c, RMR joint condition partial rating; RME, Rock Mass Excavability; J_v, volumetric joint count; DPW, distance between the plane of weakness; PSI, peak slope index from punch penetration test; RT_c, artificial rock type code; q, quartz content; γ, rock unit weight (N/m^3); $\boldsymbol{\nu}$, Poisson's ratio; K_v, the intactness index of rock mass; DRI, rock drillability index; c, cohesion; NTNU, Norwegian University of Science and Technology.

Later on, numerous TBM performance prediction models developed based on theory, laboratory test and field data. In the followings, common TBM performance prediction models used for estimating the TBM performance by means of the ROP is discussed briefly for the sake of the research. In the beginning of mid of 1970's up to present, numerous simple and also multivariable equations and models were developed from data related to rock properties and TBM parameters as given in Table 2.4. The commonly utilized equations are briefly introduced as below from simplest to the complex models for the aim of the research:

2.5.1. Simple Models

Graham (1976) derived a prediction equation based on a predominantly hard rock (uniaxial compressive strength from 140 to 200 MPa) database.

$$\mathrm{PR_{rev}} = 624 \cdot \frac{\mathrm{F_n}}{\mathrm{UCS}} \tag{2.8}$$

Where, F_n and UCS refers to individual cutter thrust per cutter (kN/cutter) and uniaxial compressive strength (MPa) of rocks to obtained the rate of penetration (PR_{rev}) in mm per revolution.

Farmer and Glossop (1980) established dataset to derive the equations base on sedimentary rocks.

$$\mathrm{PR_{rev}} = 64 \cdot \frac{\mathrm{F_n}}{\mathrm{BTS}} \tag{2.9}$$

Where, F_n and BTS refers to individual cutter thrust per cutter (kN/cutter) and Brazilian tensile strength (MPa) of rocks to obtained the rate of penetration (PR_{rev}) in mm per revolution.

Nelson et al. (1983) derived an equation from a comprehensive study on TBM

performance in sedimentary rocks such as shale, lime and sandstones.

$$R_f = 5.95 + 0.18 \cdot H_t \tag{2.10}$$

Where, R_f and H_t refers to field penetration index (kN/cuter/mm/revolution) and total hardness, which is the product of the rebound hardness (Schmitt hammer) and square root of the abrasion hardness.

2.5.2. CSM Models (1977, 1993, 2002)

This model is the most famous semi-theoretical model developed by the Colorado School of Mines (CSM) approaches. The first version of the CSM model was developed by Ozdemir (1977) and also Ozdemir et al. (1978) using shear failure for performance prediction of V–shape disc cutters. After that, the model was updated by Rostami and Ozdemir (1993) and Rostami (1997) to predict the rock cutting force requirement of constant cross section (CCS) disc cutters at a given cut spacing and depth of penetration in a rock of known properties based on tensile failure. In fact, the CSM model estimates the individual cutter forces and consequently cutterhead thrust for a given penetration (mm/rev), based on rock properties including UCS and BTS of intact rock, and CCS disc cutter and cutting geometry. The formula can be used to estimate rock cutting forces for a given penetration accordingly maximum obtainable penetration for a given set of TBM and CCS cutter specifications in a given rock, through iterations. A large database of full-scale linear cutting machine (LCM) tests performed on rock samples in the CSM laboratory were used for development of the CSM model. Obviously, the LCM tests which were conducted on the rock block obtained from the field have proven to have some shortcomings when it comes to simulating rock mass conditions in the field, especially where the TBM performance is greatly influenced by joints and discontinuities

of rock mass. Based on the assumption and deduced functions by Rostami (1997), the total estimated resultant cutting force demonstrated in Figure 2.8 was derived as follows:

$$F_t = C \cdot T \cdot R \cdot \phi \cdot \left(\frac{\sigma_c^2 \cdot \sigma_t \cdot S)}{\phi \cdot \sqrt{R \cdot T}}\right)^{1/3} \quad (2.12)$$

Where, F_t – total forces applying on disc (N); C – constant value (2.12); R – cutter radius; σ_c – uniaxial compressive strength (MPa);ϕ – angle of the area of contact (rad); σ_t-tensile strength (MPa); S – cut spacing (mm). The angle of the area can be calculated using the following equation 2.13:

$$\phi = \cos^{-1}\left(\frac{R-p}{R}\right) \quad (2.13)$$

Where, p = penetration of cutter (mm/rev)

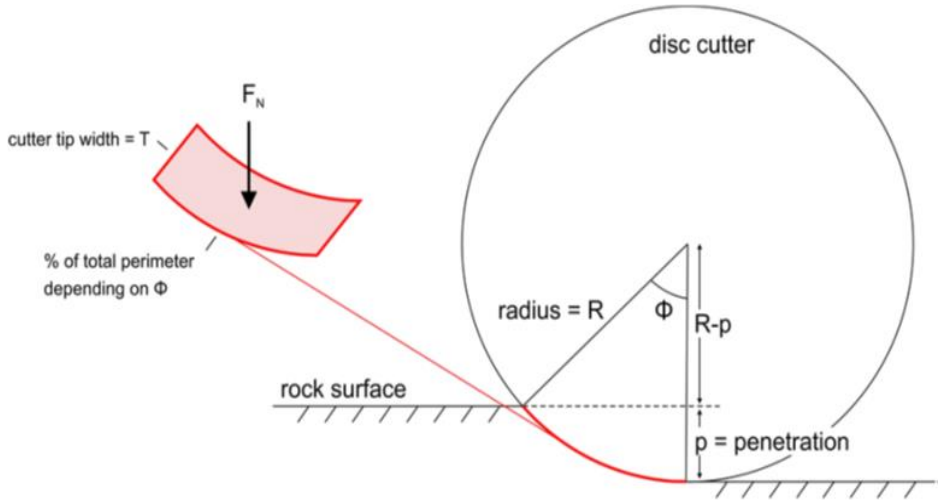

Figure 2.8. Diagram showing the interface region between disk cutter and rock (Rostami, 1997)

$$F_n = F_t \cdot \mathrm{Cos}\left(\frac{\phi}{2}\right) \quad (2.14)$$

$$F_r = F_t \cdot \mathrm{Sin}\left(\frac{\phi}{2}\right) \quad (2.15)$$

Where F_n is normal force and F_r is rolling force for individual cutters. This assumes of uniform pressure distribution $\beta = \phi/2$, angle of the resultant force from the normal) in the contact area, which has been proved to be true (Rostami, 2008).

It is clear that the CSM model prediction based on intact rock strength (UCS and BTS) was not counting the influence of discontinuities on TBM penetration. The CSM model (1997) does not systematically incorporate rock mass fracturing in the prediction model, but later some modifications have been offered for considering the effect of rock mass conditions for the prediction of TBM performance by Yagiz (2002).

Yagiz (2002) developed a Modified CSM model (MCSM) to include the effect of rock mass fracture as a function of alpha, which is the angle between plane of weakness and TBM driven direction, and spacing between the fractures and brittleness to the basic prediction formula of Rostami and Ozdemir (Wilfing, 2016). The MCSM model is based on data from a 16 km long tunnel project where the author conducted geological mapping with a special focus on joint record, laboratory testing, and TBM field data analysis. The research results in the implementation of three more parameters to consider rock mass characteristics: fracture spacing (Fs), orientation of discontinuities, and rock brittleness. For a quantitate description of discontinuities, Yagiz combined Fs and angle (α), to develop the rock fracture index (RFI). The rock brittleness index (BI) is determined by the peak slope (P_s) measured by the punch penetration test (Eq. 2.16-2.17). Consequently, he proposed equation for predicting the ROP via MCSM model as a function of adjustment indices (RFI, BI) and CSM basic penetration ($CSM_{b\text{-}rop}$) result as follow:

$$RFI = 1.44 \cdot \log(\alpha) - 0.0187 \cdot F_s \tag{2.16}$$

$$BI = 0.0157 \cdot P_s \tag{2.17}$$

$$\mathrm{ROP} = 0.859 - \mathrm{RFI} + \mathrm{BI} + 0.969 \cdot \mathrm{CSM}_{\mathrm{b-rop}} \quad (2.18)$$

The main weakness for using this model outside the United States is the need of performing punch penetration tests for obtaining the BI. The test is commonly not used in European rock mechanics laboratories which makes the determination of BI complicated; however, Yagiz (2009) proposed conversion formula to provide a solution for this problem as in Eq.2.19.

$$\mathrm{BI} = 0.198 \cdot \sigma_c - 2.174 \cdot \sigma_t + 0.913 \cdot \rho - 3.807 \quad (2.19)$$

Where, σ_c, σ_t, and ρ refers to Uniaxial compressive strength (MPa), Brazilin tensile strength (MPa) and density of rock in kN/m^3.

2.5.3. Gehring Model (1995)

The prediction model, proposed by Gehring in 1995, is based on information from preceding literature and the author's observations in four cases from Voest-Alpine with a certain TBM setup as: Cutter diameter = 432 mm; Cutter spacing=80mm; and individual cutter force (F_n) = 200kN. From the literature, several curves relating the TBM penetration rate to the intact rock's uniaxial compressive strength have been drawn (Figure 2.9) by applying the mentioned input parameters above.

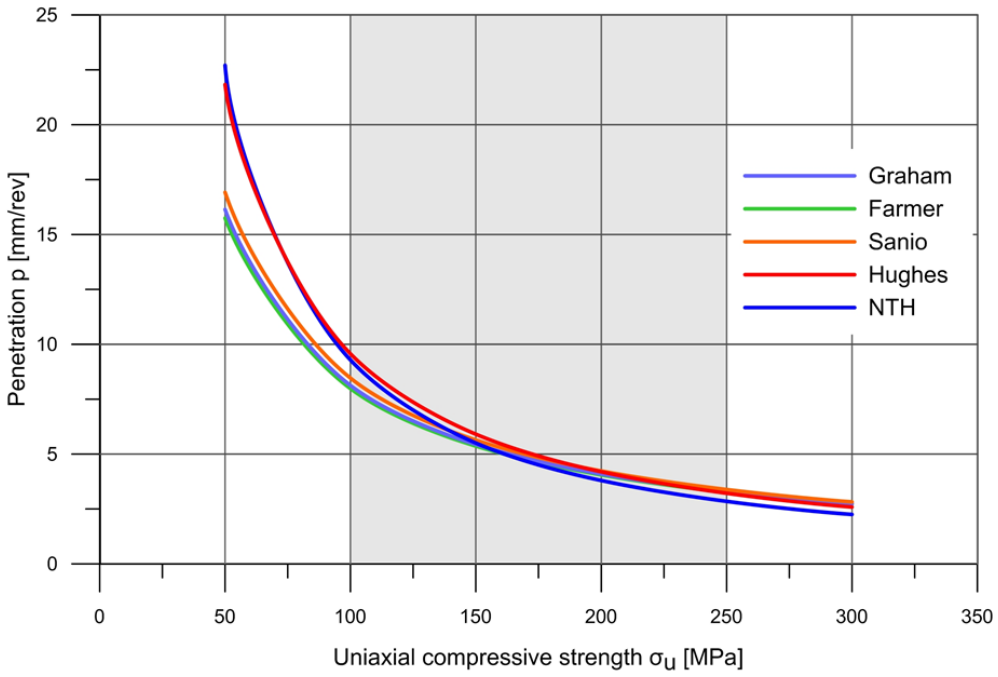

Figure 2.9. TBM basic penetration recalculated from different sources (Gehring, 1995)

The final result is the maximum penetration for a certain normal force (such as 200kN) per cutter. The formula has a modular structure and a simple linear function with independent correction factors that allow the consideration of rock mass properties, as well as different cutterhead types and geometries (Eq. 2.20).

$$\mathrm{ROP} = \frac{\mathrm{F_n}}{\sigma_c} \cdot \mathrm{k_i} \tag{2.20}$$

Where, ROP – penetration rate $(\mathrm{mm/rev})$; $\mathrm{F_n}$ – net thrust per cutter $(\mathrm{kN/cutter})$; σ_c – uniaxial compressive strength (MPa); $\mathrm{k_i}$ – correction factor

A correction factor k_i consist of k_0, k_1, k_2, k_3, k_4 and k_5 correction factors. The description of each correction factor is presented as the following: k_0 – basic penetration; k_1 – specific failure power; k_2 – rock mass material; k_3 – state of stress in rock mass; k_4 – cutter diameters; k_5 – cutter spacing.

Wilfing (2016) has modified the Gehring model (1995), called 'Alpine Model' for estimating the ROP. This approach introduces a new parameter named 'y-intercept BTS or LBC approach' in the original equation (Gehring, 1995) to assess the relation between the applied force (F_n) and resulting ROP in hard rock tunnel boring. The new parameter depends on the LCPC (Laboratoire central des Ponts et Chaussées) breakability coefficient (LBC) and the Brazilian tensile strength.

2.5.4. NTNU Model (1970, 1988, 1998, 2016)

The NTNU model has been originally introduced in the later 1970s (Johannessen, 1976; Blindheim, 1979; Lislerud, 1988, 1997) and continuously revised and improved, as new tunneling data and TBM modifications become available. The 1998 version of the NTNU model (Bruland, 1998) is based on data more than 200 km of bored tunnels mostly in Norway. Contrary to many other models the uniaxial compressive strength is not considered as a significant factor in this model but fracturing degree of rocks. In fact, the boreability is expressed by drilling rate index DRI, which is a combination of rock brittleness value (S_{20}) and Siever's miniature drill test (Sj). The Sj value expresses rock surface hardness while the S_{20}-value includes the effect of rock brittleness and therefore grain size and grain boundary strength. Input parameters of this model can be divided into two main groups including rock/rock mass parameters, and machine parameters. These parameters also depend on various individual factors related to rock mass and TBM parameters. In fact, among the all rock properties, the degree of fracturing is the most important penetration parameters for tunnel boring herein. In the NTNU model, all parameters, related to rock mass, represented by Equivalent Fracturing Factor (k_{ekv}), and all machine parameters represented by Equivalent Thrust (M_{ekv}) (kN/cutter). Then;

$$i_0 = \left(\frac{M_{ekv}}{M_1}\right)^b \quad (2.21)$$

Where, i_0, main penetration rate (mm/rev); b, penetration coefficient; M_{ekv}, equivalent thrust per cutter (kN/cutter), M_1, critical thrust for 1mm/rev penetration (kN/cutter).

The term of equivalent thrust per cutter (M_{ekv}), characterizes the influence of TBM parameters on the ROP and includes gross average cutter thrust, cutter diameter and cutter spacing. Parameters M_1 and b are highly influenced by the factor k_{ekv}, which describes rock and rock mass properties such as spacing and orientation of discontinuities, drillability and porosity of the rock material (Bruland, 1998).

The obtained ROP in mm/rev could be converted to meter per hour as follow:

$$i_0 = i_0 \cdot RPM \cdot \left(\frac{60}{1000}\right) \quad \text{(m/h)} \quad (2.22)$$

Lastly, Macias (2016) revised the NTNU model. The update includes data from new projects, which increases the empirical basis of the data. Macias (2016) updated the fracture classification, classifying both joints and fissures; he also proposed the cutterhead velocity (RPM) correction factor. The optimal cutterhead velocity appears to be influenced by rock drillability, rock mass fracturing, and/or thrust level. Low values of and applied cutter thrust indicate a lower optimal cutterhead velocity (Macias, 2016; Wilfing 2016; Salimi, 2021). The updated formula is presented herein:

$$i_0 = i_0 \cdot RPM \cdot \left(\frac{60}{1000}\right) \cdot k_{rpm} \ \text{(m/h)} \quad (2.23)$$

2.5.5. Barton Model (2000)

Based on the well-known Q-system (rock mass Quality) and data from 145 tunnels totaling more than 1000 km in length, Barton (1999, 2000) modified the Q-system into Q_{TBM} to predict TBM performance. The Q_{TBM} adds some new parameters

that take the interaction between TBM and rock mass into consideration. The components of Q_{TBM} are as follows:

$$Q_{TBM} = \frac{RQD_0}{J_n} \cdot \frac{J_r}{J_a} \cdot \frac{J_w}{SRF} \cdot \frac{SIGMA}{\frac{F^{10}}{20^9}} \cdot \frac{20}{CLI} \cdot \frac{q}{20} \cdot \frac{\sigma_\theta}{5} \quad (2.24)$$

Where, $\frac{RQD_0}{J_n} \cdot \frac{J_r}{J_a} \cdot \frac{J_w}{SRF} = Q_0$; SIGMA – rock mass strength which can be divided by favorable/unfavorable inclination values; F – net thrust per cutter $(tnf/cutter)$; CLI – cutter life index; q – quartz content (%); σ_θ – biaxial stress (MPa).

An estimation of net penetration rate based on Q_{TBM} is presented in Eq. (2.25); further, the relationship between PR (m/hr), AR (m/hr), and Q_{TBM} is shown in Figure 2.10.

$$NPR \approx 5 \cdot Q_{TBM}^{-1/5} \quad (2.25)$$

Where, NPR – net penetration rate (m/h).

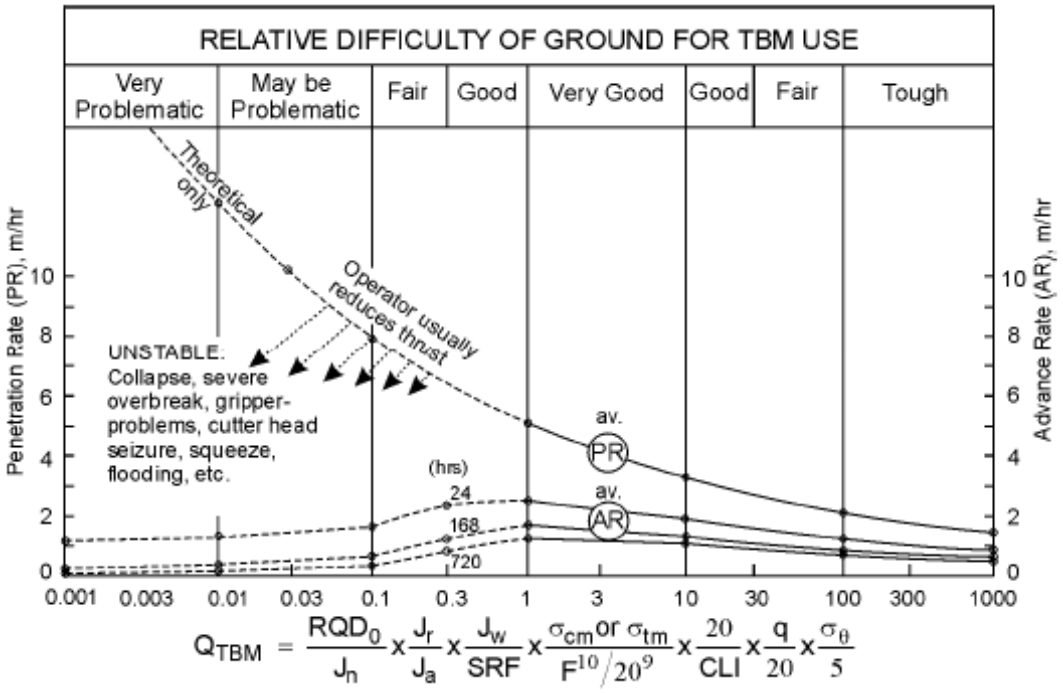

Figure 2.10. Suggested relations between the ROP, AR, and Q_{TBM} (Barton, 2000)

(2016) stated that the concepts behind this Q_{TBM} approach steps in the right direction, but the technical implementation is complicated and expensive. In sum, this model based on Q_{TBM} did not gain acceptance in the construction industry out of Norway since it contains numerous inputs, obtaining those inputs are commonly not easy in practice. Also, some of the laboratory tests such as cutter life index (CLI) and drilling index (DRI).

2.5.6. Bieniawski et al (2006, 2007, 2008)

Bieniawski, et al. (2006) developed Rock Mass Excavatability (RME) model which is similar to the RMR classification system to estimate performance of double-shield and open-type TBMs via advanced rate theoretically (ARA_T). The RME input parameters are included drillability, stand-up time, UCS of intact rock, groundwater inflow, and discontinuities at the excavation front. The RME is computed using the mentioned input variables with their ratings (Table 2.5). The sum of the ratings of the RME parameters varies between 0 and 100 points and it is expected that the higher the RME value, the easier the excavation of the tunnel; consequently, achieving the highest production rate via the ROP. Further information related to RME model can be found in the literature (e.g., Bieniawski, et al. 2007). To predict theoretical average rate of advance (ARA_T), Bieniawski, et al. (2008) proposed several equations for open TBM (Eq.2.26) and double shield TBMs (Eq.2.27) respectively using RME as below:

$$ARA_T = 0.324 \cdot RME - 6.8 \quad \text{If UCS} \leq 45 \text{ MPa} \tag{2.26}$$

$$ARA_T = 0.839 \cdot RME - 40.8 \quad \text{If UCS} > 45 \text{ MPa}$$

$$ARA_T = 0.661 \cdot RME - 20.4 \quad \text{If UCS} \leq 45 \text{ MPa} \tag{2.27}$$

$$ARA_T = 0.422 \cdot RME - 11.6 \quad \text{If UCS} > 45 \text{ MPa}$$

Table 2.5. The ratings for RME input parameters (Bieniawski et al. 2007)

Uniaxial Compressive Strength of intact rock [0-25]									
σ_c (MPa)	<5	5-30	30-90	90-180	>180				
Rating	4	14	25	14	0				
Drillability – Drilling Rate Index [0-15]									
DRI	<80	80-65	65-50	50-40	<40				
Rating	15	10	7	3	0				
Discontinuities in front of the tunnel face [0-30 points]									
Homogeneity		Number of joints per meter					Orientation with respect to tunnel axis		
Homogeneous	Mixed	0-4	4-8	8-15	15-30	>30	Perpendicular	Oblique	Parallel
Rating 10	0	2	7	15	10	0	5	3	0
Stand up time for TBM excavated tunnels [0-25 points]									
Hours	<5	5-24	24-96	96-192	>192				
Rating	0	2	10	15	25				
Groundwater inflow [0-5 points]									
Litre/sec	>100	70-100	30-70	10-30	<10				
Rating	0	1	2	4	5				

2.5.7. Yagiz (2008)

Yagiz (2008) developed TBM performance prediction model for hard rock mass rock condition using very detail and strong database obtained from Queens Fresh Water tunnel in 16km in New York City USA. The database composed of intact rock properties (such as UCS and BTS, Brittleness), rock mass properties including orientations and frequency of rock fractures with certain TBM set up (refers to TBM used for the Queens Fresh Water Tunnel in section 3.1).

$$\mathrm{ROP} = 1.093 + 0.029 \cdot \mathrm{BI} - 0.003 \cdot \mathrm{UCS} + 0.437 \cdot \log(\alpha) - 0.219 \cdot \mathrm{DPW} \qquad (2.28)$$

where ROP – rate of penetration (m/h); BI – index of brittleness (kN/mm); UCS – uniaxial compressive strength (MPa); α – the angle between the plane of weakness and TBM driven direction (°); DPW - spacing between planes of weakness (m).

Since the punch penetration test that is utilized for obtaining the BI, is commonly used in North America, but not available in many other countries around the world, Yagiz (2009) developed empirical formulate to obtain the BI as a function the UCS, BTS and density of rocks (refer to section 2.5.2). Further, the introduced equation is related to the conditions of Queens Water Tunnel and belonged single unique TBM; hence it can't be a reliable model to predict the performance of the TBM; however, the model is very common to be used in practice due to its simplicity.

2.5.8. Farrokh et al (2012)

Farrokh, et al. (2012) have presented a model based on an analysis of a comprehensive database of more than 200 TBM projects records using multivariable statistical analysis. Multivariate regression was used to evaluate the data records, which included rock mass properties and system parameters, resulting in regression equations that were used to measure the ROP. Equation 2.29 is presented how penetration rate can be calculated based on Farrokh, et al. (2012) mode.

$$PR = \frac{F_n^{0.186} \cdot RQD_c^{0.133} \cdot RT_c^{0.183} \cdot RPM^{0.363} \cdot D^{5.47} \cdot e^{(0.046 \cdot D^2)}}{5.64 \cdot UCS^{0.248} \cdot e^{(1.58 \cdot D)}} \quad (2.29)$$

Where, PR – penetration rate (m/h); F_n – normal force of disc cutter (kN); RQD_C – rock quality designation; RT_c – rock type numerical code; RPM – rotational speed (rev/min); D – diameter of tunnel (m).

They stated that despite that the model is based on data from more than 200 projects, the equation that predicts the PR has a low regression coefficient. Due to the

model's limitations, it is strongly recommended to use this model in combination with other models, especially in more complex project situations (Farrokh et al., 2012).

2.5.9. Hassanpour et al. (2009, 2011, 2016)

Hassanpour, et al. (2009a, b; 2011) developed an empirical TBM performance prediction model via Field penetration index (FPI) based on a database of actual machine performance from different hard rock TBM tunnelling projects in Iran. The database obtained from Iranian tunnels composed of shale, limestone, schist, tuff along the excavated tunnels. The relationship between different intact rock strength (UCS) and rock mass properties (such as, RQD) and cutter force (F_n) is examined to obtain the best correlation among the available parameters to estimate the FPI in kN/c/mm/rev. They recognized the Field Penetration Index (FPI), defined as the ratio between the average individual cutter force (F_n) and the ROP (Barton, 2000; Klein, et al. 1995), as the TBM performance parameter having the best correlation with the observed rock mass conditions; consequently, following equation is proposed:

$$\mathrm{FPI} = \exp(0.008 \cdot \mathrm{UCS} + 0.015 \cdot \mathrm{RQD} + 1.384) \tag{2.30}$$

Where, FPI – field penetration index ($\mathrm{kN/cutter/mm/rev}$) ; UCS – uniaxial compressive strength (MPa); RQD – rock quality designation.

Further, the rate of penetration (ROP) can be calculated by converting FPI to that.

$$\mathrm{ROP} = \frac{0.06 \cdot \mathrm{RPM} \cdot \mathrm{F_n}}{\mathrm{FPI}} \tag{2.31}$$

The formula and associated chart introduced by Hassanpour, et al. (2011) are very applicable/constructive and reflect the practical approach in an early stage of tunnel design and construction, since it has been developed based on two commonly available inputs including, and which are most often available in many tunneling projects around

the world; however, The model must be applied with caution in highly fractured rock masses and water sensitive rocks like marlstones and mudstones (Hassanpour et al., 2011).

2.5.10. Yazitova et al (2025)

Recently, Yazitova, et al. (2025) introduced empirical models for estimating the TBM penetration rate using the big database related to six different tunnel projects around the world. The database including fractured hard rock, magmatic (such as granite, diorite), metamorphic rock (e.g., variety of gneiss, calc-silicate) through the sedimentary rocks including limestone, shale, tuff with the UCS of 20 to 300MPa (refers to chapter 4 in the thesis). Utilizing UCS of intact rock, cutter head diameter (CHD), frequency of fractures via weighted fracture index, WFI (Yagiz, et al. 2024), individual cutter force (F_n) and RPM, TBM performance may be estimated by means of the ROP as follow:

$$\mathrm{ROP} = \frac{\mathrm{F_n^{0.308}} \cdot \mathrm{WFI^{0.136}} \cdot \mathrm{RPM^{-0.027}} \cdot \mathrm{CHD^{2.875}}}{8.211 \cdot \mathrm{UCS^{0.101}} \cdot \mathrm{e^{0.583 \cdot CHD}}} \tag{2.32}$$

In order to develop the model, six TBM tunnels are examined in detail and then database including rock properties and TBM and disc cutter specification are established. After that, more than hundred linear and non-linear multiple regression models were developed, and the best accurate one in terms of statistical indices is suggested herein. It is found that the obtain equation (2.32) is reliable and useful for the TBM projects where the inputs variables are available to compute the ROP. Further, information and explanation for the developed models are available in this thesis.

CHAPTER 3 : CASE STUDIES

In this thesis, the database was established using six different tunnel projects sources, those projects include Queens Water Tunnel USA; Manapouri hydropower tunnel New Zealand; Miryang Dam Tunnel S. Korea and Iranian Water Conveyance Tunnels including Karaj, Zagros and Ghomrood. Each of these tunnels was studied and raw data obtained from the laboratory and fields were also analyzed carefully for the aim. Intact rock, rock mass properties, TBM specification and Constant Cross Section (CCS) disc parameters are given in the database development section or related appendices for the aim of the research. Due to that, rock mass condition, intact rock properties and TBM specifications for each project are introduced in brief as follows.

3.1. The Queens Fresh Water Transfer (QFWT) Tunnel, USA

The Queens Fresh Water Tunnel # 3, stage 2 is intended to improve fresh water distribution throughout the City of New York, USA. The tunnel being about 7.5 km long and 7 m in diameter was excavated beneath Brooklyn and Queens at an average depth of 200 m below the sea level in West-central Queens County with using a high power TBM (Yagiz, 2008). New York City is located at the extreme southern part of the Manhattan schist, a northeast trending, deeply eroded sequence of metamorphosed Proterozoic to Paleozoic rocks into the crystalline terrains of New England (Baskerville and Mose, 1989; Merguerian, 1983, 1996). In construction area, geology is highly complex and composed of different metamorphosed igneous rock with shear zones, joint, faults, and other local weakness zones along the tunnel alignment. Five main geological formations have been identified in the area: Manhattan schist is composed of gray, medium to coarse-grained layered schist and gneiss. The Inwood Formation includes different types of marble units of white coarse-grained calcite–dolomite marble. Hartland Formation mainly consists of gray and gray weathered thinly laminated muscovite–biotite–quartz schist with minor

garnet. The Fordham Gneiss is a highly complex unit that includes black hornblende–biotite gneiss and white quartz plagioclase moderately banded gneiss (Merguerian, 2000). In the construction area, during tectonic orogeny, the Cameron's Line ductile shear zone occurred. This zone is the major tectonic restrict between the Hartland formation and the Manhattan–Inwood–Fordham Sequence (Yagiz, 2008).

In this project, the main beam high power Robbins TBM (235–282) was equipped with both 0.482 m disc cutters and a rated load capacity of 30 tons per disc cutter to excavate the Tunnel. The basic specifications of the TBM are given in Table 3.1. The TBM operational data was analyzed throughout the tunnel, since the TBM specifications (i.e., thrust and power) are very important in providing sufficient amount of force and torque to carry out the excavation operation. In order to monitor the performance of the machine in the field, the TBM was fitted with an automatic state-of-the art data logging and recording system.

Figure 3.1. High Power TBM utilized for the Queens Fresh Water Transfer Tunnel (Yagiz, 2002)

All data derived from the control system of the machine were recorded on a standard personal computer connected to the control system via local connection (Yagiz, 2008). General specification of TBM and disc cutters are given in Figure 3.1. and Table 3.1.

Table 3.1. TBM specification for the Queens Fresh Water Transfer Tunnel

TBM Specification	Queens
Machine type (Open Beam)	Open*
Diameter (m)	7.10
Number of cutters	50
Cutter type	CCS Disc
Individual cutter diameter (mm)	482.6
Cutter tip width (mm)	19.05
Revolution per minutes (RPM)	8.3
Total cutterhead thrust (kN)	16000-18000
Cutter load (kN)	250-300
Field ROP (m/h)	1.89

*Open refers to open type TBM

3.2. Manapouri Second Tail Race Hydropower Tunnel, New Zealand

The Manapouri Second Tailrace Tunnel is a significant hydroelectric infrastructure project in New Zealand, associated with the Manapouri Power Station, one of the country's largest hydroelectric power stations. The tunnel, completed in 2002, was constructed to enhance the efficiency and capacity of the power station by allowing more water to flow from Lake Manapouri through the power station to Deep Cove in Doubtful Sound. This second tunnel complements the original tailrace tunnel and significantly reduces the water pressure on the power station, increasing electricity generation capacity. The project involved extensive engineering, including drilling through hard rock and ensuring environmental sustainability in the ecologically sensitive Fiordland region (Kim, 2004). The geology of the tunnel is characterized by complex and challenging conditions due to the region's location within the Fordland area of New Zealand. The project site includes different types of rock including met-andesite, diorite,

hornblende biotite gneiss, biotite gneiss and calc-silicate gneiss with calc-silicate. In the location, with the presence of faults and fractures together with hard and abrasive rock, the construction of the tunnel was very challenging and it took more than expected to complete the project (Manapouri Project Report 2001; Kim, 2004).

Figure 3.2.TBM utilized for the Manapouri Second Tail Hydropower Tunnel (Kim, 2004)

Table 3.2. TBM specification for Manapouri Second Tail Hydropower Tunnel

TBM Specification	Manapouri
Machine type	Open
Diameter (m)	10.05
Number of cutters	68
Cutter type	CCS Disc
Cutter diameter (mm)	432
Cutter tip width (mm)	19.05
Revolution per minutes (RPM)	5.07
Total cutterhead thrust (kN)	17500-18150
Cutter load (kN)	275-300
Field ROP (m/h)	1.23

In the dataset herein, the 2km length of the tunnel (Reach 1) having 10m in diameter was examined and the raw data was extracted from report and literature and then analyzed. In this project open beam hard TBM were utilized to excavate the hard-abrasive rocks

encountered along the tunnel alignment. General specification of TBM and disc cutters are given in Figure 3.2. and Table 3.2.

3.3. Miryang Dam Tunnel, South Korea

The main purpose of the project was to deliver clean water from Miryang dam to Yangsan area through 2.6m-diameter hydro-tunnel. A 5.4 km-long hydro-tunnel was driven by open hard rock TBM from March, 1997 to October 1999 in Miryang, South Korea. Total length of this hydro-tunnel was 7.6km through mountainous area in the country. According to geological site investigation studies along the project location, most of the tunnel alignment consisted of igneous rocks that are granite from fine to medium-grained rock. Especially fine-grained granite is a very abrasive and tough rock and the compressive strength of rock is various depend on the grain size and percentage of quartz in the rock.

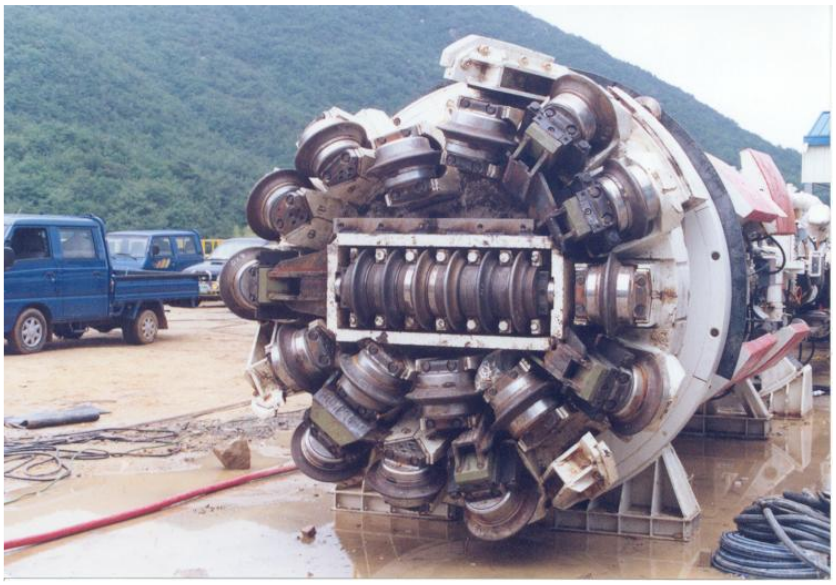

Figure 3.3. TBM utilized for Miryang Dam Tunnel (Kim, 2004)

The project which is 7.6km long is located in a mountain area in the country. It is worth mentioning that excavation in the rock mass was very challenging due to high

compressive strength and abrasiveness encountered. This project used the Drill-Blast (DB) method and TBM excavation method simultaneously from both ends of the tunnel alignment.

Table 3.3. TBM specification for Miryang Dam Tunnel (Kim, 2004)

TBM Specification	Miryang
Machine type	Open
Diameter (m)	2.6
Number of cutters	22
Cutter type	CCS Disc
Cutter diameter (mm)	393.7
Cutter tip width (mm)	15.87
Revolution per minutes (RPM)	10.0
Total cutterhead thrust (kN)	4300
Cutter load (kN)	190-200
Field ROP (m/h)	1.0

The portion of DB and TBM-excavated tunnel having 2.6m in diameter in length was 2.2 km and 5.4 km, respectively (Kim, 2004; Yagiz, et al. 2010). A total of 24 months was spent to bore the 4.7 km TBM tunnel, and total boring hours were approximately 4.753 hours with a 32% TBM utilization (Kim, 2004). An open hard rock TBM (WIRTH, Model TB 260E) was used for this project (Figure 3.3) with TBM specifications and disc properties as given in Table 3.3.

3.4. Zagros, Ghomrood and Karaj Water Transfer Tunnels, Iran

Karaj, Zagros and Ghomrood Water Conveyance Tunnels (KWCT, ZWCT, and GWCT respectively) excavated in Iran were also examined and obtained data and findings were used for the establishment of the database herein. These tunnels are recently constructed in three different geological zone of Iran (Hassanpour, et al. 2009, 2011, 2018, 2024). The main group of rocks are sedimentary, metamorphic, volcanic, and pyroclastic rocks along the alignment of tunnels. Main structure of the rock mass

changes from massive to very blocky rocks, also seen some minor fault zones, foliation and folds along the tunnels.

Table 3.4. Specification of TBMs for Zagros, Ghomrood and Karaj Water Transfer Tunnel (Goodarzi et al. 2021; Hassanpour et al. 2011)

TBM Specification	Karaj	Zagros	Ghomrood
Machine type	DS*	DS	DS
Diameter (m)	6.73	6.73	4.53
# of cutters	42	42	35
Cutter type	CCS Disc	CCS Disc	CCS Disc
Cutter dia. (mm)	432	432	432
Cutter tip width (mm)	19.0	19.0	19.0
Revolution per minutes (RPM)	6.32	5.46	10.7
Total cutterhead thrust (kN)	17000	28134	18000
Cutter load (kN)	350-400	500-600	400-500
Field ROP (m/h)	3.82	2.45	3.02

*DS refers to double shielded TBM

Since rock strength and rock mass properties including fracture spacing and frequency are more important than the type and mineralogical composition of rocks herein, detailed information related to geological formations and rock type was not given; however, those can be found in the literature (Goodarzi, et al. 2021; Yagiz, et al. 2024; Hassanpour, et al. 2024). Specifications of TBM used for the projects are given in Table 3.4 while the picture of TBM used for each project is illustrated in Figure 3.4-3.6.

Figure 3.4. TBM utilized for Ghomrood Water Transfer Tunnel (Hassanpour, et al. 2009)

Figure 3.5. TBM utilized for Karaj Water Transfer Tunnel (Hassanpour, et al. 2011)

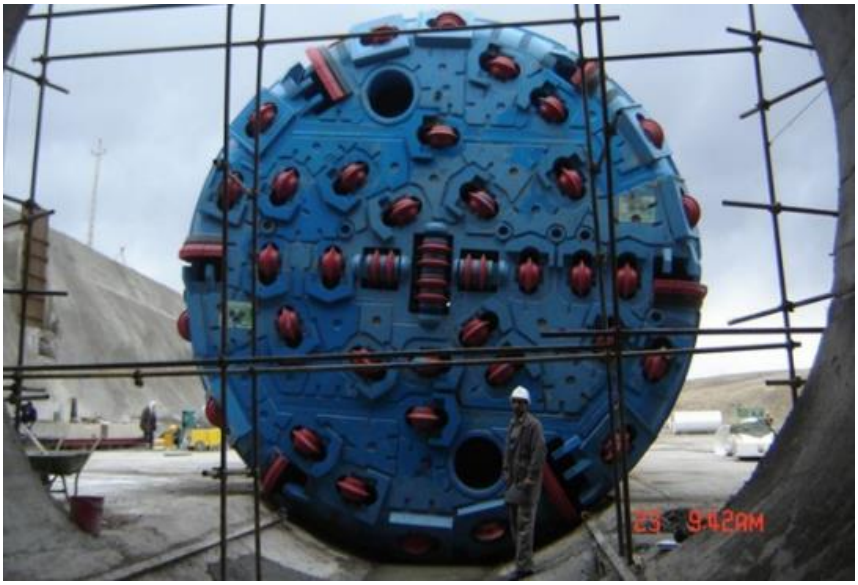

Figure 3.6. TBM utilized for Zagros Water Transfer Tunnel (Goodarzi, et al. 2021)

As seen from the configuration and specification of the TBM, the rock encountered along the tunnels were soft to medium sedimentary or volcanic rock and the type of TBM used for the projects are double shielded one.

CHAPTER 4 : DATA COLLECTION AND DATABASE ESTABLISHMENT

4.1. Data Collection

In this chapter, the selected and available projects mentioned in the chapter 3 are compiled and the database were established to use for development of empirical models to the estimation of the TBM performance in hard rock condition. The established database compiling the six different tunnel project's data has several sections including intact rock properties, rock mass properties, machine specification and TBM performance data from the field. In order to obtain the aim of the research, big database, more than 700data points, was established using intact rock properties, rock mass properties, TBM specifications and disc parameters. After examining the several intact rock properties, uniaxial compressive strength (UCS) of intact rock was chosen to represent the strength of excavated rocks. Rock mass properties especially rock type, fracture frequency and spacing between the fractures were examined carefully to obtain two new indices which are fracture index (FI) and weighted fracture index (WFI). Also, TBM specification such as cutterhead diameter (CHD), RPM, number and diameter of discs (N_c, D_c respectively) on a cutterhead and field performance parameters including cutter load (F_n) and ROP were examined.

In the dataset, each project is examined carefully to not miss any rock or machine parameters that can be input variable for the models. After establishing the database and selecting input variables, the statistical range of the dataset is checked to find the limitation of model from the scope of data availability (Table 4.1). The examining the available and nominated input parameters including both rock properties, TBM specifications and disc parameters for the purposed models, the distribution of the data range (557 datapoints) in the dataset is also controlled by developing the histogram of

each variable as given in Figure 4.1-4.11. It is obvious that data distribution and the range of data in the used dataset for both training and testing datasets is very important for the developed model in practice.

Table 4.1. Statistical distribution of the range of input variables in the dataset

Parameters	# of data	Minimum	Maximum	Mean	Std. dev	Variance
SL_e (m)	557	0.21	34.66	5.6222	6.81917	46.501
UCS (MPa)	557	20.00	300.00	155.8345	61.61448	3796.344
WFI	557	0.10	189.90	17.0537	33.02021	1090.334
MT_c	557	1.00	2.00	1.1598	0.36674	0.134
F_n	557	61.36	294.55	193.5709	65.53790	4295.217
CHD (m)	557	2.60	10.05	6.3505	2.30376	5.307
RPM (mm/rev)	557	5.07	10.70	7.9508	1.70355	2.902
N_c	557	22.00	68.00	44.8474	14.47660	209.572
D_c	557	0.39	0.48	0.4471	0.03571	0.001
ROP (m/h)	557	0.22	4.75	1.8159	0.89480	0.801

SL_e and MT_c refers to Length of tunnel segment excavate and TBM type respectively. MTc1 and MTc2 refers to O and DS respectively

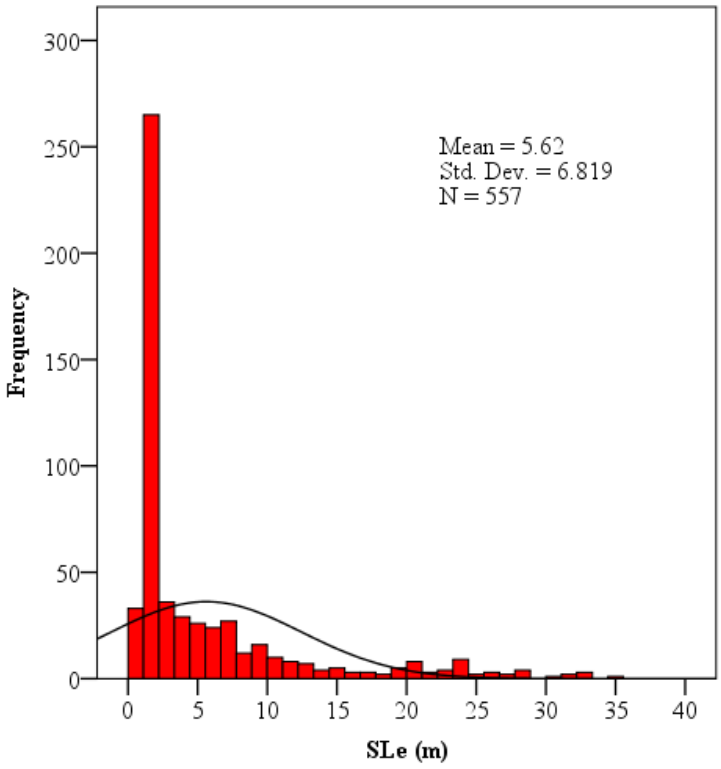

Figure 4.1. Distribution of excavated segment length in the dataset

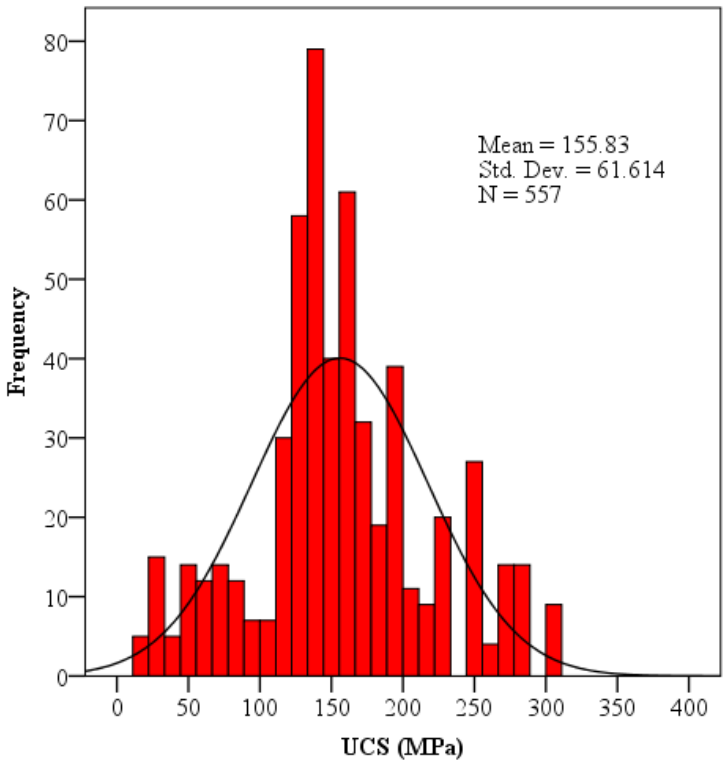

Figure 4.2. Distribution of uniaxial compressive strength in the dataset

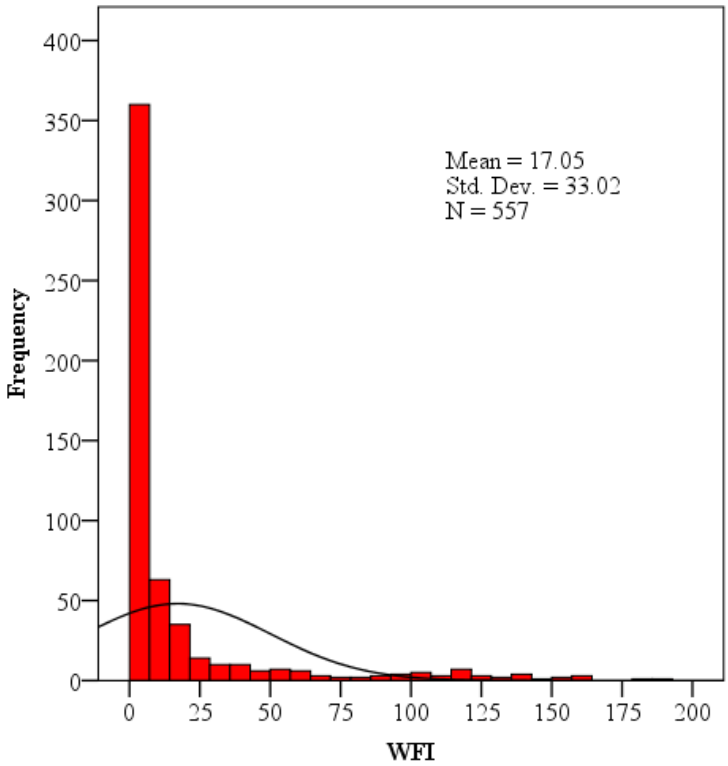

Figure 4.3. Distribution of weighted fracture index in the dataset

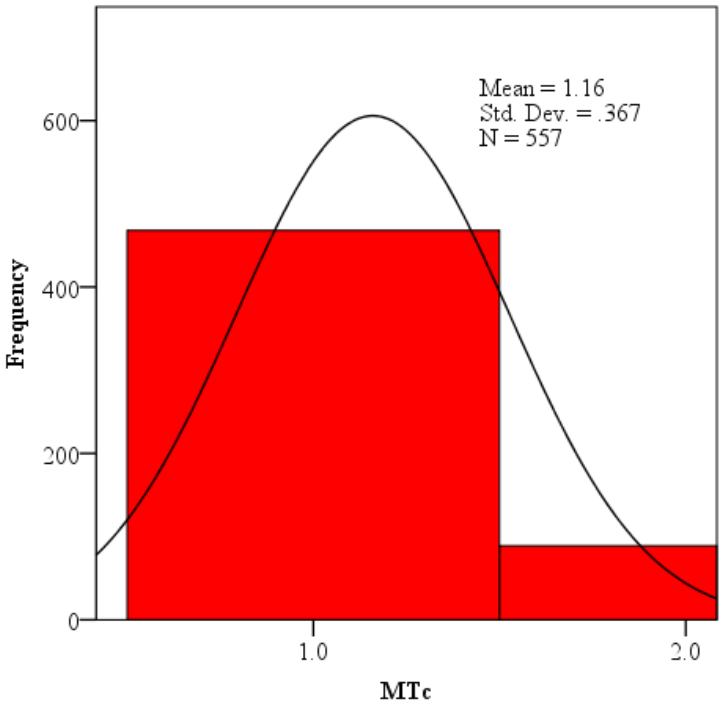

Figure 4.4. Distribution of machine types in the dataset

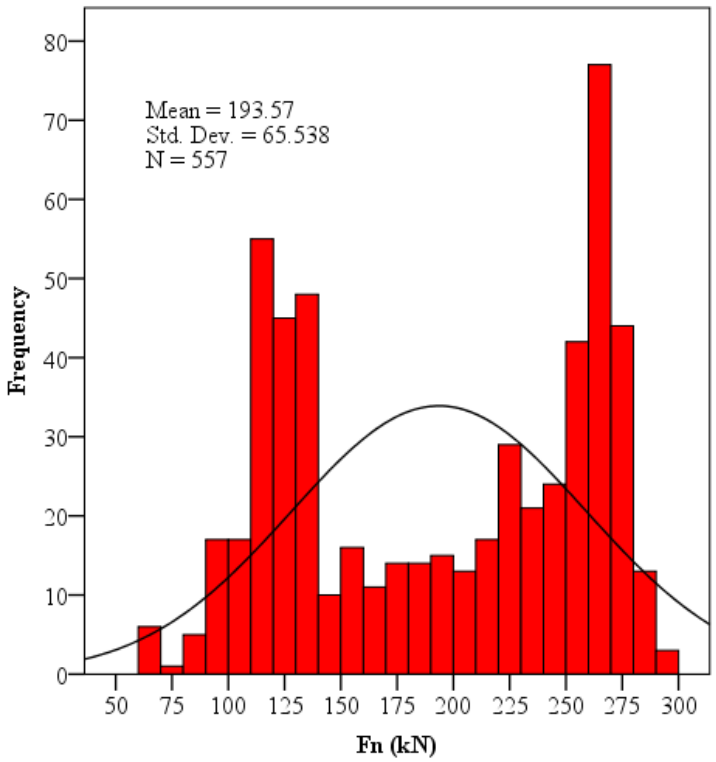

Figure 4.5. Distribution of individual cutter force in the dataset

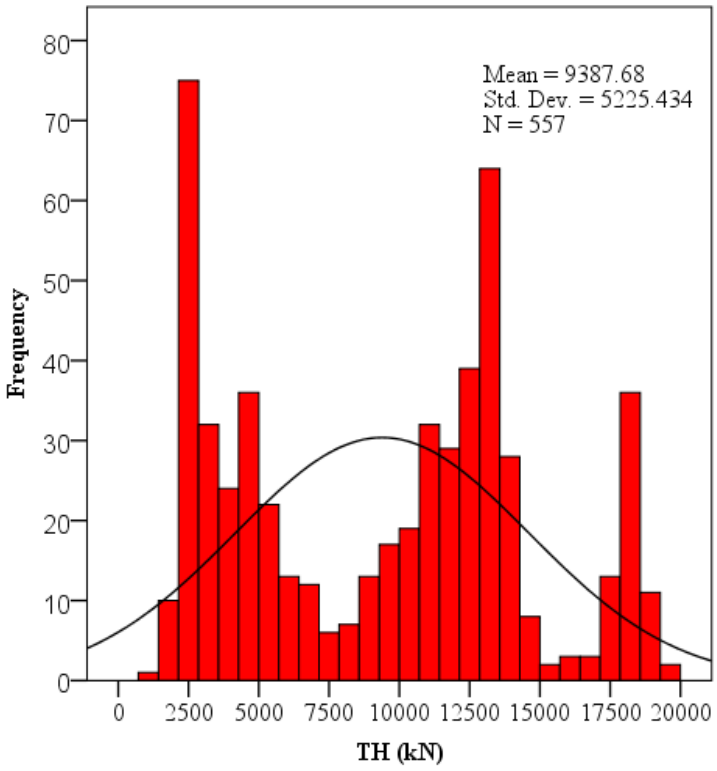

Figure 4.6. Distribution of cutterhead thrust in the dataset

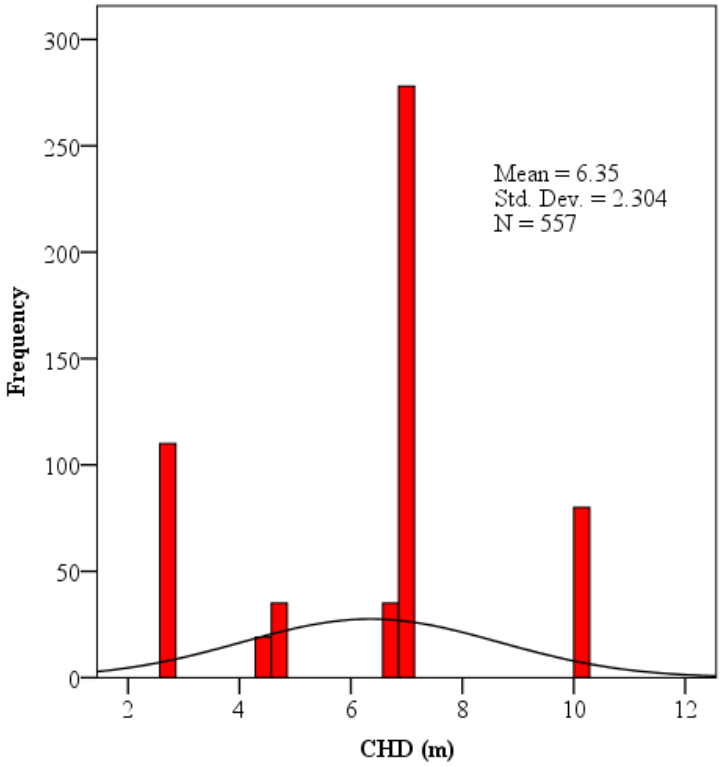

Figure 4.7. Distribution of cutterhead diameter in the dataset

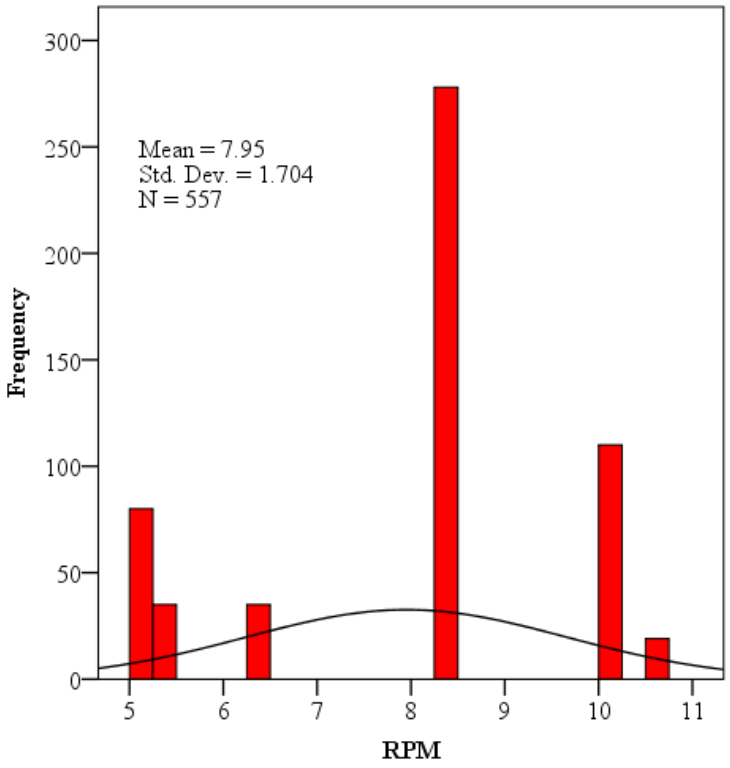

Figure 4.8. Distribution of RPM in the dataset

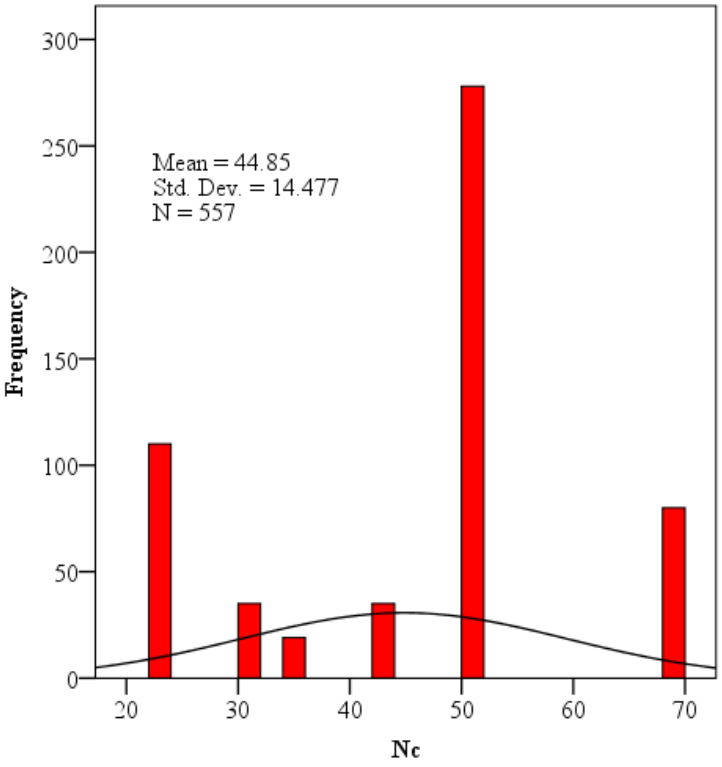

Figure 4.9. Distribution of number of cutters on the cutterhead in the dataset

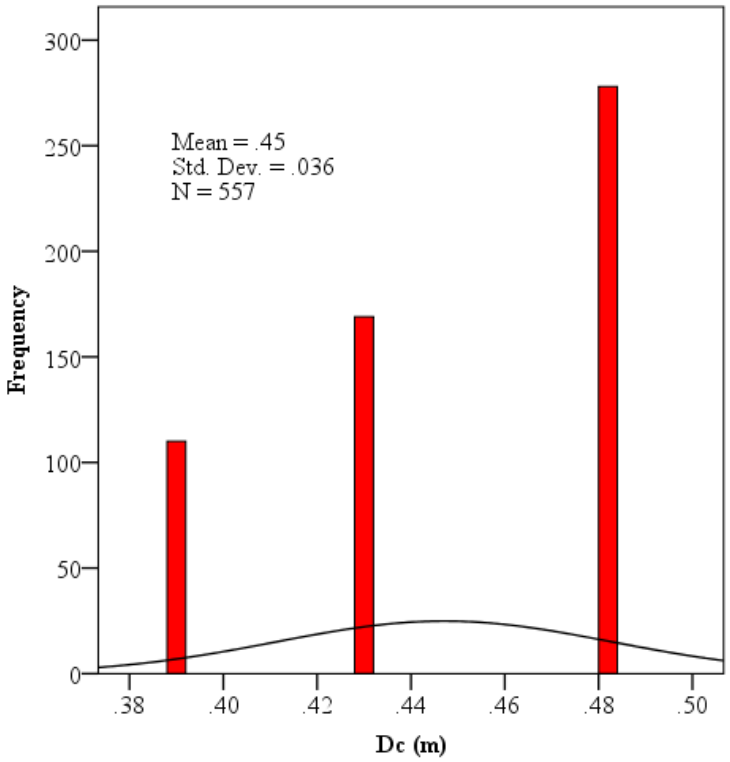

Figure 4.10. Distribution of cutter disc diameter in the dataset

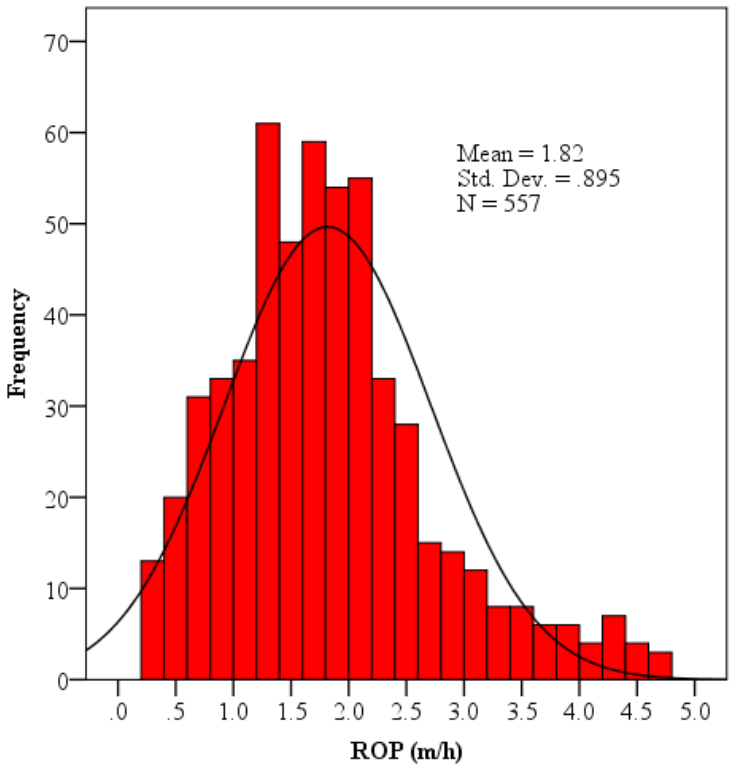

Figure 4.11. Distribution of ROP in the dataset

In order to examine the impact of machine specification and properties on the tunnel scheduling and TBM performance assessment, TBM specifications are also examined (Table 4.2). TBM type, cutter head (CH) diameter, number of cutters on the CH, Cutter type, cutter diameter and tip width are also defined and used to establishment of the dataset. As a result, each TBM specification and possible parameter are assessed for the empirical models to obtain the most suitable input parameters for the most accurate model.

Table 4.2. TBM specification for each project in the database

TBM Specification	Queens	Manapouri	Miryang	Karaj	Zagros	Ghomrood
Machine type	Open*	Open	Open	DS*	DS	DS
Diameter (m)	7.1	10.05	2.6	6.73	6.73	4.53
# of cutters	50	68	22	42	42	35
Cutter type	Disc	Disc	Disc	Disc	Disc	Disc
Cutter dia. (mm)	482.6	432	393.7	432	432	432
Cutter tip width (mm)	19.05	19.05	15.87	19.0	19.0	19.0
Total thrust (kN)	16000	18150	4300	17000	28134	18000

*Open and DS refer to Open Beam (gripper) and Double Shielded machines respectively

4.2. Introducing of Rock Fracture Index (FI)

Fracture Index (FI), which represents the fracture count over an arbitrary length of rock with similar intensity of fracturing, provides insight into the state of blackness and joint frequency in rock masses (Yagiz, et al. 2024). Further, FI also impacts rock boreability in excavation operations. Fracture frequency (F) is defined as the number of natural discontinuities in a unit length of rock mass (i.e. per meter). The most reported quantitative measures of fracture state indices are Rock Quality Designation (RQD), average joint spacing, and FI. Both these fracturing indices provide an estimate of the degree of fracturing of rock masses. Sen (2014) proposed a geomechanical classification

method based on RQD and FI to characterize local zones of heterogeneities within a rock mass. A few studies have interpreted the relationship between FI and RQD (He, et al. 2021; Vali and Arpa, 2013; Wong, et al. 2023). So, several indices can represent fracture frequency and quality of rock mass relative to its joints and discontinuities. In this study, the degree of fracturing is examined to be quantified using as an input for estimating the TBM penetration.

4.2.1. Degree of Fracturing

The Norwegian Institute of Technology (NTNU) has developed a Fracture Class System for evaluating the penetration potential of complexly deformed rocks bored by a TBM (Bruland, 1998). Fracture Class is given a Roman numeral designation based on the average spacing of joints (Sp) or fissures (St) which together allow a Fracture Class Designation to be applied to a reach of the tunnel. The class includes both the spacing between and the type of weakness planes. This classification system is good and valuable based on the average spacing of joints and fissures, however, when spacing between planes of weakness is quantified in the field, may be the actual value can be used in the analysis instead of the classification (Project Report 1-83 1983; 1-94 1995; Bruland, 1998).

Table 4.3. Fracture Class Designation (Bruland, 1998)

Fracture Class	Distance between Plane of Weakness-DPW (cm)
0	Rock mass that is set as 200
0-I	160
I-	80
I	40
II	20
III	10
IV	5

4.2.2. Fracture Index and Weighted Fracture Index Concept

Fracture index in number of fracture spacing/meter, is the number of clearly identifiable fractures per meter run of intact rock pieces or rock mass via scanline, measured over lengths of reasonably uniform rock. This index does not necessarily apply to whole core runs or along the rock mass excavated. If there is a marked change in fracture frequency during a core run, the fracture index should be calculated for each part of the run separately. In fact, FI is the quantification of fractures in certain amount of rock segment. Similarly, when dealing with rock mass, excavated segments of each rock mass should be considered separately to define the weighted fracture index (WFI) per segment (Yagiz, et al. 2024a) as follows:

$$\mathrm{FI} = \frac{1}{\mathrm{DPW}} \quad \text{(number of fractures spacing/meter)} \qquad (4.1)$$

Where FI and DPW refers to fracture index and spacing or distance between the fractures for each rock class in meter, respectively and so;

$$\mathrm{WFI} = \mathrm{FI} \cdot \mathrm{SL_e} \qquad (4.2)$$

Where WFI and SL_e refers to the weighted fracture index (number of fracture spacing/excavated segment) and length of tunnel segment excavated respectively

After several scientific reports (Project Report 1-83 and 1-94 1995; Bruland, 1998), the NTNU fracture classification systems have been frequently used in literature by different researchers (such as Yagiz, 2002, 2008). However, most of the studies focused on the quantified value of the classification rather than the Roman numeral description to be used for mechanical rock excavation (such as Yagiz 2002; Merguerian and Ozdemir, 2003; Yagiz, et al. 2024b).

4.3. Establishment of Database

Six TBM tunnel projects are examined for the aim of thesis to established database. After finding the number of inputs that is available for the model and the range of data for each variable, established database is used for development of new index that called fracture index (FI) and weighted fracture index (WFI) as mentioned previously.

In the database, the uniaxial compressive strength of intact rock, rock mass properties such as FI and WFI are introduced are the main rock related parameters. Further, TBM specifications including individual cutter load, cutterhead diameter, RPM, disc parameters such as number of discs on a cutterhead; tip width and diameter of CCS disc are added into database given as an example in Table 4.4. After that, the database is used for the development of empirical models by performing the SPPS Statistical program. Due to confidentiality, only limited datasets consisting of the rock properties and TBM parameters used in this research, are provided in **Appendix A and B.**

Table 4.4. Example of database used for the development of TBM Performance Model (see Appendices A and B)

Data	Project Name	Machine Type	SLe (m)	UCS (MPa)	WFI	FI	RT	MTc	Fn (kN/c)	TH (kN)	CHD (m)	RPM	Nc	Dc (m)	ROP (m/h)
1	Queens, USA	Open	1.8	191	4.6	2.50	3	1	227	11345	7.1	8.3	50	0.5	3.0
.	.	.	.	.	.	.	.	.	.	.	.	.	.	.	.
280	Manapouri, NZ	Open	7.7	99	3.9	0.50	7	1	286	19440	10.1	5.1	68	0.4	1.5
.	.	.	.	.	.	.	.	.	.	.	.	.	.	.	.
301	Manapouri, NZ	Open	7.3	83	18.2	2.50	6	1	274	18656	10.1	5.1	68	0.4	1.2
.	.	.	.	.	.	.	.	.	.	.	.	.	.	.	.
337	Manapouri, NZ	Open	5.3	77	2.7	0.50	6	1	269	18320	10.1	5.1	68	0.4	1.0
.	.	.	.	.	.	.	.	.	.	.	.	.	.	.	.
358	Manapouri, NZ	Open	5.0	209	6.3	1.25	7	1	174	11805	10.5	5.1	68	0.4	0.9
359	Miryang, S.K.	Open	9.0	300	3.6	0.40	8	1	123	2700	2.6	10.0	22	0.4	1.1
.	.	.	.	.	.	.	.	.	.	.	.	.	.	.	.
405	Miryang, S.K.	Open	1.8	250	0.9	0.50	8	1	135	2970	2.6	10.0	22	0.4	0.3
.	.	.	.	.	.	.	.	.	.	.	.	.	.	.	.
468	Miryang, S.K.	Open	6.0	220	3.8	0.63	8	1	115	2520	2.6	10.0	22	0.4	1.9
469	Ghomrood	D. Shield	20.5	50	137.0	6.67	9	2	116	4060	4.5	8.9	35	0.4	3.6
.	.	.	.	.	.	.	.	.	.	.	.	.	.	.	.
487	Ghomrood	D. Shield	7.2	160	12.0	1.67	13	2	130	4550	4.5	8.9	35	0.4	1.4
488	Karaj	D. Shield	18.2	30	182.1	10.00	10	2	118	3650	4.7	6.3	31	0.4	3.8
522	Karaj	D. Shield	15.6	40	62.4	4.00	11	2	112	3482	4.7	6.3	31	0.4	4.5
523	Zagros	D. Shield	13.8	30	69.0	5.00	17	2	117	4910	6.7	5.5	42	0.4	2.4
.	.	.	.	.	.	.	.	.	.	.	.	.	.	.	.
536	Zagros	D. Shield	20.8	50	138.5	6.67	11	2	98	4120	6.7	5.5	42	0.4	2.2
557	Zagros	D. Shield	15.3	60	61.1	4.00	11	2	156	6560	6.7	5.5	42	0.4	2.2

CHAPTER 5：DEVELOPMENT OF EMPIRICAL MODELS FOR PREDICTING TBM PENETRATION RATE

In order to obtain predictive equations from the appropriate datasets for prediction TBM penetration rate, the SPSS Statistics (V.24, 2024) program was used as a statistical tool for this research. Using the SPSS (2024) program, simple linear, multiple linear and non-linear regression analyses were conducted, and the resulting equations examined to obtain the most accurate predictive models. A simple regression analysis was first performed between a single variable and rate of penetration in order to evaluate the influence of each individual parameter on ROP. Multiple linear and non-linear models were subsequently run in order to obtain the most accurate equations from the datasets.

5.1. Pearson Correlation Coefficients Among the Parameters in the Database

It is well-known that to choose the input variables to estimate the unknown, the Pearson correlation among the inputs and outputs should be examined. For this reason, relations between the variable are assessed and the output of the findings is introduced in Table 5-1. The ROP and other input variable have some linear relations; however, these results are not strong enough to be solely used for the field performance of the TBM. As a result, it is found that the multiple variable and both linear and non-linear relations among the parameters should be examined and interpreted to obtain the most accurate estimation formulas for the aim.

To predict the penetration rate of the TBMs in the six tunnel cases, linear multivariable regression (LMR) and non-linear multivariable regression (NLMR) analyses were performed, after obtaining optimum valuable inputs via Pearson correlations among

the variables. To obtain the aim, numerous different LMR and NLMR models were developed with different input variables using the constructed dataset; however, five most accurate model generated from each modelling techniques were proposed herein to predict the ROP.

Table 5.1. Pearson Correlation among the input variables in the database

Pearson-Correlation (R)										
Variables	*ROP*	*SL_e*	*UCS*	*WFI*	*MT*	*F_n*	*CHD*	*RPM*	*N_c*	*D_c*
ROP	1.000	0.588	-0.632	0.634	0.635	-0.107	0.022	-0.173	-0.026	0.263
SL_e	0.588	1.000	-0.426	0.828	0.816	-0.375	-0.215	-0.227	-0.283	-0.382
UCS	-0.632	-0.426	1.000	-0.580	-0.579	-0.187	-0.519	0.640	-0.452	-0.367
WFI	0.634	0.828	-0.580	1.000	0.797	-0.392	-0.132	-0.266	-0.208	-0.180
MT_c	0.635	0.816	-0.579	0.797	1.000	-0.409	-0.172	-0.265	-0.261	-0.208
F_n	-0.107	-0.375	-0.187	-0.392	-0.409	1.000	0.712	-0.341	0.746	0.597
CHD	0.022	-0.215	-0.519	-0.132	-0.172	0.712	1.000	-0.761	0.993	0.576
RPM	-0.173	-0.227	0.640	-0.266	-0.265	-0.341	-0.761	1.000	-0.690	-0.123
N_c	-0.026	-0.283	-0.452	-0.208	-0.261	0.746	0.993	-0.690	1.000	0.599
D_c	0.263	-0.382	-0.367	-0.180	-0.208	0.597	0.576	-0.123	0.599	1.000

5.2. Simple Statistical Analysis

Commonly accepted methods to examine empirical correlations between variables are both simple and multiple regression methods using statistical software packages such as excel or SPSS statistics. In this study, linear (y=ax+b) and non-linear (y=ax^b) simple regression analyses were performed among intact rock and rock mass properties or TBM specifications and penetration rate. Rate of penetration (ROP) was used as a dependent value, while different intact rock and rock mass properties and machine parameters were used individually as an independent variable possible for prediction of TBM penetration rate. This resulted in several simple regression relations among the possible input variables and ROP. All results obtained with these simple models for prediction TBM penetration rate are summarized in Table 5-2.

Table 5.2. Simple models for prediction TBM penetration rate

#	Parameters	R^2	Regression equation	Eq.
1	UCS	0.399	ROP = 3.25+0.009 · UCS	(5.1)
2	SL_e	0.346	ROP = 1.382+0.078 · SL_e	(5.2)
3	FI	0.137	ROP=1.551+0.104· FI	(5.3)
4	WFI	0.403	ROP = 1.523+0.017 · WFI	(5.4)
5	Fn	0.011	ROP = 2.098-0.001 · Fn	(5.5)
6	MTc	0.408	ROP = -0.042+1.59 · MTc	(5.6)
7	CHD	0.001	ROP = 1.76+0.009 · CHD	(5.7)
8	RPM	0.031	ROP = 2.539-0.09 · RPM	(5.8)
9	Nc	0.001	ROP = 1.89-0.002 · Nc	(5.9)
10	Dc	0.069	ROP = -1.129+6.587 · Dc	(5.10)

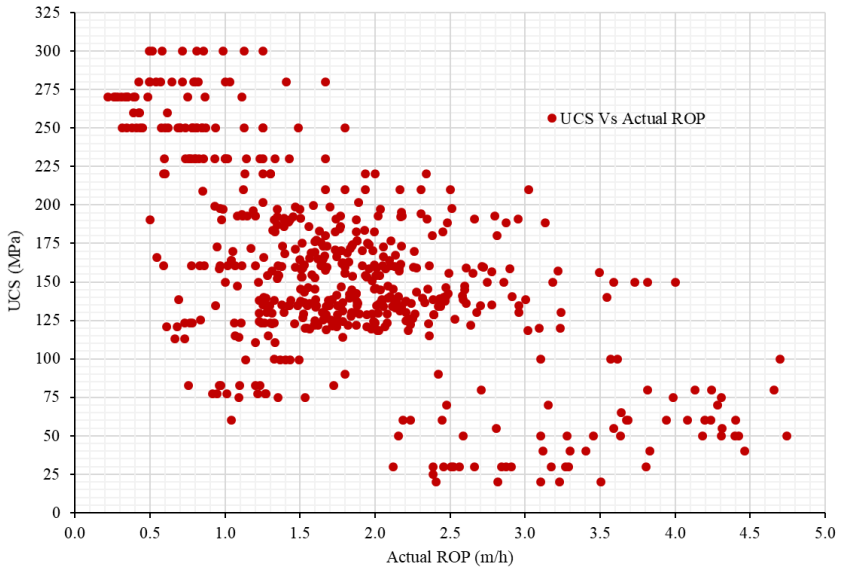

Figure 5.1. Relationship between the uniaxial compressive strength and Actual ROP

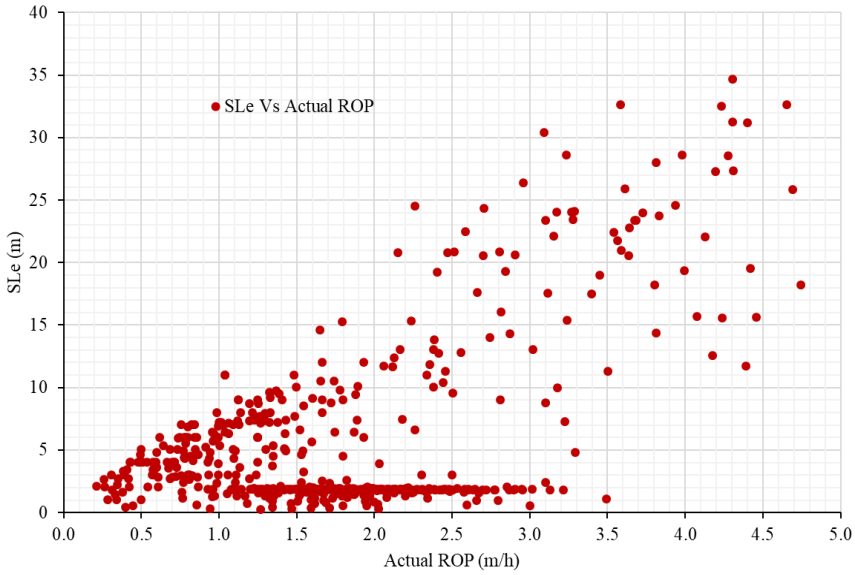

Figure 5.2. Relationship between the SL_e and Actual ROP

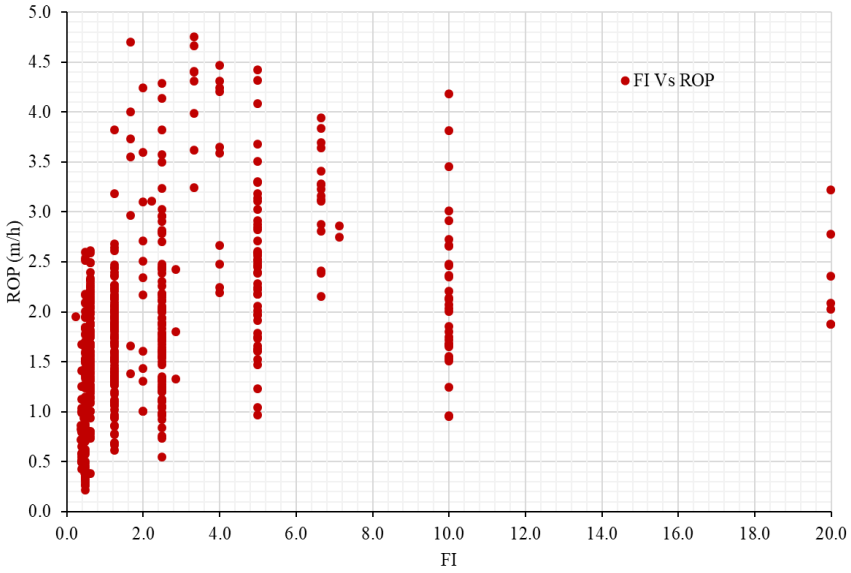

Figure 5.3. Relationship between the FI and Actual ROP

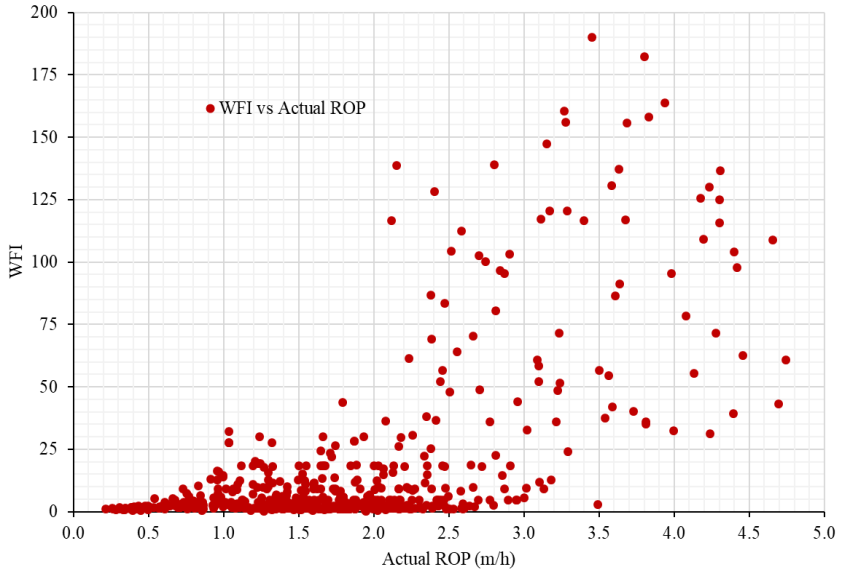

Figure 5.4. Relationship between the WFI and Actual ROP

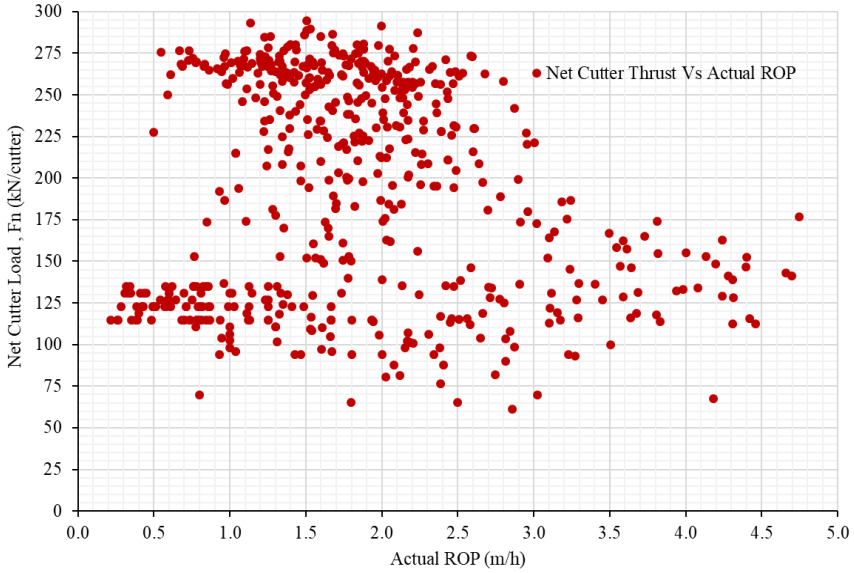

Figure 5.5. Relationship between the Individual Cutter Load (F_n) and Actual ROP

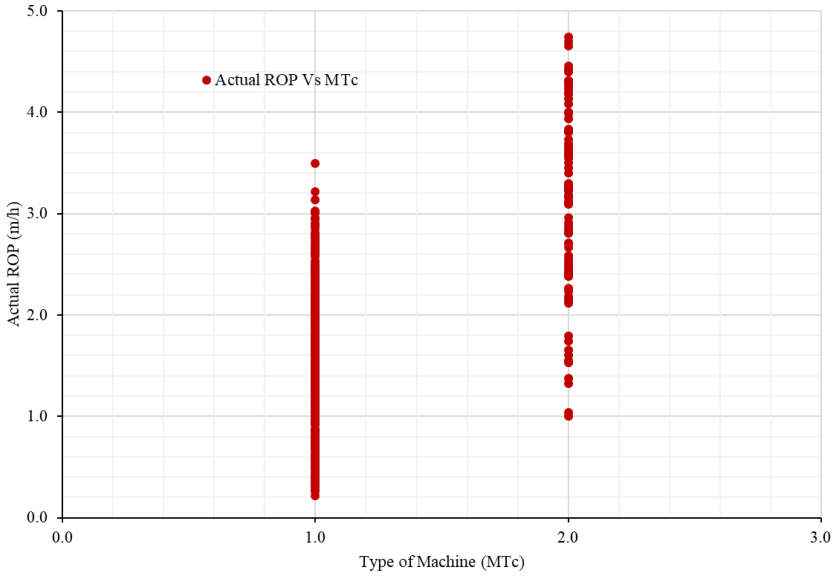

Figure 5.6. Relationship between the MTc and Actual ROP (1&2 refers to Open Bean and Double Shield TBM respectively)

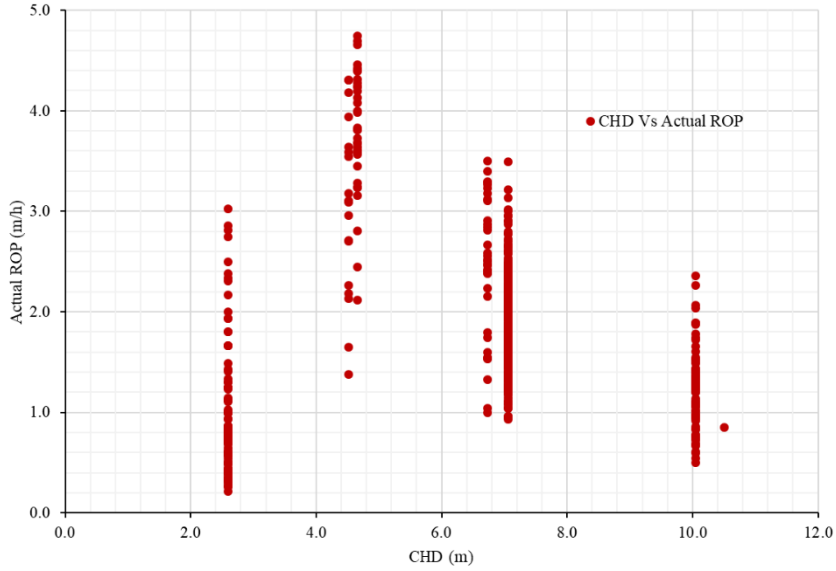

Figure 5.7. Relationship between the CHD and field ROP

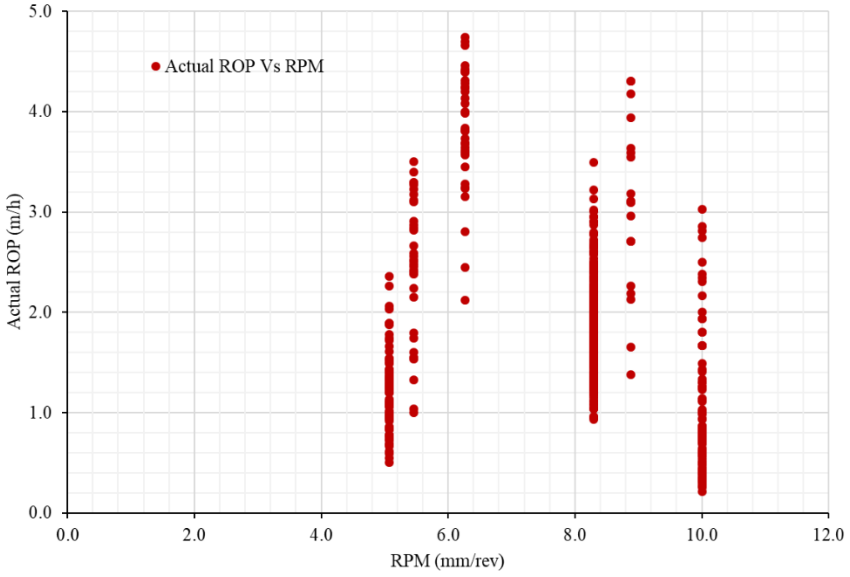

Figure 5.8. Relationship between RPM and Actual ROP

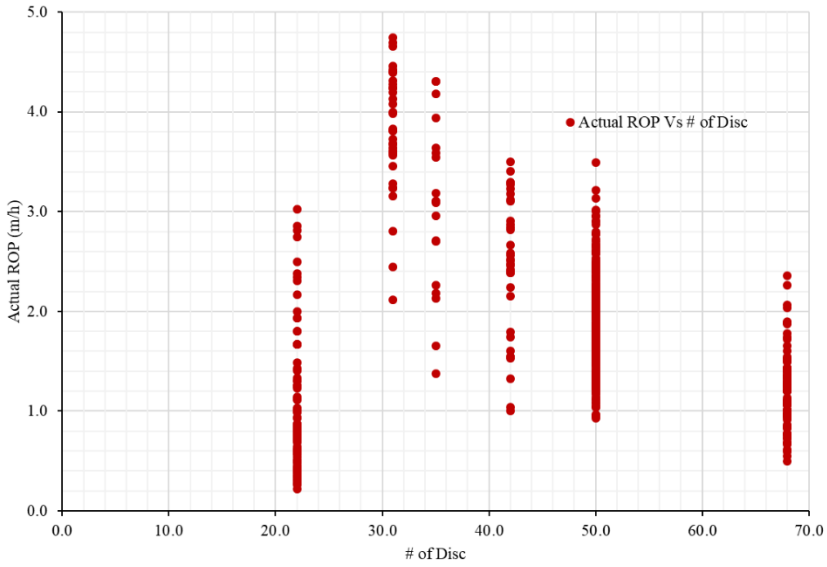

Figure 5.9. Relationship between N_c and Actual ROP

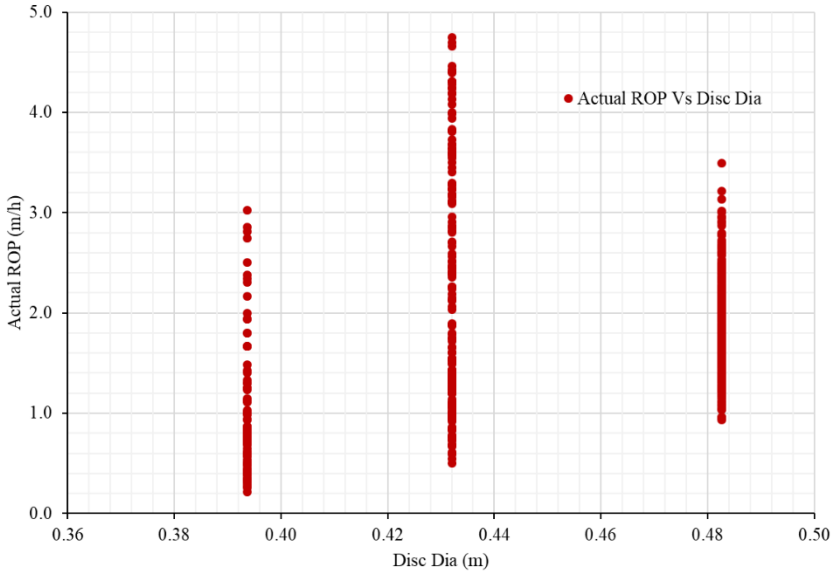

Figure 5.10. Relationship between D_c and Actual ROP

5.3. Multiple Variables Statistical Analysis

The prediction of TBM ROP is either a linear or a non-linear multivariable problem. In order to consider the concomitant effects of intact rock and rock mass properties and TBM specifications on ROP, both linear and non-linear multivariable regression analyses were performed using the SPSS Version 24 (SPSS, 2024) statistical package. Non-linear regression consists in finding a non-linear model describing the relations between a dependent variable and a set of independent variables. In a multiple regression analysis, more than two variables including intact rock and rock mass properties and machine specifications are used to derive the correlation equation. In a multiple regression analysis, both linear and non-linear methods can be used, which result in different correlation coefficients, plots, histograms, means, standard deviations, etc. In order to evaluate the differences between the two methods in the multiple regression analysis, the results are presented in Tables 5.3-5.4

according to the type of regression. In order to conduct the models, dataset is divided in two part as 80% of it for training and 20% of it for testing.

5.3.1. Linear Multiple Variables Regression Models

After examining the relations among the inputs and output of the proposed models via Pearson correlation, LMR analysis is conducted to predict the ROP from alternative input parameters including rock properties such as intact rock strength, frequency of discontinuities in rock mass, and TBM specifications such as thrust, RPM, cutterhead diameter so forth. Simple regression-type equations could be extended to a multiple-variable concept by increasing the number of inputs as follows:

$$y = a + b_1 x_1 + b_2 x_2 + b_3 x_3 + \cdots + b_n x_n \quad (5.11)$$

Where $x_1, x_2, x_3, \ldots, x_n$ are different independent variables (e.g., UCS, WFI and F_n) to predict y referring to the ROP herein.

Since one of the most common techniques is LMR to find the unknown from known variables, it is also utilized to obtain the aim in this study conducting numerous linear regression models by using the possible alternative inputs for both rock and TBM features. After trying various models with different input parameters, the five models that demonstrated acceptable performance were determined. These models can be seen in Table 5.3, where their prediction performance for the training dataset from the R^2 point of view is presented. Comparing the output of the LMR models, Model 5 shows the most accurate model with a few meaningful input parameters among the other. As a result, obtained results from training and testing data are demonstrated in Figures 5.11-5.20 respectively. It can be

stated that LMR models are not reliable or enough accurate in comparison with the non-linear multiple regression modelling approach due to the complexity of nature and rock mass as experienced from the past. Due to that, NLMR models must be considered to find the best empirical equations with the most reliable input variables for the aim.

Table 5.3. Linear multiple regression equations developed using training dataset

Models #	R^2	R	Regression Equations	Eq.
Model 1	0.516	0.718	$\mathrm{ROP} = -0.005 \cdot \mathrm{UCS} + 0.006 \cdot \mathrm{WFI} + 0.63 \cdot \mathrm{MT_c} + 1.703$	(5.12)
Model 2	0.525	0.725	$\mathrm{ROP} = -0.009 \cdot \mathrm{UCS} + 0.006 \cdot \mathrm{WFI} - 0.016 \cdot \mathrm{N_c} + 3.770$	(5.13)
Model 3	0.536	0.732	$\mathrm{ROP} = -0.008 \cdot \mathrm{UCS} + 0.004 \cdot \mathrm{WFI} + 0.33 \cdot \mathrm{MT_c} - 0.092 \cdot \mathrm{CHD} + 3.213$	(5.14)
Model 4	0.569	0.754	$\mathrm{ROP} = -0.009 \cdot \mathrm{UCS} + 0.009 \cdot \mathrm{WFI} + 0.561 \cdot \mathrm{CHD} + 0.278 \cdot \mathrm{RPM} - 0.08 \cdot \mathrm{N_c} + 0.78$	(5.15)
Model 5	0.567	0.753	$\mathrm{ROP} = -0.009 \cdot \mathrm{UCS} + 0.01 \cdot \mathrm{WFI} + 0.001 \cdot \mathrm{F_n} + 0.195 \cdot \mathrm{RPM} + 1.372$	(5.16)

In this research, there are more than 50 models with different alternative inputs was run by conduction linear multivariable regression analysis; however, the best five models were considered to present herein according to the accuracy of the LMR models. In puts, outputs and SPSS statistics results of the models are given in **Appendix B** in detail. Further, other best 20 models developed using the LMR approaches are added as **Appendix C.**

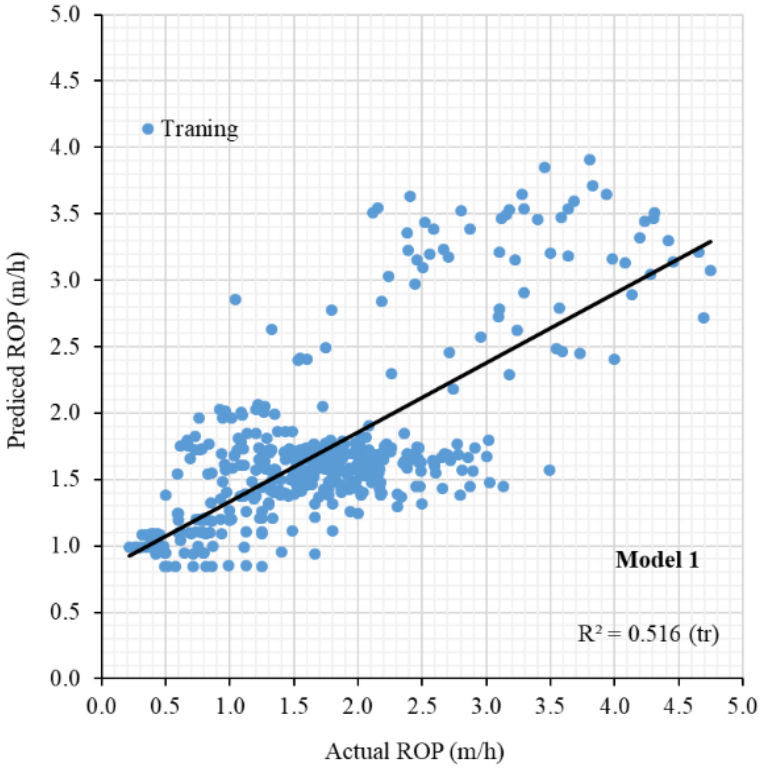

Figure 5.11. LMR model 1 for estimating TBM penetration for training dataset

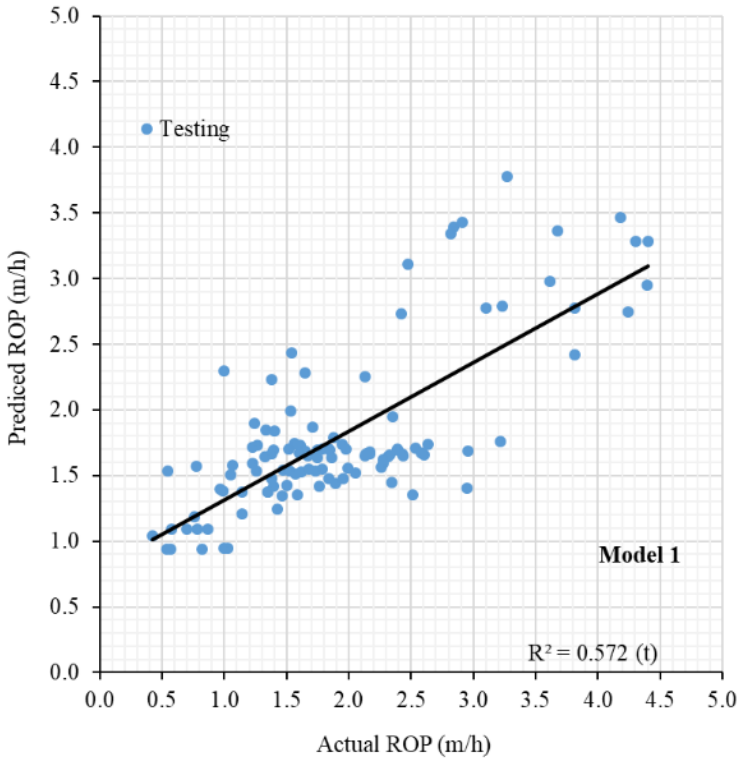

Figure 5.12. LMR model 1 for estimating TBM penetration for testing dataset

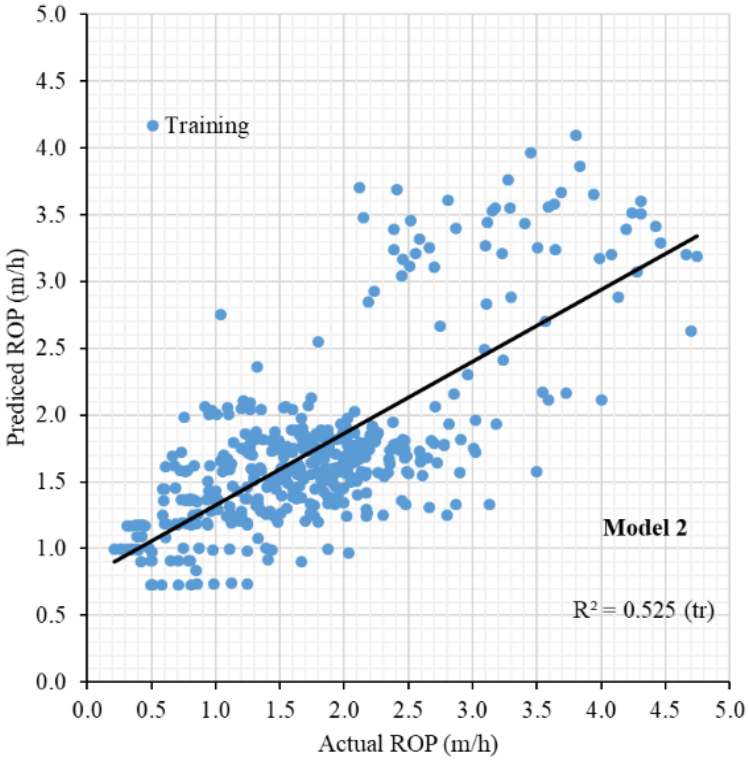

Figure 5.13. LMR model 2 for estimating TBM penetration for training dataset

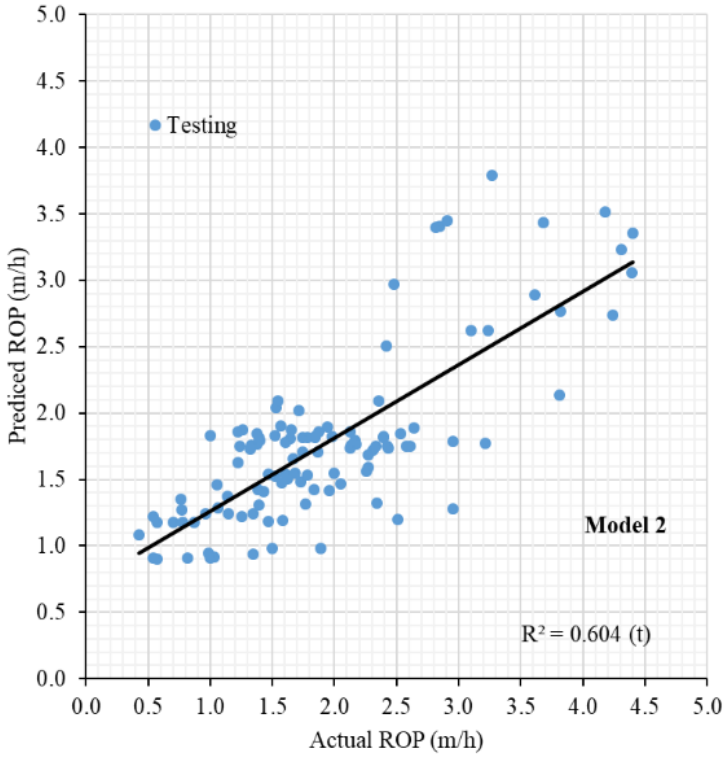

Figure 5.14. LMR model 2 for estimating TBM penetration for testing dataset

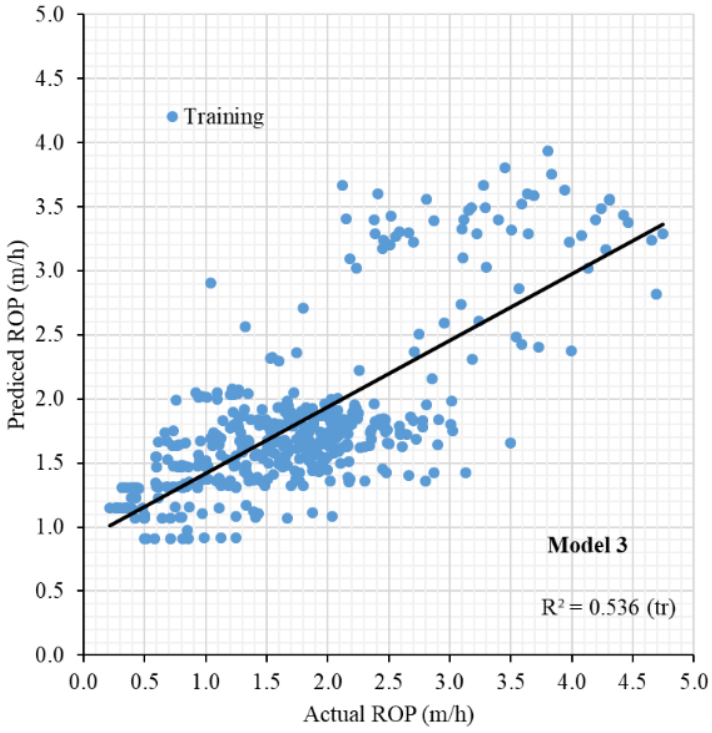

Figure 5.15. LMR model 3 for estimating TBM penetration for training dataset

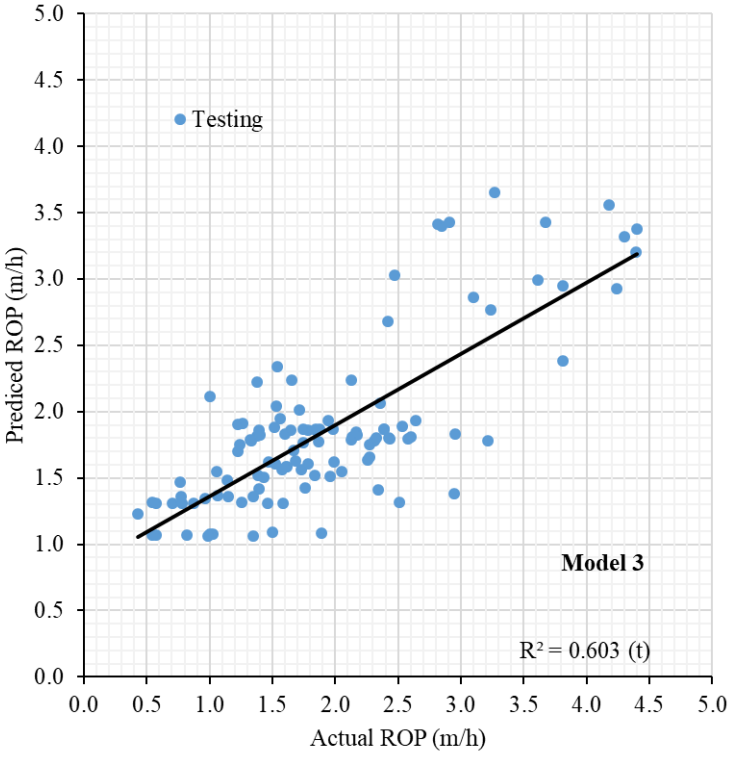

Figure 5.16. LMR model 3 for estimating TBM penetration for testing dataset

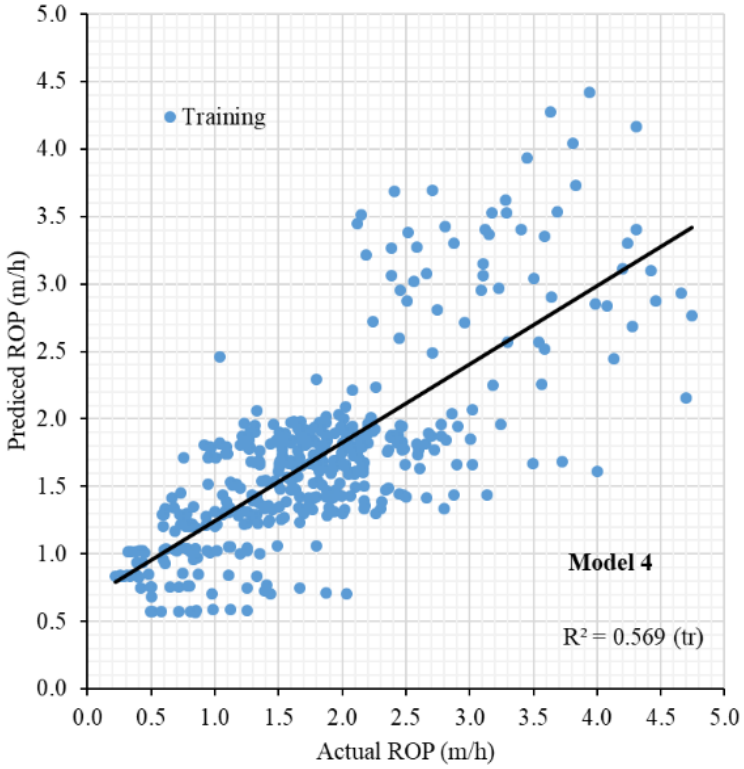

Figure 5.17. LMR model 4 for estimating TBM penetration for training dataset

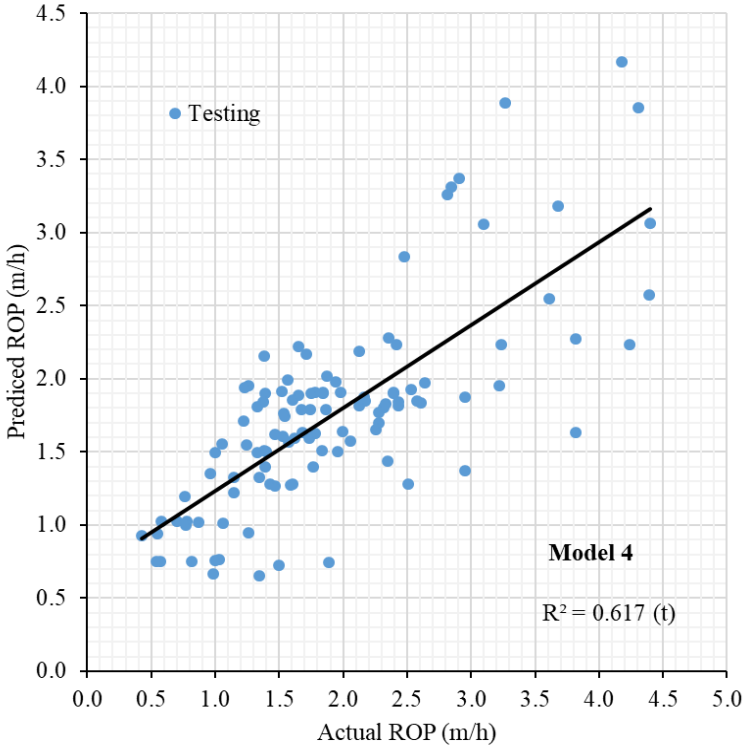

Figure 5.18. LMR model 4 for estimating TBM penetration for testing dataset

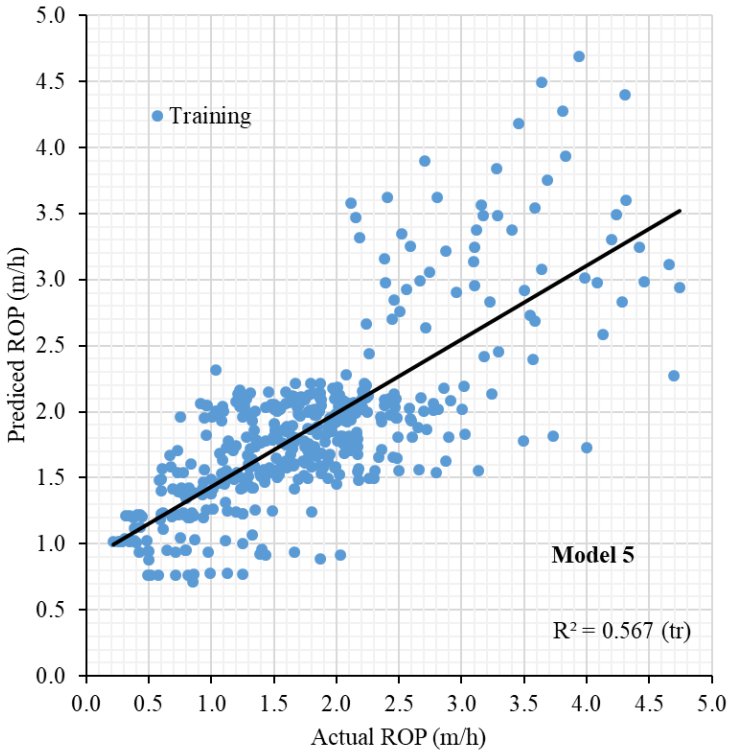

Figure 5.19. LMR model 5 for estimating TBM penetration for training dataset

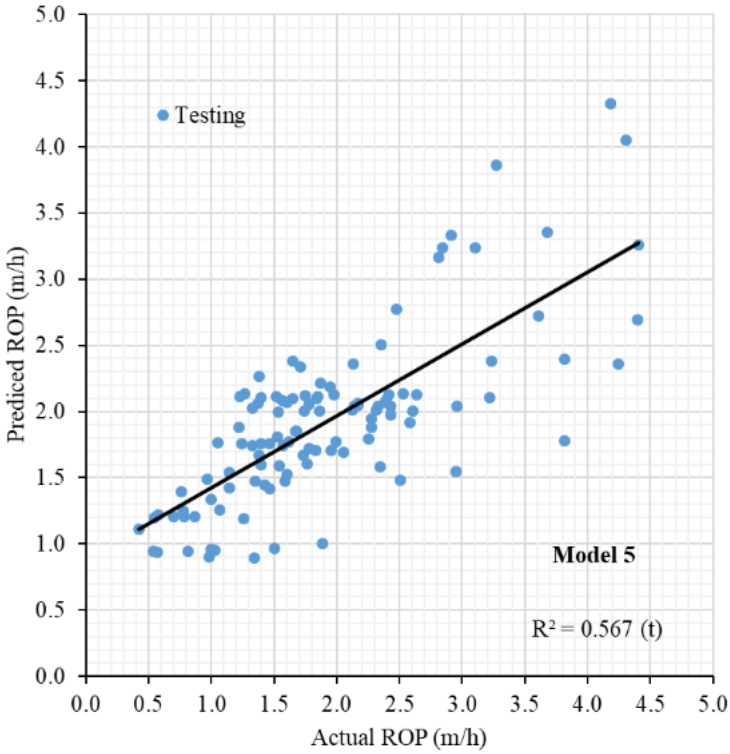

Figure 5.20. LMR model 5 for estimating TBM penetration for testing dataset

5.3.2. Non-Linear Multiple Variables Regression Models

Non-linear multiple regression (NLMR) is an approach to obtain a relation between independent as unknown and dependent variables. Unlike traditional simple linear regression, NLMR can be used to develop a model with random relationships between input and output variables, especially where complex engineering problems with multiple variables (Yagiz, et al. 2019). In the NLMR technique, both non-linear and linear relationships, such as exponential and power, can be employed as a hybrid. The NLMR approach is used for the establishment of mathematical formulas to make a prediction on dependent variables based on known independent variables in the geotechnical engineering fields in the literature (Armaghani, et al. 2016, 2017, 2021; Yagiz and Gokceoglu, 2010; Yagiz and Karahan, 2015; Yazitova and Yagiz, 2024). Using the constructed datasets, the best five NLMR equations were proposed to predict the rate of penetration as listed in Table 5.4 where the performance capacities (based on R^2) of NLMR models are higher than those of LMR models. Based on NLRM, all models, including a variety of inputs such as F_n, CHD, UCS, RPM and WFI have the potential to be used for performance prediction of TBM; further, statistical analysis was conducted among the models using the statistical several indices together to select the best one via score ranking methods in this study.

Comparing the output of the NLMR models, each model gives enough accurate result with coefficient of determination (R^2) higher than sixty five percent that means correlation coefficient (R) of more than eighty percent. Each of them has potential to be used in practice; however, Model 1 is superior in comparison with others due to few input variables but ignorable low R^2 in first glance. It is found that NLMR models are more reliable than the LMR models since the engineering problem is complex and not linear due to that, NLMR

models were considered to find the best empirical equations with the most reliable input variables for the aim.

Table 5.4. Non-linear multiple regression equations developed using training dataset

Model #	R^2	R	Regression equations	Eq.
Model 1	0.666	0.816	$ROP = \frac{F_n^{0.308} \cdot WFI^{0.136} \cdot RPM^{-0.027} \cdot CHD^{2.875}}{8.211 \cdot UCS^{0.101} \cdot e^{0.583 \cdot CHD}}$	(5.17)
Model 2	0.669	0.818	$ROP = \frac{F_n^{0.26} \cdot MT_c^{0.05} \cdot N_c^{-0.823} \cdot RPM^{0.351} \cdot SL_e^{-0.041}}{0.098 \cdot UCS^{0.15} \cdot WFI^{-0.129} \cdot e^{(CHD \cdot D_c)^{-5.476}}}$	(5.18)
Model 3	0.652	0.808	$ROP = \frac{F_n^{0.354} \cdot WFI^{0.152} \cdot RPM^{0.007} \cdot CHD^{1.185}}{7.715 \cdot UCS^{0.119} \cdot EXP(0.023 \cdot CHD^2)}$	(5.19)
Model 4	0.668	0.817	$ROP = \frac{F_n^{0.266} \cdot RPM^{0.014} \cdot CHD^{2.996} \cdot SL_e^{0.042}}{9.22 \cdot UCS^{0.087} \cdot WFI^{-0.116} \cdot e^{0.591 \cdot CHD}}$	(5.20)
Model 5	0.653	0.808	$ROP = \frac{F_n^{0.347} \cdot CHD^{1.162} \cdot RPM^{0.046} \cdot MT_c^{0.095}}{8.765 \cdot WFI^{-0.145} \cdot UCS^{0.103} \cdot EXP(0.022 \cdot CHD^2)}$	(5.21)

Further, as result of NLMR models, obtained results from training and testing data are demonstrated in Figure 5.21 to 5.30 respectively. In order to examine the accuracy of each model in detail, the developed models via both LRM and NLRM are analyzed using evaluation metric including six different statistical indices together with total score ranking for each introduced model in the following section.

In this research, there are more than 50 models with different alternative inputs was run by conduction Non-linear multivariable regression analysis; however, the best five models were considered to present herein according to the accuracy of the models. In puts, outputs and SPSS statistics results of the models are given in **Appendix D** in detail. Further, other best 20 models developed using the NLMR approaches are added as **Appendix E.**

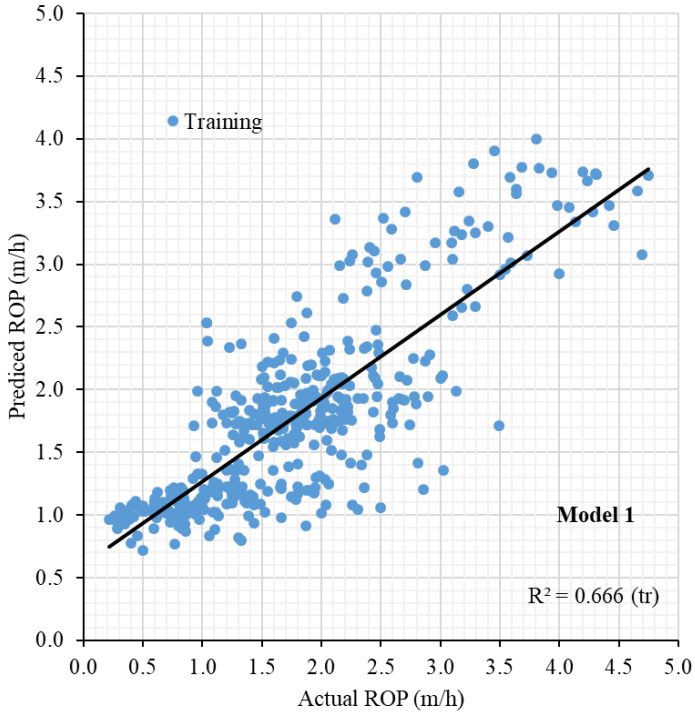

Figure 5.21. NLMR model 1 for estimating TBM penetration for training dataset

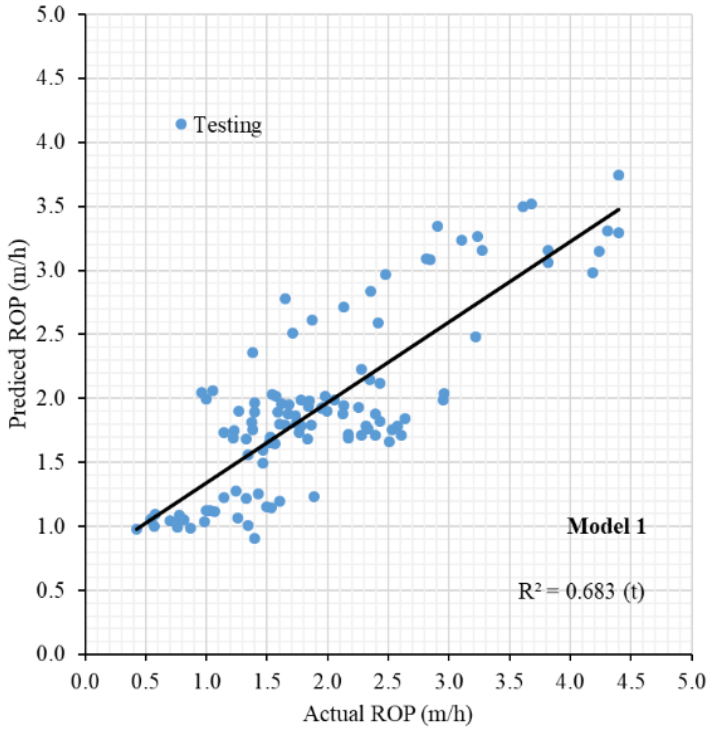

Figure 5.22. NLMR model 1 for estimating TBM penetration for testing dataset

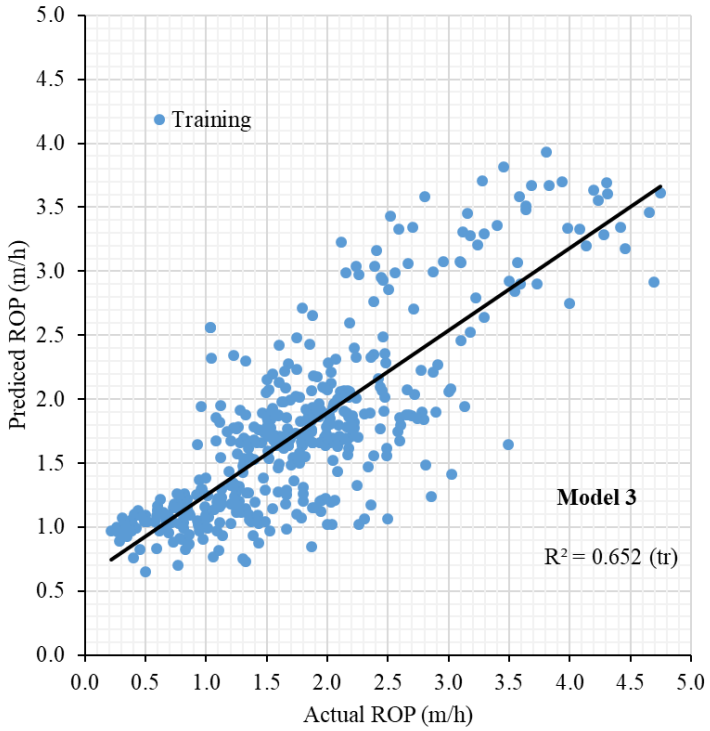

Figure 5.23. NLMR model 3 for estimating TBM penetration for training dataset

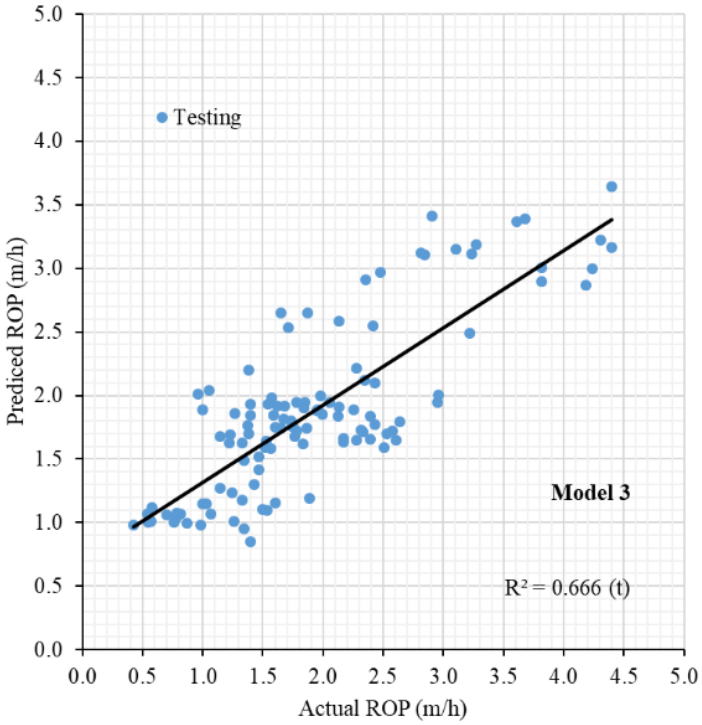

Figure 5.24. NLMR model 3 for estimating TBM penetration for testing dataset

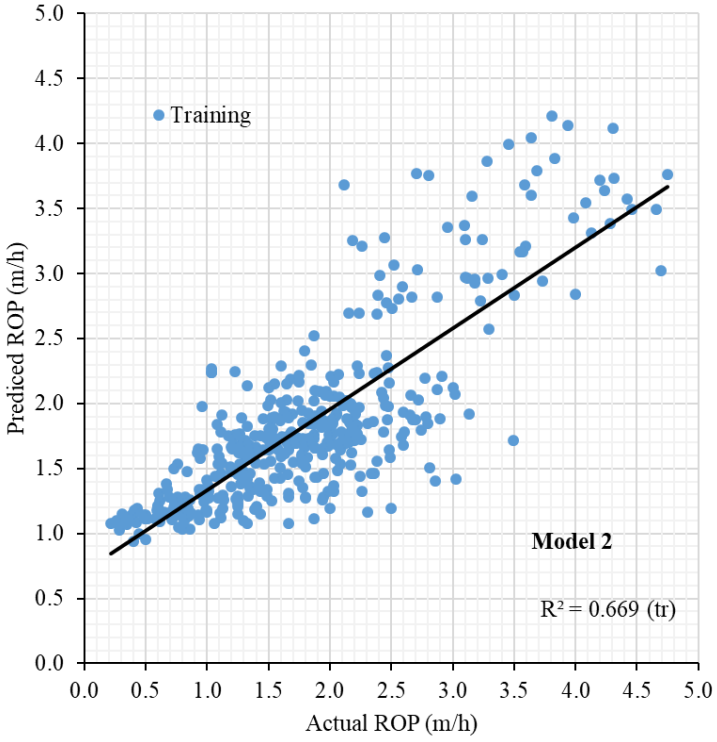

Figure 5.25. NLMR model 2 for estimating TBM penetration for training dataset

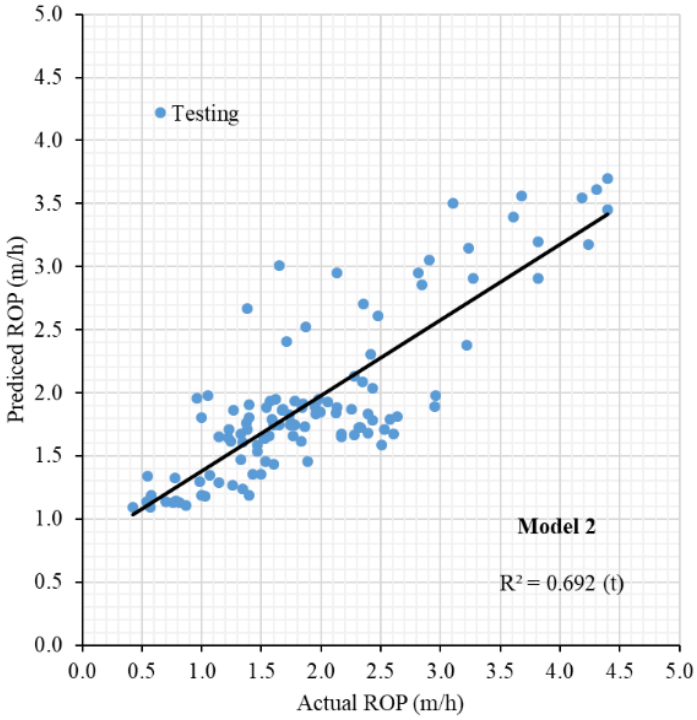

Figure 5.26. NLMR model 2 for estimating TBM penetration for testing dataset

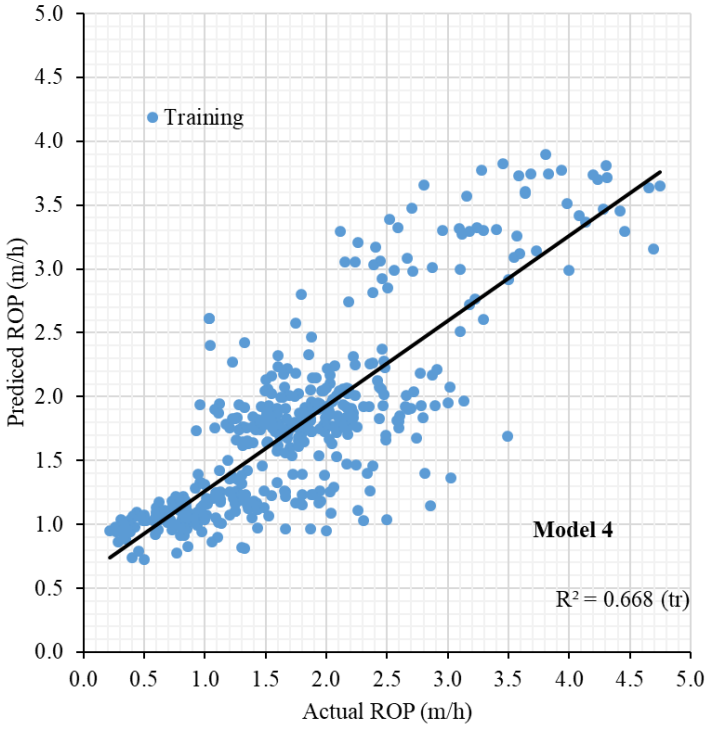

Figure 5.27. NLMR model 4 for estimating TBM penetration for training dataset

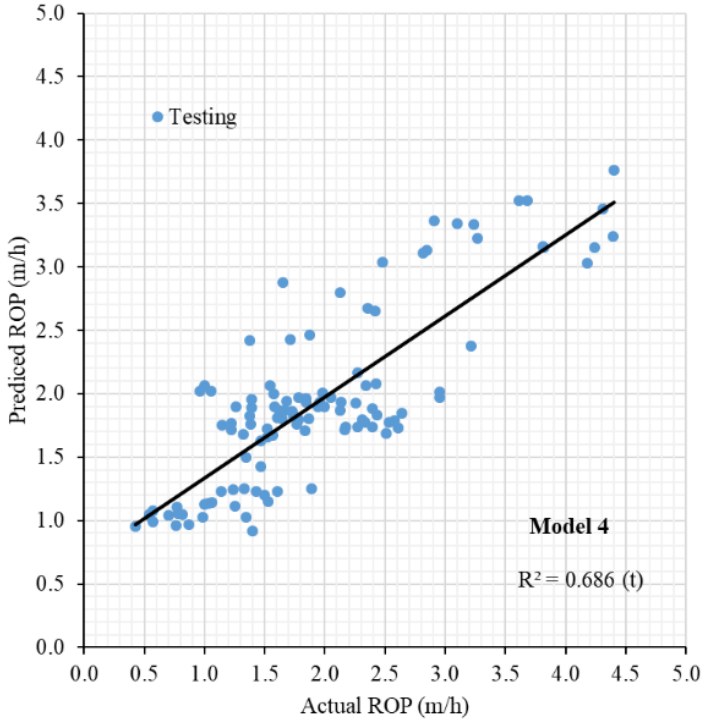

Figure 5.28. NLMR model 4 for estimating TBM penetration for testing dataset

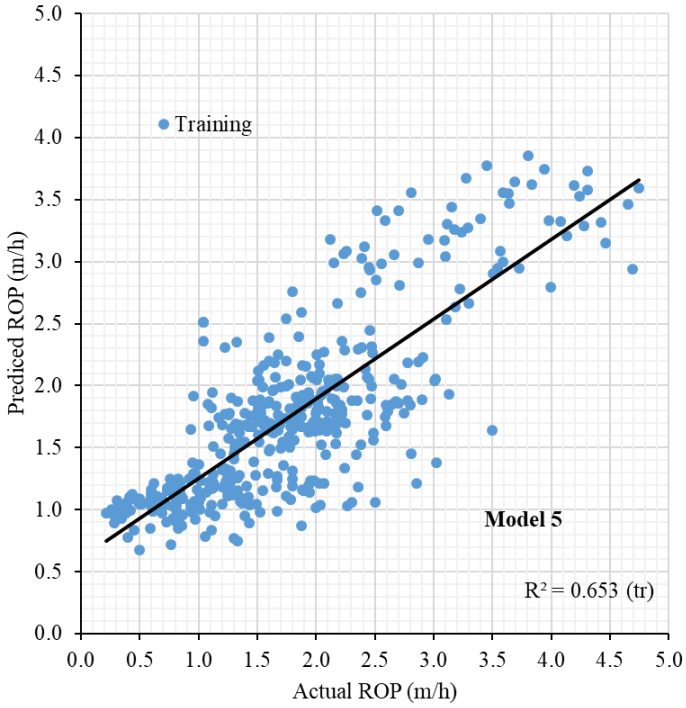

Figure 5.29. NLMR model 5 for estimating TBM penetration for training dataset

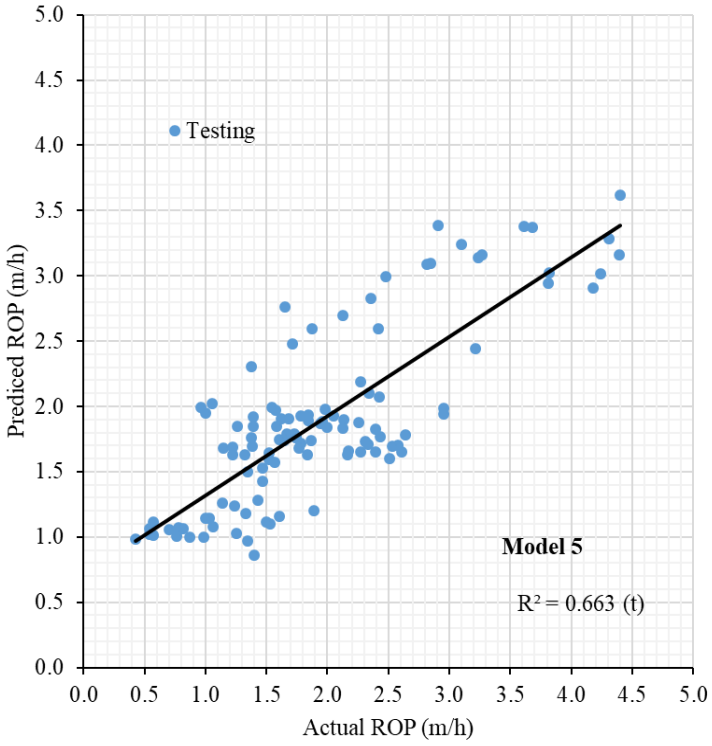

Figure 5.30. NLMR model 5 for estimating TBM penetration for testing dataset

5.4. Evaluation of Developed Models

To select the best LMR and NLMR equations for predicting the ROP, a score ranking method (Zorlu, et al. 2008) is used and the result of the analysis is summarized herein. Each performance (statistical) index was ordered in its class based on the capacity of models and the best total score of each model was found and assigned to obtain the highest rating among the models. In order to obtain the score ranking for each model, R^2, RMSE, RRMSE, MAD, MAPE and VAF were calculated and examined herein (Table 5.5). A score ranking values were calculated and assigned for each training and testing dataset separately to obtain detailed statistical indices (Table 5.6 to 5.9).

Table 5.5. Statistical performance indices used for determining the best model obtained in the study

Index	Evaluation Metric	Equations	Performance Description
1	Coefficient of determination	$R^2 = 1 - \frac{\sum_i (y_m - y_p)^2}{\sum_i (y_m - \bar{y}_p)^2}$	Higher values are better
2	Root Mean Square Error	$RMSE = \sqrt{\sum_{i=1}^{N} \frac{(y_m - y_p)^2}{N}}$	Lower values are better
3	Relative Root Mean Square Error	$RRMSE = \sqrt{\frac{\frac{1}{N}\sum_{i=1}^{N}(y_m - y_p)^2}{\sum_{i=1}^{N}(y_p)^2}}$	Lower values are better
4	Mean Absolute Deviation	$MAD = \frac{1}{N}\sum_{i=1}^{N} \frac{\lvert y_m - m \rvert}{N}$	Lower values are better
5	Mean Absolute Percentage Error	$MAPE = \frac{1}{N}\sum_{i=1}^{N} \frac{\lvert y_m - y_p \rvert}{y_m}$	Lower values are better
6	Variance Account For	$VAF = 1 - \frac{Var(y_m - y_p)}{Var(y_m)}$	Higher values are better

y_m: measured values, y_p: predicted values, $\bar{y}_p$: the mean of the predicted values, m: mean, N: total observed sample, p: number of independent variables, Var: Variance

After computing the statistical indices of each model, score ranking is performed to obtain the best model. The computation of score ranking can be explained as follows. For example, R^2 values of 0.516, 0.525, 0.536, 0.569 and 0.566 were obtained for train 1 to train 5 of the LMR technique, respectively (Table 5.6). Hence, their ratings were assigned as 1, 2, 3, 5 and 4, respectively. This procedure was repeated for each performance index as well as each predictive model (i.e. LMR and NLMR). After this process, the obtained ratings for each dataset (training and testing) were summed up separately (Table 5.7 and 5.9). For example, the rating values of the LMR training dataset 1 were assigned as 1 for R^2, 4 for RMSE, 3 for RRMSE, 5 for MAD, 4 for MAPE and 4 for VAF, so the performance rating was computed as 20 for training set (Table 5.6 to 5.9). The final stage of selecting the best models is to compute the total rank by summing up the rank value of each dataset (training and testing) as listed in Table 5.7-5.9 for LMR and NLMR. According to total rank values in these tables, Model 5 (with total rank of 41) and Model 1 (with total rank of 42) exhibited the best performance capacities for LMR and NLMR models, respectively.

Table 5.6. Performance indices of LMR analysis

Model performance indices for training dataset						
Model #	RMSE	R^2	RRMSE	MAD	MAPE	VAF
1	0.058139684	0.515951931	0.024291855	0.000809474	0.000437990	47.202945251
2	0.064157189	0.525120150	0.016103969	0.001135495	0.000648149	44.976439586
3	0.059634091	0.535568794	0.022266662	0.001066303	0.000498119	49.599968875
4	0.059102205	0.568711304	0.020594968	0.000834698	0.000526605	40.780679995
5	0.052020927	0.566454178	0.027276885	0.000878334	0.000271471	45.240638083
Model performance indices for testing dataset						
Model #	RMSE	R^2	RRMSE	MAD	MAPE	VAF
1	0.011163589	0.570535602	0.027762691	0.000382535	0.000652309	51.866870263
2	0.011820870	0.603787835	0.025829986	0.000156376	0.000576024	49.908658102
3	0.008161616	0.603385695	0.034324107	0.000216307	0.000516928	52.126622457
4	0.007480204	0.568401325	0.016413968	0.000054553	0.000496887	43.671265772
5	0.002743333	0.575769874	0.027883070	0.000174371	0.000294040	48.694431799

Table 5.7. Ranking score of the developed LMR models based on their performance according to the evaluation metrics

Ranking scores for the training dataset								
Model #	$Rank^1$	$Rank^2$	$Rank^3$	$Rank^4$	$Rank^5$	$Rank^6$	Rank of training	
1	4	1	2	5	4	4	20	
2	1	2	5	1	1	2	12	
3	2	3	3	2	3	5	18	
4	3	5	4	4	2	1	19	
5	**5**	**4**	**1**	**3**	**5**	**3**	**21**	
Ranking scores for the testing dataset								
Model #	$Rank^1$	$Rank^2$	$Rank^3$	$Rank^4$	$Rank^5$	$Rank^6$	Rank of testing	Total Score
1	2	2	3	1	1	4	13	33
2	1	4	4	4	2	3	18	30
3	3	5	1	2	3	5	19	37
4	4	1	5	5	4	1	20	39
5	**5**	**3**	**2**	**3**	**5**	**2**	**20**	**41**

*Notation number on each rank refers to the rank of each statistical index respectively.

Table 5.8. Performance indices of NLMR analysis

Model performance indices for the training dataset						
Model #	RMSE	R^2	RRMSE	MAD	MAPE	VAF
1	0.026383707	0.665854204	0.040001425	0.000278045	0.000440419	66.585175890
2	0.028407339	0.669501496	0.037452316	0.000015315	0.000297852	42.001913738
3	0.027822878	0.652016112	0.037339036	0.000245600	0.000395175	36.341383994
4	0.030746238	0.667552341	0.040878208	0.000266700	0.000410332	33.440263398
5	0.028695719	0.652637146	0.037470269	0.000236779	0.000382931	36.664559920
Model performance indices for the testing dataset						
Model #	RMSE	R^2	RRMSE	MAD	MAPE	VAF
1	0.000203491	0.683131106	0.033395432	0.000264123	0.000516482	67.869965116
2	0.001578283	0.692365030	0.037308977	0.000422114	0.000568996	48.225752363
3	0.002738501	0.665923801	0.034175020	0.000270881	0.000566562	44.618028167
4	0.000670878	0.685845306	0.033272547	0.000242707	0.000502354	40.734176507
5	0.003101137	0.663283042	0.034172482	0.000280307	0.000568398	44.246854095

Table 5.9. Ranking score of the developed NLRM models based on their performance according to the evaluation metrics

Ranking scores for training dataset								
Model #	$Rank^1$	$Rank^2$	$Rank^3$	$Rank^4$	$Rank^5$	$Rank^6$	Rank of training	
1	**5**	**3**	**2**	**1**	**1**	**5**	**17**	
2	3	5	4	5	5	4	26	
3	4	1	5	3	3	2	18	
4	1	4	1	2	2	1	11	
5	2	2	3	4	4	3	18	
Ranking scores for testing dataset								
Model #	$Rank^1$	$Rank^2$	$Rank^3$	$Rank^4$	$Rank^5$	$Rank^6$	Rank of testing	Total Score
1	5	3	4	4	4	5	25	**42**
2	3	5	1	1	1	4	15	41
3	2	2	3	3	3	3	16	34
4	4	4	5	5	5	2	24	35
5	1	1	2	2	2	1	10	28

CHAPTER 6：RESULTS AND DISCUSSIONS

In this study, empirical models consequently equations are introduced for the aim of industry, literature and academia. However, it is obvious that each model, -not only empirical, but also artificial intelligences (AI) models and theories, - has some advantages and disadvantages together with the capability and applicability of the models to the real-world problem. The most important contribution of this study to the literature is a dataset developed based on six different rock tunnels excavated into different rock types from sedimentary to gneiss rocks. Also, the obtained equations have very reliable input variables from both rock and machine specification points in practice. Since introduced WFI is a new input for estimating TBM penetration and the input parameters of these models are different than current models, comparing the output of the study with literature is not valuable. However, validation of each model was examined via testing part of the dataset.

To show the detailed quantified statistical indices of each model, the detailed score ranking of each model in LMR and NLMR are given in Figures 6.1 and 6.2 respectively. Model 5 for LMR and Model 1 for NLMR approaches are the most precise among the others. Since the problem is complex and non-linear, using NLMR is the best in comparison with linear approaches. Due to that Model 1 having less input the most accurate result obtained via NLMR is the best model among them. So, the models developed herein are crucially and significantly important for the industry. However, it should be noted that empirical models should be used for similar rock types and rock environments and geological conditions. So, the developed models herein should be used with care trying several empirical approaches both linear, non-linear or hybrid equations including both LMR and NLMR cases.

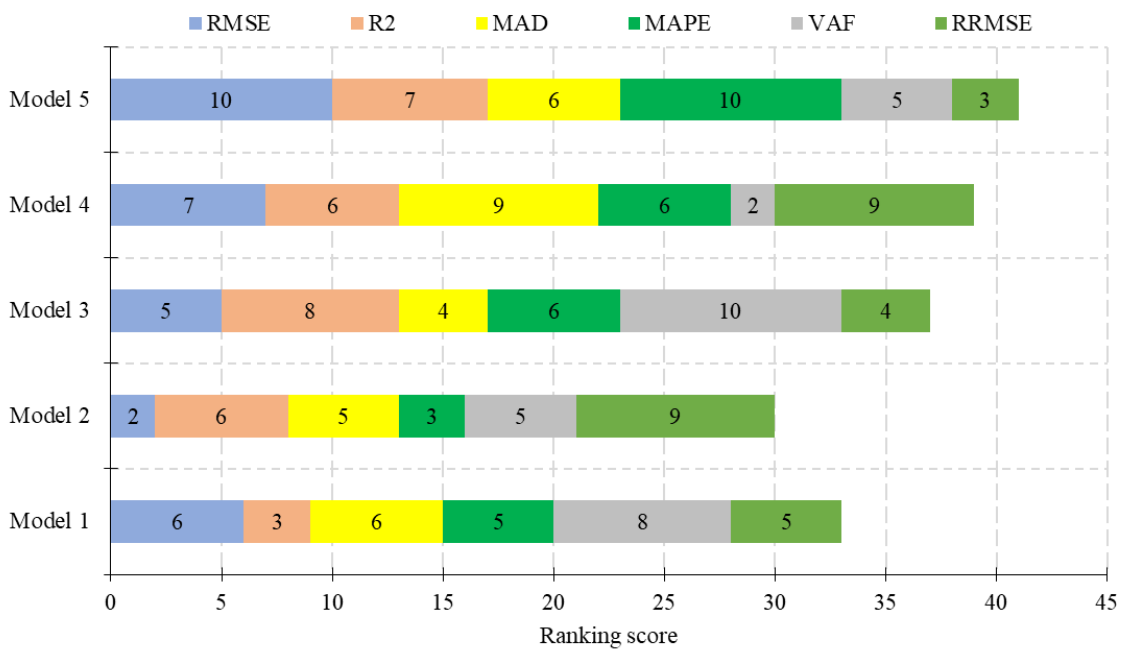

Figure 6.1. Visual presentation of ranking of the LMR models based on their performance.

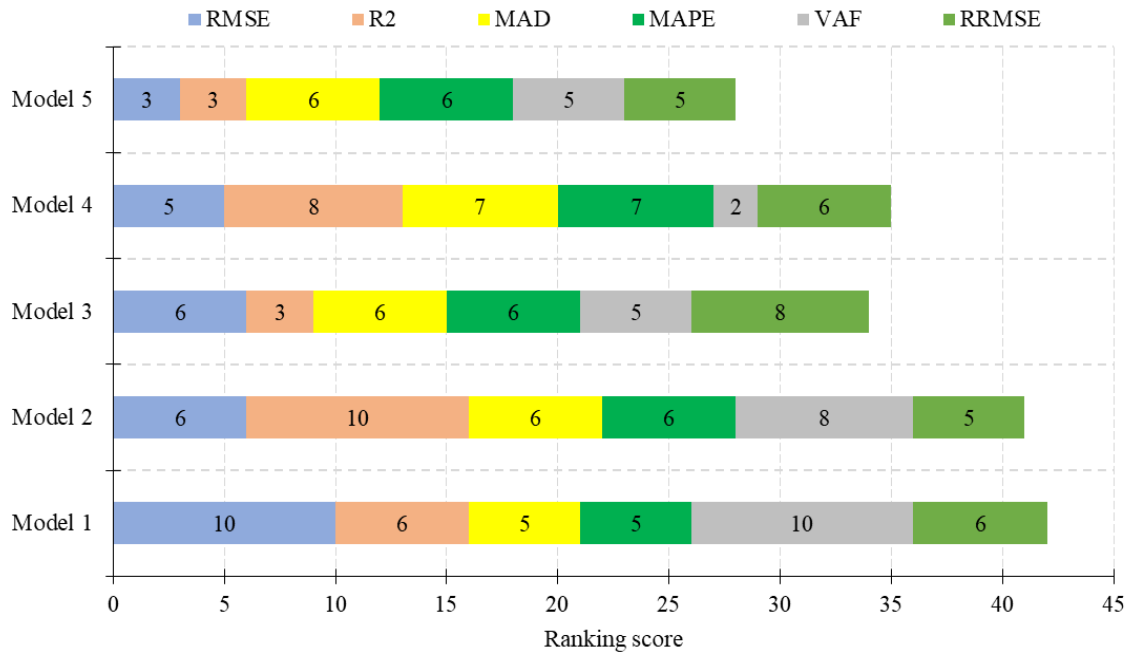

Figure 6.2. Visual presentation ranking of the NLMR models based on their performance.

The most accurate NLMR model (Eq.5.17) is compared with actual ROP obtained in the field in Figure 6.3. It is also found that Model 5 (Eq.5.18) and Model 1 (Eq.5.20) show reliable agreement with the actual ROP along the tunnel chainage, for LMR and NLMR models, respectively. Further, the Model 2 (Eq.5.18) obtained via NLMR could be utilized alternatively in the situation where selection of machine type (MTc) has a priority in the early stage of tunneling project. It should be stated that the models developed herein are good enough to estimate the rate of penetration however, scheduling including time and money as well as safety is also an important part of the construction projects; due to that, obtained results should be one of the input variables to generate a design in tunneling rather than an independent parameter. Then, the output of the models may need to be adjusted based on different rock types, and the frequency of discontinuities along the tunnels. The accuracy of LMR are lower than the NLMR models any case (Tables 5.6-5.7). Also, the equations developed via NLMR are more applicable for reality since if one of these inputs is not available, those NLMR equations (Eq.5.17-5.21) yield to zero. On the other hand, LMR equations (Eq.5.12-5.16) still give some outputs that are not accurate or reliable in practice. Also, it should be mentioned that the models do not have input for the orientation of the discontinuities. That means the obtained output for any project should be adjusted according to the alpha angle obtained as a function of tunnel direction and orientation of discontinuities in the rock mass.

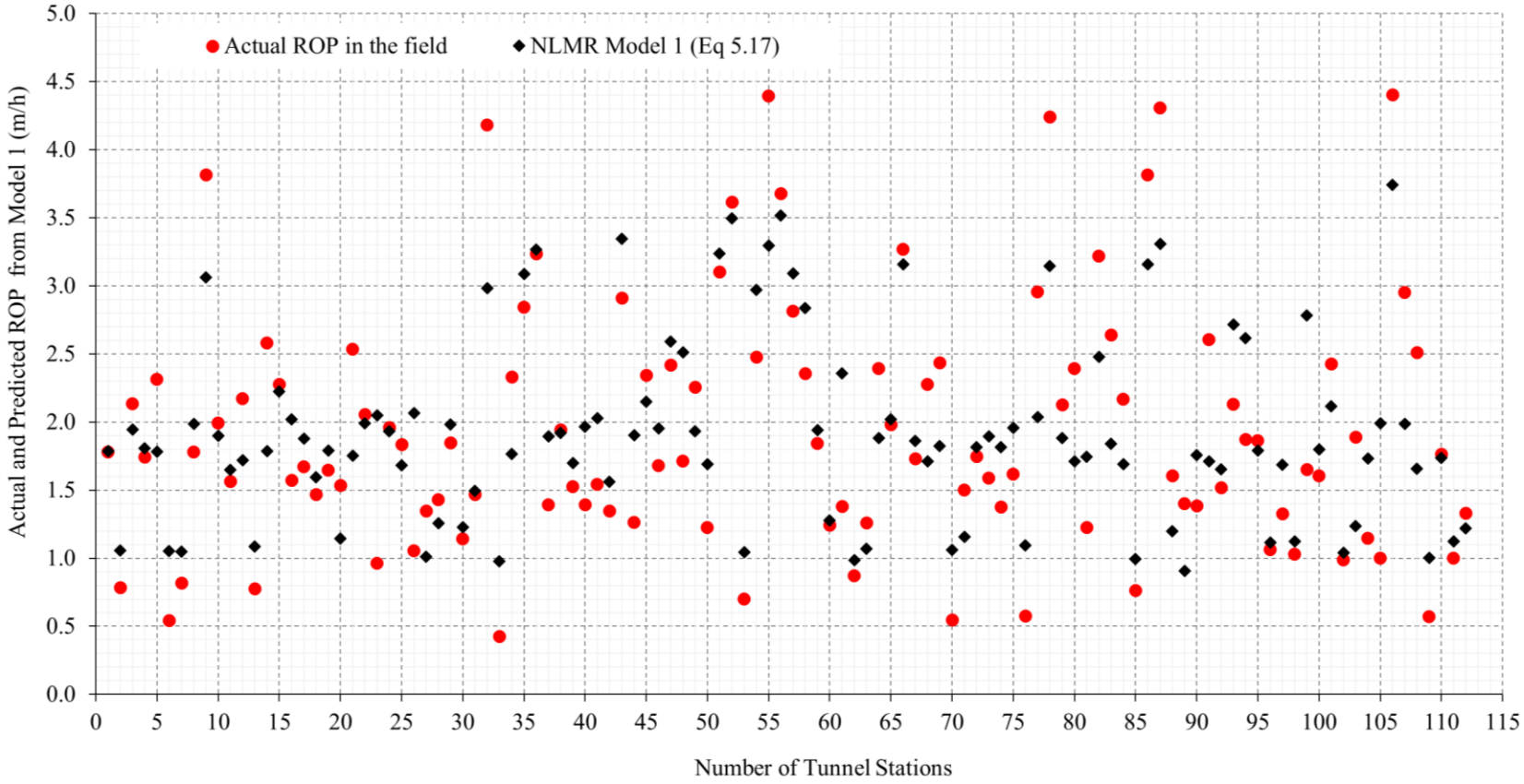

Figure 6.3. The result of the NLMR Model 1 in comparison with Actual ROP obtained in the field

CHAPTER 7：CONCLUSIONS AND RECOMMENDATIONS

7.1. Conclusions

In this thesis, numerous LMR and NLMR equations were developed using a variety of input parameters including both rock properties and machine specifications. After that, the best five LMR and five NLMR models were obtained and introduced to the literature. To select the input variables for the models, Pearson correlations and simple regression among the variables in the dataset are conducted. Then equations obtained via multiple variable regression and statistical analysis are introduced herein. To decide the best one among the developed models, statistical indices including R^2, RMSE, RRMSE, MAD, MAPE, and VAF are evaluated and the total score ranking method is used for the final decision. Based on the findings, it is stated that Model 1 developed using the NLMR approach is the most accurate one among them, since the total ranking score of the Model 1 is the highest at 42 with few input variables (Eq.5.17). Furthermore, some other models such as Model 5 for LMR and Model 2 for NLMR both having total score ranking at 41, also show good results in comparison with others; however, with high score ranking and a few reliable inputs including UCS, CHD, F_n, WFI and RPM, Model 1 via NLMR is the best capability and applicable; so, it deserves to be credited. It is concluded that the model should be used for similar rocks ranges from sedimentary to igneous and granitic gneiss as in dataset; on the other hand, the orientation of discontinuities in the rock mass, weathering degree and other unquantified rock features e.g., textural coefficient of rocks also should be considered in practice. Due to that, the developed model has the potential to be updated using the mentioned parameters of the rock mass for future research consideration.

7.2. Recommendations

In this research, empirical models are developed for the estimating TBM penetration rate in rock mass. As inputs variable, the models include the properties of intact rock, rock mases and also TBM specifications to obtain the aim. Inputs of the multi variable linear and non-linear models developed are: The uniaxial compressive strength of intact rocks; discontinuity frequency and properties in rock mass as a fracture index and weighted fracture index obtained via rock mass properties; TBM specifications including individual cutter load, RPM, CHD. It is obvious that the model obtained is reliable and acceptable from practical point of view to be used for TBM projects. However, as every model has, developed models also have some room to be improved. From this point of view, obtained models including Eq.5.17 or other non-linear multivariable models, may need some extra inputs to account of variables that influence the TBM penetration. It is known that texture of rock, rock brittleness, and also alpha angle, the angle between the plane of weakness (fractures) and TBM driving direction, have also impact on the output of the models. Due to that, the introduced models may be improved by adding those inputs such as alpha angle and texture coefficient or brittleness index into the model equations; however, these improvements should be made with care since the database used herein is very comprehensive and including wide range of rock properties and rock types and also several projects.

Nomenclature

AI = Artificial Intelligent

AR = Advance Rate

BI = Brittleness Index

BTS = Brazilian Tensile Strength

CCS = Constant Cross Section

CHD = Cutter Head Diameter

CLI = Cutter Life Index

CM = Continuous Miner

CSM = Colorado School of Mines

Dc = Diameter of discs

DB = Drill-Blast

DEM-UDEC = Discrete Element Method

DPW = Distance between Planes of Weakness

DRI = Drilling Rate Index

F_n = Cutter force

FI = Fractured Index

RFI =Rock Fracture Index

FPI = Field Penetration Index

GWCT = Ghomrood Water Conveyance Tunnel

KWCT = Karaj Water Conveyance Tunnel

LDS = Longwall Drum Shear

LBC = Breakability Coefficient

LCM = Linear Cutting Machine

LMR = Linear Multiple Regression

MAD = Mean Absolute Deviation

MAPE = Mean Absolute Percentage Error

MCSM = Codified CSM Model

MTc = Machine Type code

Nc = Number of discs

NLMR = Non-linear Multiple Regression

NPR = Net Penetration Rate

NTNU = Norwegian Institute of Technology

PR = Penetration Rate

QFWT = Queens Fresh Water Transfer

R^2 = Coefficient of determination

RBM = Raise Boring Machine

RME = Rock Mass Excavatability

RMSE = Root Mean Square Error

ROP = Rate of Penetration

RPM = Revolution Per Minutes

RRMSE = Relative Root Mean Square Error

RQD = Rock Quality Designation

RTc = Rock Type code

SER = Specific Excavation Rate

SLe = Length of tunnel segment

S_p = Spacing of joints

S_t = Spacing of fissures

SP = Specific Penetration

TBM = Tunnel Boring Machine

TH = Cutterhead net Thrust

UCS = Uniaxial Compressive Strength

VAF = Variance Account For

WFI = Weighted Fracture Index

ZWCT = Zagros Water Conveyance Tunnel

References

(1) Adoko, A.C., Gokceoglu, C, Yagiz, S. (2017) Bayesian prediction of TBM penetration rate in rock mass. Engineering Geology, 226(30), 245-256.

(2) Aeberli, U., and Wanner, H. (1978) On the Influence of Geologic Conditions at the Application of Tunnel Boring Machines. In Proc. 3rd Int. Cong., Int. Assoc. Eng. Geol., Madrid, section III, vol.2, pp.7-14.

(3) Alber, M. (2008) An integrated approach to penetration, advance rates and disc cutter wear for hard rock TBM drives, Geomechanik und Tunnelbau, 29-37.

(4) Altindag, R. (2010) Assessment of some brittleness indexes in rock-drilling efficiency. Rock Mechanics and Rock Engineering, 43:361-370.

(5) Armaghani, D.J., Mohd Amin M.F., Yagiz, S, Faradonbeh, R.S., Abdullah, RA. (2016) Prediction of the uniaxial compressive strength of sandstone using various modeling techniques. Int. J. Rock Mech. Min. Sci. 85,174-186.

(6) Armaghani, J.D., Yagiz, S., Mohamad, E.T., Zhou, J. (2021) Prediction of TBM performance in fresh through weathered granite using empirical and statistical approaches**.** Tunn. Undergr. Space Technol. 118, 104183.

(7) Armaghani, D.J., Mohamad, ET., Narayanasamy, M.S., Narita, N., Yagiz, S. (2017) Development of hybrid intelligent models for predicting TBM penetration rate in hard rock condition. Tunnelling and Underground Space Technology, 63, 29-43.

(8) Armetti, G., Migliazza, M.R., Ferrari, F., Berti A., padovesa, P. (2018) Geological and mechanical rock mass conditions for TBM performance prediction. The case of "La Maddalena" exploratory tunnel, Chiomonte (Italy). Tunneling and Underground Space technology, 77;115-126.

(9) Barton N. (1999) TBM performance estimation in rock using Q_{TBM}. Tunn. Tunn. Int. 31, 30–34.

(10) Barton, N. (2000) TBM Tunneling in Jointed and Faulted Rock. Balkema, Brookfield, p. 173.

(11) Baskerville, C.A., and Mose, G.D. (1989) The separation of the Hartland formation and Ravenswood granodiorite from the Fordham gneiss at Cameron's line in the New York City area. Northeastern Geology 11 (1), 22-28.

(12) Benardos, A., Kaliampakos, D. (2004) Modelling TBM performance with artificial neural networks, Tunnelling and Underground Space Technology 19(6):597-605.

(13) Benato, A., Oreste, P. (2015) Prediction of penetration per revolution in TBM tunneling as a function of intact rock and rock mass characteristics. Int. J. Rock Mech. Min. Sci. 74, 119–127.

(14) Bieniawski, Z.T., Celada Tamames, B., Galera Fernandez, J.M. and Hernandez Alvarez, M. (2006) Rock Mass Excavability (RME) indicator: New way to selecting the optimum tunnel construction method, Tunneling and Underground Space Tech 21, 3, 237-237.

(15) Bieniawski, Z.T., Celada, B., Galera, J.M. (2007) Predicting TBM excavatability. Tunnels and Tunnelling International, 5p.

(16) Bieniawski, Z.T., Celada, B., Galera, J.M. and Tardaguila I. (2008) New Application of the excavatability index for selection of TBM types and predicting their performance. 10p. Rapid Excavation and Tunnelling Congress, USA

(17) Bilgin, N., Copur, H., Balci, C. (2013) Mechanical excavation in mining and civil industries. CRC Press, Taylor and Francis Group, ISBM: 0429074115.

(18) Blindheim, O.T. (1979) Boreability predictions for tunneling. Ph.D.thesis. Department of geological engineering. The Norwegian Institute of Technology.

(19) Bruland, A. (1998) Hard Rock Tunnel Boring, PhD thesis, Volumes 1-10, NTNU, Norway.

(20) Cassinelli F, Cina S, Innaurato N, Mancini R, Sampaolo A. (1982) Power consumption and metal wear in tunnel-boring machines: analysis of tunnel-boring operation in hard rock. In: Tunneling 82, London. Inst. Min. Metall., pp. 73–81.

(21) Cheema, S. (1999) Development of a rock mass boreability index for the performance of tunnel boring machines. Doctoral dissertation, Department of Mining engineering, Colorado School of Mines, Gold Colorado, USA.

(22) Chen, K., Jiao, S., Wang, J. (2023) TBM Design and Construction. Springer, Berlin.

(23) Farmer, I.W., Glossop, N.H. (1980) Mechanics of disc cutter penetration. Tunnels. Tunn. Int. 12 (6), 22–25.

(24) Farrokh, E., Rostami, J. & Laughton, C. (2012). Study of various models for estimation of penetration rate of hard rock TBMs, in Tunnelling and Underground Space Tech, 30, 110-123.

(25) Fatemi, S.A., Ahmadi, M., Rostami, J. (2018). Evaluation of TBM performance prediction models and sensitivity analysis of input parameters. Bull. Eng. Geol. Environ. 77, 501–513.

(26) Gehring, K. (1995) Leistungs und Verschleißprognose im maschinellen Tunnelbau-Felsbau, 13(6): 493-448.

(27) Gertsch, R.E. (2000) Rock toughness and disc cutting, Ph.D. Thesis, T-7856, 256p, UMR, USA.

(28) Gong, M.Q., Zhao, J., Jiao, Y. (2005) Numerical modeling of the effects of joint orientation on rock fragmentation by TBM cutters. Tunnelling and Underground Space technology, 20(2), 183-191

(29) Gong, Q.M., Zhao, J. (2009) Development of a rock mass characteristics model for TBM penetration rate prediction, International Journal of Rock Mechanics, and Mining Sciences, 46(1):8–18.

(30) Goodarzi, S., Hassanpour, J., Yagiz, S., Rostami, J. (2021) Predicting TBM performance in soft sedimentary rocks, case study of Zagros Mountains water tunnel projects. Tunn. Undergr. Space Technol. 109, 103705.

(31) Graham, P.C. (1976) Rock exploration for machine manufacturers. Explor. Rock Eng. 173–180.

(32) Grima, M.A., Bruines, P.A., Verhoef, P.N.W. (2000) Modeling tunnel boring machine performance by neuro-fuzzy methods. Tunnelling and Underground Space Technology. 15(3), 259-269.

(33) Hamidi, J.K., Shahriar, K., Rezai, B., Rostami, J. (2010) Performance prediction of hard rock TBM using Rock Mass Rating (RMR) system. Tunn, Undergr. Space Technol. 25 (4), 333–345.

(34) Hassanpour, J., Rostami, J., Khamehchiyan, M., Bruland, S. (2009) Developing new equations for TBM performance prediction in carbonate-argillaceous rocks: a case history of Nowsood water conveyance tunnel. Geomechanics and Geoengineering: An International Journal. 4(4): 287-297

(35) Hassanpour, J., Rostami, J., Khamehchiyan, M., Bruland, A., Tavakoli, H.R. (2010) TBM performance analysis in pyroclastic rocks: a case history of Karaj water conveyance tunnel, Rock Mech., & Eng., 43 (4), 427-445.

(36) Hassanpour, J., Rostami, J., Zhao, J. (2011) A new hard rock TBM performance prediction model for project planning, Tunnelling and Underground Space Technology, 26 (5); 595-603.

(37) Hassanpour, J., Rostami, J., Zhao, J., Azali, S.A. (2015) TBM performance and disc cutter wear prediction based on ten years' experience of TBM tunneling in Iran. Geomechanics and Engineering, 8(3); 239-247.

(38) Hassanpour, J., Vanani, A.A., Rostami, J., Cheshomi, A. (2018) Evaluation of common TBM performance prediction models based on field data from the second lot of Zagros water conveyance tunnel (ZWCT2). Tunnelling and Underground Space Technology, 52:147-156

(39) Hassanpour, J. (2018) Development of an empirical model to estimate disc cutter wear for sedimentary and low to medium grade metamorphic rocks. Tunnelling and Underground Space Technology, 75(5), 90-99.

(40) Hassanpour, J. (2022) Personel connection and communication, University of Tehran Iran.

(41) Hassanpour, J., Kazemi, C., Rostami, J. (2024) Introduction of a modified Qtbm model for predicting TBM penetration rate in rock, based on data from mechanized tunneling project in Iran. Bull. Eng. Geol. Environ. 83,165.

(42) He, M., Zhang, Z., Li, N. (2021) Prediction of fracture frequency and RQD for the fractured rock mass using drilling logging data. B Eng Geol Environ 80(6), 4547-4557.

(43) Hucka, V., Das, B. (1974) Brittleness determination of rocks by different methods. International Journal of Rock Mechanics and Mining Sciences. 11: 389-392.

(44) Hughes, H.M. (1986) The relative cuttability of coal-measures stone. Min. Sci. Technol. 3 (2), 95–109.

(45) IBM SPSS Statistics (2024) https://www.ibm.com/support/pages/downloading-ibm-spss-statistics-24

(46) Innaurato, N., Mancini, A., Rondena, E., Zaninetti, A. (1991) Forecasting and Effective TBM Performances in a Rapid Excavation of a Tunnel in Italy. 7th International ISRM Congress. International Society for Rock Mechanics and Rock Engineering.

(47) Johannessen, O. (1976) New prediction model for full-face tunnel boring. Rock Blasting Conference, 14, 61.

(48) Khosravi, M., Ramezanzadeh, A., Zare, S. (2021) Effects of joint orientation and spacing on the boreability of jointed rock mass using tunnel boring machines. Arabian J of Geosciences, 14,61.

(49) Kim, T. (2004) Development of a Fuzzy Logic Based Utilization Predictor Model for Hard Rock Tunnel Boring Machines, PhD Thesis, Colorado School of Mines 2004.

(50) Klein, S., Schmoll, M., Avery, T. (1995) TBM performance at four hard rock tunnels in California. In: Williamson, G., Gowing, S. (eds.), Proc.RETC, S. Francisco, 61-75.

(51) Lislerud, A. (1988) Hard rock tunnel boring: prognosis and costs. Tunneling and Underground Space Technology 3 (1), 9–17.

(52) Lislerud, A. (1997). Principles of Mechanical Excavation. Possiva report 97-12, Helsinki, Finland (1997). ISBN 951-652-037-5.

(53) Macias, F.J., Jakobsen, P.D., Seo, Y., Bruland, A. (2014) Influence of rock mass fracturing on the net penetration rates of hard rock TBMs. Tunn. Undergr. Sp. Technol. 44,108-120.

(54) Macias, F.J. (2016) Hard Rock Tunnel Boring; Performance Predictions and Cutter Life Assessments, PhD Thesis, 2016:350 NTNU, Trondheim, Norway.

(55) Maidl, B., Schmid, L., Ritz W., Herrenknecht, M. (2008). Hard Rock Tunnel Boring Machines. Erns and Sohn, ISBN 978-3-433-01676-3.

(56) Manapouri Project Report (2001) Evaluation of geologic condition and boreability. Reach 1, Manapouri Second Tailrace Tunnel No.2.Rocky Mountain Consultants, Colorado USA.

(57) Merguerian, C., Ozdemir, L. (2003) Rock mass properties and hard rock TBM penetration rate investigations, Queens Tunnel Complex, NYC Water Tunnel #3, Stage 2, In: Robinson, R.A. and Marquardt, J.M. (eds.) Proceedings of Rapid Excavation and Tunneling Conferences, 1019–1036.

(58) Merguerian, C. (1983) Tectonic significance of Cameron's Line in the vicinity of the Hodges Complex--an imbricate thrust model for Western Connecticut: American Journal of Science, v. 283, p. 341-368.

(59) Merguerian, C. (1996) Stratigraphy, structural geology, and ductile- and brittle faults of New York City, p. 53-77 in Benimoff, A. I. and Ohan A. A., chm., The Geology of New York City and Vicinity, Field guide and Proceedings, New York State Geological Association, 68th Annual Meeting, Staten Island, NY, 178 p.

(60) Nelson, P.P., Orourke, D., Kulhawy, F.H. (1983) Factors affecting TBM penetration rates in sedimentary rocks. 24th of US Symposium on Rock Mechanics. 227-238pp.

(61) Nelson, P.P. (1993) TBM performance analysis with reference to rock properties. Comprehensive Rock Engineering, Volume 4, Chapter 10. 261-289.

(62) Oraee, K., Khorami, M.T., Hosseini, N. (2012) Prediction of the penetration rate of TBM using adaptive neuro fuzzy inference system (ANFIS). In: Proceeding of SME Annual Meeting & Exhibit, From the Mine to the Market, Now It's Global, Seattle, WA, USA, pp. 297–302.

(63) Ozdemir, L. (1977). Development of theoretical equations for predicting tunnel borability. PhD, Thesis, T-1969, Colorado School of Mines, Golden, Co, USA, 1977.

(64) Ozdemir, L., Miller, R., Wang, F. (1978) Mechanical tunnel boring prediction and machine design. -Annual Report; Washington.

(65) Paltrinieri, E. (2015). Analysis of TBM tunneling performance in faulted and highly fractured rocks. Thesis no.6724, Ecole Polytechnique Federale De Lausanne, Switzerland.

(66) Pourhashemi, S.M., Ahangari, K., Hassanpour, J., Eftekhari, S.M. (2021) Evaluating the influence of engineering geological parameters on TBM performance during grinding process in limestone strata. Bull. Eng. Geol. Environ. 80, 3023–3040.

(67) Project report 1-83. (1985) Hard Rock Tunnel Boring. The Norwegian Institute of Technology.

(68) Project report 1-94. (1995) Hard Rock Tunnel Boring: The Norwegian Institute of Technology.

(69) Queens Project Report (2000) Rock properties and TBM performance evaluation reports. Vol.1-2, Earth Mechanics Institute of Colorado School of Mines, Golden Co USA.

(70) Rayatdust, H., Shahriar, K., Ahangari, K., Kamali-Bandpey, H. (2012) A Statistical Model for Prediction TBM Performance using Rock Mass Characteristics in the TBM Driven Alborz Tunnel Project. Res. J. Appl. Sci. Eng. Technol. 4, 5048–5054.

(71) Rostami, J. & Ozdemir, L (1993). A new model for performance prediction of hard rock TBMs. Retc Proc, Colorado School of Mines, Golden, Co, 793-809.

(72) Rostami, J. (1997) Development of a force estimation model for rock fragmentation with disc cutters through theoretical modeling and physical measurement of crushed zone pressure, PhD. Thesis, CSM, USA.

(73) Rostami, J. (2008) Hard Rock TBM cutterhead modeling for design and performance prediction, Geomechanik und Tunnelbau, Ernst & Sohn, January 2008.

(74) Rostami, J. (2016) Performance prediction of hard rock Tunnel Boring Machines (TBMs) in difficult ground, Tunnelling and Underground S pace technology, 57; 173-182.

(75) Rostami, J. (2022). Personel Connection and Communication, Colorado School of Mines, USA

(76) Roxborough, F. and Phillips, R. (1975). Rock Excavation by Disc Cutter. Int. J. Rock. Min. Sci & Geomech. Abstr. Vol. 12, 361-366.

(77) Salimi, A. (2021) Investigation and Evaluation of Rock Mass Characteristics for Development of New TBM Performance Prediction Model in Hard Rock Conditions. Ph.D. thesis. Institute of Geotechnical Engineering (IGS), University of Stuttgart, Stuttgart.

(78) Salimi, A. Esmaeilia, M. (2013) Utilising of linear and non-linear prediction tools for evaluation of penetration rate of Tunnel Boring Machine in hard rock condition. International Journal of Mining and Mineral Engineering, 4(3); 249-264

(79) Sanio, H.P. (1985) Prediction of the performance of disc cutters in anisotropic rocks. International Journal of Rock Mechanics and Mining Science & Geomechanics abstracts 22 (1985), No.3, p.153-161.

(80) Sapigni, M., Berti, M., Behtaz, E., Busillo, A., Cardone, G. (2002) TBM performance estimation using rock mass classification. Int J RockMech Min Sci 39:771–788.

(81) Sato, K., Gong, F., Itakura, K. (1991) Prediction of disc cutter performance using a circular rock cutting ring, in: proceedings 1st international mine mechanization and automation symposium, June, CSM, Golden Colorado.

(82) Sen, Z. (2014) Rock quality designation-fracture intensity index method for geomechanical classification. Arab J Geoscience. 7(7), 2915–2922.

(83) She L, Hu C, Li Y, Zhang S, Wang C, Wang Y, He M, Li S, Wang S. (2024) An empirical method for estimating TBM penetration rate using tunnelling specific energy. Tunn. Undergr. Space Technol. 144, 105525.

(84) Snowdon, R., Ryley, M., Temporal, J. (1982). A study of disc cutting in selected British rocks, Int. J. Rock Mech. and Min. Sci & Geomech. Abstr, 19, 3, 107-121.

(85) Stevenson, G. (1999) Empirical estimates of TBM performance in hard rock. In: Proceedings of the rapid excavation and tunneling conference, pp 993–1010

(86) Tang, S., Zang, X., Liu, Q., Zhang, Q., Li, X., Wang, H. (2024) Experimental study on the influences of cutter geometry and material on scraper wear during shield TBM tunnelling in abrasive sandy ground. J of Rock Mech and Geotechnical Eng., 16(2), 410-425 115, 104065.

(87) Tarkoy, P.J., Marconi, N. (1991) Difficult rock comminution and associated geological conditions. In Tunnelling’91. 14-18 April, pp.195-207

(88) Thuro, K., Plinninger, R.J. (2006) Hard rock tunnel boring, cutting, drilling and blasting: rock parameters for excavatability, In: Proceedings of the 10th ISRM International Congress, South Africa, 2003, 1227-1234.

(89) Torabi, S.R., Shirazi, H., Hajali, H., Monjezi, M. (2013) Study of the influence of geotechnical parameters on the TBM performance in Tehran-Shomal highway project using ANN and SPSS. Arab. J. Geoscience. 6, 1215–1227.

(90) Vali, B., Arpa, G. (2013) Finding the relationship between RQD and fracture frequency in the different Ok tedilithologies. Procedia Earth Planet Sci 6,403–410.

(91) Wanner, H. (1975) On the influence of geological conditions at the application of tunnel boring machines. Bulletin of the International Association of Engineering Geology. 12, 21–28.

(92) Wilfing, L.S.F. (2016) The Influence of Geotechnical Parameters on Penetration Prediction in TBM Tunneling in Hard Rock. PhD Thesis, Munich Technical University.

(93) Xu, H.Y., Gong, Q.M., Lu, J.W., Yin, L.J., Yang, F.W. (2021) Setting up simple estimating equations of TBM penetration rate using rock mass classification parameters. Tunn. Undergr. Space Technol. 115, 104065.

(94) Yagiz, S. (2002) Development of rock fracture and brittleness indices to quantify the effects of rock mass features and toughness in the CSM Model basic penetration for hard rock tunneling machines. PhD Thesis. Colorado School of Mines, Golden, Colorado, USA.

(95) Yagiz, S. (2008) Utilizing rock mass properties for predicting TBM performance in hard rock condition. Tunn. Undergr. Space Technol. 23 (3), 326–339.

(96) Yagiz, S., Gokceoglu, C., Sezer, E., Iplikci, S. (2009) Application of two non-linear prediction tools to the estimation of tunnel boring machine performance. Eng. Appl. Artif. Intell. 22, 808–814.

(97) Yagiz, S., Gokceoglu, C. (2010) Application of fuzzy inference system and nonlinear regression models for predicting rock brittleness. Expert Syst. Appl. 37, 2265–2272.

(98) Yagiz, S., Merguerian, C., Kim, T. (2010) Geological controls on the breakthrough of tunnel boring machines in hard rock crystalline terrains. ISRM International Symposium - EUROCK 2010, Lausanne, Switzerland, June 2010 5p.

(99) Yagiz, S. (2017) New equations for predicting the field penetration index of tunnel boring machines in fractured rock mass. Arab. J. Geoscience. 10, 33.

(100) Yagiz, S., Hassanpour, J., Rostami, J. (2024a) Introducing the concept of fracture index for performance prediction of hard rock TBMs. In Eurock2024-New challenges in rock mechanics and rock engineering, Spain 1513-1520.

(101) Yagiz, S., Yazitova, A., Smirnov, G., Thyagarajan, V.M., Hassanpour, J. (2024b) Appraisal of boreability characteristics of rocks to estimate the TBM advancement. 58th U.S. Rock Mechanics/Geomechanics Symposium, Golden, Colorado, USA, June 2024. Paper Number: ARMA-2024-0982.

(102) Yazitova, A., Yagiz, S. (2024) Performance analysis of drilling machines based on rock properties and machines specifications. Bull. Eng. Geol. Environ. 83, 37.

(103) Yazitova, A., Adoko, A.C., Hassanpour, J., Yagiz, S. (2025) Empirical models for estimating penetration rate of tunnel boring machines in rock mass. Bull. Eng. Geol. Environ. 84:55.

(104) Zorlu, K., Gokceoglu, C., Ocakoglu, F., Nefeslioglu, H.A., Acikalin, S. (2008) Prediction of uniaxial compressive strength of sandstones using petrography-based models. Eng. Geol. 96, 141–15.

Appendix A
Intact Rock and Rock Mass Properties
(Limited dataset)

Appendix A: Intact Rock and Rock Mass Properties (Continue)

Case #	SL_e (m)	FI (f/m)	WFI -	UCS (MPa)	Lithology and Rock Types (RT)
1	1.83	2.5	4.57	191	Massive Garnet Amphibolite and larger Mafic dikes
2	0.95	10	9.52	191	Massive Garnet Amphibolite and larger Mafic dikes
3	1.13	10	11.3	191	Massive Garnet Amphibolite and larger Mafic dikes
4	1.82	1.25	2.28	193	Massive Garnet Amphibolite and larger Mafic dikes
5	1.81	2.5	4.51	194	Massive Garnet Amphibolite and larger Mafic dikes
6	1.83	2.5	4.57	195	Massive Garnet Amphibolite and larger Mafic dikes
7	1.82	5.0	9.11	198	Massive Garnet Amphibolite and larger Mafic dikes
8	1.83	2.5	4.57	199	Massive Garnet Amphibolite and larger Mafic dikes
9	1.82	1.25	2.28	199	Massive Garnet Amphibolite and larger Mafic dikes
10	1.99	1.25	2.49	200	Massive Garnet Amphibolite and larger Mafic dikes
11	1.82	0.63	1.14	199	Massive Garnet Amphibolite and larger Mafic dikes
12	1.79	0.5	0.9	198	Mafic to Mesocratic Gneiss, Amphibolite, and Schist
13	1.79	5.0	8.95	188	Massive Garnet Amphibolite and larger Mafic dikes
14	1.8	5.0	9.0	188	Mafic to Mesocratic Gneiss, Amphibolite, and Schist
15	1.83	5.0	9.13	188	Mafic to Mesocratic Gneiss, Amphibolite, and Schist
16	1.81	1.25	2.26	191	Mafic to Mesocratic Gneiss, Amphibolite, and Schist
17	1.81	1.25	2.26	191	Mafic to Mesocratic Gneiss, Amphibolite, and Schist
18	1.82	0.63	1.14	192	Granitoid (felsic) Gneiss and Orthogneiss
19	1.81	1.25	2.26	193	Granitoid (felsic) Gneiss and Orthogneiss
20	1.81	1.25	2.26	194	Granitoid (felsic) Gneiss and Orthogneiss
21	0.72	0.63	0.45	197	Mafic to Mesocratic Orthogneiss
22	1.82	0.63	1.14	186	Mafic to Mesocratic Orthogneiss
23	1.81	0.63	1.13	185	Mafic to Mesocratic Gneiss, Amphibolite, and

Appendix A: Intact Rock and Rock Mass Properties (Continue)

Case #	SLe (m)	FI (f/m)	WFI -	UCS (MPa)	Lithology and Rock Types (RT)
24	1.81	0.63	1.13	184	Granitoid (felsic) Gneiss and Orthogneiss
25	1.81	1.25	2.26	183	Granitoid (felsic) Gneiss and Orthogneiss
26	1.82	1.25	2.27	183	Granitoid (felsic) Gneiss and Orthogneiss
27	1.84	1.25	2.3	182	Granitoid (felsic) Gneiss and Orthogneiss
28	1.82	2.5	4.55	182	Granitoid (felsic) Gneiss and Orthogneiss
29	1.15	1.25	1.44	183	Mafic to Mesocratic Orthogneiss
30	1.83	1.25	2.29	183	Mafic to Mesocratic Orthogneiss
31	1.83	1.25	2.28	186	Mafic to Mesocratic Orthogneiss
32	1.83	1.25	2.29	191	Mafic to Mesocratic Orthogneiss
33	1.82	0.63	1.14	193	Mafic to Mesocratic Orthogneiss
34	1.83	0.63	1.14	193	Mafic to Mesocratic Orthogneiss
35	1.83	0.63	1.14	193	Mafic to Mesocratic Orthogneiss
36	1.28	2.5	3.2	193	Massive Garnet Amphibolite and larger Mafic dikes
37	0.94	2.5	2.36	193	Mafic to Mesocratic Gneiss, Amphibolite, and Schist
38	1.83	2.5	4.58	193	Granitoid (felsic) Gneiss and Orthogneiss
39	0.94	2.5	2.36	193	Mafic to Mesocratic Gneiss, Amphibolite, and Schist
40	0.38	2.5	0.95	193	Mafic to Mesocratic Orthogneiss
41	1.83	0.5	0.91	191	Granitoid (felsic) Gneiss and Orthogneiss
42	1.79	0.63	1.12	189	Mafic to Mesocratic Orthogneiss
43	1.84	0.63	1.15	187	Mafic to Mesocratic Orthogneiss
44	1.82	2.5	4.56	186	Mafic to Mesocratic Gneiss, Amphibolite, and Schist
45	1.81	5	9.07	183	Mafic to Mesocratic Gneiss, Amphibolite, and Schist
46	1.81	10	18.11	173	Mafic to Mesocratic Orthogneiss
47	1.81	0.63	1.13	165	Mafic to Mesocratic Orthogneiss
48	1.83	1.25	2.28	164	Mafic to Mesocratic Orthogneiss
49	1.8	0.63	1.12	161	Mafic to Mesocratic Orthogneiss
50	1.82	0.63	1.14	161	Massive Garnet Amphibolite and larger Mafic dikes
51	1.82	2.5	4.55	159	Massive Garnet Amphibolite and larger Mafic dikes
52	0.59	5.0	2.96	145	Mafic to Mesocratic Orthogneiss
53	1.83	10	18.26	141	Mafic to Mesocratic Orthogneiss
54	1.82	10	18.16	140	Mafic to Mesocratic Orthogneiss
55	1.81	0.63	1.13	137	Mafic to Mesocratic Orthogneiss
56	1.82	1.25	2.27	137	Mafic to Mesocratic Orthogneiss

Appendix A: Intact Rock and Rock Mass Properties

Case #	SLe (m)	FI (f/m)	WFI -	UCS (MPa)	Lithology and Rock Types (RT)
57	1.8	2.5	4.5	135	Mafic to Mesocratic Gneiss, Amphibolite
58	1.8	5.0	8.99	136	Massive Garnet Amphibolite and larger Mafic dikes
59	1.82	2.5	4.56	136	Massive Garnet Amphibolite and larger Mafic dikes
60	1.81	1.25	2.27	136	Massive Garnet Amphibolite and larger dikes
61	1.82	0.63	1.14	137	Mafic to Mesocratic Gneiss, Amphibolite, and Schist
62	1.81	1.25	2.26	137	Mafic to Mesocratic Orthogneiss
63	1.83	0.63	1.14	138	Mafic to Mesocratic Orthogneiss
64	1.11	0.63	0.7	138	Mafic to Mesocratic Orthogneiss
65	1.82	0.63	1.14	139	Mafic to Mesocratic Gneiss, Amphibolite, and Schist
66	1.82	0.5	0.91	139	Mafic to Mesocratic Gneiss, Amphibolite, and Schist
67	1.82	0.5	0.91	139	Mafic to Mesocratic Gneiss, Amphibolite, and Schist
68	1.56	0.63	0.97	140	Mafic to Mesocratic Gneiss, Amphibolite, and Schist
69	1.83	0.63	1.14	141	Mafic to Mesocratic Gneiss, Amphibolite, and Schist
70	1.82	0.63	1.14	141	Mafic to Mesocratic Gneiss, Amphibole, schist
71	1.81	0.63	1.13	140	Mafic to Mesocratic Gneiss, Amphibolite, and Schist
72	1.81	1.25	2.26	139	Mafic to Mesocratic Gneiss, Amphibolite, and Schist
73	1.81	1.25	2.26	139	Mafic to Mesocratic Gneiss, Amphibolite, and Schist
74	1.65	0.63	1.03	137	Mafic to Mesocratic Gneiss, Amphibolite, and Schist
75	1.82	0.63	1.14	136	Mafic to Mesocratic Gneiss, Amphibolite, and Schist
76	1.82	0.63	1.14	136	Mafic to Mesocratic Gneiss, Amphibolite, and Schist
77	1.8	0.5	0.9	134	Granitoid (felsic) Gneiss and Orthogneiss
78	1.77	0.5	0.89	131	Mafic to Mesocratic Gneiss, Amphibolite, and Schist
79	1.82	0.63	1.14	130	Mafic to Mesocratic Gneiss, and Schist
80	1.82	0.63	1.14	129	Mafic to Mesocratic Gneiss, Amphibolite, and Schist

Appendix B

Tunnel Boring Machine Specifications and its performance in the field

(Limited dataset)

Appendix B: TBM Specifications and its performance in the field (Continue)

Case #	MTc	Fn (kN/c)	CHD (m)	RPM	Dc (m)	Nc -	ROP (m/h)
1	1	227	7.06	8.3	0.48	50	2.95
2	1	197	7.06	8.3	0.48	50	2.66
3	1	195	7.06	8.3	0.48	50	2.34
4	1	217	7.06	8.3	0.48	50	1.77
5	1	209	7.06	8.3	0.48	50	2.30
6	1	202	7.06	8.3	0.48	50	2.17
7	1	187	7.06	8.3	0.48	50	0.96
8	1	246	7.06	8.3	0.48	50	1.70
9	1	192	7.06	8.3	0.48	50	0.93
10	1	257	7.06	8.3	0.48	50	1.59
11	1	207	7.06	8.3	0.48	50	1.47
12	1	261	7.06	8.3	0.48	50	2.51
13	1	242	7.06	8.3	0.48	50	2.87
14	1	168	7.06	8.3	0.48	50	3.13
15	1	264	7.06	8.3	0.48	50	2.48
16	1	221	7.06	8.3	0.48	50	1.74
17	1	238	7.06	8.3	0.48	50	1.39
18	1	262	7.06	8.3	0.48	50	1.45
19	1	248	7.06	8.3	0.48	50	2.02
20	1	254	7.06	8.3	0.48	50	1.11
21	1	263	7.06	8.3	0.48	50	1.19
22	1	268	7.06	8.3	0.48	50	1.56
23	1	268	7.06	8.3	0.48	50	1.76
24	1	270	7.06	8.3	0.48	50	1.32
25	1	267	7.06	8.3	0.48	50	1.93
26	1	222	7.06	8.3	0.48	50	1.87
27	1	212	7.06	8.3	0.48	50	2.00
28	1	264	7.06	8.3	0.48	50	2.45
29	1	262	7.06	8.3	0.48	50	1.73
30	1	270	7.06	8.3	0.48	50	1.33
31	1	260	7.06	8.3	0.48	50	1.39
32	1	266	7.06	8.3	0.48	50	1.50
33	1	269	7.06	8.3	0.48	50	1.20
34	1	269	7.06	8.3	0.48	50	1.14
35	1	268	7.06	8.3	0.48	50	1.08
36	1	267	7.06	8.3	0.48	50	1.12
37	1	258	7.06	8.3	0.48	50	2.80
38	1	267	7.06	8.3	0.48	50	2.18
39	1	201	7.06	8.3	0.48	50	2.17
40	1	208	7.06	8.3	0.48	50	1.35

Appendix B: TBM Specifications and its performance in the field (Continue)

Case #	MTc	Fn (kN/c)	CHD (m)	RPM	Dc (m)	Nc -	ROP (m/h)
41	1	230	7.06	8.3	0.48	50	1.39
42	1	263	7.06	8.3	0.48	50	1.42
43	1	267	7.06	8.3	0.48	50	1.35
44	1	249	7.06	8.3	0.48	50	1.77
45	1	174	7.06	8.3	0.48	50	1.63
46	1	189	7.06	8.3	0.48	50	1.68
47	1	256	7.06	8.3	0.48	50	1.56
48	1	231	7.06	8.3	0.48	50	2.09
49	1	262	7.06	8.3	0.48	50	2.10
50	1	261	7.06	8.3	0.48	50	2.05
51	1	174	7.06	8.3	0.48	50	2.01
52	1	216	7.06	8.3	0.48	50	2.60
53	1	174	7.06	8.3	0.48	50	2.91
54	1	226	7.06	8.3	0.48	50	2.46
55	1	255	7.06	8.3	0.48	50	2.20
56	1	258	7.06	8.3	0.48	50	2.14
57	1	189	7.06	8.3	0.48	50	2.78
58	1	249	7.06	8.3	0.48	50	2.24
59	1	258	7.06	8.3	0.48	50	2.03
60	1	253	7.06	8.3	0.48	50	1.53
61	1	184	7.06	8.3	0.48	50	2.04
62	1	257	7.06	8.3	0.48	50	2.47
63	1	277	7.06	8.3	0.48	50	1.44
64	1	274	7.06	8.3	0.48	50	1.33
65	1	273	7.06	8.3	0.48	50	2.58
66	1	275	7.06	8.3	0.48	50	1.83
67	1	274	7.06	8.3	0.48	50	2.08
68	1	217	7.06	8.3	0.48	50	1.25
69	1	270	7.06	8.3	0.48	50	1.87
70	1	258	7.06	8.3	0.48	50	2.10
71	1	265	7.06	8.3	0.48	50	2.31
72	1	211	7.06	8.3	0.48	50	2.43
73	1	211	7.06	8.3	0.48	50	2.43
74	1	267	7.06	8.3	0.48	50	2.33
75	1	238	7.06	8.3	0.48	50	1.79
76	1	230	7.06	8.3	0.48	50	2.61
77	1	258	7.06	8.3	0.48	50	2.17
78	1	244	7.06	8.3	0.48	50	2.17
79	1	263	7.06	8.3	0.48	50	1.65
80	1	273	7.06	8.3	0.48	50	1.75

Appendix C
SPPS Program Output for the Best Five LMR Models

Model 1-Linear Multiple Regression Model

Variables Entered/Removed[a]

Model	Variables Entered	Variables Removed	Method
1	MT_c, UCS, WFI[b]	.	Enter

a. Dependent Variable: ROP

b. All requested variables entered.

Model Summary

Model	R	R Square	Adjusted R Square	Std. Error of the Estimate
1	.719[a]	.516	.513	.62221

a. Predictors: (Constant), MTc, UCS, WFI

ANOVA[a]

Model		Sum of Squares	df	Mean Square	F	Sig.
1	Regression	182.205	3	60.735	156.880	.000[b]
	Residual	170.730	441	.387		
	Total	352.935	444			

a. Dependent Variable: ROP

b. Predictors: (Constant), MTc, UCS, WFI

Coefficients[a]

Model		Unstandardized Coefficients B	Unstandardized Coefficients Std. Error	Standardized Coefficients Beta	t	Sig.
1	(Constant)	1.703	.202		8.445	.000
	UCS	-.005	.001	-.336	-8.042	.000
	WFI	.006	.002	.233	4.058	.000
	MT_c	.630	.145	.253	4.349	.000

a. Dependent Variable: ROP

$$\mathbf{ROP} = -\mathbf{0.005} \cdot \mathbf{UCS} + \mathbf{0.006} \cdot \mathbf{WFI} + \mathbf{0.63} \cdot \mathbf{MT_c} + \mathbf{1.703}$$

End

Model 2-Linear Multiple Regression Model

Variables Entered/Removed[a]

Model	Variables Entered	Variables Removed	Method
1	N_c, WFI, UCS[b]	.	Enter

a. Dependent Variable: ROP

b. All requested variables entered.

Model Summary

Model	R	R Square	Adjusted R Square	Std. Error of the Estimate
1	.725[a]	.525	.522	.61633

a. Predictors: (Constant), N_c, WFI, UCS

ANOVA[a]

Model		Sum of Squares	df	Mean Square	F	Sig.
1	Regression	185.418	3	61.806	162.708	.000[b]
	Residual	167.517	441	.380		
	Total	352.935	444			

a. Dependent Variable: ROP

b. Predictors: (Constant), N_c, WFI, UCS

Coefficients[a]

Model		Unstandardized Coefficients B	Unstandardized Coefficients Std. Error	Standardized Coefficients Beta	t	Sig.
1	(Constant)	3.770	.272		13.880	.000
	UCS	-.009	.001	-.620	-10.285	.000
	WFI	.006	.001	.222	4.121	.000
	N_c	-.016	.003	-.266	-5.267	.000

a. Dependent Variable: ROP

$$\mathbf{ROP} = -\mathbf{0.009} \cdot \mathbf{UCS} + \mathbf{0.006} \cdot \mathbf{WFI} - \mathbf{0.016} \cdot \mathbf{N_c} + \mathbf{3.770}$$

End

Model 3-Linear Multiple Regression Model

Variables Entered/Removed[a]

Model	Variables Entered	Variables Removed	Method
1	CHD, WFI, MT_c, UCS[b]	.	Enter

a. Dependent Variable: ROP

b. All requested variables entered.

Model Summary

Model	R	R Square	Adjusted R Square	Std. Error of the Estimate
1	.732[a]	.536	.532	.61016

a. Predictors: (Constant), CHD, WFI, MT_c, UCS

ANOVA[a]

Model		Sum of Squares	df	Mean Square	F	Sig.
1	Regression	189.127	4	47.282	127.003	.000[b]
	Residual	163.807	440	.372		
	Total	352.935	444			

a. Dependent Variable: ROP

b. Predictors: (Constant), CHD, WFI, MT_c, UCS

Coefficients[a]

Model		Unstandardized Coefficients		Standardized Coefficients		
		B	Std. Error	Beta	t	Sig.
1	(Constant)	3.213	.402		7.989	.000
	UCS	-.008	.001	-.585	-8.262	.000
	WFI	.004	.002	.157	2.650	.008
	MT_c	.330	.158	.133	2.089	.037
	CHD	-.092	.021	-.245	-4.312	.000

a. Dependent Variable: ROP

$$\mathbf{ROP} = -\mathbf{0.008} \cdot \mathbf{UCS} + \mathbf{0.004} \cdot \mathbf{WFI} + \mathbf{0.33} \cdot \mathbf{MT_c} - \mathbf{0.092} \cdot \mathbf{CHD} + \mathbf{3.213}$$

End

Model 4-Linear Multiple Regression Model

Variables Entered/Removed[a]

Model	Variables Entered	Variables Removed	Method
1	N_c, WFI, RPM, UCS, CHD[b]	.	Enter

a. Dependent Variable: ROP

b. All requested variables entered.

Model Summary

Model	R	R Square	Adjusted R Square	Std. Error of the Estimate
1	.754[a]	.569	.564	.58851

a. Predictors: (Constant), N_c, WFI, RPM, UCS, CHD

ANOVA[a]

Model		Sum of Squares	df	Mean Square	F	Sig.
1	Regression	200.891	5	40.178	116.008	.000[b]
	Residual	152.044	439	.346		
	Total	352.935	444			

a. Dependent Variable: ROP

b. Predictors: (Constant), N_c, WFI, RPM, UCS, CHD

Coefficients[a]

Model		Unstandardized Coefficients B	Unstandardized Coefficients Std. Error	Standardized Coefficients Beta	t	Sig.
1	(Constant)	.780	.639		1.221	.223
	UCS	-.009	.001	-.606	-8.953	.000
	WFI	.009	.001	.350	6.378	.000
	CHD	.561	.311	1.497	1.807	.071
	RPM	.278	.058	.540	4.763	.000
	N_c	-.080	.044	-1.336	-1.810	.071

a. Dependent Variable: ROP

$$\mathbf{ROP = -0.009 \cdot UCS + 0.009 \cdot WFI + 0.561 \cdot CHD + 0.278 \cdot RPM - 0.08 \cdot N_c + 0.78}$$

End

Model 5-Linear Multiple Regression Model

Variables Entered/Removed[a]

Model	Variables Entered	Variables Removed	Method
1	RPM, WFI, F_n, UCS[b]	.	Enter

a. Dependent Variable: ROP

b. All requested variables entered.

Model Summary

Model	R	R Square	Adjusted R Square	Std. Error of the Estimate
1	.753[a]	.567	.563	.58917

a. Predictors: (Constant), RPM, WFI, F_n, UCS

ANOVA[a]

Model		Sum of Squares	df	Mean Square	F	Sig.
1	Regression	200.203	4	50.051	144.190	.000[b]
	Residual	152.732	440	.347		
	Total	352.935	444			

a. Dependent Variable: ROP

b. Predictors: (Constant), RPM, WFI, F_n, UCS

Coefficients[a]

Model		Unstandardized Coefficients		Standardized Coefficients		
		B	Std. Error	Beta	t	Sig.
1	(Constant)	1.372	.249		5.498	.000
	UCS	-.009	.001	-.645	-11.944	.000
	WFI	.010	.001	.379	7.815	.000
	F_n	.001	.001	.048	1.136	.257
	RPM	.195	.023	.378	8.488	.000

a. Dependent Variable: ROP

$$\mathbf{ROP} = -\mathbf{0.009} \cdot \mathbf{UCS} + \mathbf{0.01} \cdot \mathbf{WFI} + \mathbf{0.001} \cdot \mathbf{F_n} + \mathbf{0.195} \cdot \mathbf{RPM} + \mathbf{1.372}$$

End

Appendix D
SPPS Program Output for the Best Five NLMR Models

Model 1-Non-linear Multiple Regression Model

Iteration History[b]

Iteration Number[a]	Residual Sum of Squares	Parameter						
		b1	b2	b3	b4	b5	b6	b7
1.0	4237616.007	.010	.010	.010	.010	.010	.010	.010
1.1	1073759.934	.014	.013	.009	.057	.020	.013	.019
2.0	1073759.934	.014	.013	.009	.057	.020	.013	.019
2.1	276339.562	.021	.017	.006	.146	.041	.018	.037
3.0	276339.562	.021	.017	.006	.146	.041	.018	.037
3.1	73734.287	.035	.026	.002	.310	.084	.026	.070
4.0	73734.287	.035	.026	.002	.310	.084	.026	.070
4.1	21414.088	.060	.041	-.002	.590	.175	.040	.125
5.0	21414.088	.060	.041	-.002	.590	.175	.040	.125
5.1	6215.945	.088	.060	-.016	1.006	.359	.062	.208
6.0	6215.945	.088	.060	-.016	1.006	.359	.062	.208
6.1	889.237	.074	.069	-.091	1.514	.542	.103	.309
7.0	889.237	.074	.069	-.091	1.514	.542	.103	.309
7.1	293.235	.098	.087	-.136	2.148	.910	.130	.436
8.0	293.235	.098	.087	-.136	2.148	.910	.130	.436
8.1	257.408	.157	.103	-.124	2.547	1.647	.129	.517
9.0	257.408	.157	.103	-.124	2.547	1.647	.129	.517
9.1	127.626	.163	.102	-.144	2.647	2.015	.133	.541
10.0	127.626	.163	.102	-.144	2.647	2.015	.133	.541
10.1	126.359	.197	.110	-.118	2.721	2.752	.126	.556
11.0	126.359	.197	.110	-.118	2.721	2.752	.126	.556
11.1	120.557	.207	.112	-.112	2.737	3.120	.125	.559
12.0	120.557	.207	.112	-.112	2.737	3.120	.125	.559
12.1	120.407	.230	.118	-.090	2.768	3.857	.119	.564
13.0	120.407	.230	.118	-.090	2.768	3.857	.119	.564
13.1	119.121	.238	.119	-.084	2.779	4.225	.117	.566
14.0	119.121	.238	.119	-.084	2.779	4.225	.117	.566
14.1	118.898	.255	.124	-.068	2.802	4.961	.113	.570
15.0	118.898	.255	.124	-.068	2.802	4.961	.113	.570
15.1	118.443	.269	.127	-.056	2.821	5.698	.110	.573
16.0	118.443	.269	.127	-.056	2.821	5.698	.110	.573
16.1	118.178	.282	.130	-.046	2.839	6.435	.107	.576
17.0	118.178	.282	.130	-.046	2.839	6.435	.107	.576
17.1	118.033	.293	.133	-.037	2.854	7.171	.104	.579

18.0	118.033	.293	.133	-.037	2.854	7.171	.104	.579
18.1	117.967	.304	.135	-.029	2.869	7.908	.102	.582
19.0	117.967	.304	.135	-.029	2.869	7.908	.102	.582
19.1	117.924	.308	.136	-.027	2.874	8.215	.101	.583
20.0	117.924	.308	.136	-.027	2.874	8.215	.101	.583
20.1	117.923	.308	.136	-.027	2.875	8.209	.101	.583
21.0	117.923	.308	.136	-.027	2.875	8.209	.101	.583
21.1	117.923	.308	.136	-.027	2.875	8.211	.101	.583

Derivatives are calculated numerically.

a. Major iteration number is displayed to the left of the decimal, and minor iteration number is to the right of the decimal.

b. Run stopped after 42 model evaluations and 21 derivative evaluations because the relative reduction between successive residual sums of squares is at most SSCON = 1.00E-008.

Parameter Estimates

			95% Confidence Interval	
Parameter	Estimate	Std. Error	Lower Bound	Upper Bound
b1	.308	.060	.189	.426
b2	.136	.013	.111	.161
b3	-.027	.098	-.220	.165
b4	2.875	.238	2.408	3.342
b5	8.211	2.710	2.885	13.537
b6	.101	.039	.024	.178
b7	.583	.046	.492	.674

Correlations of Parameter Estimates

	b1	b2	b3	b4	b5	b6	b7
b1	1.000	.276	-.004	-.269	.555	.308	-.120
b2	.276	1.000	.260	-.212	.665	-.338	-.275
b3	-.004	.260	1.000	-.355	.304	.487	-.470
b4	-.269	-.212	-.355	1.000	.196	-.432	.965
b5	.555	.665	.304	.196	1.000	-.219	.162
b6	.308	-.338	.487	-.432	-.219	1.000	-.388
b7	-.120	-.275	-.470	.965	.162	-.388	1.000

ANOVA[a]

Source	Sum of Squares	df	Mean Squares
Regression	1656.222	7	236.603
Residual	117.923	438	.269
Uncorrected Total	1774.145	445	
Corrected Total	352.935	444	

Dependent variable: ROP[a]

a. R squared = 1 – (Residual Sum of Squares) / (Corrected Sum of Squares) = .666.

Then,

$\mathrm{ROP} = \frac{\mathrm{F_n^{b1}} \cdot \mathrm{WFI^{b2}} \cdot \mathrm{RPM}^{b3} \cdot \mathrm{CHD^{b4}}}{\mathrm{b5} \cdot \mathrm{UCS^{b6}} \cdot \mathrm{e^{b7.CHD}}}$, and

$$\mathbf{ROP} = \frac{\mathbf{F_n^{0.308} \cdot WFI^{0.136} \cdot RPM^{-0.027} \cdot CHD^{2.875}}}{\mathbf{8.211 \cdot UCS^{0.101} \cdot e^{0.583 \cdot CHD}}}$$

End

Model 2-Non-linear Multiple Regression Model

Iteration History[b]

Iteration Number[a]	Residual Sum of Squares	Parameter								
		b1	b2	b3	b4	b5	b6	b7	b8	b9
1.0	603346.042	.010	.010	.010	.010	.010	.010	.010	.010	.010
1.1	107912.491	.016	.027	-.114	.045	.013	.017	.016	.004	-.093
2.0	107912.491	.016	.027	-.114	.045	.013	.017	.016	.004	-.093
2.1	13292.908	.029	.047	-.364	.110	.019	.022	.029	-.008	-.332
3.0	13292.908	.029	.047	-.364	.110	.019	.022	.029	-.008	-.332
3.1	1217.826	.054	.013	-.846	.213	.035	.014	.055	-.034	-.981
4.0	1217.826	.054	.013	-.846	.213	.035	.014	.055	-.034	-.981
4.1	55272.006	.062	-.352	-1.367	.255	.065	.001	.105	-.069	-3.002
4.2	192.292	.045	.141	-.868	.166	-.022	.016	.101	-.083	-1.255
5.0	192.292	.045	.141	-.868	.166	-.022	.016	.101	-.083	-1.255
5.1	135.124	.070	.069	-.912	.215	-.034	.019	.145	-.114	-1.992
6.0	135.124	.070	.069	-.912	.215	-.034	.019	.145	-.114	-1.992
6.1	124.629	.154	-.120	-.953	.272	-.025	.025	.178	-.118	-3.539
7.0	124.629	.154	-.120	-.953	.272	-.025	.025	.178	-.118	-3.539
7.1	130.197	.221	-.060	-.911	.285	-.045	.038	.186	-.126	-4.721
7.2	120.472	.200	-.039	-.943	.263	-.048	.029	.192	-.123	-3.878
8.0	120.472	.200	-.039	-.943	.263	-.048	.029	.192	-.123	-3.878
8.1	121.053	.233	-.037	-.929	.281	-.048	.039	.187	-.125	-4.592
8.2	119.482	.223	-.035	-.948	.269	-.049	.033	.192	-.123	-4.151
9.0	119.482	.223	-.035	-.948	.269	-.049	.033	.192	-.123	-4.151
9.1	119.342	.240	-.027	-.927	.283	-.049	.041	.186	-.125	-4.685

10.0	119.342	.240	-.027	-.927	.283	-.049	.041	.186	-.125	-4.685
10.1	118.049	.244	-.016	-.918	.289	-.048	.046	.182	-.126	-4.868
11.0	118.049	.244	-.016	-.918	.289	-.048	.046	.182	-.126	-4.868
11.1	118.044	.248	-.003	-.891	.304	-.046	.055	.175	-.126	-5.211
12.0	118.044	.248	-.003	-.891	.304	-.046	.055	.175	-.126	-5.211
12.1	117.384	.249	.005	-.882	.309	-.046	.060	.171	-.126	-5.289
13.0	117.384	.249	.005	-.882	.309	-.046	.060	.171	-.126	-5.289
13.1	117.385	.252	.018	-.861	.323	-.044	.070	.165	-.127	-5.434
13.2	117.250	.250	.012	-.872	.316	-.045	.065	.168	-.127	-5.348
14.0	117.250	.250	.012	-.872	.316	-.045	.065	.168	-.127	-5.348
14.1	117.250	.253	.025	-.853	.329	-.043	.075	.162	-.127	-5.460
15.0	117.250	.253	.025	-.853	.329	-.043	.075	.162	-.127	-5.460
15.1	117.020	.255	.031	-.847	.334	-.043	.080	.159	-.128	-5.436
16.0	117.020	.255	.031	-.847	.334	-.043	.080	.159	-.128	-5.436
16.1	117.040	.257	.041	-.831	.344	-.041	.090	.154	-.128	-5.521
16.2	116.983	.256	.036	-.841	.338	-.042	.084	.157	-.128	-5.449
17.0	116.983	.256	.036	-.841	.338	-.042	.084	.157	-.128	-5.449
17.1	116.983	.258	.044	-.828	.347	-.041	.093	.153	-.128	-5.517
18.0	116.983	.258	.044	-.828	.347	-.041	.093	.153	-.128	-5.517
18.1	116.947	.260	.050	-.828	.351	-.040	.096	.151	-.129	-5.268
19.0	116.947	.260	.050	-.828	.351	-.040	.096	.151	-.129	-5.268

19.1	116.978	.258	.043	-.818	.346	-.041	.097	.152	-.128	-6.048
19.2	116.942	.259	.048	-.825	.349	-.041	.096	.151	-.128	-5.492
20.0	116.942	.259	.048	-.825	.349	-.041	.096	.151	-.128	-5.492
20.1	116.945	.260	.051	-.825	.352	-.040	.098	.150	-.129	-5.305
20.2	116.941	.260	.049	-.825	.350	-.041	.097	.151	-.128	-5.467
21.0	116.941	.260	.049	-.825	.350	-.041	.097	.151	-.128	-5.467
21.1	116.941	.260	.049	-.823	.350	-.041	.098	.151	-.129	-5.509
22.0	116.941	.260	.049	-.823	.350	-.041	.098	.151	-.129	-5.509
22.1	116.941	.260	.050	-.824	.351	-.040	.098	.150	-.129	-5.424
22.2	116.941	.260	.050	-.824	.351	-.041	.098	.151	-.129	-5.475
23.0	116.941	.260	.050	-.824	.351	-.041	.098	.151	-.129	-5.475
23.1	116.941	.260	.050	-.823	.351	-.041	.098	.150	-.129	-5.490
24.0	116.941	.260	.050	-.823	.351	-.041	.098	.150	-.129	-5.490
24.1	116.941	.260	.050	-.823	.351	-.041	.098	.150	-.129	-5.473
25.0	116.941	.260	.050	-.823	.351	-.041	.098	.150	-.129	-5.473
25.1	116.941	.260	.050	-.823	.351	-.041	.098	.150	-.129	-5.490
25.2	116.941	.260	.050	-.823	.351	-.041	.098	.150	-.129	-5.477
26.0	116.941	.260	.050	-.823	.351	-.041	.098	.150	-.129	-5.477
26.1	116.941	.260	.050	-.823	.351	-.041	.098	.150	-.129	-5.476

Derivatives are calculated numerically.

a. Major iteration number is displayed to the left of the decimal, and minor iteration number is to the right of the decimal.

b. Run stopped after 61 model evaluations and 26 derivative evaluations because the relative reduction between successive residual sums of squares is at most SSCON = 1.00E-008.

Parameter Estimates

Parameter	Estimate	Std. Error	95% Confidence Interval	
			Lower Bound	Upper Bound
b1	.260	.066	.130	.390
b2	.050	.107	-.159	.260
b3	-.823	.110	-1.039	-.608
b4	.351	.088	.178	.524
b5	-.041	.029	-.098	.017
b6	.098	.040	.020	.177
b7	.150	.043	.066	.234
b8	-.129	.018	-.164	-.093
b9	-5.476	5.651	-16.584	5.631

Correlations of Parameter Estimates

	b1	b2	b3	b4	b5	b6	b7	b8	b9
b1	1.000	.062	-.653	.028	-.257	.103	.190	-.443	.232
b2	.062	1.000	-.111	.065	-.225	.247	-.575	.096	.411
b3	-.653	-.111	1.000	.006	.170	.534	-.087	.343	-.620
b4	.028	.065	.006	1.000	.402	.350	.251	.040	.426
b5	-.257	-.225	.170	.402	1.000	.104	.085	.527	.286
b6	.103	.247	.534	.350	.104	1.000	-.340	-.125	-.164
b7	.190	-.575	-.087	.251	.085	-.340	1.000	.174	-.194
b8	-.443	.096	.343	.040	.527	-.125	.174	1.000	-.130
b9	.232	.411	-.620	.426	.286	-.164	-.194	-.130	1.000

ANOVA[a]

Source	Sum of Squares	df	Mean Squares
Regression	1657.204	9	184.134
Residual	116.941	436	.268
Uncorrected Total	1774.145	445	
Corrected Total	352.935	444	

Dependent variable: ROP[a]

a. R squared = 1 – (Residual Sum of Squares) / (Corrected Sum of Squares) = .669.

Then,

$$\mathbf{ROP} = \frac{\mathbf{F_n^{0.26} \cdot MT_c^{0.05} \cdot N_c^{-0.823} \cdot RPM^{0.351} \cdot SL_e^{-0.041}}}{\mathbf{0.098 \cdot UCS^{0.15} \cdot WFI^{-0.129} \cdot e^{(CHD \cdot D_c)^{-5.476}}}}$$

End

Model 3- Non-linear Multiple Regression Model

Iteration History[b]

Iteration Number[a]	Residual Sum of Squares	Parameter						
		b1	b2	b3	b4	b5	b6	b7
1.0	2219433.552	.010	.010	.010	.010	.010	.010	.010
1.1	564129.166	.015	.013	.010	.034	.020	.014	.010
2.0	564129.166	.015	.013	.010	.034	.020	.014	.010
2.1	146439.729	.025	.020	.011	.081	.041	.022	.011
3.0	146439.729	.025	.020	.011	.081	.041	.022	.011
3.1	40065.286	.042	.032	.013	.165	.084	.035	.012
4.0	40065.286	.042	.032	.013	.165	.084	.035	.012
4.1	12459.033	.074	.051	.018	.305	.180	.053	.013
5.0	12459.033	.074	.051	.018	.305	.180	.053	.013
5.1	3893.736	.107	.073	.012	.500	.370	.079	.015
6.0	3893.736	.107	.073	.012	.500	.370	.079	.015
6.1	591.595	.096	.085	-.056	.718	.561	.122	.017
7.0	591.595	.096	.085	-.056	.718	.561	.122	.017
7.1	252.543	.131	.103	-.101	.966	.942	.146	.019
8.0	252.543	.131	.103	-.101	.966	.942	.146	.019
8.1	145.879	.161	.108	-.133	1.065	1.323	.154	.021
9.0	145.879	.161	.108	-.133	1.065	1.323	.154	.021
9.1	156.338	.220	.121	-.099	1.109	2.086	.145	.021
9.2	130.356	.185	.111	-.139	1.086	1.618	.153	.021
10.0	130.356	.185	.111	-.139	1.086	1.618	.153	.021
10.1	131.876	.221	.120	-.105	1.108	2.207	.145	.021
10.2	128.336	.199	.114	-.130	1.093	1.847	.151	.021
11.0	128.336	.199	.114	-.130	1.093	1.847	.151	.021
11.1	127.769	.224	.120	-.104	1.109	2.305	.145	.021
12.0	127.769	.224	.120	-.104	1.109	2.305	.145	.021
12.1	126.032	.242	.125	-.086	1.120	2.764	.142	.022
13.0	126.032	.242	.125	-.086	1.120	2.764	.142	.022
13.1	124.982	.258	.129	-.071	1.129	3.222	.138	.022
14.0	124.982	.258	.129	-.071	1.129	3.222	.138	.022
14.1	125.702	.287	.136	-.044	1.147	4.140	.132	.022
14.2	124.333	.268	.131	-.062	1.135	3.553	.136	.022
15.0	124.333	.268	.131	-.062	1.135	3.553	.136	.022
15.1	124.055	.287	.136	-.044	1.147	4.215	.132	.022
16.0	124.055	.287	.136	-.044	1.147	4.215	.132	.022
16.1	123.456	.303	.140	-.031	1.156	4.877	.129	.022

17.0	123.456	.303	.140	-.031	1.156	4.877	.129	.022
17.1	123.098	.317	.143	-.020	1.164	5.538	.126	.022
18.0	123.098	.317	.143	-.020	1.164	5.538	.126	.022
18.1	122.887	.329	.146	-.010	1.171	6.200	.123	.022
19.0	122.887	.329	.146	-.010	1.171	6.200	.123	.022
19.1	122.771	.340	.149	-.001	1.177	6.861	.121	.022
20.0	122.771	.340	.149	-.001	1.177	6.861	.121	.022
20.1	122.721	.351	.151	.006	1.183	7.523	.119	.023
21.0	122.721	.351	.151	.006	1.183	7.523	.119	.023
21.1	122.687	.353	.152	.008	1.185	7.717	.119	.023
22.0	122.687	.353	.152	.008	1.185	7.717	.119	.023
22.1	122.687	.353	.152	.007	1.184	7.713	.119	.023
23.0	122.687	.353	.152	.007	1.184	7.713	.119	.023
23.1	122.687	.354	.152	.007	1.185	7.715	.119	.023

Derivatives are calculated numerically.

a. Major iteration number is displayed to the left of the decimal, and minor iteration number is to the right of the decimal.

b. Run stopped after 49 model evaluations and 23 derivative evaluations because the relative reduction between successive residual sums of squares is at most SSCON = 1.00E-008.

Parameter Estimates

			95% Confidence Interval	
Parameter	Estimate	Std. Error	Lower Bound	Upper Bound
b1	.354	.062	.232	.475
b2	.152	.013	.127	.177
b3	.007	.102	-.193	.207
b4	1.185	.121	.947	1.422
b5	7.715	2.584	2.635	12.794
b6	.119	.040	.040	.197
b7	.023	.002	.019	.026

Correlations of Parameter Estimates

	b1	b2	b3	b4	b5	b6	b7
b1	1.000	.265	-.036	-.369	.570	.289	-.060
b2	.265	1.000	.218	-.064	.695	-.378	-.192
b3	-.036	.218	1.000	-.214	.304	.495	-.482
b4	-.369	-.064	-.214	1.000	.197	-.446	.848

b5	.570	.695	.304	.197	1.000	-.206	.147
b6	.289	-.378	.495	-.446	-.206	1.000	-.386
b7	-.060	-.192	-.482	.848	.147	-.386	1.000

ANOVA[a]

Source	Sum of Squares	df	Mean Squares
Regression	1651.458	7	235.923
Residual	122.687	438	.280
Uncorrected Total	1774.145	445	
Corrected Total	352.935	444	

Dependent variable: ROP[a]

a. R squared = 1 – (Residual Sum of Squares) / (Corrected Sum of Squares) = .652.

Then,

$$\mathbf{ROP} = \frac{\mathbf{F_n^{0.354}} \cdot \mathbf{WFI^{0.152}} \cdot \mathbf{RPM^{0.007}} \cdot \mathbf{CHD}^{\mathbf{1.185}}}{\mathbf{7.715} \cdot \mathbf{UCS^{0.119}} \cdot \mathbf{EXP}(\mathbf{0.023} \cdot \mathbf{CHD^2})}$$

End

Model 4- Non-linear Multiple Regression Model

Iteration History[b]

Iteration Number[a]	Residual Sum of Squares	Parameter							
		b1	b2	b3	b4	b5	b6	b7	b8
1.0	4070886.037	.010	.010	.010	.010	.010	.010	.010	.010
1.1	1033320.790	.013	.010	.061	.011	.020	.013	.008	.020
2.0	1033320.790	.013	.010	.061	.011	.020	.013	.008	.020
2.1	266995.672	.018	.010	.159	.013	.041	.017	.003	.039
3.0	266995.672	.018	.010	.159	.013	.041	.017	.003	.039
3.1	71923.888	.028	.011	.339	.016	.084	.026	-.005	.073
4.0	71923.888	.028	.011	.339	.016	.084	.026	-.005	.073
4.1	21363.282	.045	.015	.644	.021	.178	.038	-.020	.131
5.0	21363.282	.045	.015	.644	.021	.178	.038	-.020	.131
5.1	6271.904	.066	.008	1.079	.026	.365	.059	-.039	.215
6.0	6271.904	.066	.008	1.079	.026	.365	.059	-.039	.215
6.1	899.610	.060	-.075	1.567	.018	.553	.102	-.055	.315
7.0	899.610	.060	-.075	1.567	.018	.553	.102	-.055	.315
7.1	295.372	.087	-.123	2.188	.013	.929	.128	-.078	.440
8.0	295.372	.087	-.123	2.188	.013	.929	.128	-.078	.440
8.1	258.240	.139	-.108	2.592	.015	1.681	.126	-.094	.520
9.0	258.240	.139	-.108	2.592	.015	1.681	.126	-.094	.520
9.1	127.480	.150	-.131	2.681	.012	2.058	.130	-.096	.543
10.0	127.480	.150	-.131	2.681	.012	2.058	.130	-.096	.543
10.1	126.152	.177	-.101	2.768	.017	2.810	.122	-.100	.559
11.0	126.152	.177	-.101	2.768	.017	2.810	.122	-.100	.559
11.1	120.318	.184	-.094	2.788	.019	3.186	.120	-.101	.562
12.0	120.318	.184	-.094	2.788	.019	3.186	.120	-.101	.562
12.1	120.120	.200	-.068	2.832	.024	3.939	.113	-.104	.568
13.0	120.120	.200	-.068	2.832	.024	3.939	.113	-.104	.568
13.1	118.808	.206	-.061	2.846	.026	4.315	.111	-.105	.570
14.0	118.808	.206	-.061	2.846	.026	4.315	.111	-.105	.570
14.1	118.536	.219	-.042	2.879	.029	5.067	.105	-.108	.574
15.0	118.536	.219	-.042	2.879	.029	5.067	.105	-.108	.574
15.1	118.031	.230	-.028	2.905	.032	5.820	.101	-.109	.578
16.0	118.031	.230	-.028	2.905	.032	5.820	.101	-.109	.578
16.1	117.718	.239	-.016	2.929	.035	6.572	.097	-.111	.581
17.0	117.718	.239	-.016	2.929	.035	6.572	.097	-.111	.581
17.1	117.528	.247	-.006	2.950	.037	7.325	.094	-.113	.584
18.0	117.528	.247	-.006	2.950	.037	7.325	.094	-.113	.584

18.1	117.418	.255	.004	2.969	.039	8.077	.091	-.114	.587
19.0	117.418	.255	.004	2.969	.039	8.077	.091	-.114	.587
19.1	117.367	.262	.012	2.987	.041	8.829	.088	-.115	.590
20.0	117.367	.262	.012	2.987	.041	8.829	.088	-.115	.590
20.1	117.336	.266	.015	2.996	.041	9.226	.087	-.116	.591
21.0	117.336	.266	.015	2.996	.041	9.226	.087	-.116	.591
21.1	117.334	.266	.014	2.996	.042	9.218	.087	-.116	.591
22.0	117.334	.266	.014	2.996	.042	9.218	.087	-.116	.591
22.1	117.334	.266	.014	2.996	.042	9.220	.087	-.116	.591

Derivatives are calculated numerically.

a. Major iteration number is displayed to the left of the decimal, and minor iteration number is to the right of the decimal.

b. Run stopped after 44 model evaluations and 22 derivative evaluations because the relative reduction between successive residual sums of squares is at most SSCON = 1.00E-008.

Parameter Estimates

			95% Confidence Interval	
Parameter	Estimate	Std. Error	Lower Bound	Upper Bound
b1	.266	.067	.135	.397
b2	.014	.101	-.184	.213
b3	2.996	.251	2.503	3.489
b4	.042	.028	-.013	.096
b5	9.220	3.119	3.090	15.350
b6	.087	.040	.008	.165
b7	-.116	.019	-.153	-.079
b8	.591	.046	.500	.682

Correlations of Parameter Estimates

	b1	b2	b3	b4	b5	b6	b7	b8
b1	1.000	-.133	-.372	-.428	.390	.367	-.481	-.162
b2	-.133	1.000	-.221	.290	.343	.384	.046	-.408
b3	-.372	-.221	1.000	.340	.260	-.471	.381	.944
b4	-.428	.290	.340	1.000	.224	-.221	.735	.136
b5	.390	.343	.260	.224	1.000	-.264	-.275	.189
b6	.367	.384	-.471	-.221	-.264	1.000	.066	-.402
b7	-.481	.046	.381	.735	-.275	.066	1.000	.281
b8	-.162	-.408	.944	.136	.189	-.402	.281	1.000

ANOVA[a]

Source	Sum of Squares	df	Mean Squares
Regression	1656.811	8	207.101
Residual	117.334	437	.268
Uncorrected Total	1774.145	445	
Corrected Total	352.935	444	

Dependent variable: ROP[a]

a. R squared = 1 – (Residual Sum of Squares) / (Corrected Sum of Squares) = .668.

Then,

$$\mathbf{ROP} = \frac{\mathbf{F_n^{0.266} \cdot RPM^{0.014} \cdot CHD^{2.996} \cdot SL_e^{0.042}}}{\mathbf{9.22.UCS^{0.087} \cdot WFI^{-0.116} \cdot e^{0.591 \cdot CHD}}}$$

End

Model 5-Non-linear Multiple Regression Model

Iteration History[b]

Iteration Number[a]	Residual Sum of Squares	Parameter							
		b1	b2	b3	b4	b5	b6	b7	b8
1.0	2084590.098	.010	.010	.010	.010	.010	.010	.010	.010
1.1	527676.092	.015	.035	.010	.010	.020	.006	.015	.010
2.0	527676.092	.015	.035	.010	.010	.020	.006	.015	.010
2.1	136002.028	.024	.083	.010	.010	.041	-.001	.024	.011
3.0	136002.028	.024	.083	.010	.010	.041	-.001	.024	.011
3.1	36838.463	.042	.170	.010	.010	.084	-.015	.038	.012
4.0	36838.463	.042	.170	.010	.010	.084	-.015	.038	.012
4.1	11394.892	.074	.314	.015	.008	.177	-.037	.059	.013
5.0	11394.892	.074	.314	.015	.008	.177	-.037	.059	.013
5.1	3581.844	.111	.520	.001	-.013	.365	-.066	.088	.015
6.0	3581.844	.111	.520	.001	-.013	.365	-.066	.088	.015
6.1	550.376	.120	.769	-.095	-.099	.552	-.089	.141	.018
7.0	550.376	.120	.769	-.095	-.099	.552	-.089	.141	.018
7.1	245.544	.162	1.028	-.154	-.143	.928	-.115	.167	.021
8.0	245.544	.162	1.028	-.154	-.143	.928	-.115	.167	.021
8.1	144.926	.192	1.121	-.187	-.144	1.303	-.122	.172	.023
9.0	144.926	.192	1.121	-.187	-.144	1.303	-.122	.172	.023
9.1	156.135	.236	1.140	-.131	-.081	2.053	-.129	.154	.022
9.2	129.964	.210	1.133	-.187	-.126	1.585	-.123	.168	.023
10.0	129.964	.210	1.133	-.187	-.126	1.585	-.123	.168	.023
10.1	131.453	.236	1.138	-.139	-.082	2.149	-.128	.155	.022
10.2	128.178	.220	1.133	-.173	-.109	1.799	-.124	.163	.023
11.0	128.178	.220	1.133	-.173	-.109	1.799	-.124	.163	.023
11.1	127.654	.237	1.136	-.137	-.078	2.228	-.128	.155	.022
12.0	127.654	.237	1.136	-.137	-.078	2.228	-.128	.155	.022
12.1	126.112	.250	1.137	-.109	-.053	2.657	-.130	.148	.022
13.0	126.112	.250	1.137	-.109	-.053	2.657	-.130	.148	.022
13.1	125.135	.261	1.138	-.087	-.033	3.085	-.131	.143	.022
14.0	125.135	.261	1.138	-.087	-.033	3.085	-.131	.143	.022
14.1	125.696	.281	1.144	-.049	5.480E-5	3.943	-.135	.133	.022
14.2	124.502	.268	1.139	-.073	-.019	3.411	-.132	.139	.022
15.0	124.502	.268	1.139	-.073	-.019	3.411	-.132	.139	.022
15.1	124.216	.283	1.144	-.047	.003	4.062	-.135	.132	.022

16.0	124.216	.283	1.144	-.047	.003	4.062	-.135	.132	.022
16.1	123.544	.294	1.146	-.028	.022	4.714	-.137	.127	.022
17.0	123.544	.294	1.146	-.028	.022	4.714	-.137	.127	.022
17.1	123.118	.305	1.149	-.011	.038	5.365	-.139	.122	.022
18.0	123.118	.305	1.149	-.011	.038	5.365	-.139	.122	.022
18.1	122.843	.314	1.152	.003	.051	6.017	-.140	.117	.022
19.0	122.843	.314	1.152	.003	.051	6.017	-.140	.117	.022
19.1	123.229	.332	1.159	.029	.075	7.320	-.143	.109	.022
19.2	122.676	.319	1.153	.010	.059	6.392	-.141	.115	.022
20.0	122.676	.319	1.153	.010	.059	6.392	-.141	.115	.022
20.1	122.607	.329	1.157	.024	.071	7.144	-.143	.111	.022
21.0	122.607	.329	1.157	.024	.071	7.144	-.143	.111	.022
21.1	122.513	.338	1.159	.035	.083	7.895	-.144	.107	.022
22.0	122.513	.338	1.159	.035	.083	7.895	-.144	.107	.022
22.1	122.475	.346	1.162	.046	.093	8.646	-.145	.104	.022
23.0	122.475	.346	1.162	.046	.093	8.646	-.145	.104	.022
23.1	122.444	.347	1.162	.046	.095	8.761	-.145	.103	.022
24.0	122.444	.347	1.162	.046	.095	8.761	-.145	.103	.022
24.1	122.444	.347	1.162	.046	.095	8.764	-.145	.103	.022
25.0	122.444	.347	1.162	.046	.095	8.764	-.145	.103	.022
25.1	122.444	.347	1.162	.046	.095	8.765	-.145	.103	.022

Derivatives are calculated numerically.

a. Major iteration number is displayed to the left of the decimal, and minor iteration number is to the right of the decimal.

b. Run stopped after 54 model evaluations and 25 derivative evaluations because the relative reduction between successive residual sums of squares is at most SSCON = 1.00E-008.

Parameter Estimates

			95% Confidence Interval	
Parameter	Estimate	Std. Error	Lower Bound	Upper Bound
b1	.347	.063	.224	.470
b2	1.162	.123	.920	1.404
b3	.046	.108	-.166	.258
b4	.095	.102	-.105	.295
b5	8.765	3.111	2.651	14.878
b6	-.145	.015	-.175	-.116
b7	.103	.043	.018	.188
b8	.022	.002	.017	.026

Correlations of Parameter Estimates

	b1	b2	b3	b4	b5	b6	b7	b8
b1	1.000	-.326	-.098	-.157	.475	-.301	.326	.029
b2	-.326	1.000	-.261	-.193	.123	-.050	-.324	.818
b3	-.098	-.261	1.000	.365	.383	.017	.271	-.569
b4	-.157	-.193	.365	1.000	.336	.515	-.395	-.489
b5	.475	.123	.383	.336	1.000	-.386	-.317	-.039
b6	-.301	-.050	.017	.515	-.386	1.000	.100	-.110
b7	.326	-.324	.271	-.395	-.317	.100	1.000	-.113
b8	.029	.818	-.569	-.489	-.039	-.110	-.113	1.000

ANOVA[a]

Source	Sum of Squares	df	Mean Squares
Regression	1651.701	8	206.463
Residual	122.444	437	.280
Uncorrected Total	1774.145	445	
Corrected Total	352.935	444	

Dependent variable: ROP[a]

a. R squared = 1 – (Residual Sum of Squares) / (Corrected Sum of Squares) = .653.

Then,

$$\mathbf{ROP} = \frac{\mathbf{F_n^{0.347} \cdot CHD^{1.162} \cdot RPM^{0.046} \cdot MT_c^{0.095}}}{\mathbf{8.765 \cdot WFI^{-0.145} \cdot UCS^{0.103} \cdot EXP(0.022 \cdot CHD^2)}}$$

End

Appendix E

Output of 20 Developed Models conducting LMR Models

Models #	Linear Multiple Regression Model Equations	R^2
Model **1**	$ROP = -0.005 \cdot UCS + 0.006 \cdot WFI + 0.63 \cdot MT_c + 1.703$	0.516
Model 2	$ROP = -0.009 \cdot UCS + 0.009 \cdot WFI + 0.189 \cdot RPM + 1.605$	0.566
Model **3**	$ROP = -0.009 \cdot UCS + 0.006 \cdot WFI - 0.016 \cdot N_c + 3.770$	0.525
Model 4	$ROP = -0.009 \cdot UCS + 0.097 \cdot RM_c + 1.148 \cdot MT_c - 0.127 \cdot CHD + 1.740$	0.571
Model 5	$ROP = -0.009 \cdot UCS + 0.095 \cdot RM_c + 1.561 \cdot MT_c + 0.2 \cdot RPM - 1.157$	0.608
Model **6**	$ROP = -0.008 \cdot UCS + 0.004 \cdot WFI + 0.33 \times MT_c - 0.092 \cdot CHD + 3.213$	0.536
Model 7	$ROP = -0.009 \cdot UCS + 0.009 \cdot WFI + 0.001 \cdot CHD + 0.19 \cdot RPM + 1.588$	0.566
Model 8	$ROP = -0.008 \cdot UCS + 0.003 \cdot WFI + 0.095 \cdot RM_c + 0.967 \cdot MT_c - 0.113 \cdot CHD + 1.698$	0.576
Model 9	$ROP = -0.008 \cdot UCS + 0.042 \cdot WFI + 0.083 \cdot RM_c + 0.651 \cdot MT_c + 0.028 \cdot SL_e - 0.108 \cdot CHD + 1.916$	0.599
Model 10	$ROP = -0.009 \cdot UCS + 0.07 \cdot WFI + 0.046 \cdot SL_e + 0.044 \cdot RM_c - 0.183 \cdot CHD + 0.003 \cdot F_n + 2.907$	0.608
Model 11	$ROP = -0.004 \cdot UCS + 0.006 \cdot WFI + 0.082 \cdot RM_c + 1.240 \cdot MT_c + 0.094$	0.547
Model 12	$ROP = -0.006 \cdot UCS + 0.013 \cdot WFI + 0.149 \cdot RPM + 5.889 \cdot D_c - 1.275$	0.60
Model 13	$ROP = -0.007 \cdot UCS + 0.009 \cdot WFI - 0.025 \cdot N_c + 10.170 \cdot D_c - 0.771$	0.626
Model 14	$ROP = -0.008 \cdot UCS + 0.094 \cdot RM_c + 1.597 \cdot MT_c + 0.01 \cdot CHD + 0.208 \cdot RPM - 1.351$	0.595
Model **15**	$ROP = -0.009 \cdot UCS + 0.009 \cdot WFI + 0.561 \cdot CHD + 0.278 \cdot RPM - 0.08 \cdot N_c + 0.78$	0.569
Model 16	$ROP = -0.008 \cdot UCS + 0.005 \cdot WFI + 0.412 \cdot MT_c + 0.002 \cdot F_n - 0.129 \cdot CHD + 2.871$	0.547
Model **17**	$ROP = -0.009 \cdot UCS + 0.01 \cdot WFI + 0.001 \cdot F_n + 0.195 \cdot RPM + 1.372$	0.567
Model 18	$ROP = -0.01 \cdot UCS + 0.008 \cdot WFI + 0.047 \cdot RM_c + 0.002 \cdot F_n - 0.17 \cdot CHD + 3.581$	0.572
Model 19	$ROP = -0.009 \cdot UCS + 0.062 \cdot WFI + 0.056 \cdot SL_e - 0.025 \cdot CHD + 0.189 \cdot RPM + 0.002 \cdot F_n + 0.918$	0.624
Model 20	$ROP = -0.009 \cdot UCS + 0.062 \cdot WFI + 0.056 \cdot SL_e - 0.025 \cdot CHD + 0.189 \cdot RPM + 0.002 \cdot F_n + 0.918$	0.624

*Red colored models were examined in detail at content

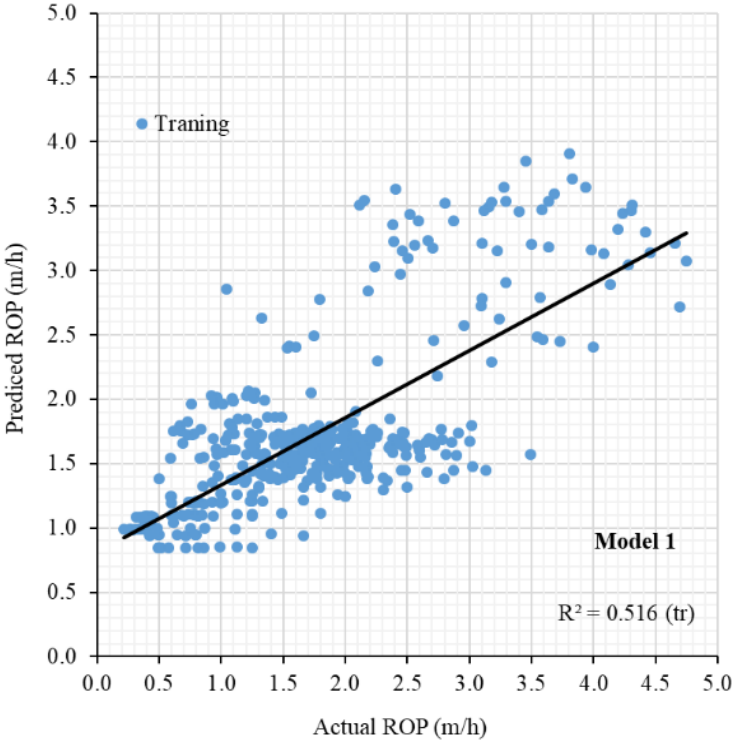

Figure E1. LMR model 1 for estimating TBM penetration for training dataset

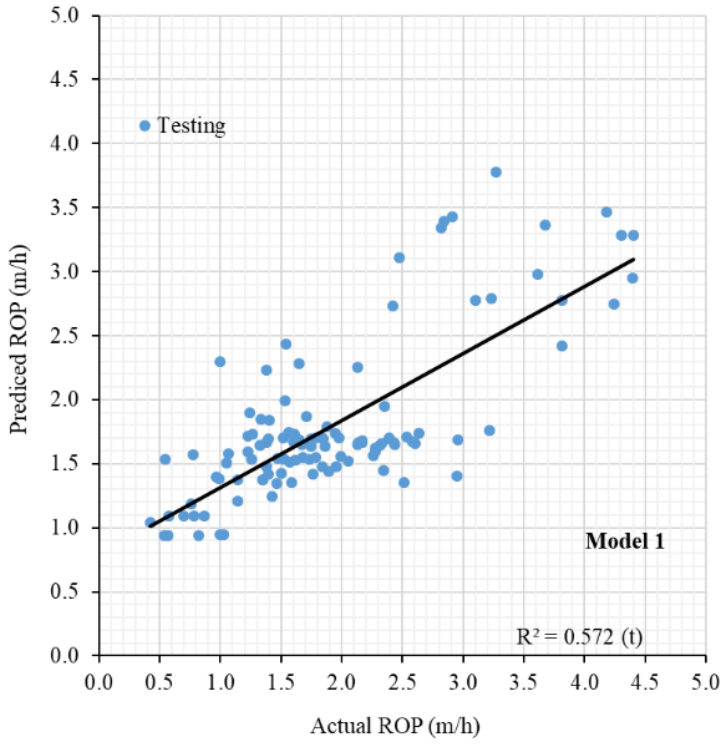

Figure E2. LMR model 1 for estimating TBM penetration for testing dataset

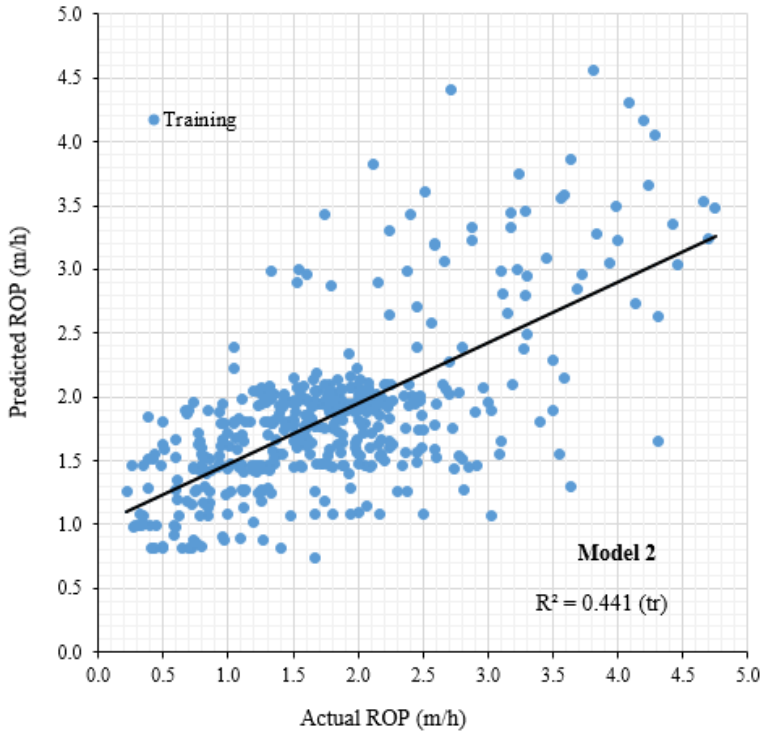

Figure E3. LMR model 2 for estimating TBM penetration for training dataset

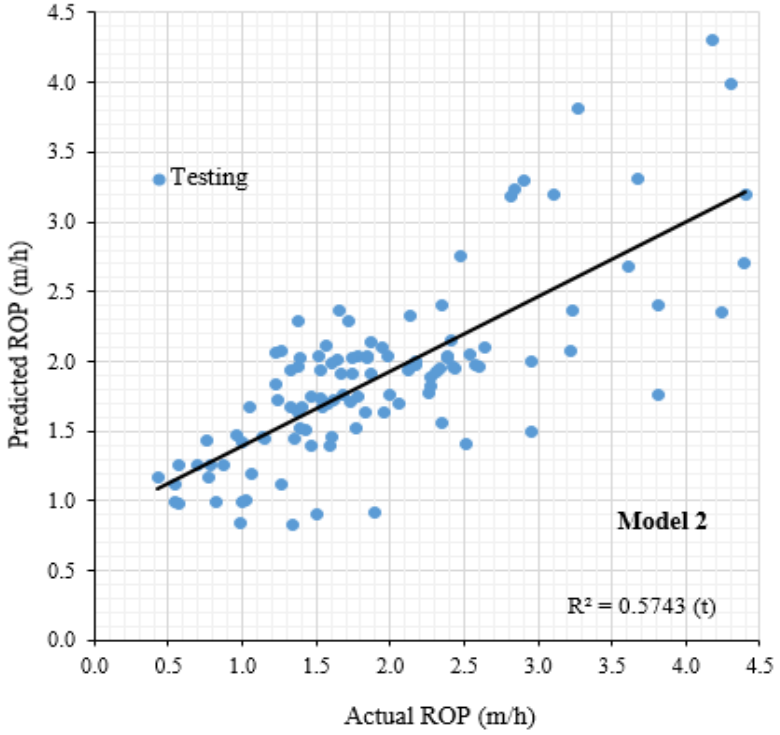

Figure E4. LMR model 2 for estimating TBM penetration for testing dataset

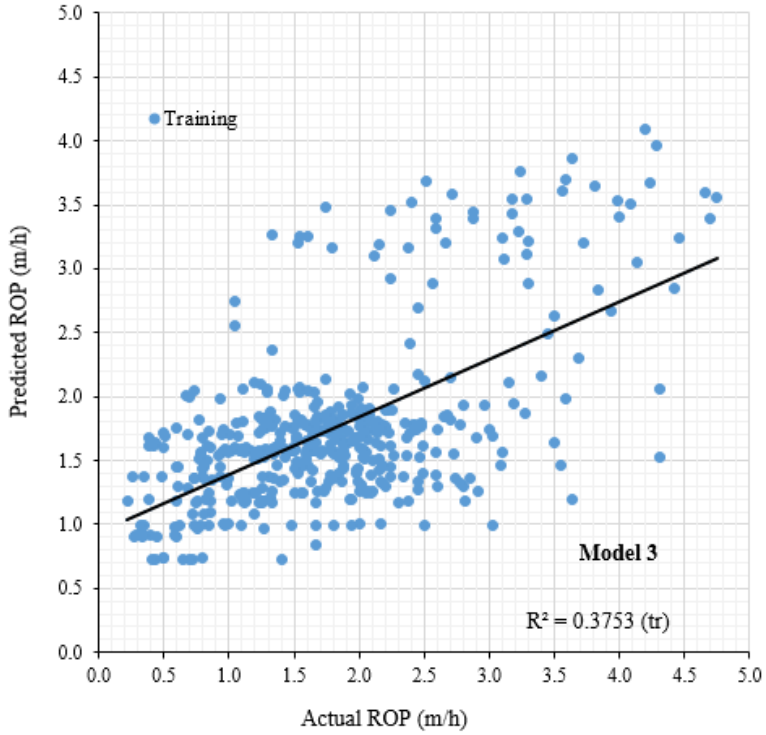

Figure E5. LMR model 3 for estimating TBM penetration for training dataset

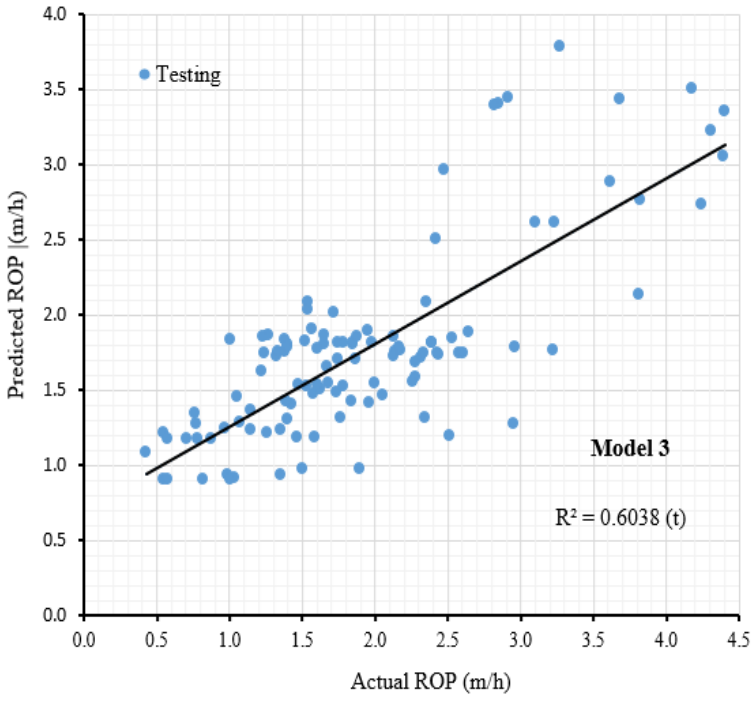

Figure E6. LMR model 3 for estimating TBM penetration for testing dataset

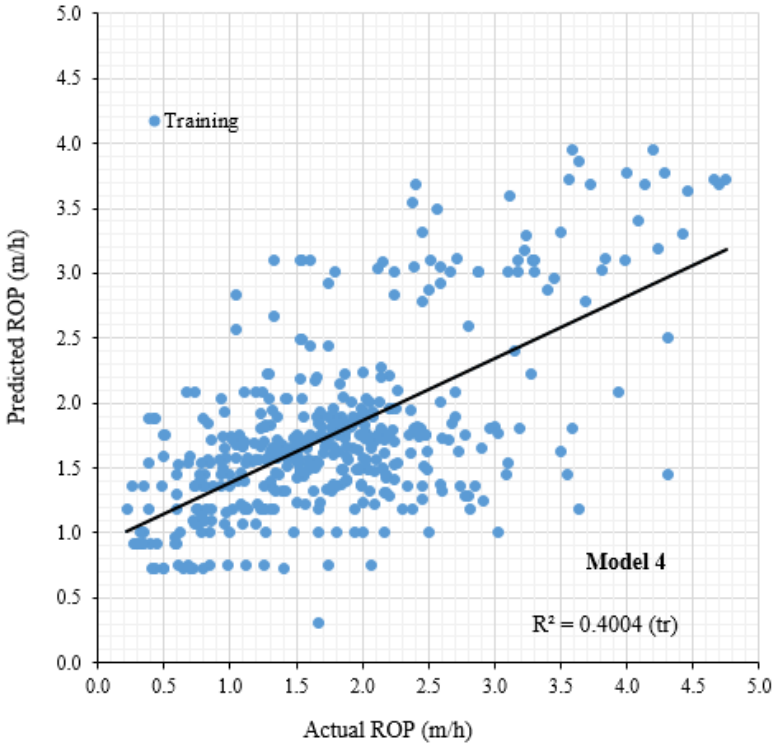

Figure E7. LMR model 4 for estimating TBM penetration for training dataset

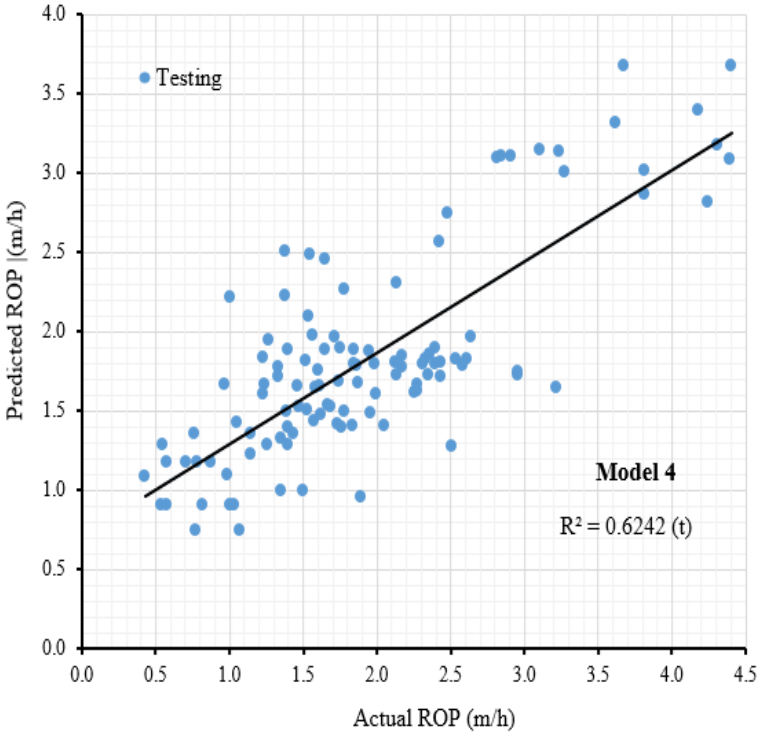

Figure E8. LMR model 4 for estimating TBM penetration for testing dataset

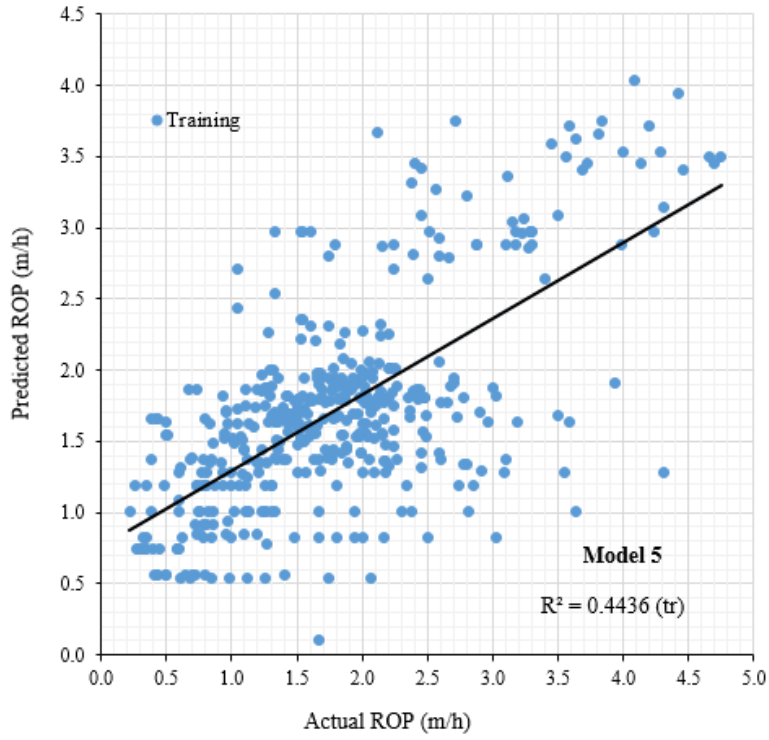

Figure E9. LMR model 5 for estimating TBM penetration for training dataset

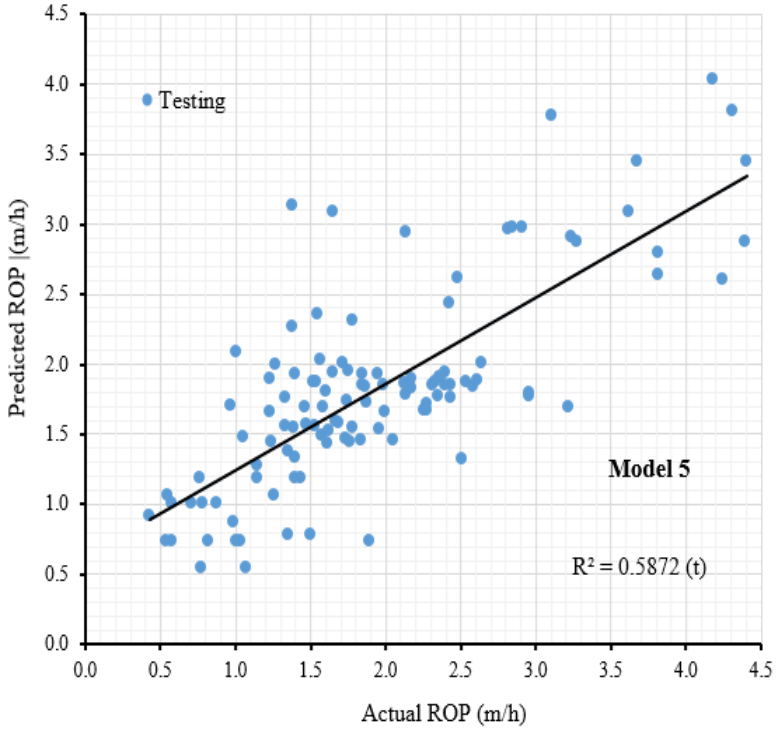

Figure E10. LMR model 5 for estimating TBM penetration for testing dataset

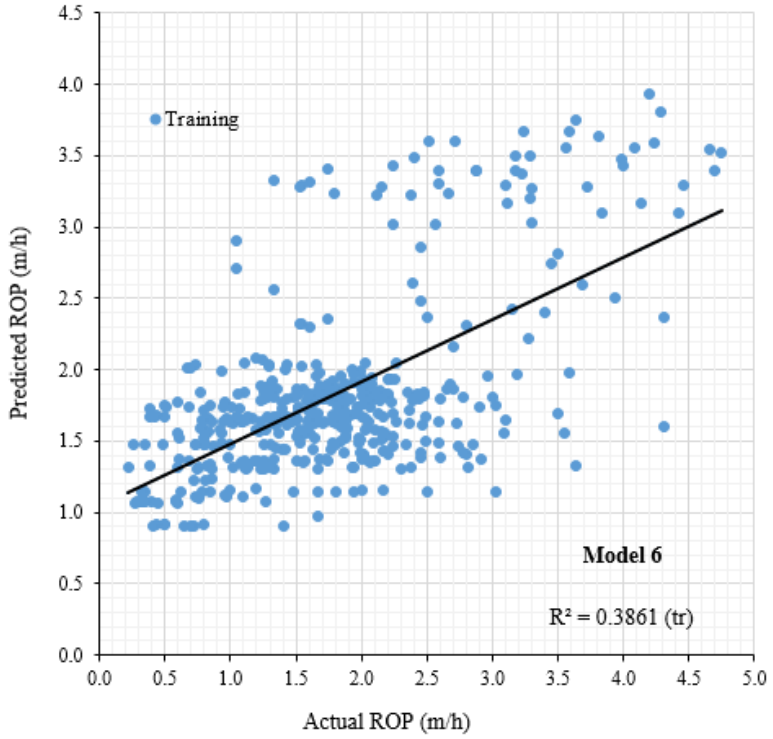

Figure E11. LMR model 6 for estimating TBM penetration for training dataset

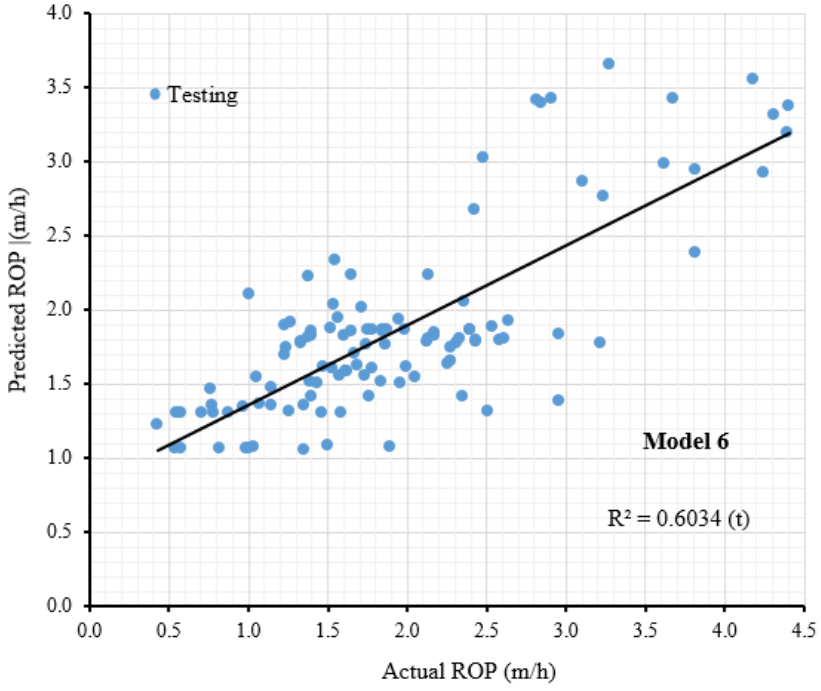

Figure E12. LMR model 6 for estimating TBM penetration for testing dataset

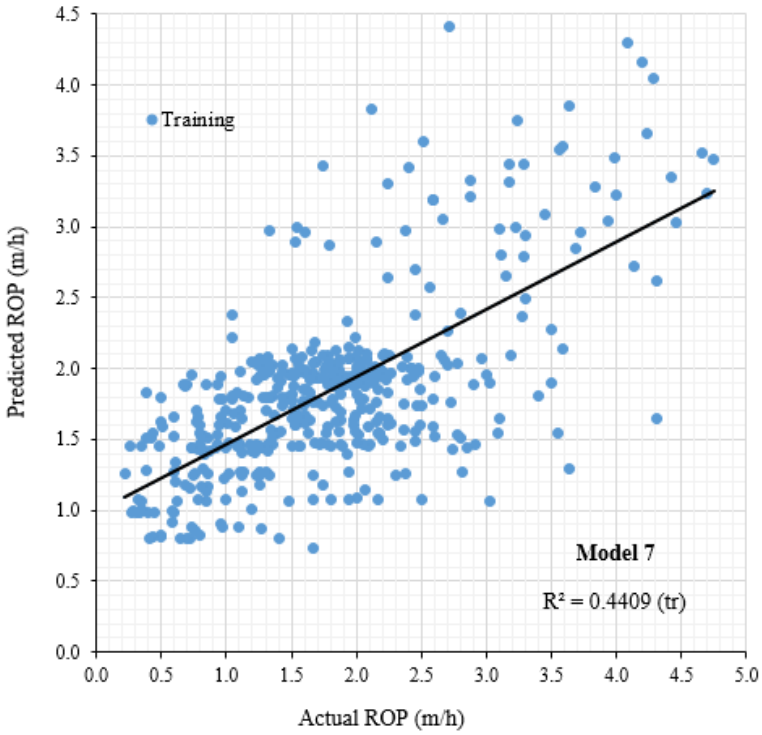

Figure E13. LMR model 7 for estimating TBM penetration for training dataset

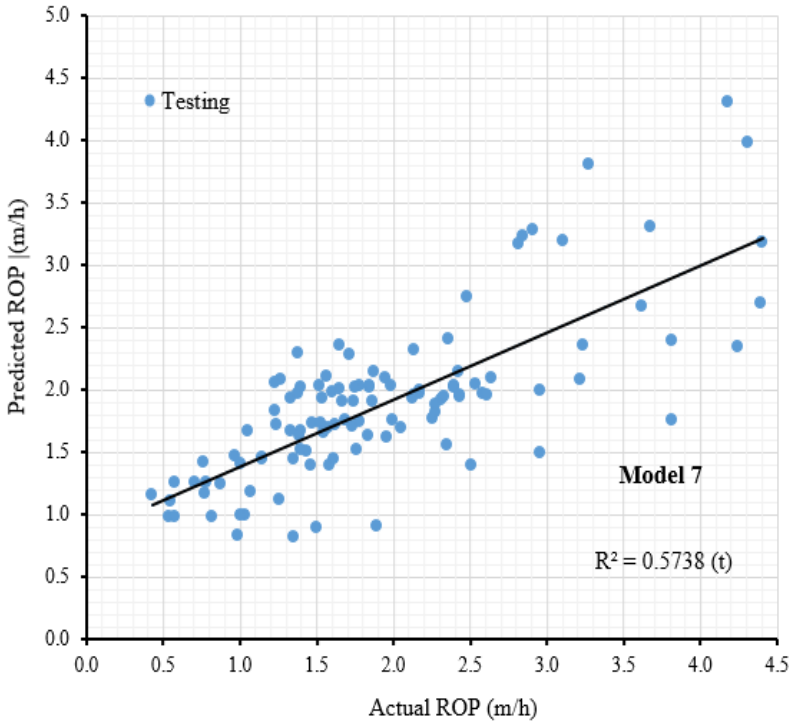

Figure E14. LMR model 7 for estimating TBM penetration for testing dataset

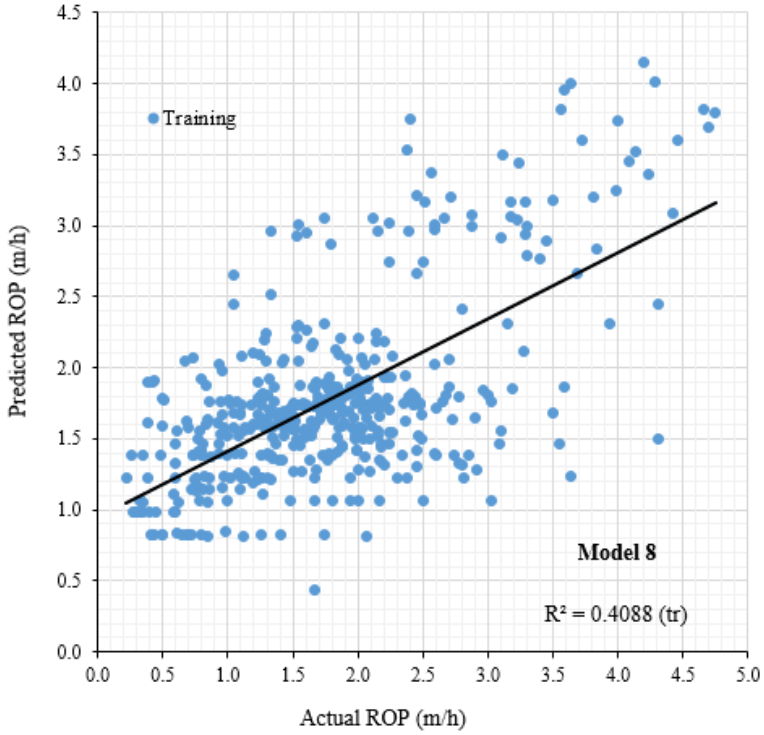

Figure E15. LMR model 8 for estimating TBM penetration for training dataset

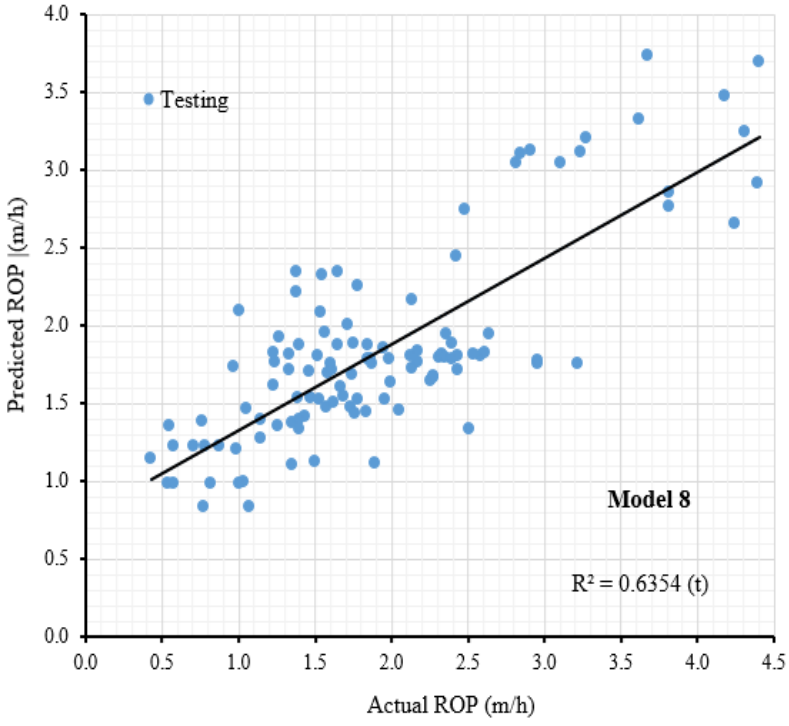

Figure E16. LMR model 8 for estimating TBM penetration for testing dataset

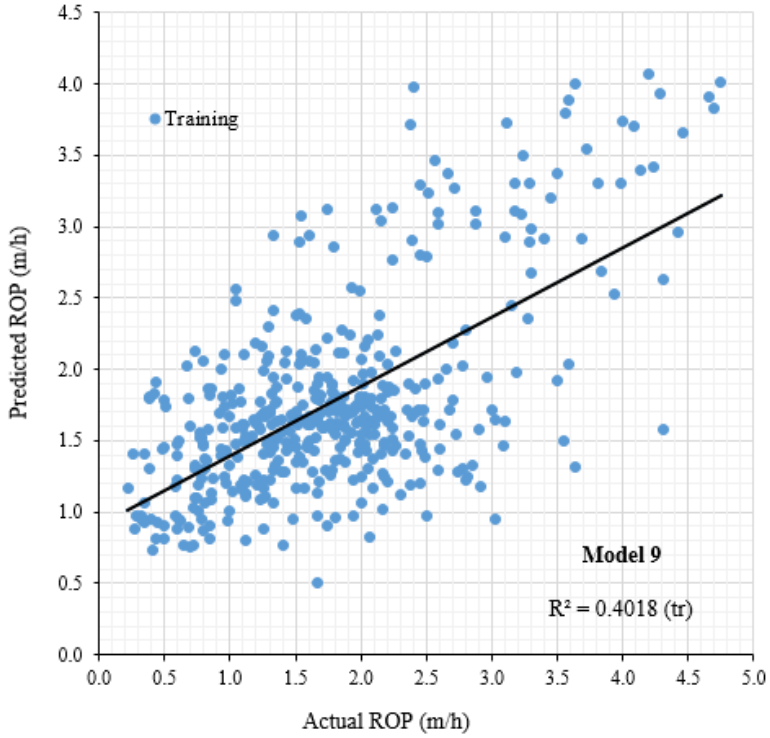

Figure E17. LMR model 9 for estimating TBM penetration for training dataset

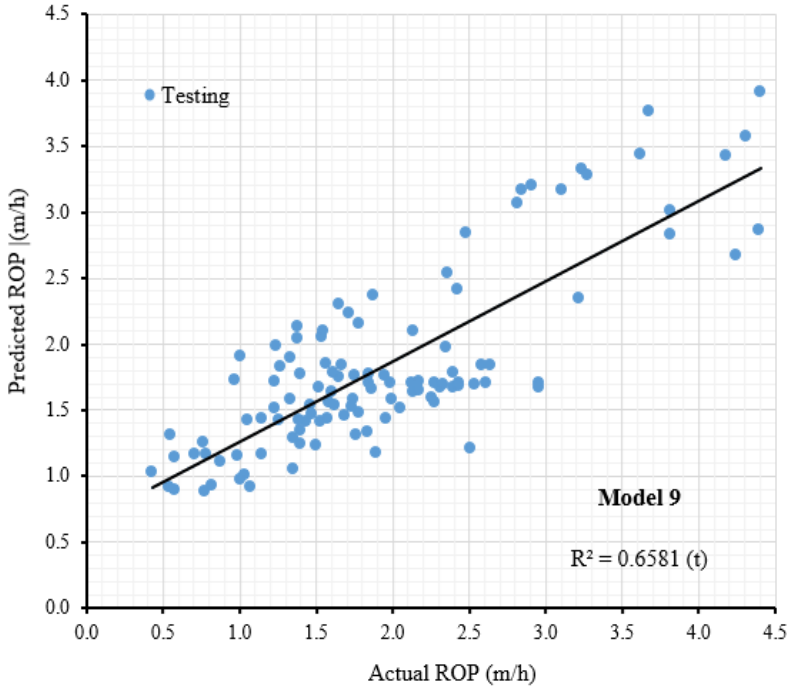

Figure E18. LMR model 9 for estimating TBM penetration for testing dataset

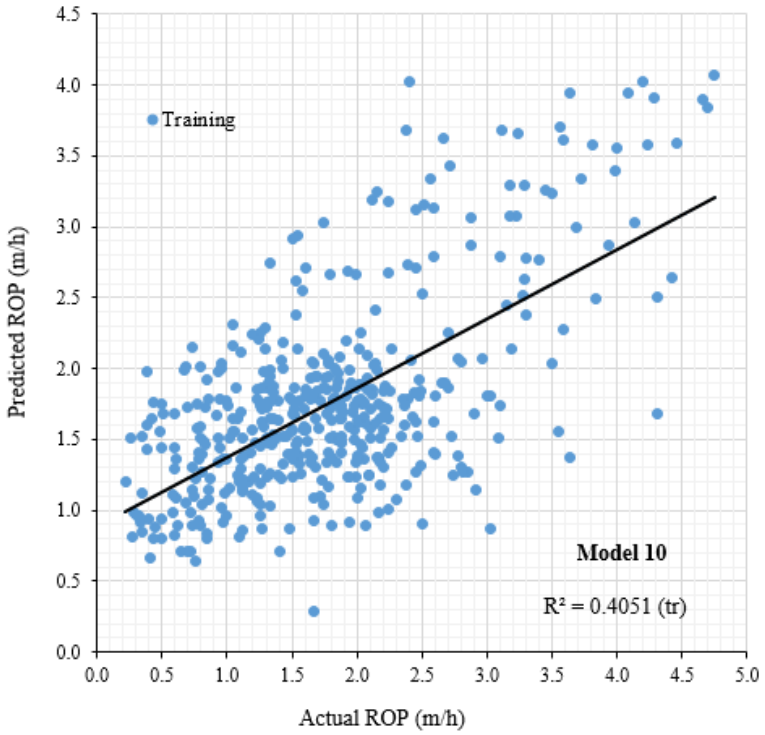

Figure E19. LMR model 10 for estimating TBM penetration for training dataset

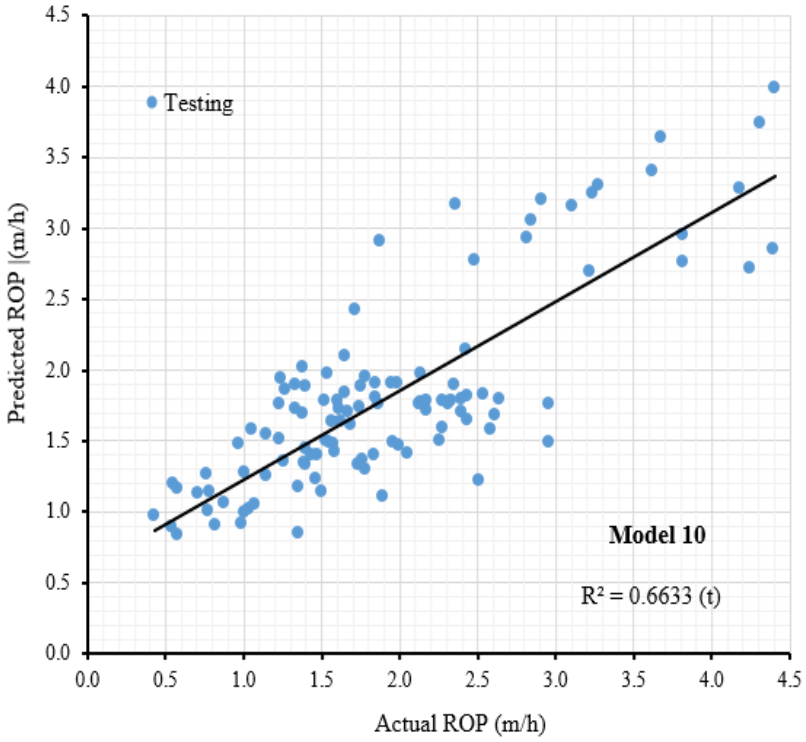

Figure E20. LMR model 10 for estimating TBM penetration for testing dataset

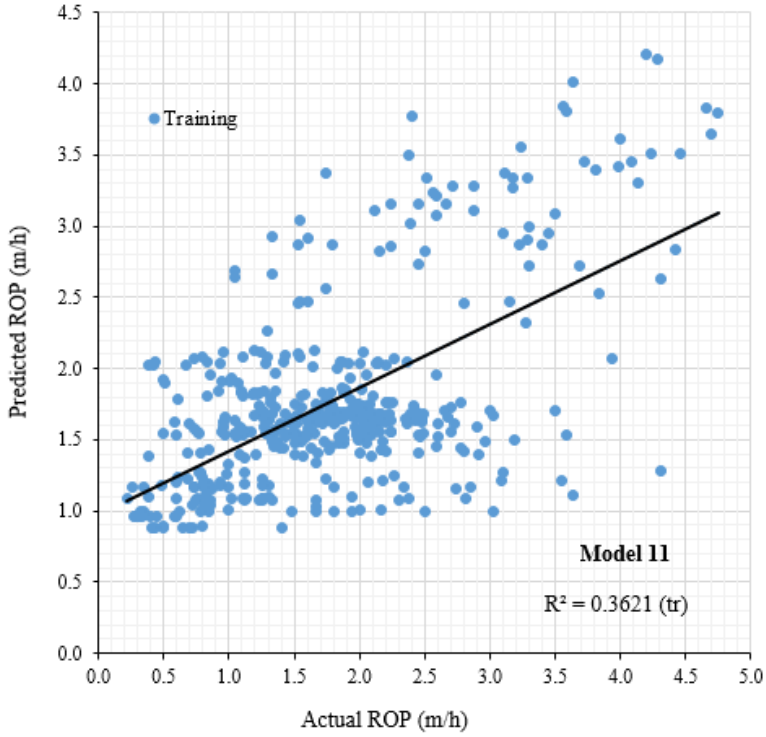

Figure E21. LMR model 11 for estimating TBM penetration for training dataset

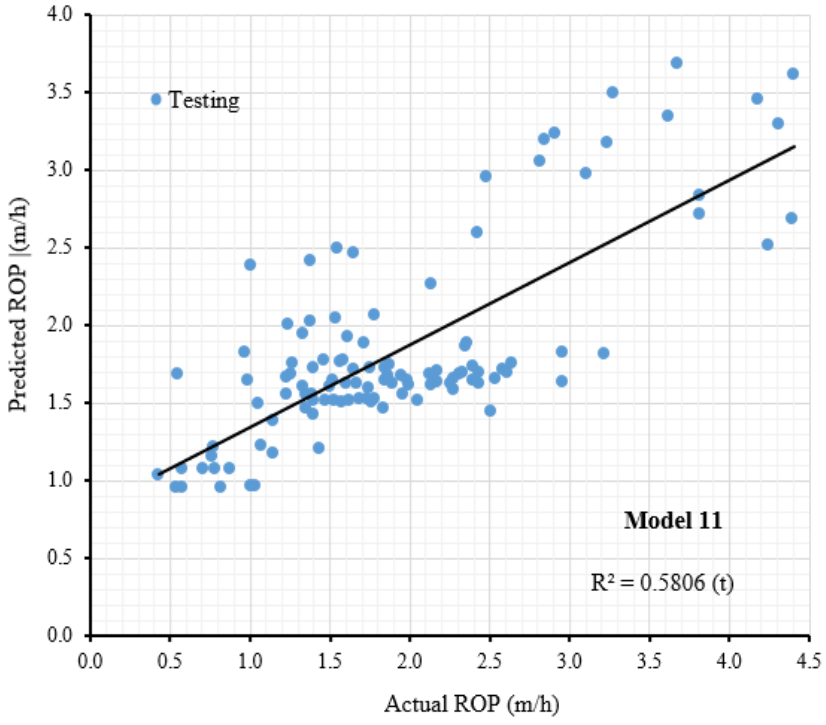

Figure E22. LMR model 11 for estimating TBM penetration for testing dataset

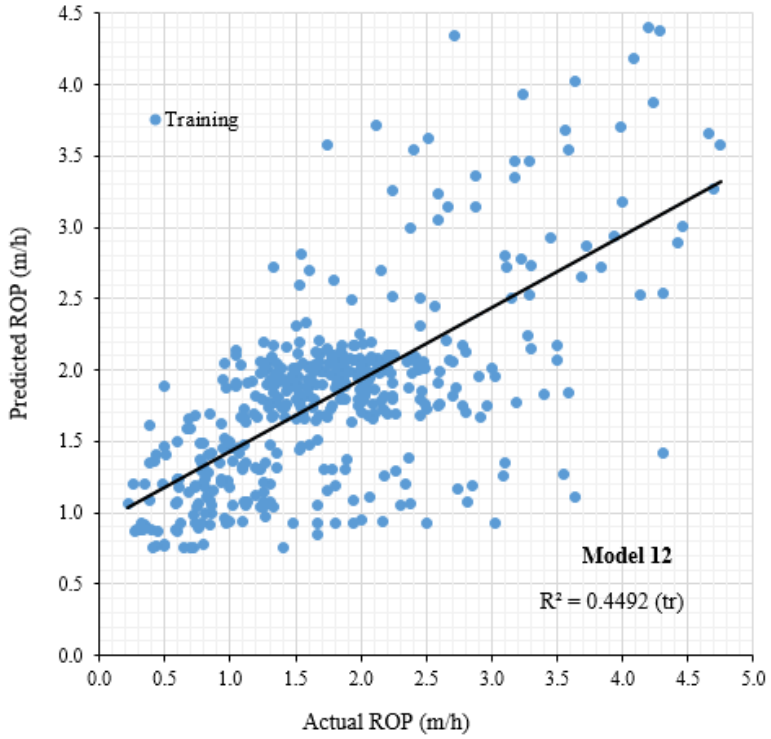

Figure E23.LMR model 12 for estimating TBM penetration for training dataset

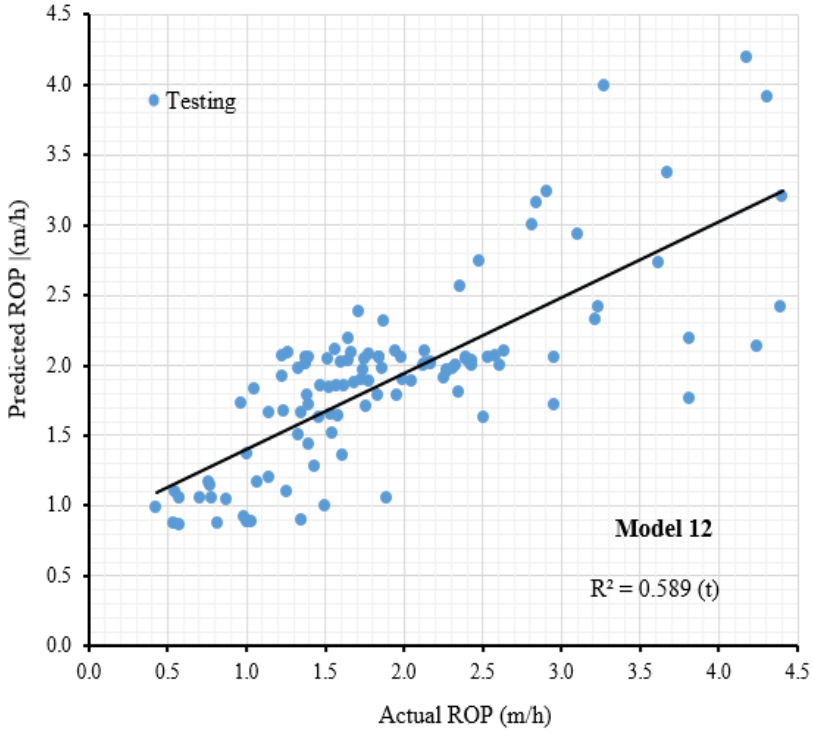

Figure E24. LMR model 12 for estimating TBM penetration for testing dataset

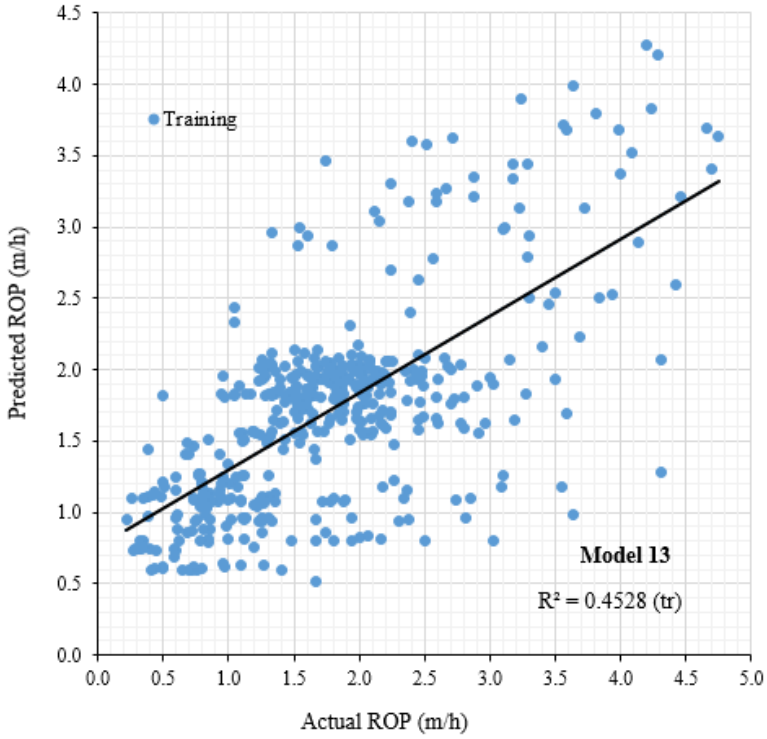

Figure E25. LMR model 13 for estimating TBM penetration for training dataset

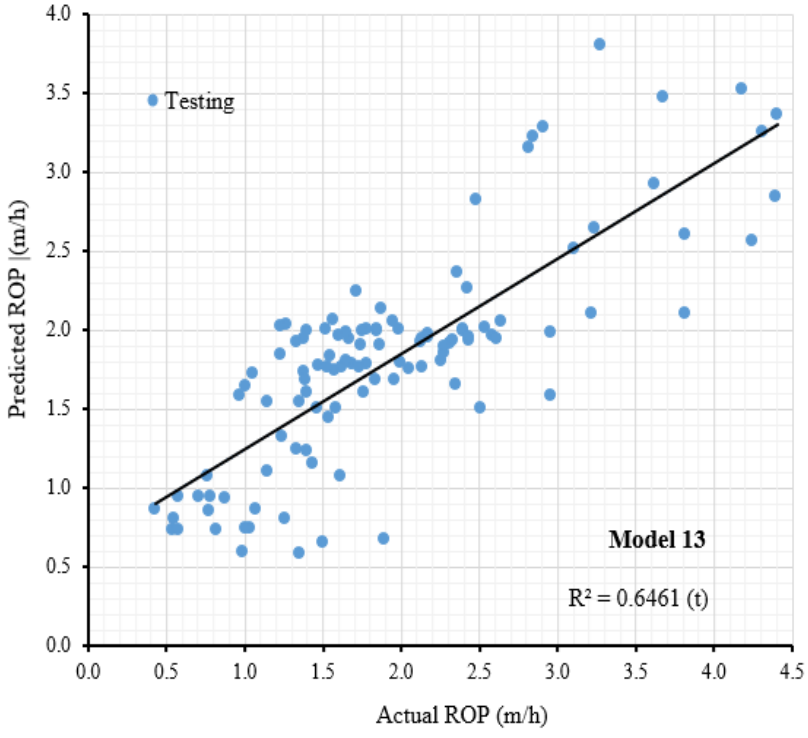

Figure E26. LMR model 13 for estimating TBM penetration for testing dataset

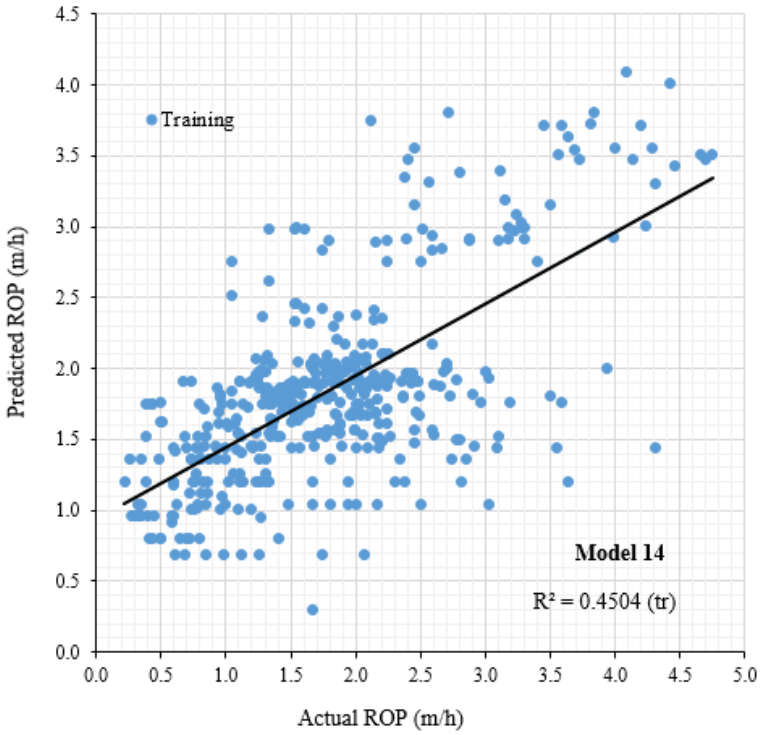

Figure E27. LMR model 14 for estimating TBM penetration for training dataset

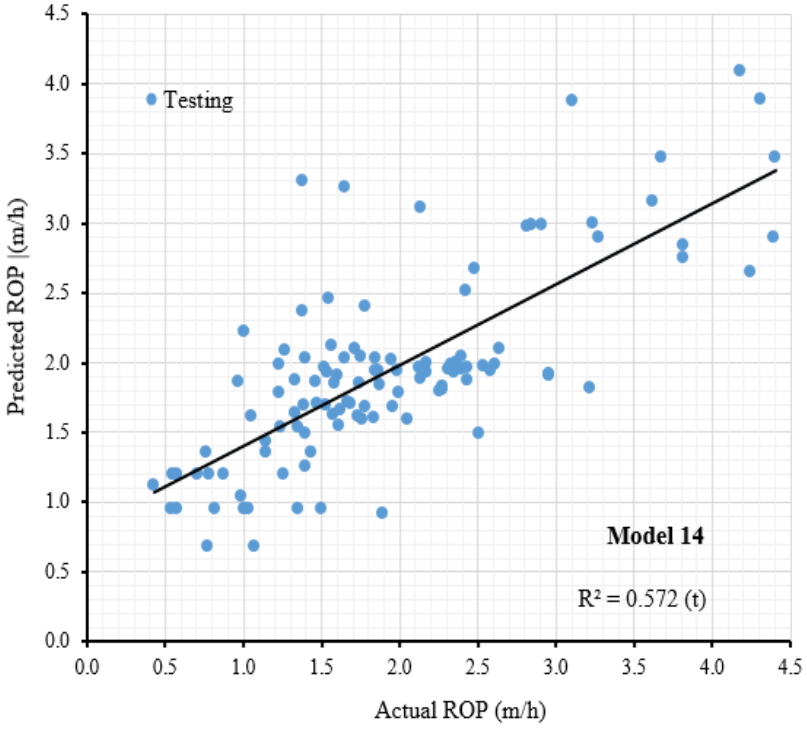

Figure E28. LMR model 14 for estimating TBM penetration for testing dataset

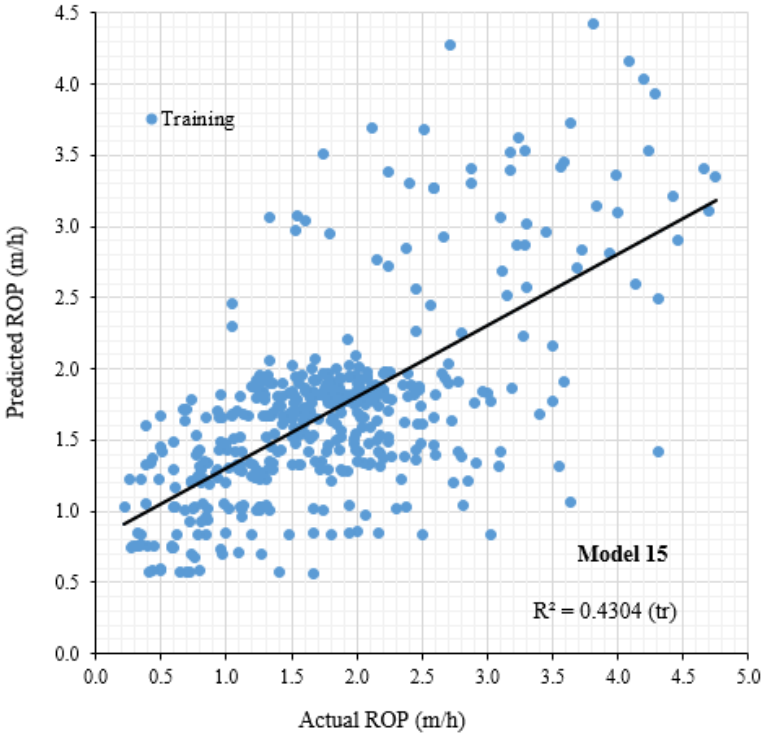

Figure E29. LMR model 15 for estimating TBM penetration for training dataset

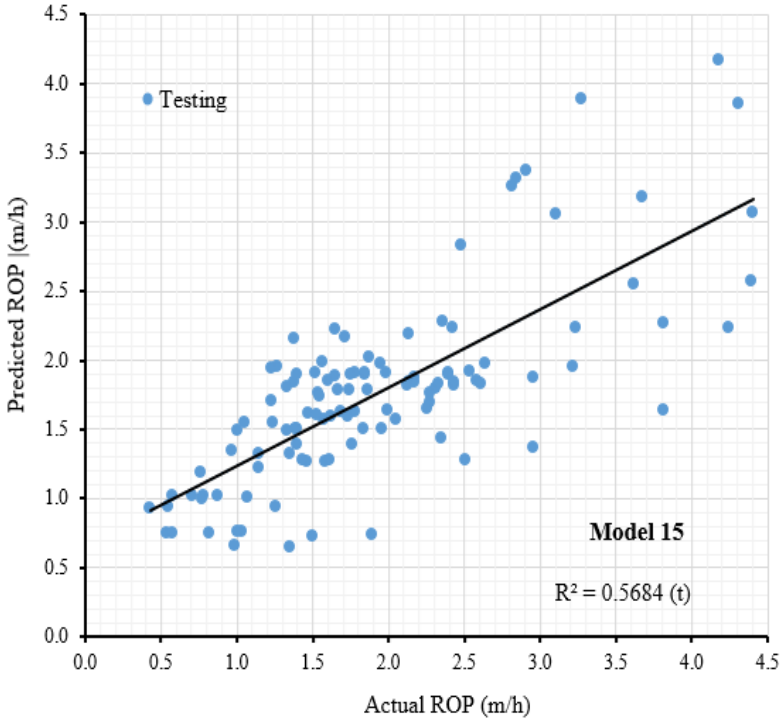

Figure E30. LMR model 15 for estimating TBM penetration for testing dataset

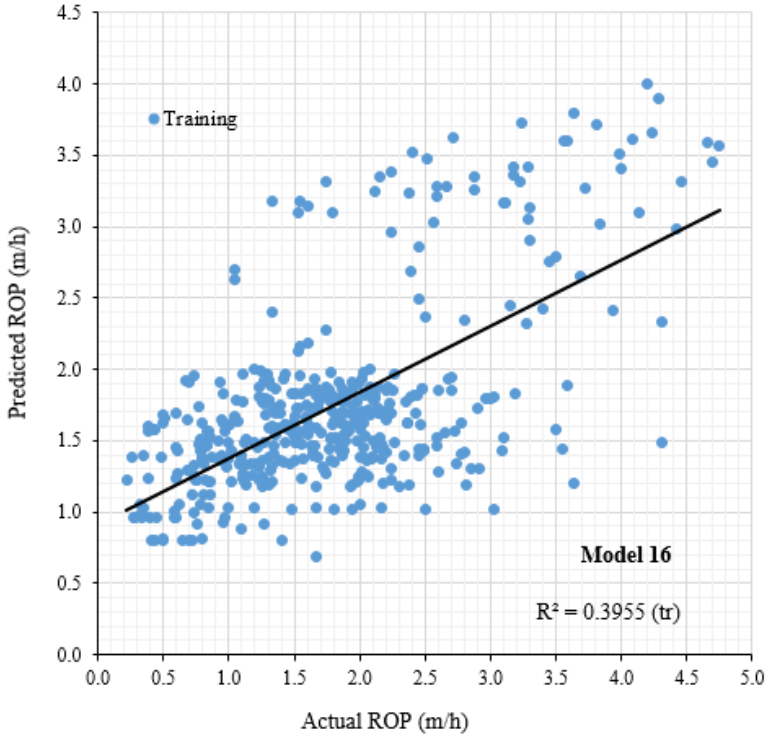

Figure E31. LMR model 16 for estimating TBM penetration for training dataset

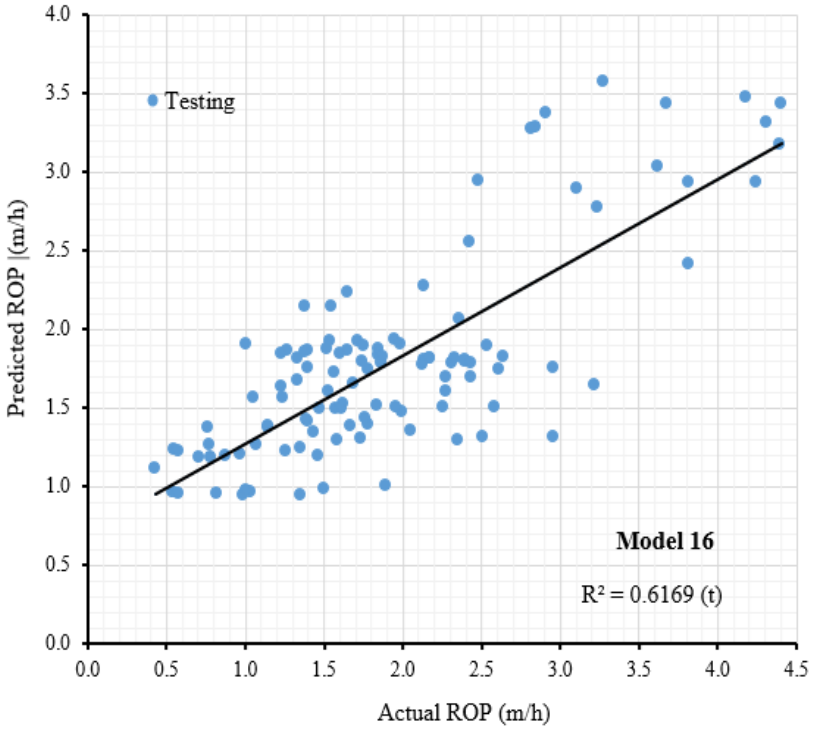

Figure E32. LMR model 16 for estimating TBM penetration for testing dataset

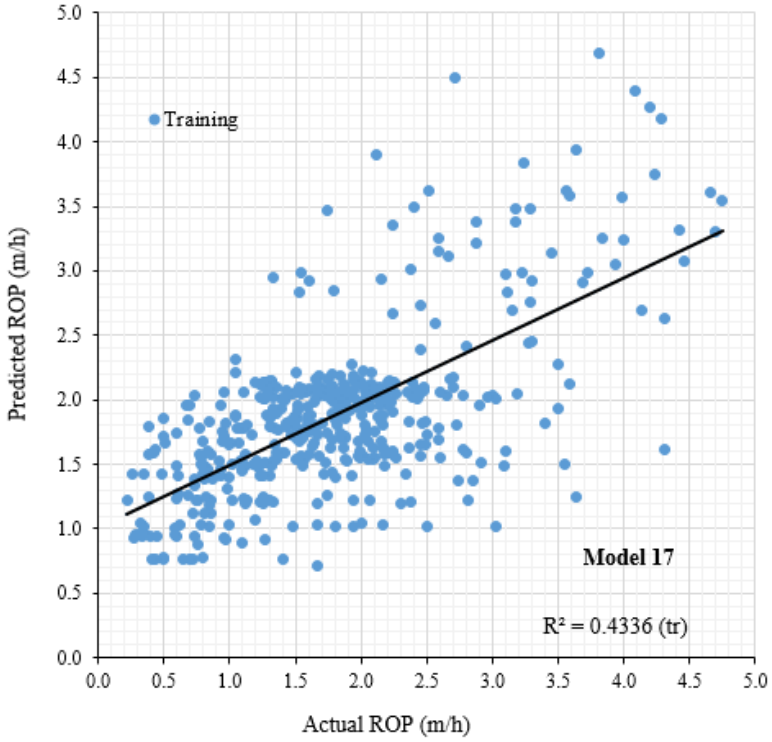

Figure E33. LMR model 17 for estimating TBM penetration for training dataset

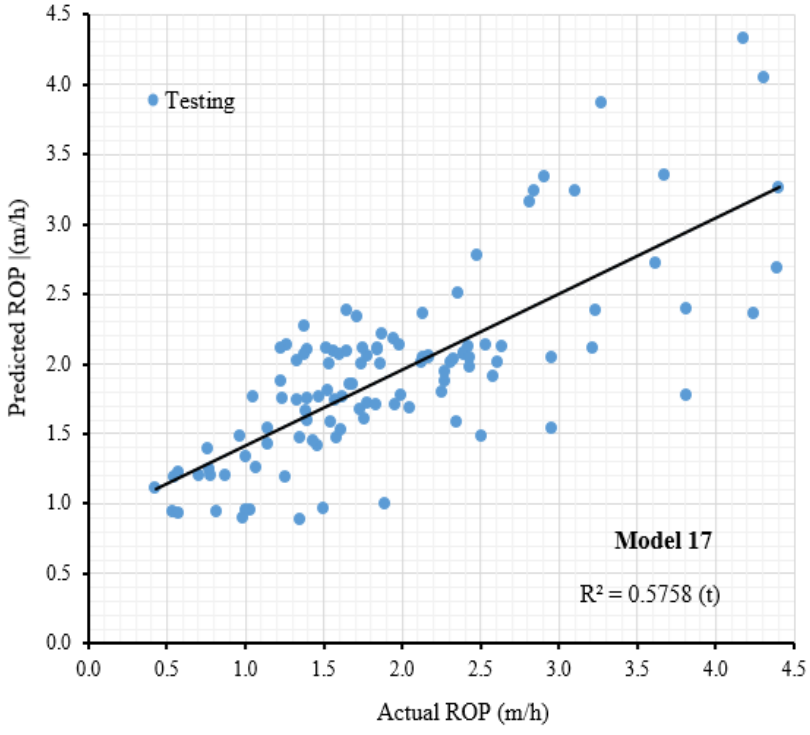

Figure E34. LMR model 17 for estimating TBM penetration for testing dataset

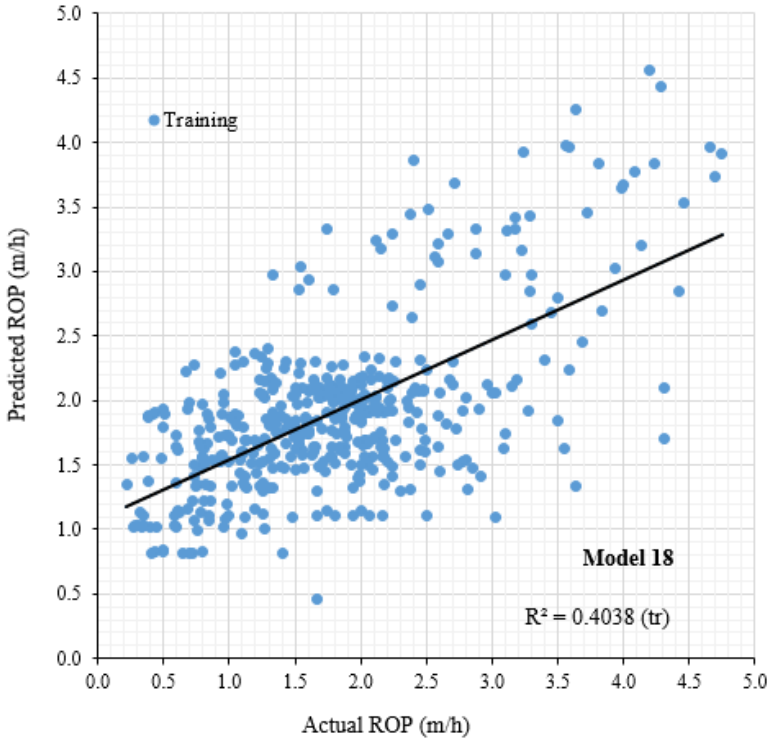

Figure E35. LMR regression model 18 for estimating TBM penetration for training dataset

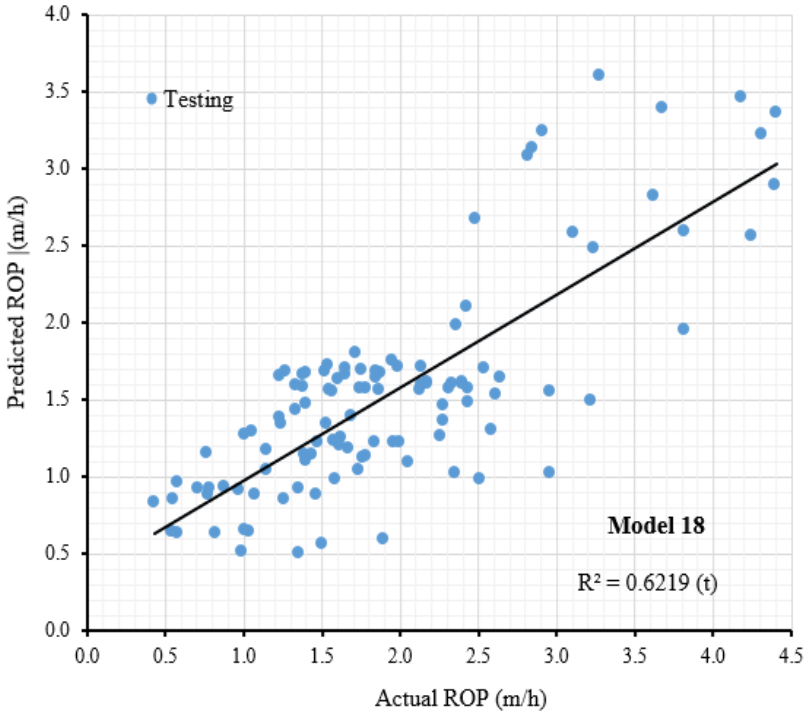

Figure E36. LMR regression model 18 for estimating TBM penetration for testing dataset

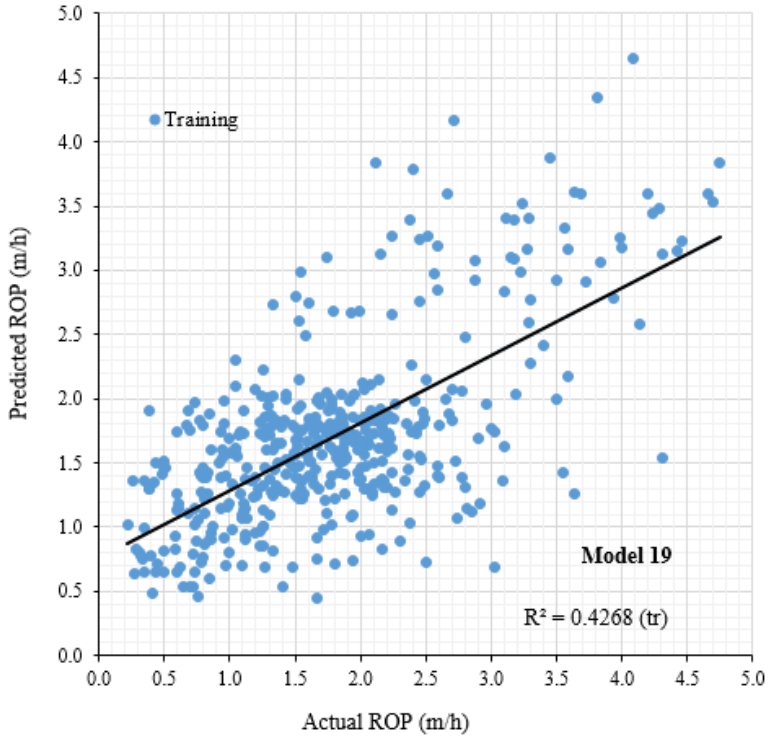

Figure E37. LMR regression model 19 for estimating TBM penetration for training dataset

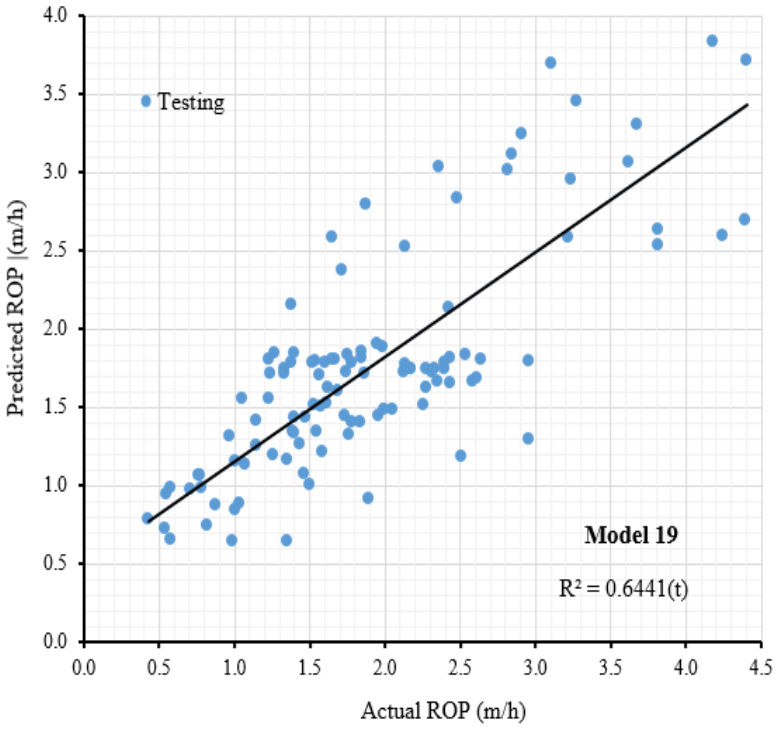

Figure E38. LMR regression model 19 for estimating TBM penetration for testing dataset

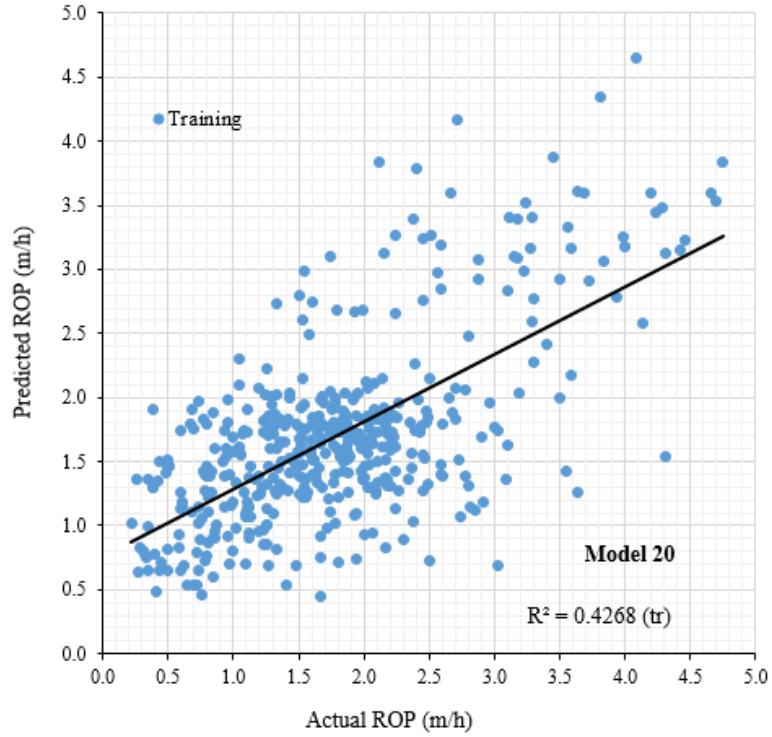

Figure E39. LMR regression model 20 for estimating TBM penetration for training dataset

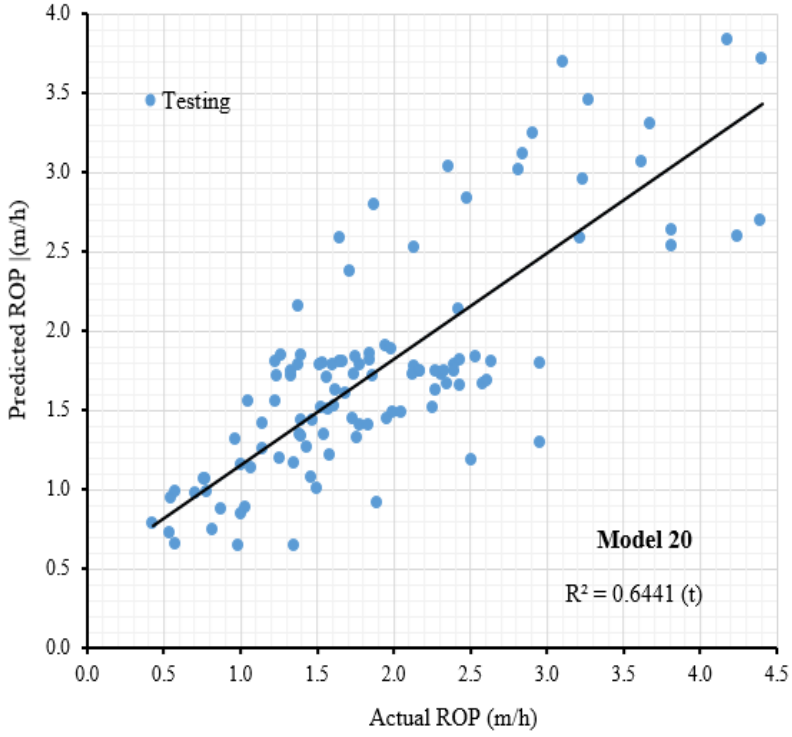

Figure E40. LMR regression model 20 for estimating TBM penetration for testing dataset

Appendix F

Output of 20 Developed Models conducting NLMR Model

Appendix F

Models #	Non-linear Multiple Regression Model Equations	R^2
Model **1**	$ROP = \frac{F_n^{0.308} \cdot WFI^{0.136} \cdot RPM^{-0.027} \cdot CHD^{2.875}}{8.211 \cdot UCS^{0.101} \cdot EXP(0.583 \cdot CHD)}$	0.666
Model 2	$ROP = \frac{MT_c^{0.837} \cdot RPM^{0.817} \cdot TH^{0.101} \cdot WFI^{0.098}}{6.724 \cdot CHD^{-0.242} \cdot UCS^{0.247} \cdot RM_c^{-0.197}}$	0.594
Model 3	$ROP = \frac{TH^{0.187} \cdot MT_c^{0.344} \cdot RPM^{-0.057} \cdot SL_e^{0.078} \cdot CHD^{2.116}}{0.772 \cdot WFI^{-0.099} \cdot EXP\left(\left(CHD/D_c\right)^{0.594}\right) \cdot UCS^{0.144} \cdot RM_c^{-0.061}}$	0.68
Model 4	$ROP = \frac{F_n^{0.181} \cdot MT_c^{0.335} \cdot RPM^{0.01} \cdot SL_e^{0.08} \cdot CHD^{2.116}}{0.566 \cdot WFI^{-0.099} \cdot EXP\left(\left(CHD/D_c\right)^{0.589}\right) \cdot UCS^{0.144} \cdot RM_c^{-0.063}}$	0.68
Model 5	$ROP = \frac{TH^{0.233} \cdot MT_c^{0.165} \cdot RPM^{1.469} \cdot FI^{-0.067} \cdot \left(CHD/D_c\right)^{-0.68}}{0.036 \cdot WFI^{-0.175} \cdot EXP\left(\left(CHD/N_c\right)^{-0.889}\right) \cdot UCS^{0.159} \cdot RM_c^{-0.093}}$	0.672
Model 6	$ROP = \frac{TH^{0.326} \cdot MT_c^{0.736} \cdot RPM^{1.222} \cdot FI^{0.12} \cdot CHD^{-0.722}}{0.137 \cdot UCS^{0.197} \cdot EXP\left(\left(CHD/N_c\right)^{-0.817}\right) \cdot RM_c^{-0.13}}$	0.638
Model 7	$ROP = \frac{TH^{0.032} \cdot MT_c^{0.111} \cdot RPM^{1.96} \cdot CHD^{-0.3} \cdot SL_e^{0.198}}{0.02 \cdot UCS^{0.201} \cdot EXP\left(\left(CHD/N_c\right)^{-0.959}\right) \cdot RM_c^{-0.14}}$	0.647
Model 8	$ROP = \frac{TH^{0.281} \cdot MT_c^{0.267} \cdot RPM^{1.546} \cdot CHD^{-0.697}}{0.095 \cdot WFI^{-0.13} \cdot EXP\left(\left(CHD/N_c\right)^{-0.899}\right) \cdot UCS^{0.16} \cdot RM_c^{-0.103}}$	0.666
Model 9	$ROP = \frac{TH^{0.153} \cdot MT_c^{0.259} \cdot RPM^{0.271} \cdot CHD^{-0.769} \cdot SL_e^{-0.037}}{0.481 \cdot WFI^{-0.113} \cdot EXP((CHD \cdot D_c)^{-4.862}) \cdot UCS^{0.179} \cdot RM_c^{-0.073}}$	0.658
Model 10	$ROP = \frac{F_n^{0.215} \cdot MT_c^{0.11} \cdot RPM^{1.728} \cdot CHD^{-0.386} \cdot SL_e^{0.072}}{0.048 \cdot WFI^{-0.106} \cdot EXP\left(\left(CHD/N_c\right)^{-0.92}\right) \cdot UCS^{0.16} \cdot RM_c^{-0.106}}$	0.669
Model 11	$ROP = \frac{F_n^{0.201} \cdot RMc^{0.066} \cdot MTc^{0.24} \cdot RPM^{0.281} \cdot CHD^{-0.67} \cdot SL_e^{-0.043}}{0.413 \cdot WFI^{-0.119} \cdot UCS^{0.181} \cdot EXP(CHD \cdot D_c)^{-4.851}}$	0.661
Model 12	$ROP = \frac{F_n^{0.375} \cdot WFI^{0.454} + MTc^{0.842} \cdot RPM^{1.883} \cdot CHD^{0.147}}{0.058 \cdot UCS^{0.131} \cdot \left(CHD/N_c\right)^{-3.276} \cdot RM_c^{-0.169}}$	0.63
Model 13	$ROP = \frac{F_n^{0.285} \cdot MT_c^{0.321} \cdot N_c^{-4.776} \cdot RPM^{1,567} \cdot CHD^{4.449}}{0.002 \cdot UCS^{0.171} \cdot WFI^{-0.131} \cdot RM_c^{-0.127}}$	0.66
Model **14**	$ROP = \frac{F_n^{0.26} \cdot MT_c^{0.05} \cdot N_c^{-0.823} \cdot RPM^{0.351} \cdot SL_e^{-0.041}}{0.098 \cdot UCS^{0.15} \cdot WFI^{-0.129} \cdot EXP((CHD \cdot D_c)^{-5.476})}$	0.669
Model **15**	$ROP = \frac{F_n^{0.354} \cdot WFI^{0.152} \cdot RPM^{0.007} \cdot CHD^{1.185}}{7.715 \cdot UCS^{0.119} \cdot EXP(0.023 \cdot CHD^2)}$	0.652
Model 16	$ROP = \frac{3.977 \cdot F_n^{0.103} \cdot WFI^{0.11} \cdot RPM^{0.423} \cdot MTc^{0.874}}{UCS^{0.142} \cdot D_c^{-2.582} \cdot RM_c^{-0.123}}$	0.657
Model **17**	$ROP = \frac{F_n^{0.266} \cdot RPM^{0.014} \cdot CHD^{2.993} \cdot SL_e^{0.042}}{9.22 \cdot UCS^{0.087} \cdot WFI^{-0.116} \cdot EXP(0.591 \cdot CHD)}$	0.668
Model 18	$ROP = \frac{MT_c^{0.131} \cdot RPM^{-0.002} \cdot TH^{0.269} \cdot CHD^{2.555}}{11.881 \cdot UCS^{0.151} \cdot WFI^{-0.128} \cdot EXP(0.559 \cdot CHD) \cdot RM_c^{-0.081}}$	0.672
Model **19**	$ROP = \frac{F_n^{0.347} \cdot CHD^{1.162} \cdot RPM^{0.046} \cdot MT_c^{0.095}}{8.765 \cdot WFI^{-0.145} \cdot UCS^{0.103} \cdot EXP(0.022 \cdot CHD^2)}$	0.653
Model 20	$ROP = \frac{F_n^{0.310} \cdot WFI^{0.149} \cdot RPM^{1.632} \cdot CHD^{-0.58}}{0.035 \cdot UCS^{0.177} \cdot EXP\left(\left(CHD/N_c\right)^{-0.928}\right) \cdot RM_c^{-0.071}}$	0.662

*Red colored models were examined in detail at content

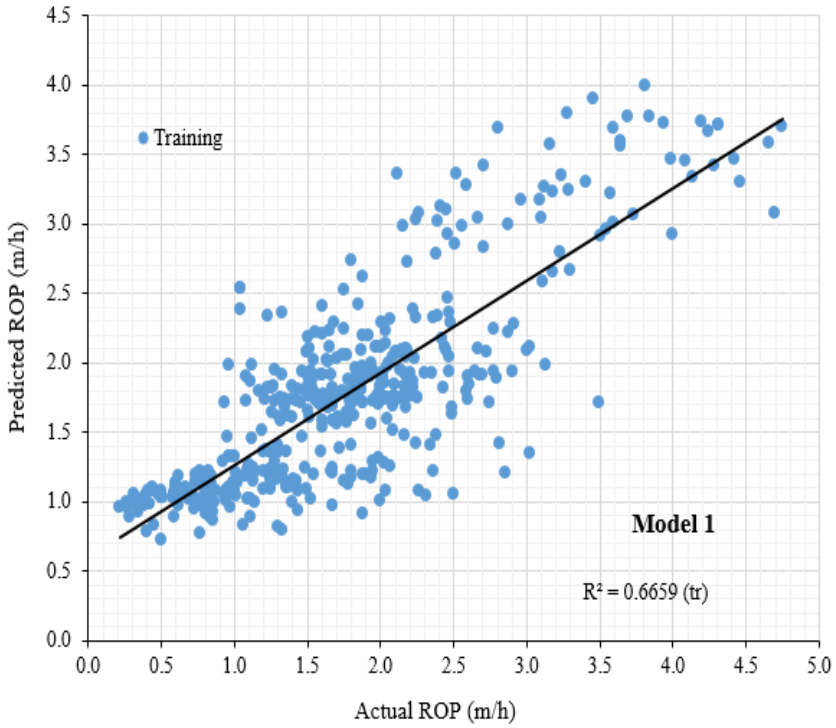

Figure F1. NLMR model 1 for estimating TBM penetration for training dataset

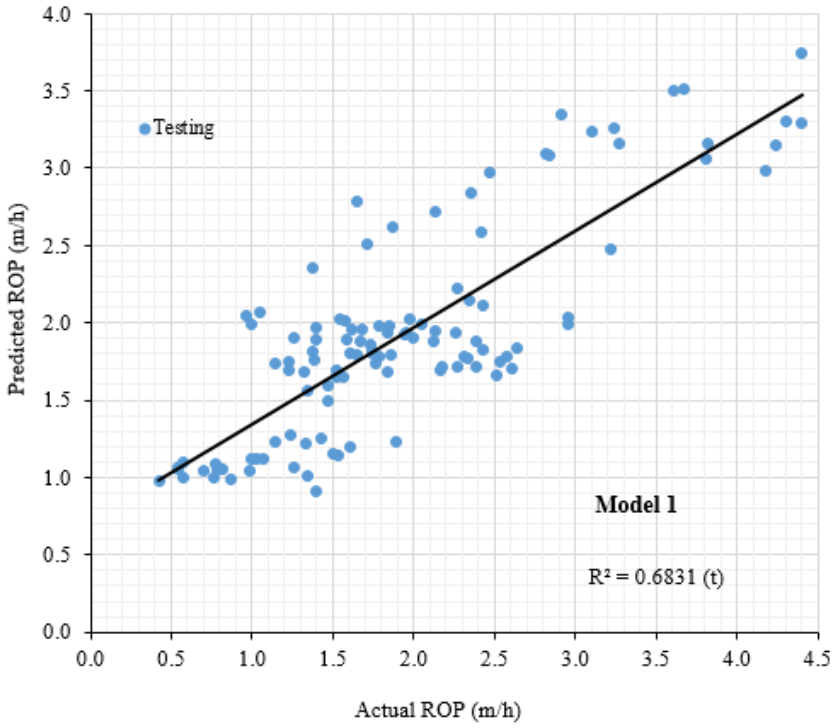

Figure F2. NLMR model 1 for estimating TBM penetration for testing dataset

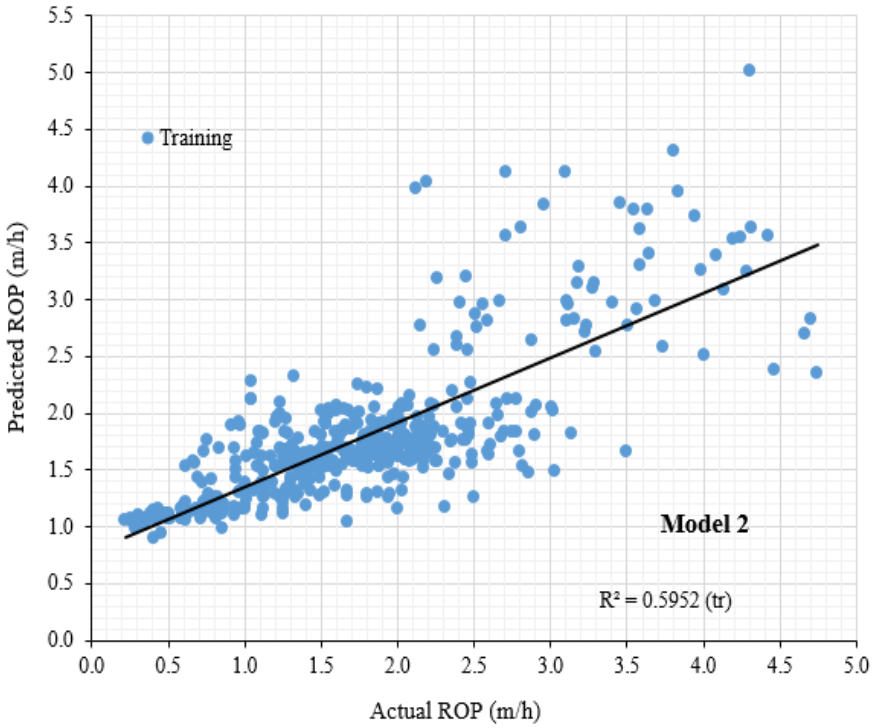

Figure F3. NLMR model 2 for estimating TBM penetration for training dataset

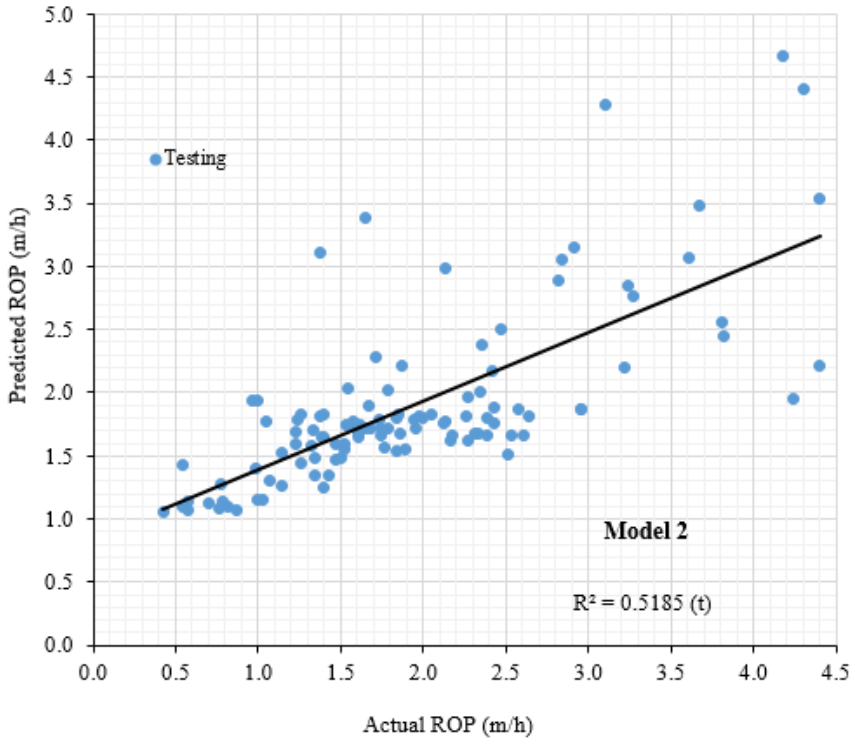

Figure F4. NLMR model 2 for estimating TBM penetration for testing dataset

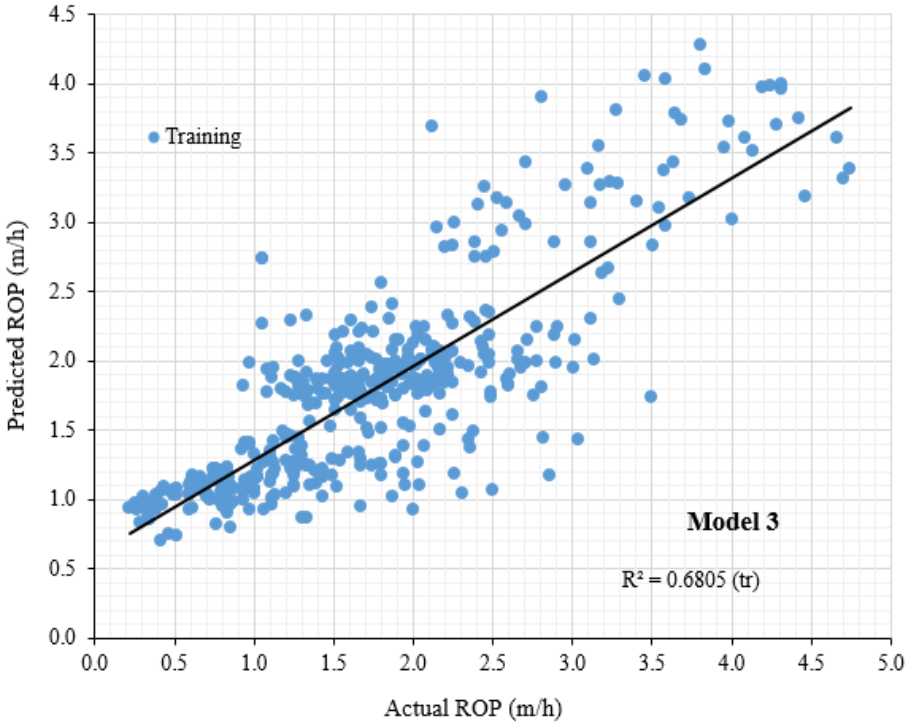

Figure F5. NLMR model 3 for estimating TBM penetration for training dataset

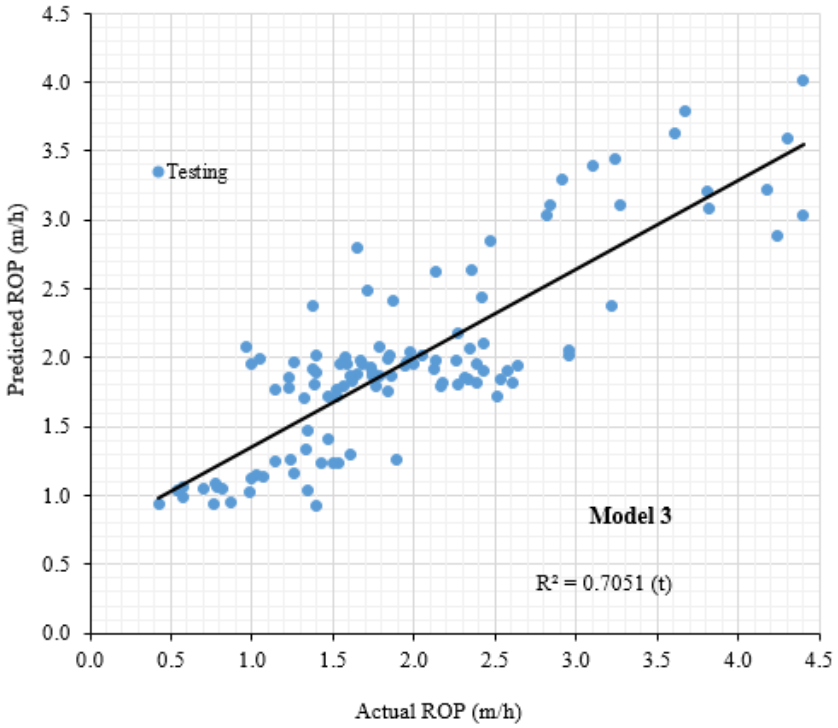

Figure F6. NLMR model 3 for estimating TBM penetration for testing dataset

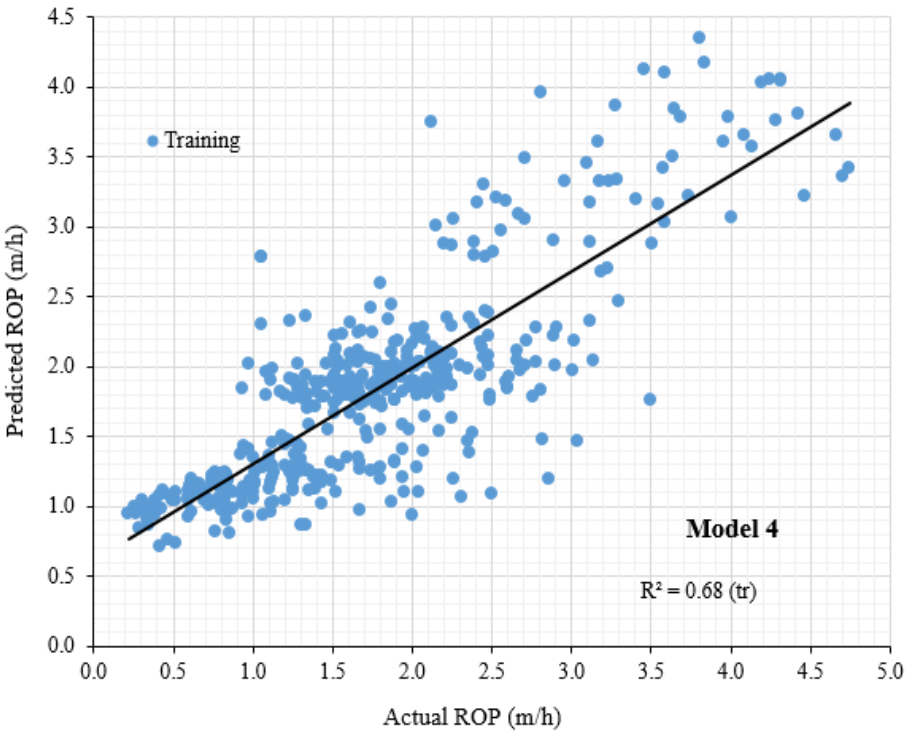

Figure F7. NLMR model 4 for estimating TBM penetration for training dataset

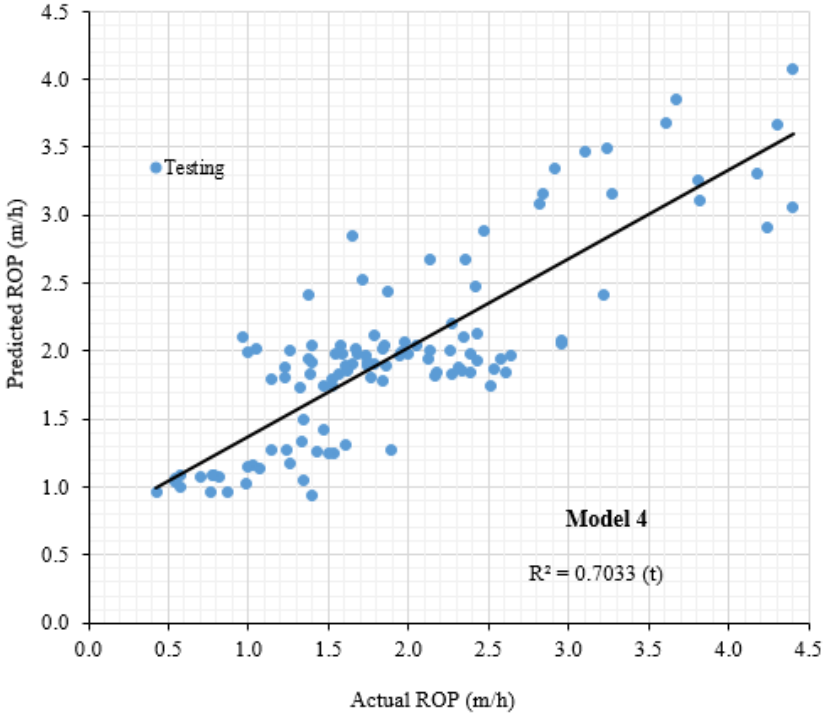

Figure F8. NLMR model 4 for estimating TBM penetration for testing dataset

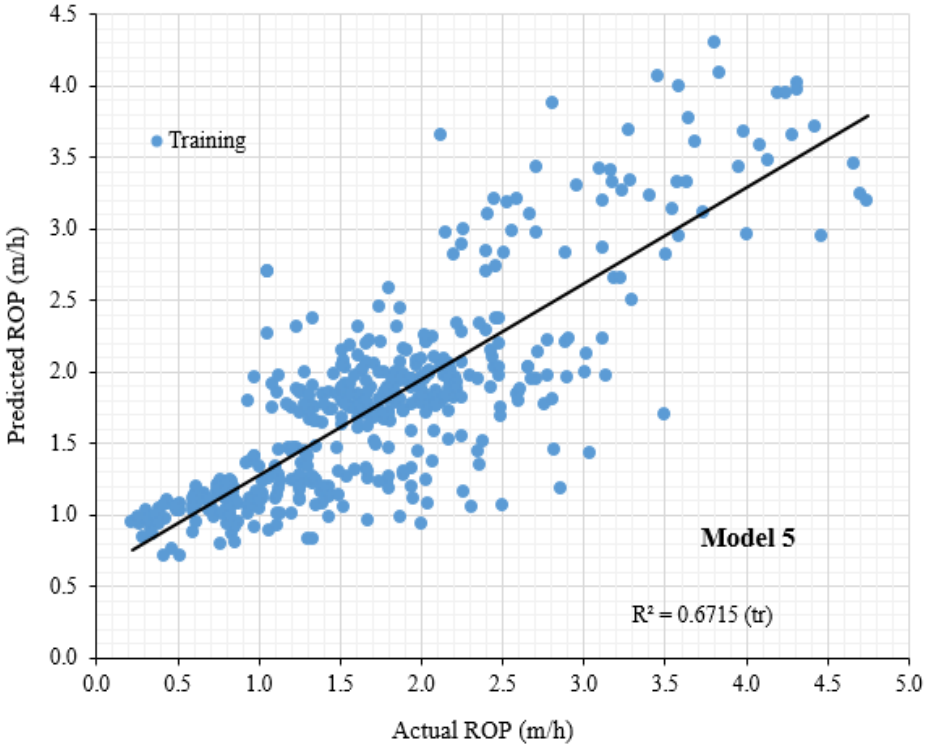

Figure F9. NLMR model 5 for estimating TBM penetration for training dataset

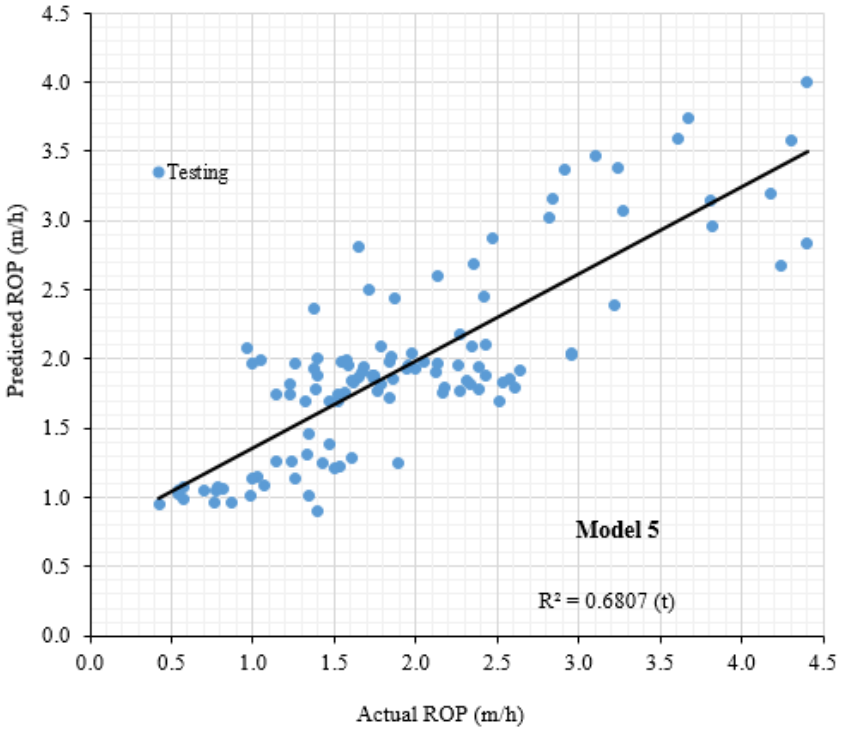

Figure F10. NLMR model 5 for estimating TBM penetration for testing dataset

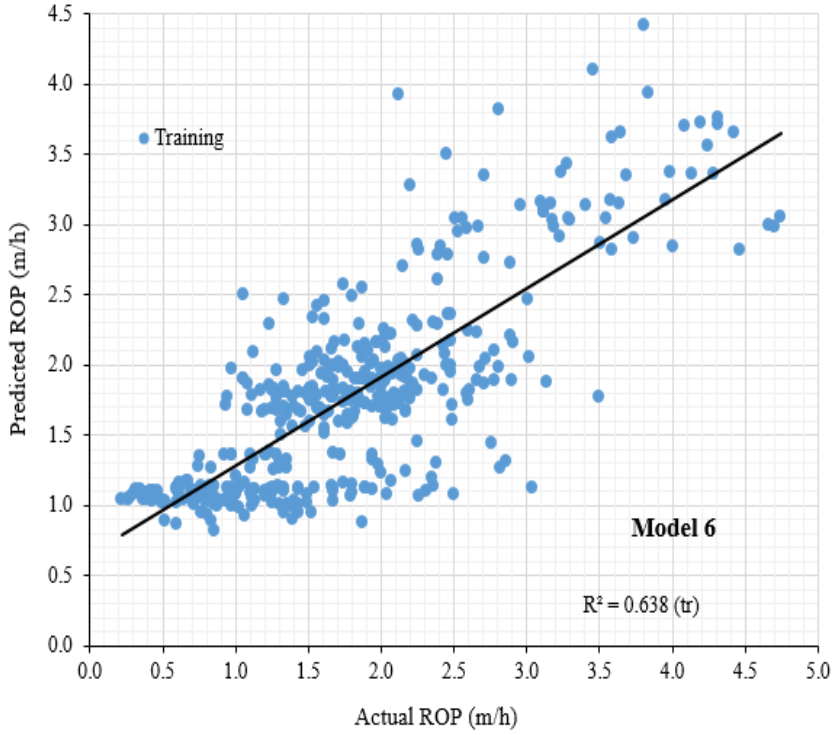

Figure F11. NLMR model 6 for estimating TBM penetration for training dataset

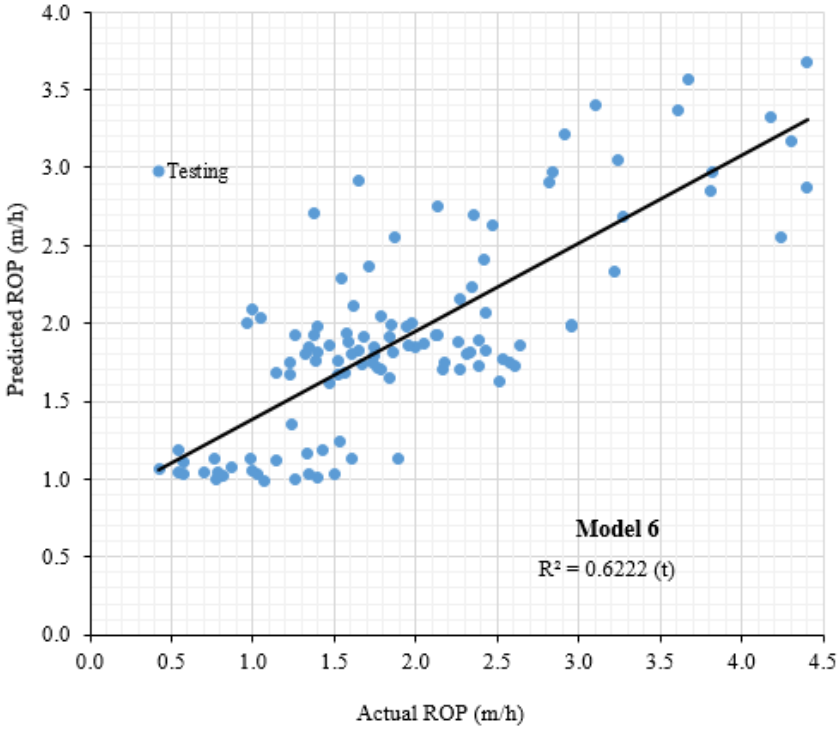

Figure F12. NLMR model 6 for estimating TBM penetration for testing dataset

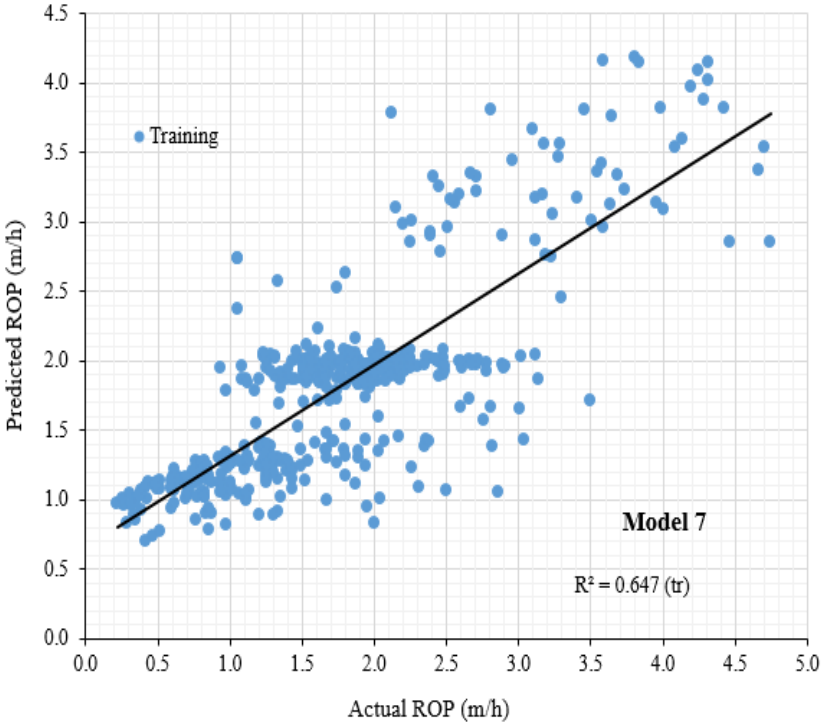

Figure F13. NLMR model 7 for estimating TBM penetration for training dataset

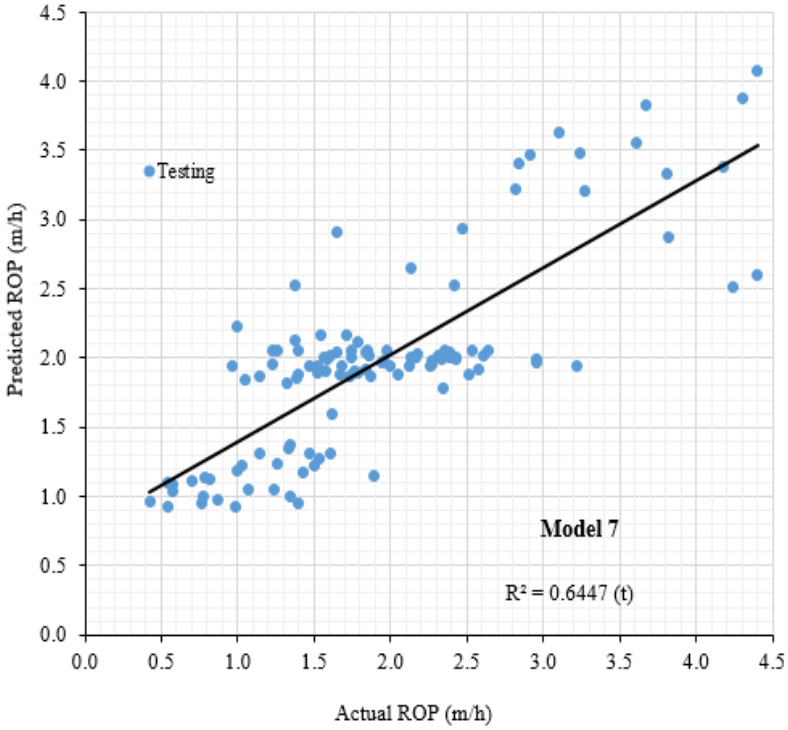

Figure F14. NLMR model 7 for estimating TBM penetration for testing dataset

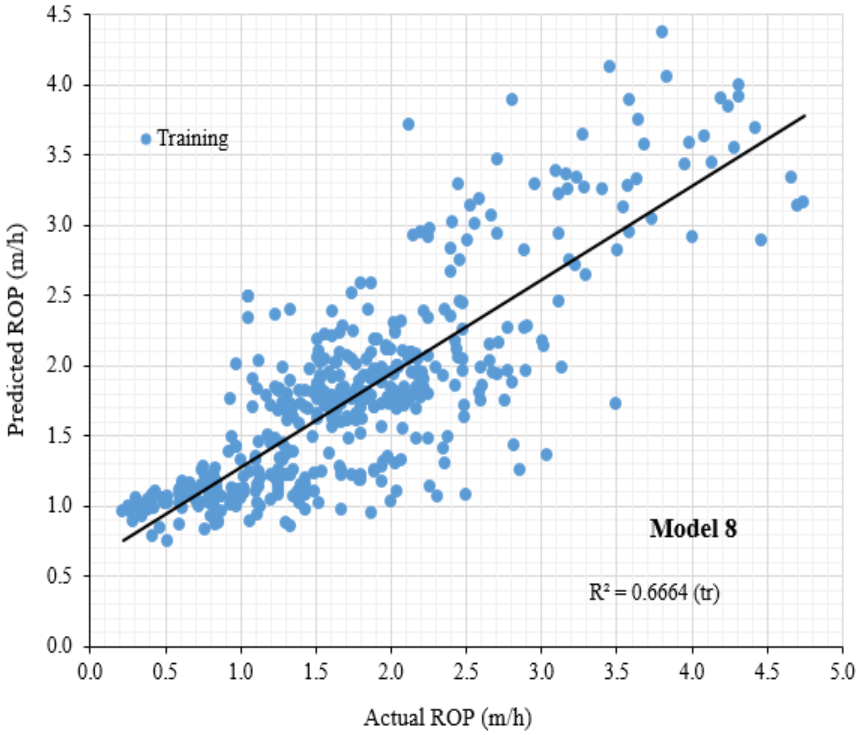

Figure F15. NLMR model 8 for estimating TBM penetration for training dataset

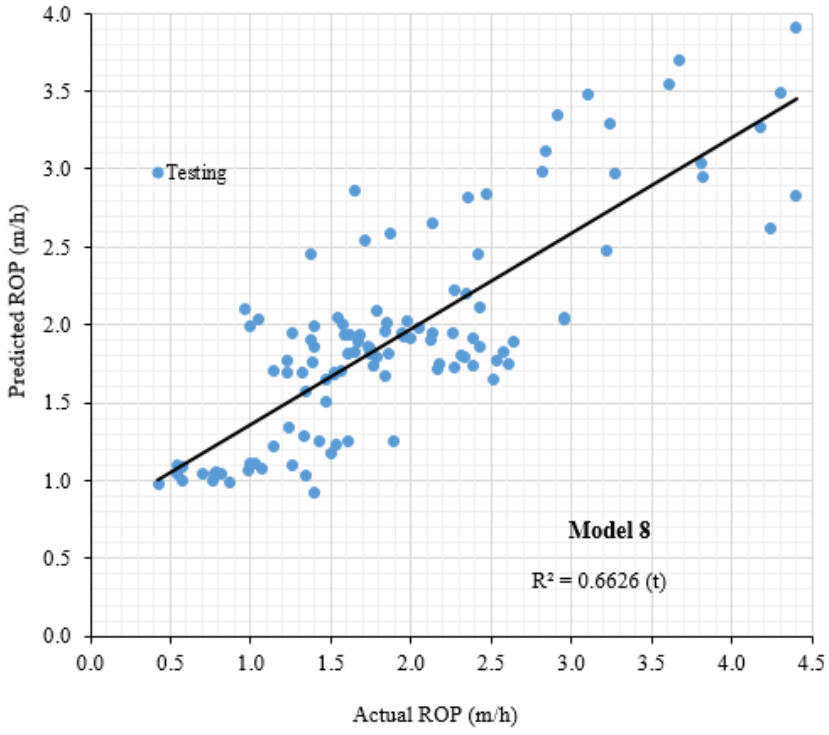

Figure F16. NLMR model 8 for estimating TBM penetration for testing dataset

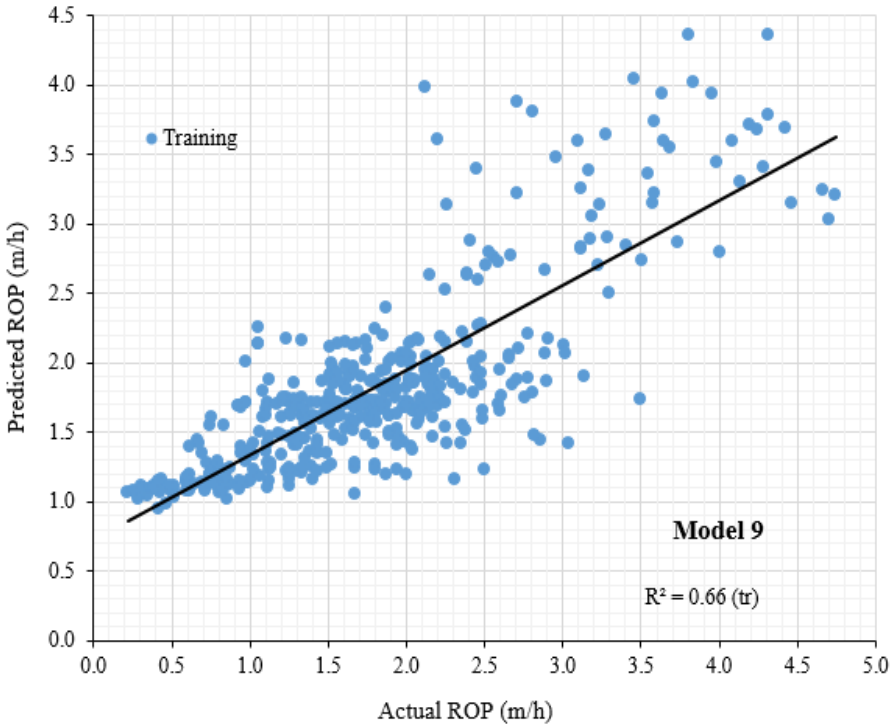

Figure F17. NLMR model 9 for estimating TBM penetration for training dataset

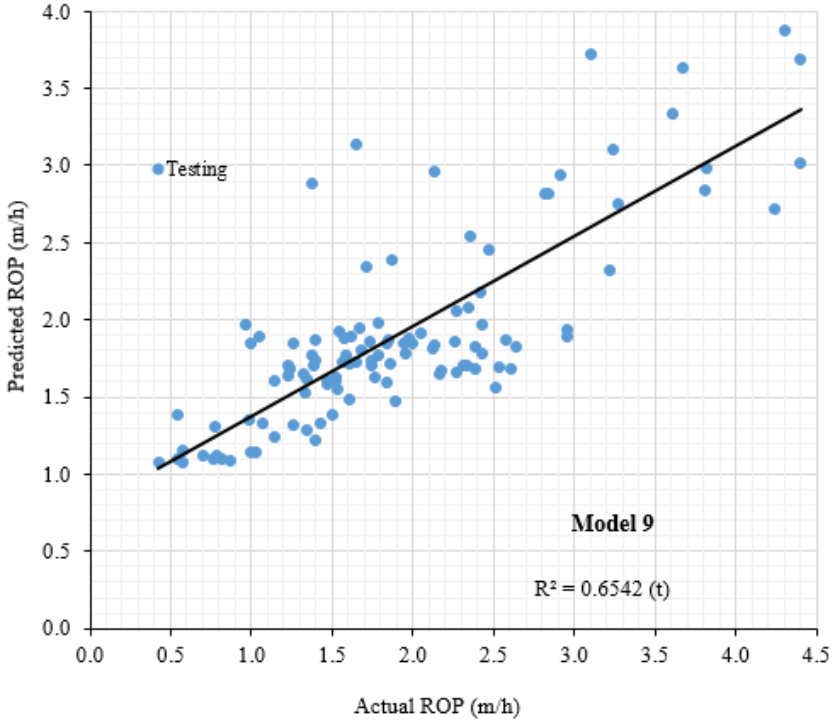

Figure F18. NLMR model 9 for estimating TBM penetration for testing dataset

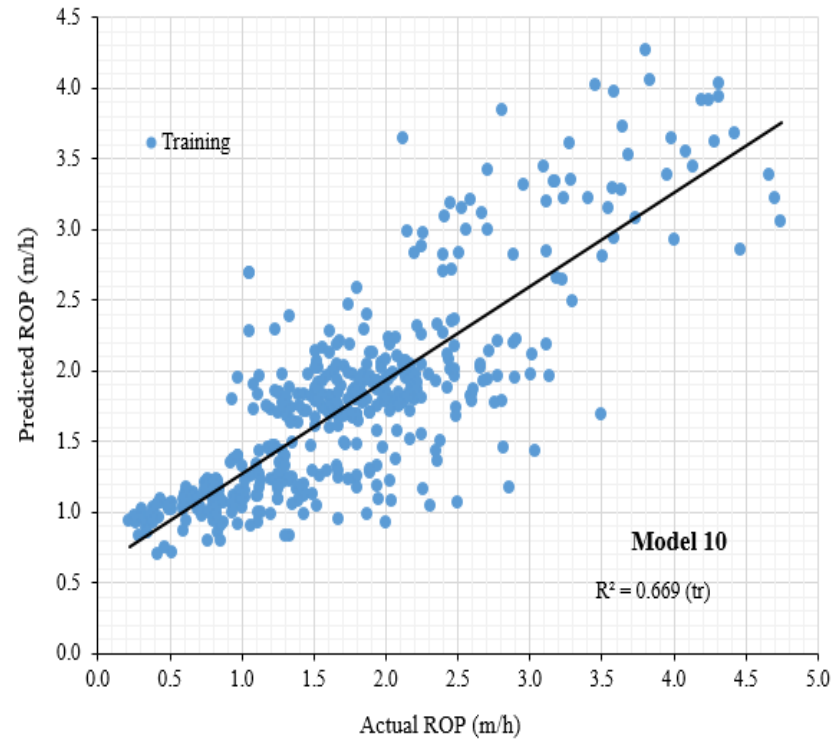

Figure F19. NLMR model 10 for estimating TBM penetration for training dataset

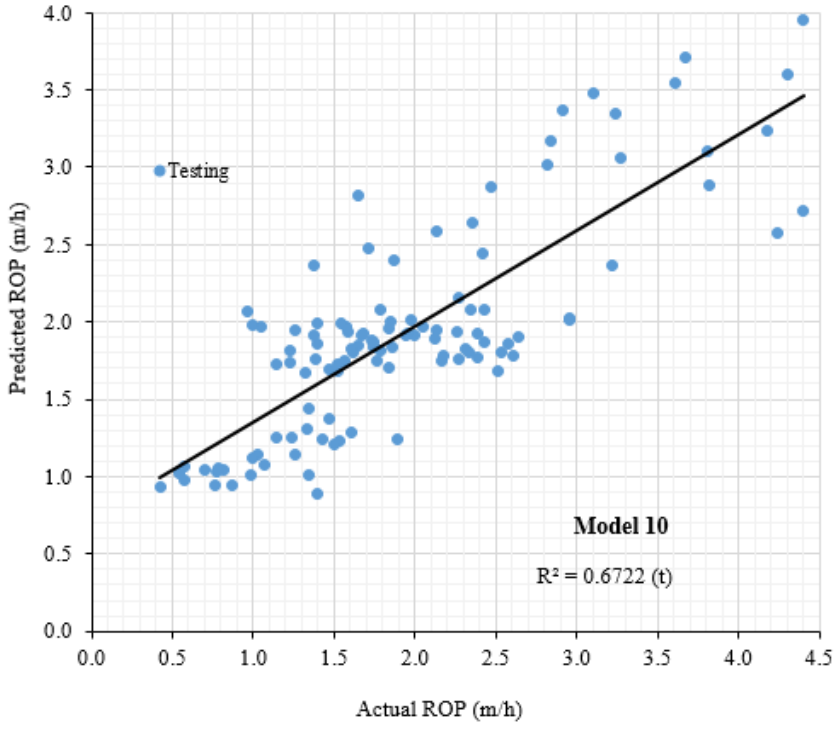

Figure F20. NLMR model 10 for estimating TBM penetration for testing dataset

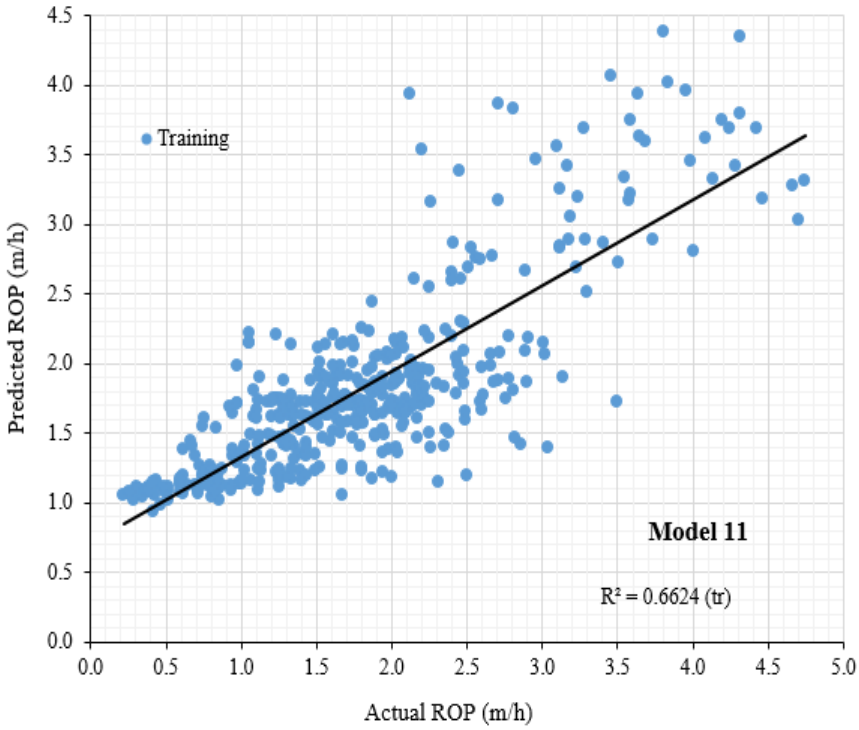

Figure F21. NLMR model 11 for estimating TBM penetration for training dataset

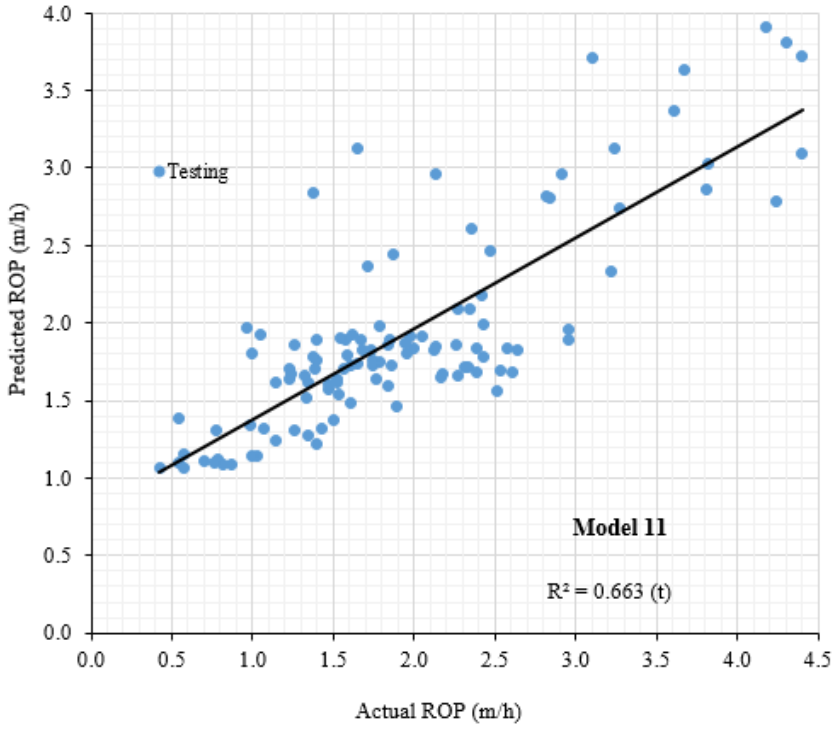

Figure F22. NLMR model 11 for estimating TBM penetration for testing dataset

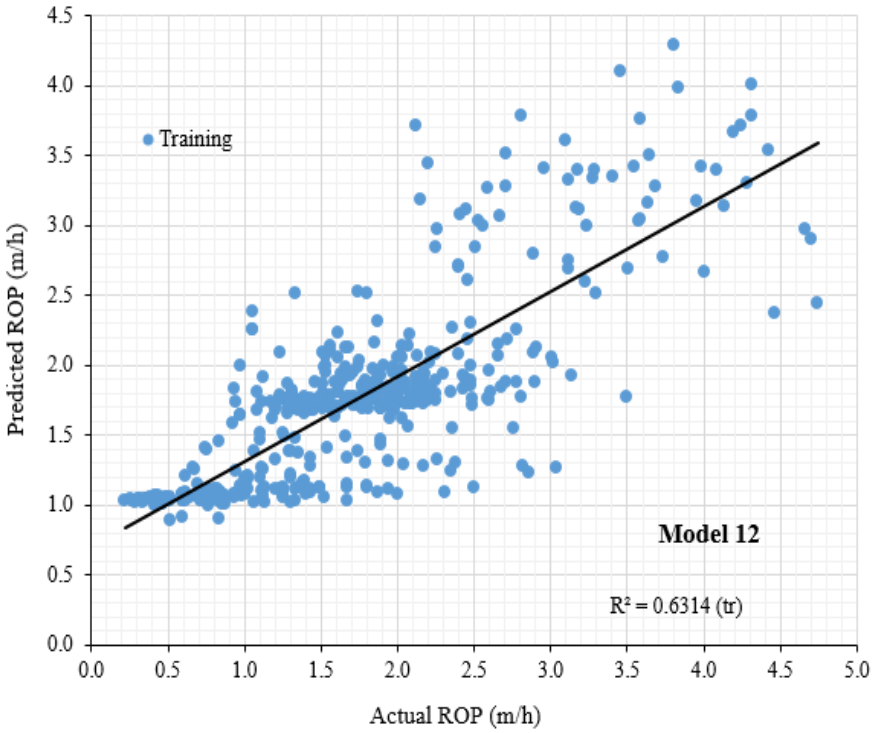

Figure F23. NLMR model 12 for estimating TBM penetration for training dataset

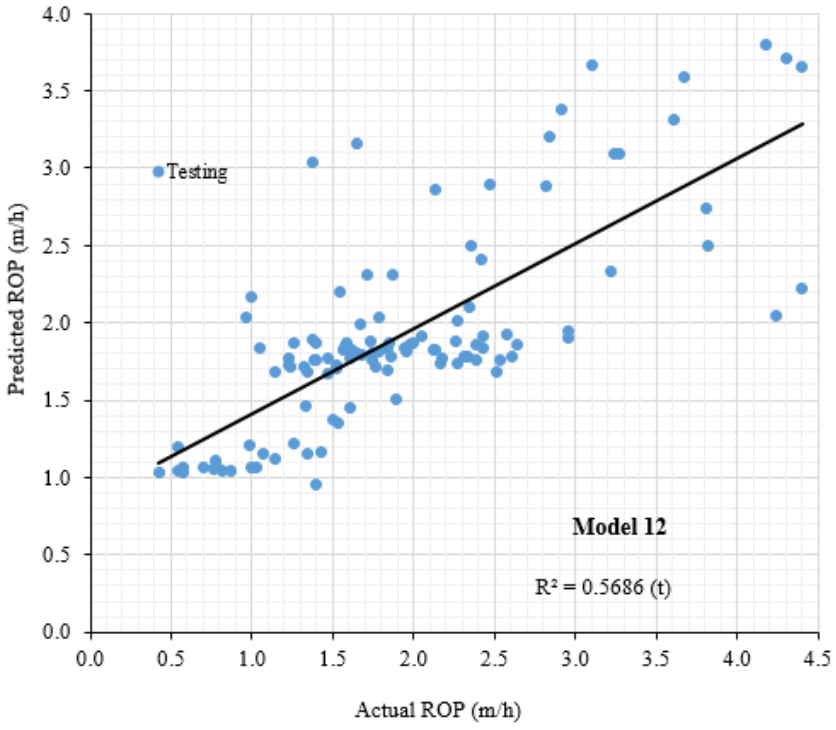

Figure F24. NLMR model 12 for estimating TBM penetration for testing dataset

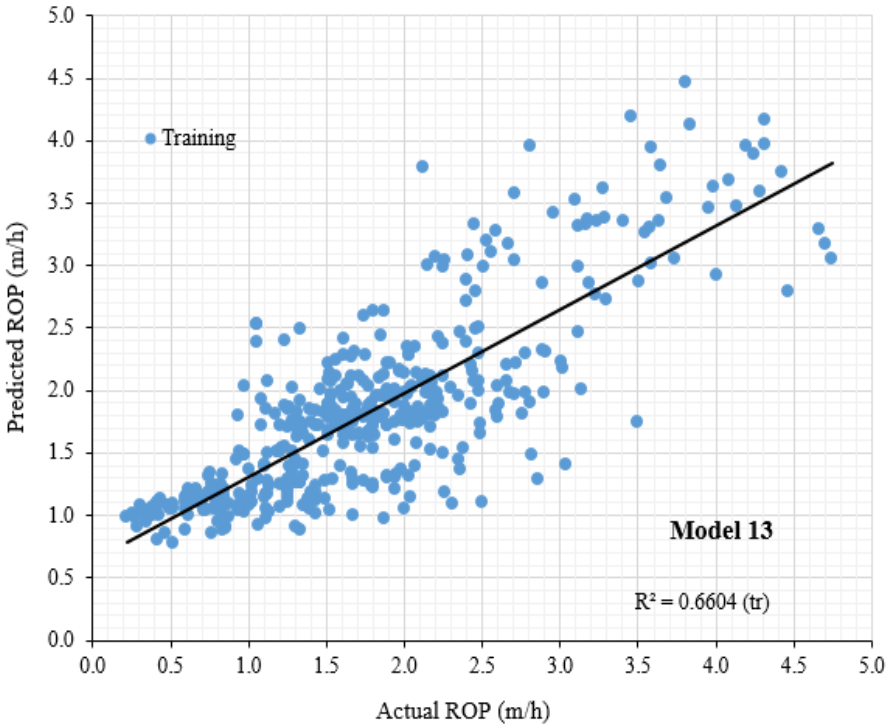

Figure F25. NLMR model 13 for estimating TBM penetration for training dataset

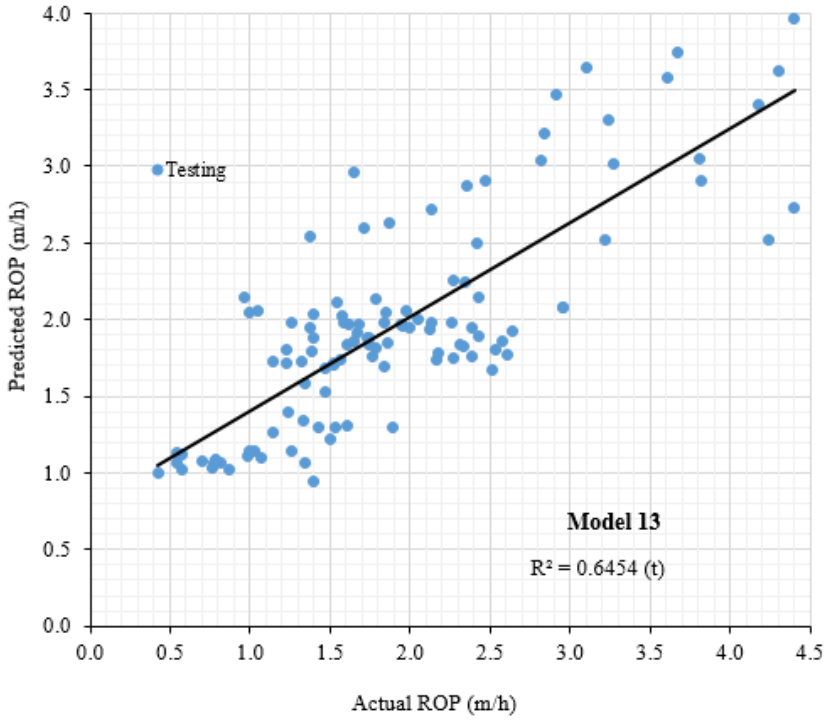

Figure F26. NLMR model 13 for estimating TBM penetration for testing dataset

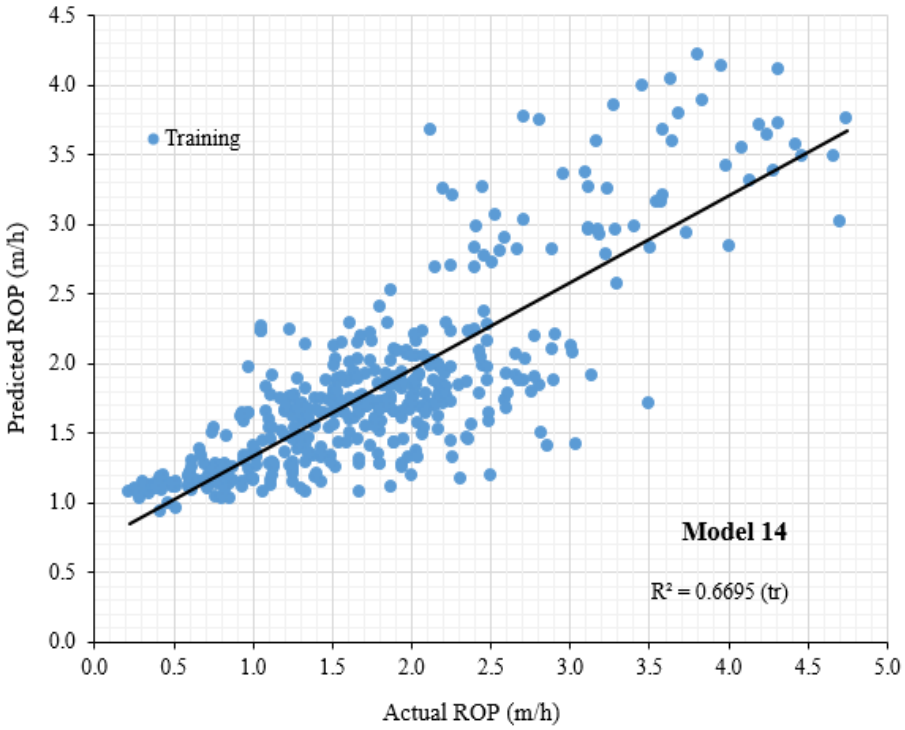

Figure F27. NLMR model 14 for estimating TBM penetration for training dataset

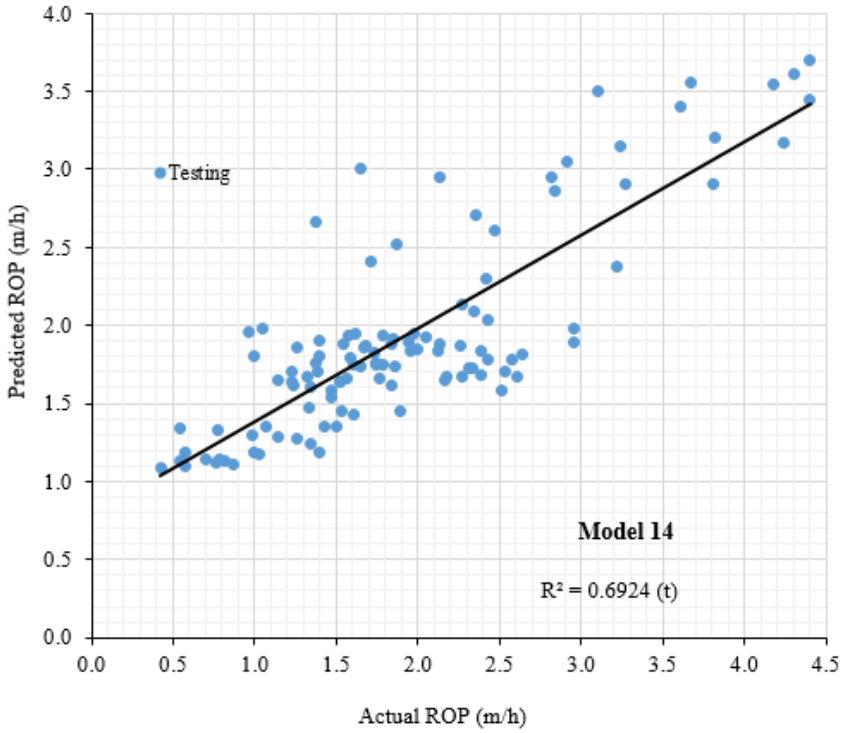

Figure F28. NLMR model 14 for estimating TBM penetration for testing dataset

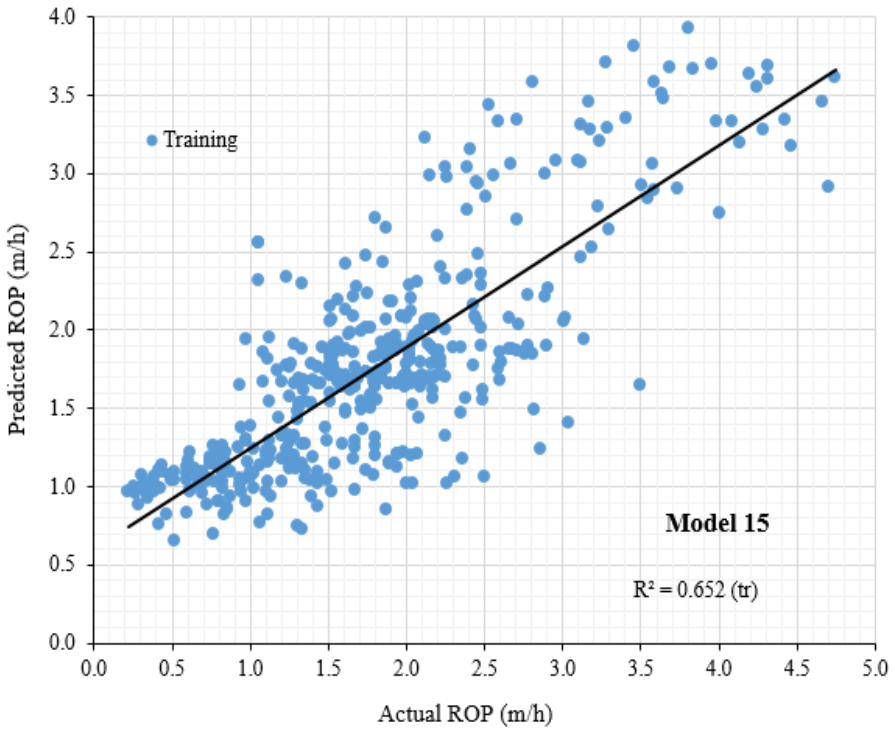

Figure F29. NLMR model 15 for estimating TBM penetration for training dataset

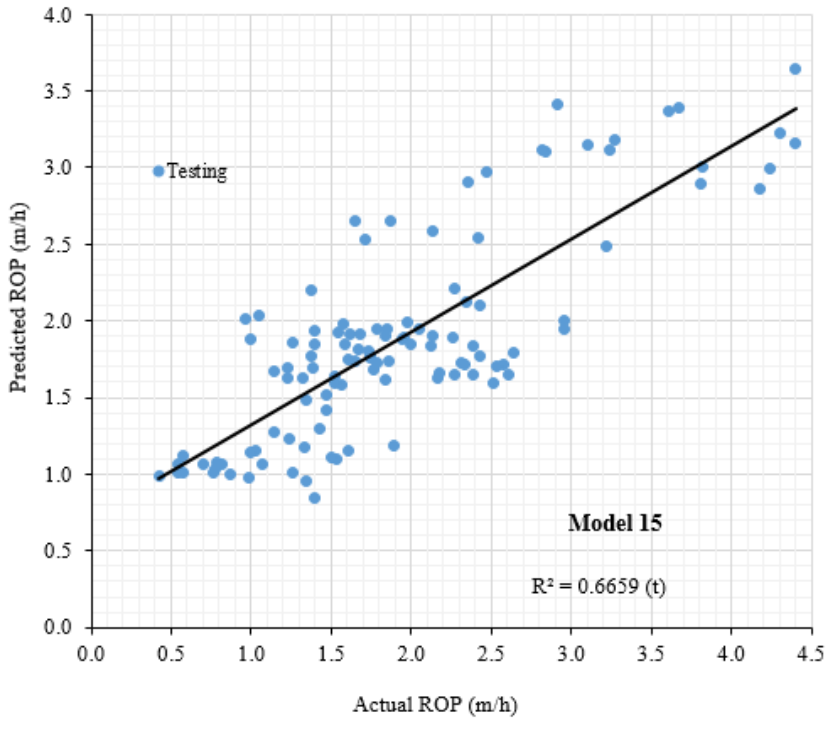

Figure F30. NLMR model 15 for estimating TBM penetration for testing dataset

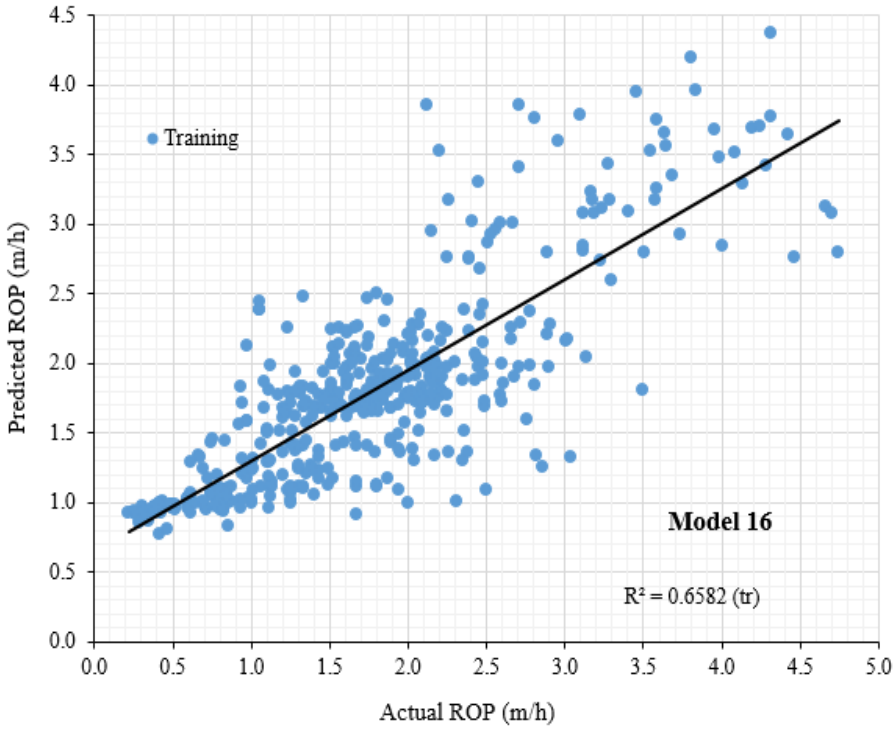

Figure F31. NLMR model 16 for estimating TBM penetration for training dataset

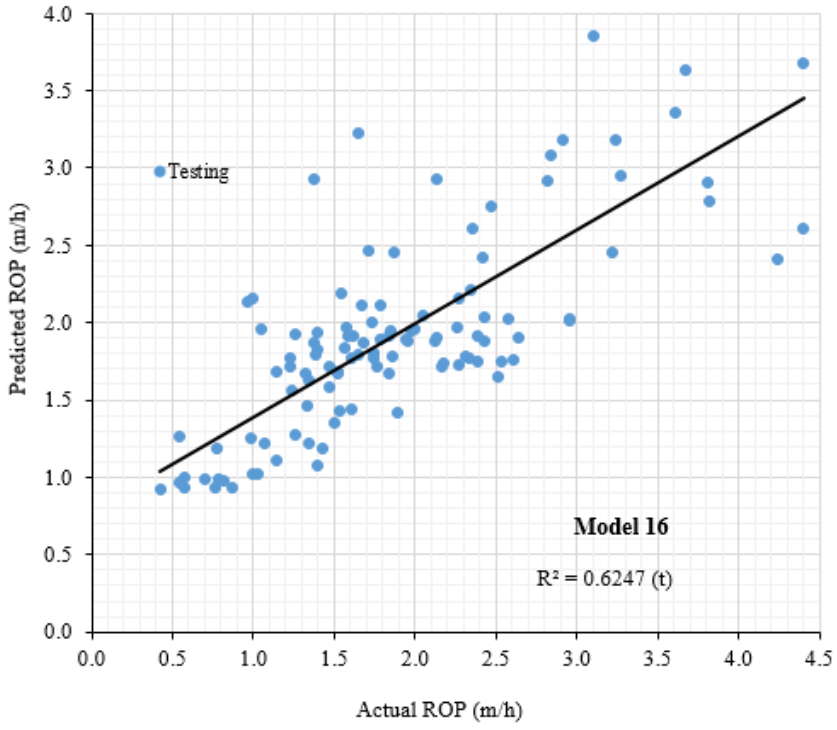

Figure F32. NLMR model 16 for estimating TBM penetration for testing dataset

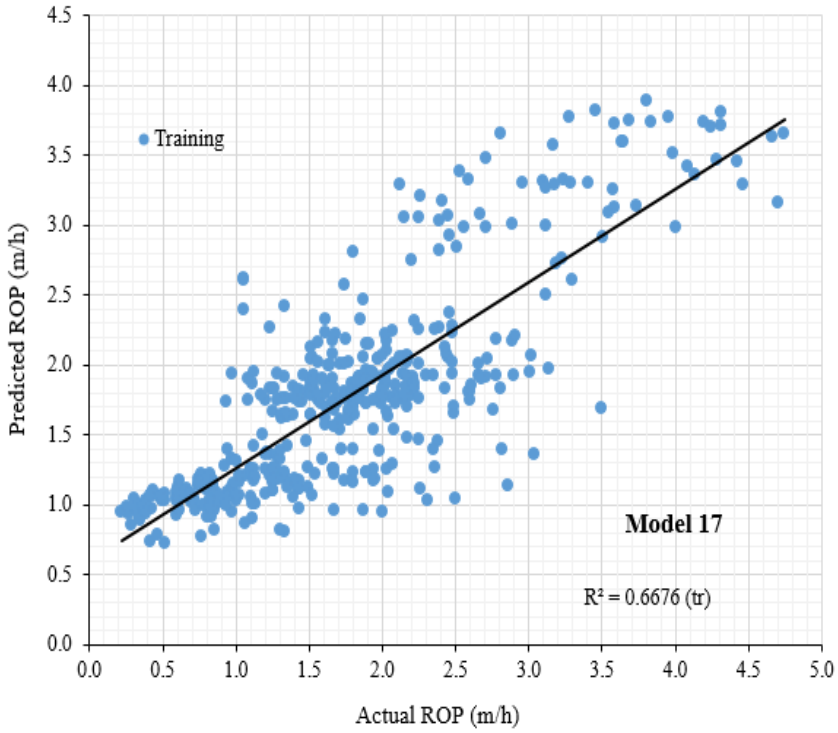

Figure F33. NLMR model 17 for estimating TBM penetration for training dataset

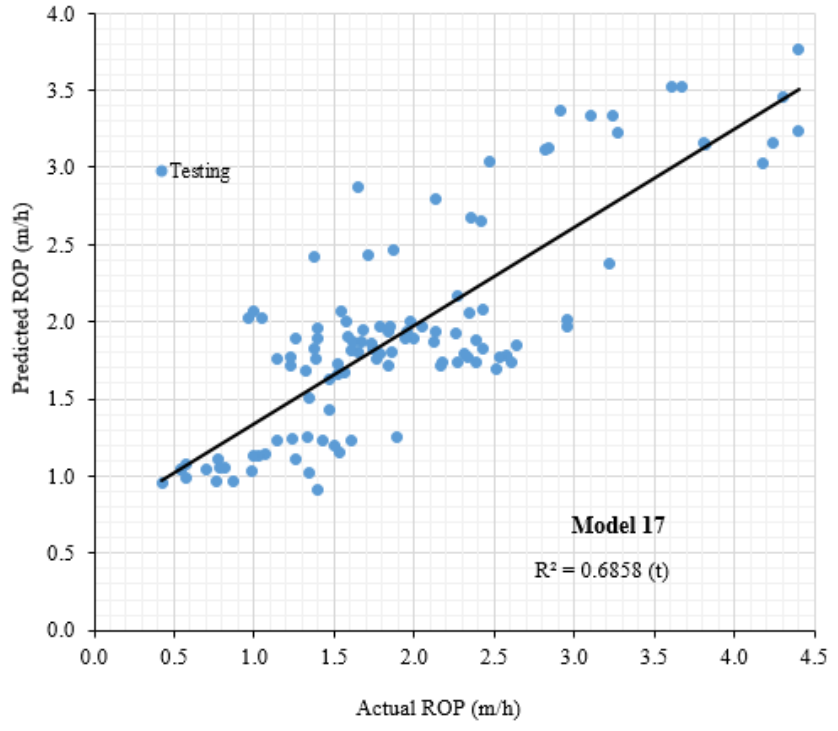

Figure F34. NLMR model 17 for estimating TBM penetration for testing dataset

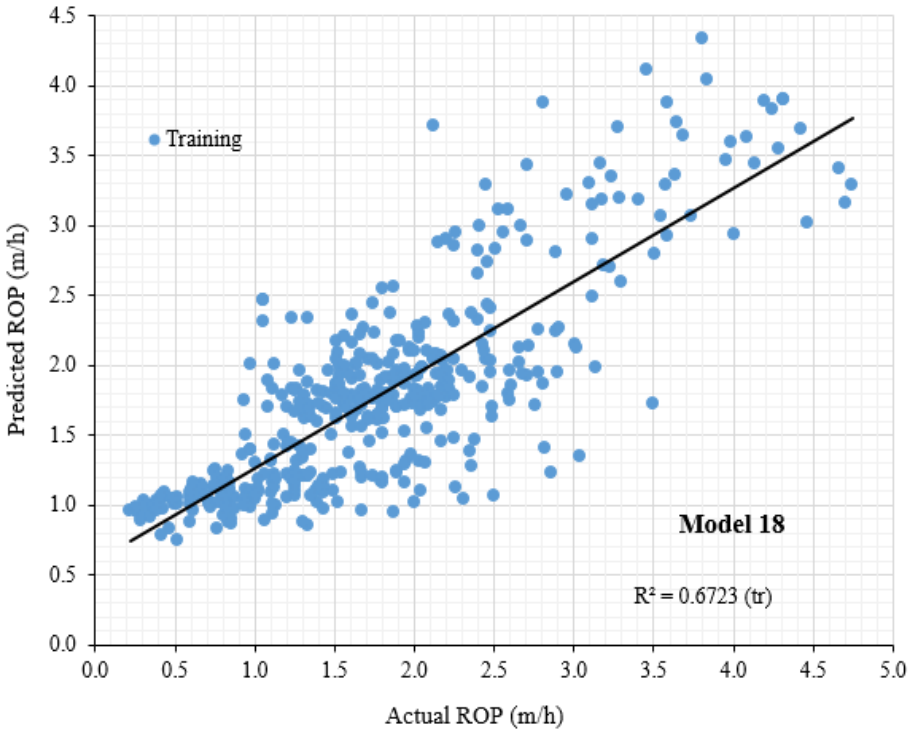

Figure F35. NLMR model 18 for estimating TBM penetration for training dataset

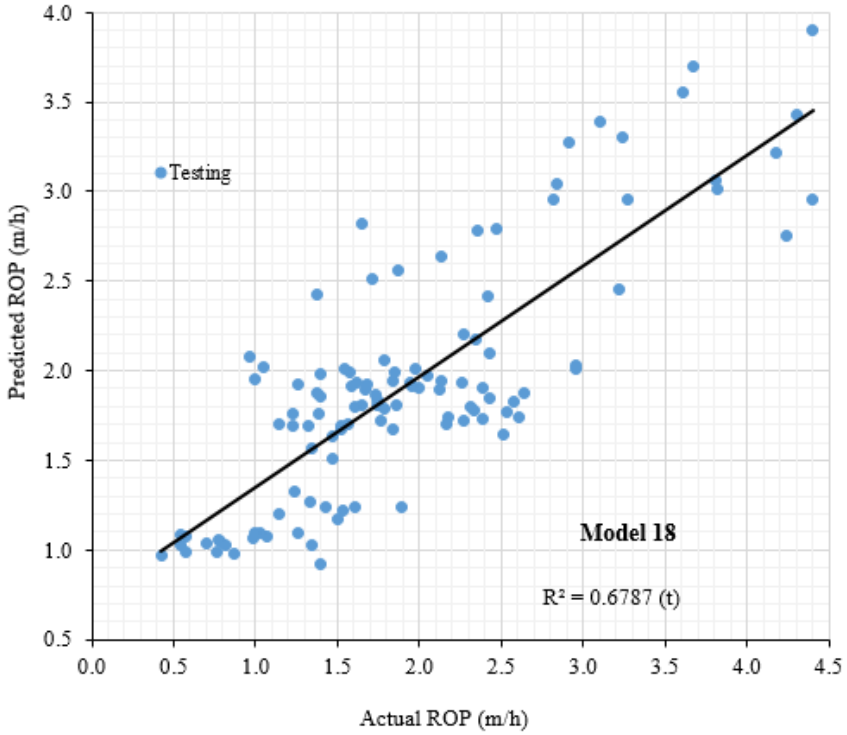

Figure F36. NLMR model 18 for estimating TBM penetration for testing dataset

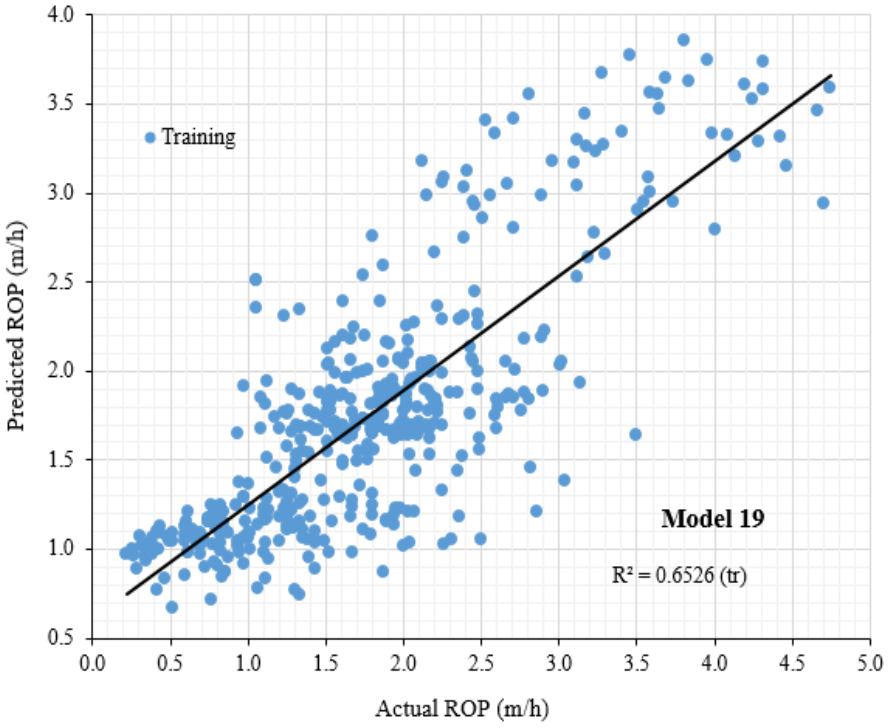

Figure F37. NLMR model 19 for estimating TBM penetration for training dataset

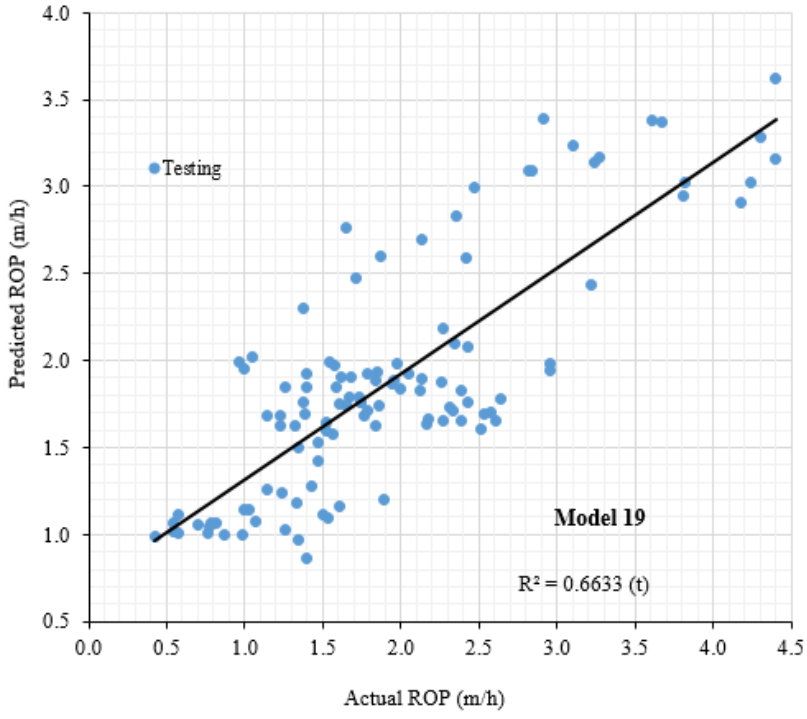

Figure F38. NLMR model 19 for estimating TBM penetration for testing dataset

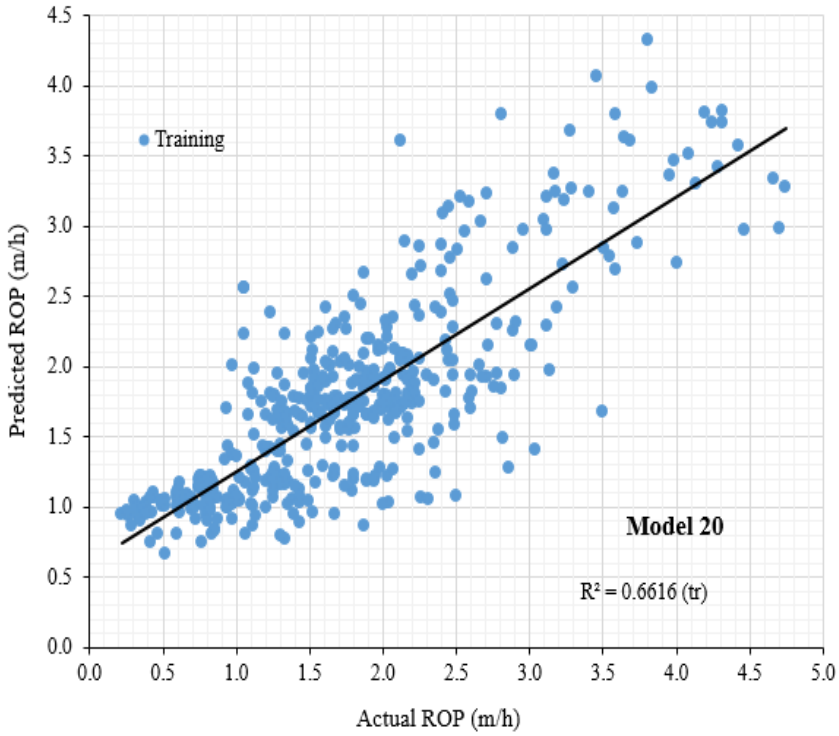

Figure F39. NLMR model 20 for estimating TBM penetration for training dataset

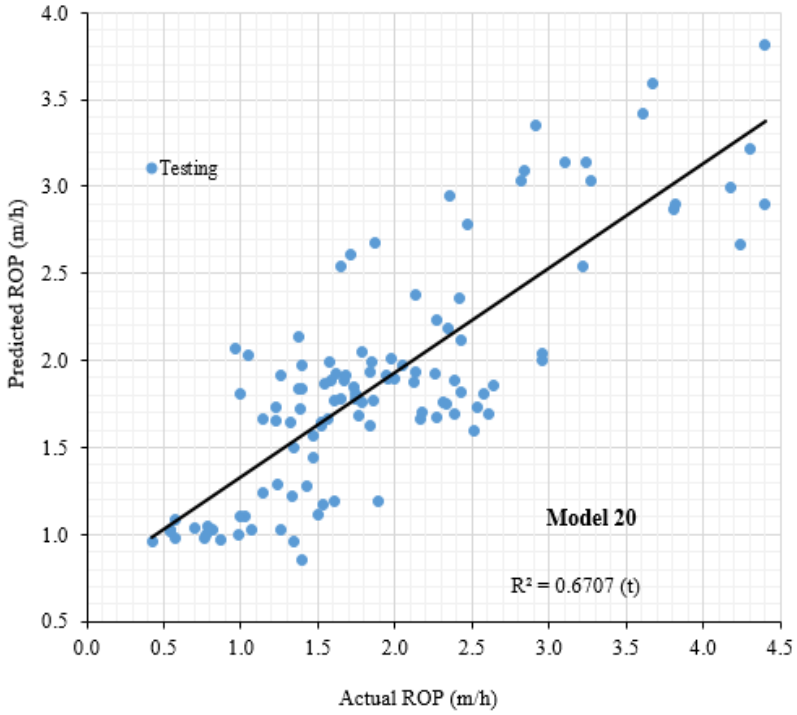

Figure F40. NLMR model 20 for estimating TBM penetration for testing

List of Publications (Dr. Aitolkyn Yazitova)

Manuscripts

1) **Yazitova, A.,** Adoko, A.C., Hassanpour J., Yagiz, S. Empirical models for estimating penetration rate of tunnel boring machine in rock mass. Bulletin of Eng., Geology and the Environment. 84(1):55 https://doi.org/10.1007/s10064-024-04062-5
2) **Yazitova, A.,** Yagiz, S. Performance analysis of drilling machines based on rock properties and machine's specifications. (2024) Bulletin of Engineering Geology and the Environment, 83 (1):37. https://doi.org/10.1007/s10064-023-03499-4
3) Yagiz, S., **Yazitova, A.,** Karahan, H. Application of differential evolution algorithm and comparing its performance with literature to predict rock brittleness for excavatability, (2020) International Journal of Mining, Reclamation and Environment, 34 (9):672-685. https://doi.org/10.1080/17480930.2019.1709012

Proceedings Paper & Presentations

1) **Yazitova, A.**, Yagiz, S. 2024. A model development for estimating TBM penetration in rocks. 13th of Asian Rock Mechanics Symposium (ARMS): Advances in Rock Mechanics-Infrastructure Development. New Delhi India. (Early Career Abstract Presentation)
2) Yagiz, S., **Yazitova, A**., Smirnov, G., Thyagarajan, MT., Hassanpour, J. Appraisal of Boreability Characteristics of Rocks to Estimate the TBM Advancement. 58th U.S. Rock Mechanics/Geomechanics Symposium, Golden, Colorado, USA, June 2024. Paper Number: ARMA-2024-0982. doi.org/10.56952/ARMA-2024-0982.
3) Yermukhanbetov K., **Yazitova A.,** Yagiz S. Comparison of strength-based rock brittleness indices with the brittleness index measured via Yagiz's approaches. (2021) IOP Conference Series: Earth and Environmental Science, 833 (1), art. no. 012038.
4) Yagiz S., Shaterpour-Mamaghani A., **Yazitova A**., Yermukhanbetov K., Dogan E., Erdogan T., Copur H. empirical models for estimating performance and operational parameters of raise boring machine in mining applications. (2021) IOP Conference Series: Earth and Environmental Science, 833 (1), art. no. 012129.
5) Yagiz S., Yermukhanbetov K., **Yazitova A.**, Rostami J. Utilizing linear cutting machine test for estimating cutting force via intact rock properties. (2021) 55th U.S. Rock Mechanics / Geomechanics Symposium 2021, 1, pp. 353 - 357.
6) **Yazitova A.,** Yagiz S. Estimation of drilling rate of diamond driller using rock properties and driller specifications. (2020) ISRM International Symposium -EUROCK2020.
7) **Yazitova A.,** Yagiz S. Prediction of drilling rate utilizing common rock properties and driller specifications: percussion drilling. WTC2020, Kuala Lumpur, Malaysia, 973-977pp.
8) Yagiz S., **Yazitova A.** Using intact rock brittleness for assessing TBM penetration. (2019) World Congress on Civil, Structural, and Environmental Engineering, article no. 122.

Academic CV of PhD candidate

Aitolkyn Yazitova

aitolkyn.yazitova@nu.edu.kz +77055126863 Astana

Education

PhD in Mining Engineering 2020 - 2025
Nazarbayev University, Astana, Kazakhstan

Master's Degree in Mining Engineering 2017 - 2019
Nazarbayev University, Astana, Kazakhstan

Bachelor's Degree in Petroleum Engineering 2013 - 2017
Kazakh-British Technical University, Almaty, Kazakhstan

Employment

Research assistant 2019 - 2020
Nazarbayev University, Astana, Kazakhstan
Geochemical study of the corrosion at Uzen oil field

Internship 2018 - 2018
Kazzinc Shakhtostroy, Ridder, Kazakhstan
Determining drilling directions underground using a theodolite in a mine

Internship 2017 - 2017
Kazakhoil Aktobe, Aktobe, Kazakhstan
Compilation of technical reports concerning the Kozhasai field.

Internship 2016 - 2016
Karachganak Petroleum Operating B.V., Aksay, Kazakhstan
An introductory exploration into the separation of gas and liquid phases and the utilization of compressors for gas re-injection to maintain reservoir pressure equilibrium

Publications

- Yazitova A., Adoko AC, Hassanpour J., Yagiz S. (2025) Empirical models for estimating penetration rate of tunnel boring machines in rock mass. Bull.Eng.Geol.Environ. 84:55
- Yazitova A., Yagiz S. Performance analysis of drilling machines based on rock properties and machine's specifications. (2024) Bulletin of Engineering Geology and the Environment, 83 (1):37
- Yazitova A, Yagiz S. (2024) A model development for estimating TBM penetration in rocks. 13th of Asian Rock Mechanics Symposium (ARMS): Advances in Rock Mechanics-Infrastructure Development. New Delhi India. (Early Career Abstract Presentation)
- Yagiz S., Yazitova A., Smirnov G., Thyagarajan MT., Hassanpour J. (2024) Appraisal of Boreability Characteristics of Rocks to Estimate the TBM Advancement. 58th U.S. Rock Mechanics/Geomechanics Symposium, Golden, Colorado, USA
- Yagiz S., Shaterpour-Mamaghani A., Yazitova A., Yermukhanbetov K., Dogan E., Erdogan T., Copur H. (2021) Empirical models for estimating performance and operational parameters of raise

Skills

Petroleum Engineering: Petrel

Mining Engineering: Micromine, Ventsim, Isatis

Statistical programs: IBM SPSS Statistics 25

Geochemical software: SUPCRT92

General Programs: Microsoft Office (Word, Excel, PowerPoint), Sigma-Plot

Languages

Kazakh

English

Russian

Hobbies

- Reading
- Swimming
- Music: singing
- Martial arts (boxing, kickboxing, muay thai)
- Composing poems
- Les mills instructor
- Fitness trainer
- I have a passion for a long-distance running, particularly distances like 10 kilometers (10K) and half-marathons of 21 kilometers (21K)

boring machine in mining applications. IOP Conference Series: Earth and Environmental Science, 833 (1), art. no. 012129

- Yagiz S., Yazitova A., Karahan H. (2020) Application of differential evolution algorithm and comparing its performance with literature to predict rock brittleness for excavatability, International Journal of Mining, Reclamation and Environment, 34 (9):672-685
- Yazitova A., Yagiz S. (2020) Prediction of drilling rate utilizing common rock properties and driller specifications: percussion drilling. WTC2020, Kuala Lumpur, Malaysia, 973-977pp.
- Yazitova A., Yagiz S. (2020) Estimation of drilling rate of diamond driller using rock properties and driller specifications. ISRM International Symposium -EUROCK2020
- Yagiz S., Yazitova A. (2019) Using intact rock brittleness for assessing TBM penetration. World Congress on Civil, Structural, and Environmental Engineering, article no. 122

Participating in conferences/forums

ConnectEd2024 2024

Mining & Exploration Forum (MINEX) 2019

Volunteer of the IX Central Asian MINEX 2018

New Generation. Across the Universe 2016
forum in Moscow

Organizer of the SPE VI, VII International Scientific and Practical Conference " Problems of innovative development of the oil and gas industry 2015

Honors & Awards

Selected as one of the eight young rock engineers to participate in the 9th ISRM Early Career Forum 2024
New Delhi, India

Participant of intellectual game "GeoGames 2016

1st place in the regional intellectual team game "GeoQuestions" 2016

The winner of Kurmangazy Petroleum Company 2016- 2017 Scholarship 2016

1st place in The VII International Scientific and Practical Conference 'Innovative Development Problems in Oil and Gas Industry' with project 'Kinematics of a parallel Mechanisms with two-end effectors 2015

Marathons, participating in 10km and 21km distances several times

Qualities

- Hardworking and responsible
- Effective communication and presentation skills
- Team player
- Outstanding abilities in organization
- Capacity to rapidly grasp scientific software applications
- Pursuing advancement and personal development in a professional capacity
- I take pleasure in upholding discipline

Blank Page